Department of Radiation Biology

FACULTY OF HEALTH AND MEDICAL SCIENCES
UNIVERSITY OF COPENHAGEN

PhD thesis

Signe Regner Michaelsen, MSc

Analysis of molecules related to angiogenesis for advancement of glioblastoma treatment

Head Supervisor
Hans Skovgaard Poulsen

Submitted
This thesis has been submitted October 2017 to the Graduate School of the Faculty of Health and Medical Sciences, University of Copenhagen

Author
Signe Regner Michaelsen, MSc
Department of Radiation Biology, Finsen Center
Rigshospitalet, Section 6321
Blegdamsvej 9
DK-2100 Copenhagen
Denmark
E-mail: signe.regner.michaelsen@regionh.dk, signerm@gmail.com

Supervised by
Hans Skovgaard Poulsen, MD, DMSc
Department of Radiation Biology,
Rigshospitalet

Ulrik Lassen, MD, PhD
Department of Oncology,
Rigshospitalet

Petra Hamerlik, MSc, PhD
Brain Tumor Group
The Danish Cancer Society Research Center

Opponents
Julia Sidenius Johansen, Professor, MD, DMSc (Chairman)
Department of Clinical Medicine,
Herlev Hospital,
University of Copenhagen, DK

Bjarne Winther Kristensen, Professor, MD, PhD
Department of Clinical Pathology,
Odense University Hospital,
University of Southern Denmark, DK

Simone Niclou, Professor, MSc, PhD
NORLUX Neuro-Oncology Laboratory,
Luxembourg Institute of Health, LU

Preface

The present thesis "Analysis of angiogenesis related molecules for advancement of glioblastoma treatment" has been submitted October 30, 2017, in order to achieve the PhD degree from the Faculty of Health and Medical Sciences, University of Copenhagen, Denmark. The thesis is based on work of which the majority was carried out at the Department of Radiation Biology, Rigshospitalet, while minor experimental parts were conducted at other sites at Rigshospitalet; at the Department of Experimental Medicine, Faculty of Health and Medical Sciences, University of Copenhagen; and at the Danish Cancer Society Research Center.

The thesis covers three original manuscripts included in the result section:

I. ***Michaelsen SR***, Staberg M, Nedergaard MK, Majewski WW, Broholm H, Meulengracht C, Urup T, Villingshøj M, Lucacova S, Kjær A, Lassen U, Stockhausen MT, Poulsen HS, Hamerlik: VEGF-C sustains VEGFR-2 activation under bevacizumab therapy and promotes cellular maintenance in glioblastoma. Submitted.

II. Staberg M*, ***Michaelsen SR****, Olsen LS, Nedergaard MK, Villingshøj M, Hamerlik P, Poulsen HS: Combined EGFR- and notch inhibition display additive inhibitory effect on glioblastoma cell viability and glioblastoma-induced endothelial cell sprouting in vitro. Cancer Cell International. Apr 26;16:34. 2016. *shared first authorship. Manuscript has previously been part of PhD thesis by M. Staberg.

III. ***Michaelsen SR***, Urup T, Olsen LR, Broholm H, Lassen U, Poulsen HS: Molecular profiling of short-term and long-term surviving patients identifies CD34 mRNA levels as prognostic for glioblastoma survival. Submitted.

Financial support for the PhD study was granted from The Faculty of Health and Medical Sciences, University of Copenhagen; Arvid Nilssons Foundation; Torben and Alice Frimodts Foundation; King Christian X's Foundation, Dansk Kraeftforsknings Foundation, Manufacturer Einar Willumsens Memorial Foundation and Sejer Perssons and Lis Klüwers Foundation.

Acknowledgements

Making it as a PhD require a combination of hard work, some talent, a bit of luck and lots of support from good people, and in regard to the latter I would like to express my sincere gratitude to a number of persons that have been important during my PhD life:

…My three supervisors for setting a frame that made this project possible. Specific thanks should go to *Hans Skovgaard Poulsen* for accompanying me in my science travel for many years and involving me in all sorts of research related work. Although, your high expectations and trust in my abilities have been very challenging at times, it has with no doubt also been highly developing. *Ulrik Lassen* should be especially acknowledged for always meeting me and my project with a positive mind and helping in establishing financial support for the project. Finally, huge thanks should go to *Petra Hamerlik* for stepping in with great supervision during difficult times and developing my science skills to a new level.

…The team at the Department of Radiation Biology, which I consider as my extended family and with whom I have shared many good hours of both the scientific and not-so scientific kind. Special thanks should go to *Thomas Urup* for fantastic teamwork on our common projects, wise words when frustration level reached maximum and our many great (mostly too late in the night) scientific discussions; *Mikkel Staberg* for being my lab buddy as well as supportive friend during dark (lab) days and definitely making Fridays more fun; *Mette Villingshøj* for fantastic technical input, for turning the world in our office on daily basis and for decorating my desk with wonderful flowers; *Dorte Nørøxe, Kirsten Grunnet* and *Camilla Bjørnbak Holst* for bringing an uplifting positive attitude into the lab life and Medical students, *Anders*, *Sofie*, *Sidsel*, *Sarah* and *Maria,* for creating a fun and pleasant environment and still dropping by for a coffee to catch up. Also former members of the lab, including *Karina Kristoffersen*, *Frederik Cramer*, *Marie Stockhausen* and *Pia Pedersen*, for shaping my early science life in a good direction and for encouraging me to keep on in the tough process of establishing the funding for the this project.

…The team of the Brain Tumor Biology Group at the Danish Cancer Society, especially *Kamilla Ellermann Jensen* and *Rikke Darling Rasmussen*, for welcoming me in their lab and always being extremely helpful and kind.

…My fantastic collaborators, in particular *Helle Broholm*, *Mette Kjølhede Nedergaard* and *Ib Jarle Christensen*, for great project input and educating me in each of their specialties.

…Finally my parents for listening to my endless talk about my science world of which I guess you did not understand half and always helping me out when my life was struck by bad planning (which it often is). And last but not least my wonderful friends, especially *Line*, *Malin*, *Mette*, *Sofie* and *Henriette*, for cheering on me and remembering me on that there is a world besides science.

Thanks to you all,

Signe Regner Michaelsen

Copenhagen, October 2017

Table of Contents

Summary

Glioblastoma, the most malignant primary brain cancer in adults, is an aggressively developing disease presenting very short survival and hence, new treatment modalities are in great demand. Recent year's research has improved the understanding of the genetic background and key phenotypic features in glioblastoma, but also unfolded how heterogeneous glioblastoma tumors are. One of the phenotypic traits of glioblastoma that have been greatly examined as a treatment target is tumor vascularization. However, although glioblastomas present a high level of formation of new blood-vessels, i.e. angiogenesis, very little effect has been achieved upon clinical testing of the anti-angiogenic drug bevacizumab in glioblastoma patients. Accordingly, the overall aim of this PhD dissertation was to examine molecules related to angiogenesis or efficacy of anti-angiogenic therapy for improvement of glioblastoma treatment.

One of the studied molecules was the vascular endothelial growth factor (VEGF) – C, found to be heterogeneously expressed among glioblastoma patient tumors as well as cultured cells. VEGF-C was further shown to engage in autocrine activation of angiogenic- and oncogenic receptor VEGFR2 in glioblastoma cells and to promote cell survival, cell-cycle progression, invasion and tumor growth. The results thereby point at VEGF-C as a potential treatment target in glioblastoma, but also highlight the relevance of combination with other treatments like bevacizumab. In line with this recognition, a more closely exploration was conducted of the potential of combined targeting of several angiogenesis-related molecules overexpressed in subpopulations of glioblastoma cells. In specific, inhibition of signaling via epidermal growth factor receptor (EGFR) and Notch was examined via *in vitro* assays using relevant glioblastoma cell models. Data showed the combination of EGFR-targeting drug *Iressa* and Notch-pathway-inhibitor *DAPT* to decrease pro-survival signaling, cell viability and angiogenic capacity more efficiently than single drug treatment, thereby highlighting the potential of this combination as a treatment strategy in glioblastoma. Finally, an explorative approach was used to identify molecules among 792 genes, for which a varying expression pattern correlated to the survival of glioblastoma patients treated with radiation-, chemo- and bevacizumab therapy. Analysis of

two independent datasets pointed at the vessel marker CD34 as an identifier of survival outliers and as being an independent prognostic variable in glioblastoma. These results encourage further study of CD34 level and vessel composition for treatment optimization in glioblastoma.

Collectively, thesis results provide novel insight into molecular signaling related to angiogenesis, which can be exploited in the battle against glioblastoma. Evidence is presented for a possible therapeutic value in glioblastoma of targeting VEGF-C, targeting of Notch- and EGFR-signaling in combination, and estimation of CD34 expression level as indicator of patient prognosis.

Dansk Resumé

Glioblastom, den mest ondartede primære hjernekræft hos voksne, er en aggressiv udviklende sygdom med meget kort overlevelse, hvorfor der er stort behov for nye behandlingsmuligheder. Senere års forskning har forbedret forståelsen af sygdommens genetiske baggrund samt af vigtige fænotypiske karakteristika, men har også påvist, hvor utroligt forskelligartede glioblastom kræftsvulster (tumorer) er. Et af de særegne karakteristika ved glioblastom, der er meget velundersøgt som behandlingsmål, er tumorernes blodforsyning. På trods af at glioblastomer har et højt niveau af blodkardannelse, såkaldt angiogenese, har effekten ved klinisk afprøvning af anti-angiogenese lægemidlet bevacizumab været ringe hos glioblastom patienter. Som følge heraf var det overordnede formål i denne ph.d.-afhandling at undersøge molekyler relateret til angiogenese eller effekt af anti-angiogen behandling, til forbedring af behandlingen i glioblastom. Et af de studerede molekyler var ”vascular endothelial growth factor” (VEGF) – C, som blev vist at have et heterogent udtryk blandt glioblastom patienttumorer såvel som i cellekulturer. VEGF-C blev yderligere påvist i glioblastom tumorceller til at indgå i et aktiverings loop for receptoren VEGFR2 samt at fremme celledeling, celleoverlevelse, tumorvækst samt cellernes evne til at invadere omkringliggende miljø. Resultaterne peger derved på VEGF-C som et potentielt

behandlingsmål i glioblastom, men fremhæver også relevans af kombinationen med andre behandlinger såsom bevacizumab. I overensstemmelse med denne anerkendelse blev potentialet af en kombineret målrettet behandling mod flere angiogenese-relaterede molekyler, der er set overudtrykt i subpopulationer af glioblastomceller undersøgt. Helt specifikt blev hæmning af signalering via molekylerne "epidermal growth factor receptor" (EGFR) og Notch undersøgt i glioblastom via cellebaserede forsøg i relevante modeller. Data viste, at der ved kombination af EGFR hæmmeren Iressa og Notch-signalvejs hæmmeren DAPT kunne opnås øget reduktion af cellevækst samt øget reduktion af kræftcellernes evne til at stimulere angiogenese i forhold til ved enkelt-stof behandling. Endeligt indeholder tesen et eksplorativt studie af 792 gener. Disse blev undersøgt for, hvorvidt et varierende ekspressionsmønster korrelerede med overlevelsen for glioblastom patienter behandlet med stråling, kemo- og bevacizumab-terapi. Analyser i to uafhængige datasæt viste, at genudtryk af blodkar markøren CD34 kan anvendes til at estimere overlevelsen for glioblastom patienter. Disse resultater fordrer yderligere undersøgelser af variation i CD34 udtryk og blodkarmønstre i glioblastom.

Samlet set giver afhandlingens resultater et nyt indblik i molekylær signalering relateret til angiogenese, som kan udnyttes i kampen mod sygdommen glioblastom. De fremlagte data påviser en mulig terapeutisk værdi i glioblastom for behandling målrettet mod VEGF-C, behandling målrettet mod Notch og EGFR-signalering i kombination samt for estimering af CD34 udtryk som indikator for patient prognose.

Abbreviations

2-HG	2-hydroxylglutarate
ADAM	A disintegrin and metalloprotease
ATRX	Alpha-thalassemia/ mental retardation X-linked
BBB	Blood-brain barrier
BMDCs	Bone marrow-derived cells
CHI3L1	Chitinase-3-like protein 1
Chr	Chromosome
CSCs	Cancer stem cells
CSL	CBF1, Suppressor of Hairless, Lag-1
CT	Computed tomography
Dll	Delta-like
ECM	Extracellular matrix
EGFR	Epidermal growth factor receptor
FFPE	Formalin-fixed paraffin embedded
G-CIMP	Glioma-CpG island methylator phenotype
GFAP	Glial fibrillary acidic protein
GSCs	Glioblastoma stem-like cells
GSIs	γ-secretase inhibitors
HBMVECs	Human brain microvascular endothelial cells
HES	Hairy/Enhancer of Split
HIF	Hypoxia inducible factor
HRE	Hypoxia response elements
HSPG	Heparan sulfate proteoglycans
IDH	Isocitrate dehydrogenase
IHC	Immunohistochemistry
IRES	Internal ribosome entry site
LTS	Long-term survivors
MGMT	O^6-methylguanine-DNA methyltransferase
MR	Magnetic resonance

MVA	Microvessel area
MVD	Micro vessel density
NF1	Neurofibromatosis type 1
NFκB	Nuclear factor κB
NICD	Notch intracellular domain
NK	Natural killer
NLSs	Nuclear localization signals
NRP	Neurophilin
OLIG2	Oligodendrocyte transcription factor 2
OS	Overall survival
PAS	Periodic acid-Schiff
PDGFRA	Platelet-derived growth factor receptor alpha
PET	Positron emission tomography
PFS	Performance-free survival
PlGF	Placental growth factor
PTEN	Phosphatase and tensin homolog
rCBV	Relative cerebral blood volume
RTKs	Receptor tyrosine kinases
Shh	Sonic Hedgehog
SNP	Single-nucleotide-polymorphism
STS	Short-term survivors
TCGA	The Cancer Genome Atlas
TERT	Telomerase reverse transcriptase
TGF	Transforming growth factor
tGLI1	Glioma-associated oncogene homolog 1
TKI	Tyrosine kinase inhibitor
VEGF	Vascular endothelial growth factor
VHD	VEGF homology domain
WHO	World Health Organization

1. Background

1.1 Glioblastoma – prevalence, histological characteristics and risk factors

Brain cancer can be of either primary origin arising in the brain or secondary origin metastasizing from lesion sites outside the cranial cavity. Primary brain tumors are subdivided according to the World Health Organization (WHO) grading system into low grade (grade I-II) and high grade (grade III-IV) tumors. This grading is based on histological features with increasing grade correlating to enhanced aggressiveness and poorer patient prognosis [1]. Among the primary brain tumors, glioblastoma (grade IV glioma) is the most malignant and frequent in adults, accounting for around 67% of cases and having an incidence rate of 3-4 cases/100.000 population in western countries [2].

Histological characteristics of glioblastoma include high mitotic activity, nuclear atypia with presentation of multinucleated cells, as well as pleomorphic cells being irregular in shape and size and having varying level of differentiation. Further on, these tumors presents proliferating micro-vasculature and areas of necrosis often surrounded by dense accumulation of "palisading" tumor cells [1]. Upon diagnostic imaging analysis (typically by magnetic resonance (MR) imaging or computed tomography (CT) scans), patients most often present a single lesion appearing solid in form with relative defined borders. However, histological analysis of glioblastoma tumors have shown a high degree of diffusely spreading tumor cells into the surrounding brain parenchyma [3], suggestion that glioblastoma should be considered as a systemic disease within the brain.

As summarized by Walsh et al., little is known regarding the causes leading to the development of glioblastoma with cases originating of hereditary familial genomic alterations being infrequent. The few recognized risk factors are increasing age, gender (male over female), race (White over African-American and Asian) and prior radiation of the head (e.g. for treatment of childhood tumors). In contrary, various allergic conditions and prior infection with varicella-zoster virus (i.e. chickenpox) are suspected for having a protective function, but this is less documented. Beside this, studies have pointed at influence of specific germline single-nucleotide-polymorphism (SNP) variants in known glioma associated onco- and tumor

suppressor genes as well as increased telomere length for being related to higher risk of developing glioma [2].

1.2 Glioblastoma diversity

1.2.1 IDH1 status as a defining alteration

Glioblastomas can arise *de novo* as a primary disease or as a secondary tumor developing from a lower grade glioma. Secondary glioblastomas are highly associated with mutations in the isocitrate dehydrogenase (IDH) -1 gene, while these mutations are only rarely seen in primary glioblastomas [4] and consequently IDH status rather than clinical history is today used to subdivide glioblastomas into two diagnostic entities [1]. Tissue of IDH wildtype and -mutated glioblastomas are practically indistinguishable based on histology [1], although the IDH mutated glioblastomas have some tendency towards being less necrotic and having focal areas with oligodendroglial tumor morphology [5]. In contrary, IDH wildtype and -mutated glioblastomas differ significantly in respect to their clinical profile with IDH1 mutated glioblastomas, comprising around 10 % of the patients, presenting younger age, a higher tendency of having a frontal tumor brain location, a more gender balanced ratio and longer survival [5-8]. Moreover, IDH wildtype and -mutated tumors separates by having distinct molecular features. Typically genomic alterations associated with IDH1 wildtype glioblastomas are mutation in the oncogene EGFR (epidermal growth factor receptor), the tumor-suppressor gene PTEN (phosphatase and tensin homolog) and in the promoter for the TERT (telomerase reverse transcriptase) gene, resulting in transcriptional activation of this telomerase component. Contrary, IDH mutated glioblastomas frequently presents loss of ATRX (alpha-thalassemia/ mental retardation X-linked), a gene important for epigenetic and telomere maintenance, and inactivating mutation in the gene for tumor suppressor P53 [9-11]. Additionally, mutations in IDH mediates a glioma-CpG island methylator phenotype (G-CIMP) by generating highly increased levels of the oncometabolite 2-hydroxylglutarate (2-HG) inducing global DNA hypermethylation [12]. An overview of differences between IDH wildtype and -mutated tumors are shown in Table 1.

Table 1: Comparison of IDH-wildtype and –mutated glioblastomas. Modified from Louis et al. [1].

	IDH-wildtype glioblastoma	IDH-mutant glioblastoma
Synonym	Primary glioblastoma, IDH-wildtype	Secondary glioblastoma, IDH-mutant
Precursor lesion	Not identifiable; develops de novo	Diffuse astrocytoma Anaplastic astrocytoma
Proportion of glioblastomas	~90%	~10%
Median age at diagnosis	~62 years	~44 years
Male-to-female ratio	1.42:1	1.05:1
Mean length of clinical history	4 months	15 months
Median overall survival Surgery + radiotherapy Surgery + radiotherapy + chemotherapy	 9.9 months 15 months	 24 months 31 months
Location	Supratentorial	Preferentially frontal
Unique pathological features	Extensive necrosis	Limited necrosis Oligodendroglioma -like component
TERT promoter mutations	72%	26%
TP53 mutations	27%	81%
ATRX mutations	Exceptional	71%
EGFR amplification	35%	Exceptional
PTEN mutations	24%	Exceptional
G-CIMP phenotype	No	Yes

1.2.2 Glioblastoma subtyping

A decade of huge effort to characterize genomic alterations and expression signatures in glioblastoma has led to realization that these tumors represent a heterogeneous population, widely differing in their molecular profiles. However, it has also shown that some order exist in the chaos by the identification of specific genetic subtyping profiles for grouping of glioblastoma tumors [13]. Based on examination of gene expression profiles from WHO grade III-IV gliomas, Phillips et al. suggested three subtypes termed proneural, mesenchymal and

proliferative [14]. This was later supplemented by analysis by Verhaak et al. based on genomic screenings of glioblastoma tumors from The Cancer Genome Atlas (TCGA), identifying and characterizing four subtypes (proneural, mesenchymal, classical and neural) [15]. These were further refined in a recent publication by Wang et al. specifically examining expression profiles of glioblastoma tumor cells by filtering out profiles supplemented from the microenvironment. This study suggested that the neural subtype is non-tumor specific and consequently that only the Verhaak subtypes proneural, mesenchymal and classical proved to be relevant [16]. Upon comparison of the Phillips and Verhaak subclassification systems, overlap is found [17] as shown in Table 2 and as also described below. Key features for proneural tumors are: Mutation in IDH1, P53 and PDGFRA (Platelet-derived growth factor receptor alpha) as well as OLIG2 (Oligodendrocyte transcription factor 2) overexpression; for mesenchymal tumors they are: Loss of chromosome (chr) 10, gain of chr 7, mutation in NF1 (Neurofibromatosis type 1) and PTEN and overexpression of CHI3L1 (Chitinase-3-like protein 1), CD44, MET as well as NFκB (Nuclear factor κB) pathway members; while for proliferative/classical tumors they are: Loss of chr 10, gain of chr 7, EGFR and PTEN mutation and increased activity of Akt-, Notch- and Shh- (Sonic Hedgehog) pathways [14, 15].

The Wang et al. study also confirmed previous findings of glioblastoma subtype plasticity during disease course, with around 50% of tumors presenting other subtype at recurrence as compared to time of diagnosis [14, 16]. However, it did not support a specific shift from proneural to mesenchymal subtype as previous suggested [14, 18], but found ability of all three subtypes to shift to all of the other profiles [16]. Further, intra-tumoral heterogeneity with mixture of tumor cells of variable subtypes within the single tumor has been shown via single cell sequencing analysis [19] and consequently fluctuation in tumor clonal composition

Table 2: Genomic features of glioblastoma subtypes.

Phillips	Verhaak	Signature*
Proneural	Proneural	Mut:, IDH1, P53, PDGFRA Sig. exp: OLIG2
Mesenchymal	Mesenchymal	Mut: chr 10 loss, chr 7 gain, NF1, PTEN Sig. exp: CHI3L1, CD44, MET, NFκB pathway
Proliferative	Classical	Mut: chr 10 loss, chr 7 gain, EGFR, PTEN Sig. exp: Akt pathway, Notch pathway, Shh pathway

*Mut = Mutations, Sig. Exp = signature overexpression

during disease course could likely be the founder of the observed subtype shifts. This instability and heterogeneity of the current subtypes also complicates clinical implementation, although specific subtypes have been linked to better outcome with certain therapies in glioblastoma patients [18, 20, 21].

1.3 Therapy and effect

1.3.1 Established treatment for glioblastoma

Primary treatment for glioblastoma consists of maximal safe surgical resection followed by treatment according to Stupp's regimen i.e. radiation therapy with concomitant and up to six cycles of adjuvant temozolomide, an alkylating chemotherapy agent. This therapy was established as standard of care for patients younger than 70 years following the NCIC-EORTC phase 3 clinical trial demonstrating increased median overall survival (OS) (14.6 *versus* 12.1 months) and improved two year survival rate (27.5% *versus* 10.4%) upon combined radiation-temozolomide therapy as compared to radiation therapy alone [22]. Contrary, treatment of elderly glioblastoma patients have for long been controversial. However, a recent report by Perry et al. from a clinical phase 3 trial in glioblastoma patients older than 65 years provide evidence that these patients should also be given the combination therapy. This study, which randomized for short course radiation with concomitant and adjuvant temozolomide therapy or radiation therapy alone, showed significantly increased OS (9.3 months *versus* 7.6 months) as well as two year survival rate (10.4% *versus* 2.8%) of the combination regimen in comparison to single treatment [23].

At disease relapse, which is nearly inevitable in glioblastoma, no standard treatment exists, with most of the many tested therapeutic options failing. Yet, selected trials have indicated positive effect of certain treatments [24], and accordingly patients in Denmark, if not participating in clinical protocols, are evaluated for relapse surgery, followed by therapy with the antiangiogenic agent bevacizumab in combination with chemotherapy, currently in form of the alkylating agent CCNU (lomustine) [25].

1.3.2 Factors associated with survival

Besides IDH status, other factors have been established as prognostic for glioblastoma survival. This include clinical variables associated with worse prognosis such as increasing patient age, increasing performance status, limited extent of primary surgery, use of corticosteroids at therapy start, and presence of multiple lesion sites [26-28]. Although many molecular variables have been examined for association with survival, only promoter methylation of the O^6-methylguanine-DNA methyltransferase (MGMT) gene have been validated repeatedly as being correlated with better survival in temozolomide treated glioblastoma patients [23, 29-32]. MGMT promoter methylation is inversely correlated to MGMT protein expression [30, 32], and influence of MGMT on clinical outcome is believed to result from ability of MGMT protein to inhibit DNA damaging from chemotherapy, by removing methyl-groups delivered to the DNA by the therapeutic agents [33].

1.4 Glioblastoma development, cancer stem cells and implication for preclinical modelling

The cell(s) of origin for glioblastoma is still not well defined, but as summarized by Jiang et al. literature suggests that these tumors arise from neural stem cells, glial precursor cells or more differentiated glial cells [34]. Also, different theories exist for tumor initiation and formation of heterogeneous cell populations within glioblastoma (Figure 1). One is a stochastic model where a given cell obtains tumorigenic potential through series of mutations enabling it for unlimited division. Acquisition of additional mutations later on in selected cells then give rise to sub-clones having other genetic profiles and consequently different proliferative abilities and treatment sensitivity. Accordingly, during disease course clonal composition will change as a result of selection of therapy resistant sub-clones. Elimination of the tumors will therefore require either the use of combinations of treatments enabling targeting of all clones or the use of treatment with ubiquitous sensitivity, e.g. by targeting early genetic events. Alternatively, the hierarchical model suggests existence of cancer cells with stem cell-like abilities, able to self-renew and give rise to a heterogeneous clonal population of more differentiated bulk cells. Consequently, if these cancer stem cells (CSCs), although only constituting a small subset of cells, are not eliminated, tumors will regrow following treatment [35, 36].

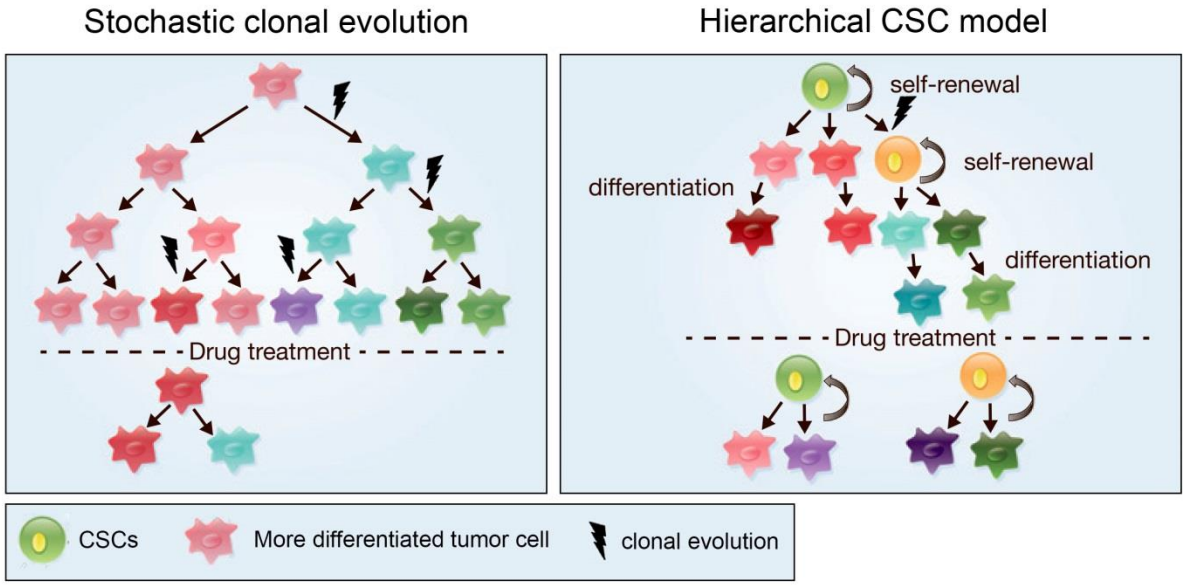

Figure 1. Models for glioblastoma development. In the stochastic clonal evolution model, heterogeneity is caused by a combination of cell expansion intervened by acquirement of multiple new mutations. Upon drug exposure selected clones will survive and expand to generate a relapse tumor with a new molecular profile. According to the hierarchical CSC model, cancer cells with stem cell properties are both able to self-renew and differentiate into a spectrum of different cells thereby generating tumor heterogeneity. Additional mutations can be acquired in the CSCs, also causing a heterogeneous population of CSCs. In this model, the CSCs possess high resistance to treatment and will expand the tumor following exposure to treatment. Modified from Bonovia et al. [36]

The existence of glioblastoma stem-like cells (GSCs) is supported by identification of glioblastoma tumor cells expressing various stem cell markers including CD133, Oct4, Sox2 and Nestin. Moreover, these cells have been shown to be multipotent in nature with ability to differentiate into all of the three neural linages i.e. astrocytes, oligodendrocytes and neurons [37-39]. The cells further possess high tumor initiating capacity, as demonstrated by the ability of a few hundred CD133-positive glioblastoma cells to form orthotropic xenografts in immune-deficient mice, whereas transplantation of up to several millions CD133-negative cells did not result in tumor formation [37]. As compared to their stem cell marker negative counterparts, GSCs also presents decreased sensitivity to radiation- and chemotherapy, related to elevated expression of genes important for multi-drug resistance, DNA mismatch repair and inhibition

of apoptosis [37, 40, 41]. Evidence for the existence of GCSs is further supported by the finding, that glioblastoma cell model establishment and maintenance in growth media normally used for neural-stem cells, give rise to cultures having expression profiles more similar to that of the parental tumor, as compared to culturing in traditional serum containing media [42]. Further, culturing in neural-stem cell media has been shown specifically to maintain glioblastoma cells in an undifferentiated state with preserved multipotent potential and expression of stem cell markers [42, 43]. Consequently, this way of culturing is today the *state of the art* within glioblastoma *in vitro* modelling, and accordingly used in studies of this thesis concerning glioblastoma cells.

1.5 Targeting of the glioblastoma vasculature

1.5.1 Vasculature and angiogenesis in glioblastoma

Compared to normal brain and low grade brain tumors, glioblastomas harbors more extensive vascularization and ranks among the most vascularized cancers overall [44]. Glioblastoma vasculature is characterized by abnormal disorganized leaky vessels being irregular in diameter and perfusion [45], as well as by microvascular proliferation resulting in formation of so-called glomeruloid bodies, a histopathological hallmark of glioblastoma [1]. Consequently this leads to development of tumor regions with deprived oxygenation (hypoxia), blood-brain barrier (BBB) disruption and increased interstitial pressure ultimately causing edema [46].

Angiogenesis is the formation of new vasculature via sprouting from already existing vessels, a process stimulated by a range of pro-angiogenic mediators secreted from the tumor cells or originating from other host sources such as immune cells [46]. The main driver of angiogenesis in glioblastoma is the hypoxic response [46], initiated in the tumor cells when oxygen levels reaches below 1-2%, which is significantly lower than the 3.4% normally observed in the brain [47]. During oxygen deprivation, hypoxia inducible factor (HIF) 1/2α proteins are stabilized from degradation allowing for complex formation with the constitutively expressed HIF1β protein and nuclear co-activator CBP/p300. This complex initiate transcription by binding to hypoxia response elements (HREs) in gene promoter regions, leading to the production of angiogenic promoting molecules, whereof vascular

endothelial growth factor (VEGF)-A is among the most prominent [48]. Besides hypoxia, VEGF-A level in glioblastoma is also increased by acidosis [49, 50], mechanical stress from extracellular compaction [51], nitric oxide [52], and stimulation via growth factors such as transforming growth factor (TGF) -β [53].

1.5.2 The VEGF family and its receptors

In mammals five VEGF family members have been identified, comprising VEGF-A, VEGF-B, VEGF-C, VEGF-D and placental growth factor (PlGF). These are further subdivided into biologically distant isoforms as a result of alternative splicing (VEGF-A and –B and PlGF) or proteolytic processing (VEGF-C and VEGF-D) [54]. A common feature of all VEGF family members is the presence of a defined VEGF homology domain (VHD), a region containing the receptor binding sites. Additionally, most VEGFs contain accessory domains influencing their specificity [55]. Receptors binding the VEGFs include the VEGFR-1, -2, -3, being receptor tyrosine kinases (RTKs) - a type of receptors characterized by an extracellular ligand binding domain, a transmembrane domain and a cytoplasmic domain with the tyrosine kinase. Upon ligand binding, monomeric forms of the receptors undergo homo-dimerization and intracellular auto-phosphorylation, recruiting and activating downstream signaling pathways. Receptor activity is regulated via various co-receptors including neurophilin (NRP-1 and -2), heparan sulfate proteoglycans (HSPG) and integrins, as well as by existence of soluble receptor isoforms trapping available ligand [54]. Moreover, the receptors also form heterodimers, resulting in deviating phosphorylation patterns and thereby changed downstream signaling [56, 57]. Functionally, VEGFR2 is the main mediator of VEGF-A stimulated angiogenesis via extensive effects on adherence junctions, proliferation, motility and differentiation in endothelial cells. VEGFR-1 mainly mediates negative regulatory function on VEGFR2 signaling, whereas VEGFR3 is the main mediator of lymphangiogenesis (the formation of new lymphatic vessels from pre-existing lymphatic vessels), but may also play a role in angiogenesis given its expression on normal vascular endothelial cells [58]. Overview of receptor binding and function are shown in Figure 2.

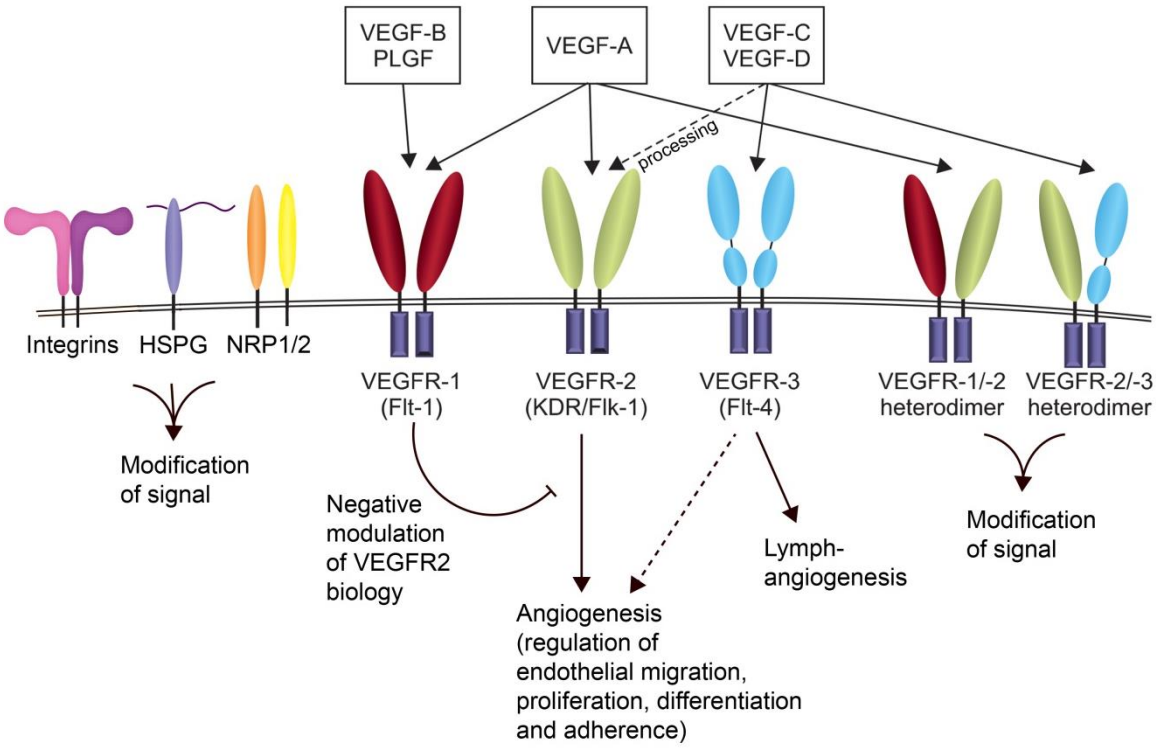

Figure 2. VEGF-VEGFR signaling. Overview of VEGF family members, their receptors and downstream effect of signaling. Modified from Bae et al. [59].

1.5.3 Efficacy of anti-angiogenic therapy

Originally anti-angiogenic therapy was believed to diminish vasculature development, leading to non-vascular dormant tumors with inhibited ability to grow [60]. Later on the theory of vasculature normalization was presented, in which the treatment initially result in a transient period of improved vessel integrity and perfusion. This creates a “therapeutic window” with better delivery of cytotoxic agents such as chemotherapy and increased sensitivity to radiation therapy due to elevated oxygenation levels [61]. This ability to normalize tumor vessels and thereby re-establish the BBB, presents a challenge for evaluation of treatment efficacy in glioblastoma, as it can result in decreased contrast enhancement on MR imaging without a real antitumor effect, a phenomena known as “pseudoresponse” [62].

Other proposed mechanisms of action for anti-angiogenic therapy in cancer, including glioblastoma, are induced immune reactivity due to increased recruitment of immune effector

cells and inhibition of VEGF-A mediated suppressive effect on maturation of immune cells [63]. Moreover, specific function of VEGFR-2 in glioblastoma tumor cells maintenance, including the GSC population [64-67], argue for direct cytotoxic effect of anti-angiogenic therapy in the glioblastoma tumor cells.

1.5.4 Anti-angiogenic therapy for glioblastoma – a telling about bevacizumab

Based on the high vascularity of brain tumors, Judah Folkman in 1971 proposed that "it is possible that "anti-angiogenesis" would be extremely important in the therapy of brain tumors" [60]. Multiple clinical trials of anti-angiogenic therapy have been conducted in glioblastoma, but survival benefit of tested agents has been limited. Strategies have mainly focused on VEGF-A targeting using the humanized monoclonal antibody bevacizumab, but also VEGF-A targeting by soluble decoy-VEGFRs and tyrosine kinase inhibitor (TKI)-driven VEGFR targeting have been examined [68].

Functionally, bevacizumab binds all isoforms of VEGF-A, but not other VEGF members such as VEGF-B and -C, and neutralizes the biological activity by steric blocking the VEGFR binding site [69]. Bevacizumab was implemented at many clinical institutions for treatment of recurrent glioblastoma based on results from phase II clinical trials, showing high response rate as well as increased performance-free survival (PFS) and OS compared to historical data, upon treatment with bevacizumab combined with irinotecan, a topoisomerase I inhibitor [70, 71]. More recently, two randomized placebo controlled phase III studies, AVAGlio and RTOG 0825, tested addition of bevacizumab to first-line radiation and temozolomide therapy. These reported increased PFS of 3-4 months in the treatment arm receiving bevacizumab, but not improved OS [72, 73]. Similar results was found in the phase II randomized GLARIUS trial, testing combination of bevacizumab-, radiation- and irinotecan therapy *versus* standard radiation- and temozolomide therapy in the first-line setting for non-MGMT promoter methylated glioblastoma [74]. Further questioning the efficacy of bevacizumab is the recent EORTC 26101 phase III clinical trial comparing bevacizumab plus CCNU *versus* CCNU single therapy for recurrent glioblastoma. As the other phase III trials, this study did not show improved OS of the combinational regimen, although PFS was increased [75].

Still, published data argue for therapeutic benefit of bevacizumab treatment in a subpopulation of glioblastoma patient. Several studies have reported improved survival for patients experiencing a durable response as compared to non-responding patients [76-78]. Also, clinical benefits have been reported for bevacizumab therapy re-challenging in patients previous treated with bevacizumab [79, 80]. Moreover, sub-analysis of two of the conducted clinical trials found indications for improved OS in the proneural and classical glioblastoma subtypes, respectively, upon bevacizumab combination therapy, despite no clinical benefit in the total trial population [20, 21].

1.5.5 Mechanisms behind bevacizumab resistance

Insensitivity towards anti-angiogenic drugs such as bevacizumab has been proposed to arise in several ways (Figure 3). One is the establishment of tumor vasculature in an angiogenesis independent manner for which different mechanisms have been described in glioblastoma. This includes vessel co-option, in which the cancer cells exploit the normal vasculature to migrate and grow along [81-83]. Also vascular mimicry with incorporation of glioblastoma tumor cells into the vessel lining has been suggested, a process driven by adaptation of vascular cell-like abilities of the GSC tumor subpopulation and found to be unaffected by VEGF-A blocking antibodies [84-87]. Moreover, neo-vascularization, vasculogenesis, initiated by recruitment and differentiation of circulating bone marrow-derived (vascular progenitor) cells (BMDCs) may contribute to the tumor vasculature in glioblastomas [88]. Although this process was found to be stimulated by VEGF-A, alternative molecular drivers were proposed to sustain it under anti-VEGF-A therapy [89].

Additionally, covering of tumor vessels by pericytes has shown to protect the endothelial lining from anti-angiogenic therapy by supportive expression of endothelial stimulating factors such as VEGF-A [90]. Studies have also pointed at a bevacizumab-induced phenotypic shift in glioblastoma, from a vascularized towards a more invasive growth pattern. This shift has been linked to subclass transition from a proneural to a more mesenchymal subtype, increased immune infiltration and signaling via the RTK c-Met [91, 92]. Additionally, signaling by alternative pro-angiogenic factors can sustain or rebuild glioma vessel formation under

depression of active VEGF-A. This includes both alternative activators of VEGFR signaling or completely alternative pro-angiogenic pathways [93]. Finally, VEGFR2 signaling, including activation by VEGF-A, can possible occur within the intracellular compartments, not requiring available ligand outside the cell. This type of “intracrine” signaling has been shown in non-small cell lung cancer and colorectal cancer [94, 95], but if this phenomenon also play a role in bevacizumab resistance in glioblastoma remains to be explored.

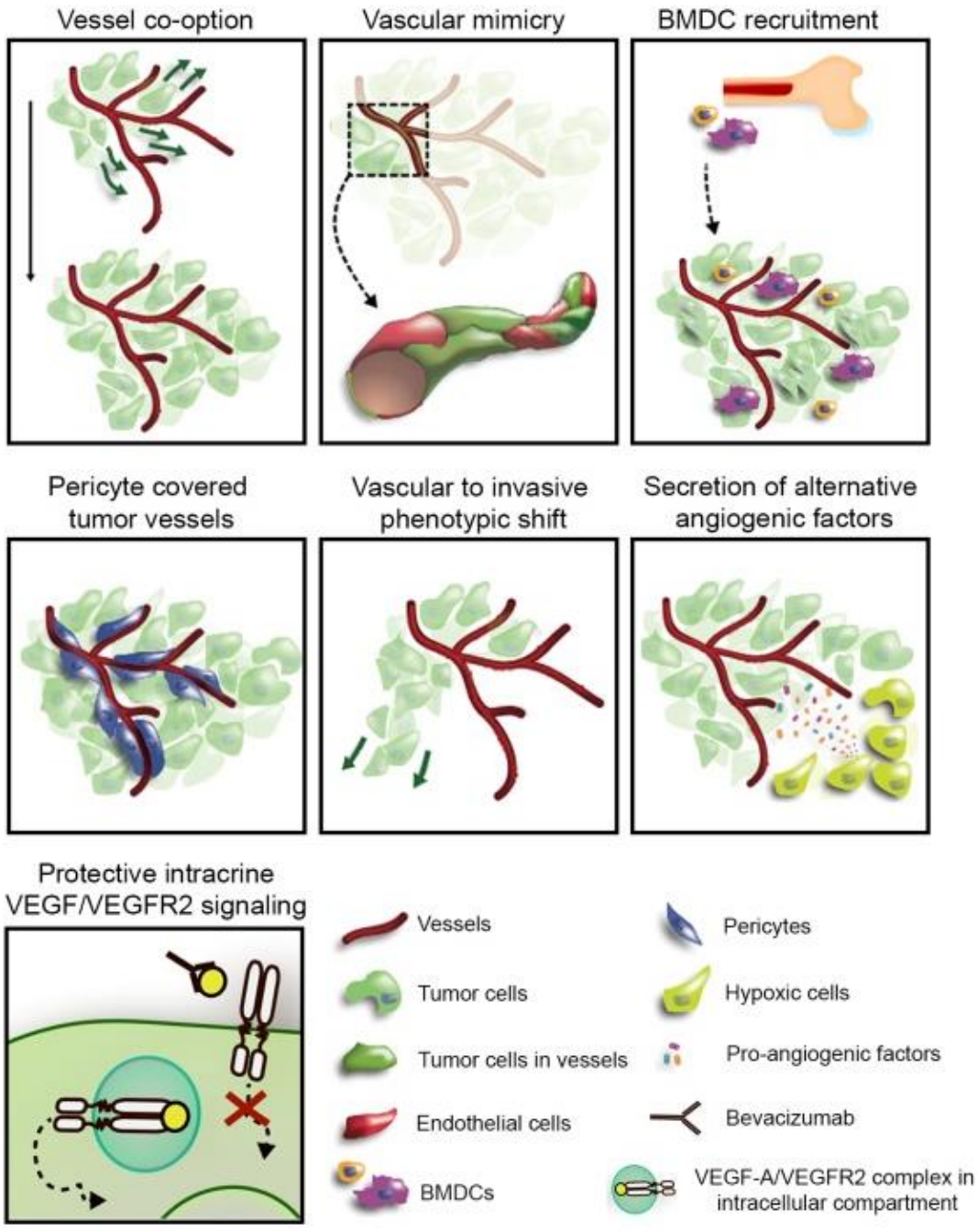

Figure 3. Modes of bevacizumab resistance. Proposed mechanisms cover alternative ways for establishment of tumor vessel network (by vessel co-option, vascular mimicry by tumor cells and vessel formation by recruited BMDC's), protection for VEGF-A targeting (by pericyte vessel covering and intracrine signaling), vascular independency (by shift towards invasive phenotype) and VEGF-A independent stimulation of angiogenesis (by secretion of alternative pro-angiogenic factors from hypoxic tumor cells). Modified from Lu-Emerson et al. [68].

1.6 Putative molecular targets in glioblastoma

The limited clinical efficacy of tested therapies directed toward VEGF-A signaling, emphasizes a need for identification of alternative strategies for targeting angiogenesis. The following section describes molecular targets examined in this thesis (VEGF-C and EGFR-Notch crosstalk); related to stimulation of angiogenesis, but also influencing other cancer hallmarks.

1.6.1 VEGF-C – processing and targets

VEGF-C is synthesized as a 419 aa precursor protein containing unique C- and N-terminal extensions flanking the VHD, and sharing sequence homology of 30% to VEGF-A (isoform 165) and 48% to VEGF-D [96, 97] (Figure 4). This precursor protein now undergoes a complex series of proteolytic processing, important for regulation of VEGF-C activity (Figure 4). Simplified, first the C-terminal is cleaved off inside the cell, followed by protein secretion and extracellular N-terminal processing [98]. While immature precursor forms of VEGF-C can bind VEGFR3, the processing increases its receptor affinity and activating abilities, giving VEGF-C the capability to also bind VEGFR2 [98], with same potency as VEGF-A [96]. VEGF-C also interacts with NRP-1 and NRP-2, but mainly in its partly processed immature form [99]. Functionally, participation of NRP-2 in the binding complex between VEGF-C and VEGFR2 and -R3, respectively, has been found to increase receptor sensitivity for ligand activation [100]. Further on, VEGF-C was demonstrated to co-internalize into the cell together with VEGFR3 and NRP-2 upon binding [99], indicating that signaling of mature VEGF-C occurs both extracellularly and intracellularly.

1.6.2 VEGF-C – function in normal and malignant cells

VEGF-C induces the proliferation and migration of endothelial cells [101]. During embryogenesis it is, via activation of VEGFR3, central for sprouting of lymphatic endothelial cells and thereby essential in formation of the lymphatic vessel-system [102]. In adults, it is also a main driver of physiological (e.g. upon wound healing) and pathological (e.g. under tumor development) induced lymphangiogenesis, but VEGF-C also possesses strong angiogenic potency via its ability to activate VEGFR2 and presumable also VEGFR3 [103, 104].

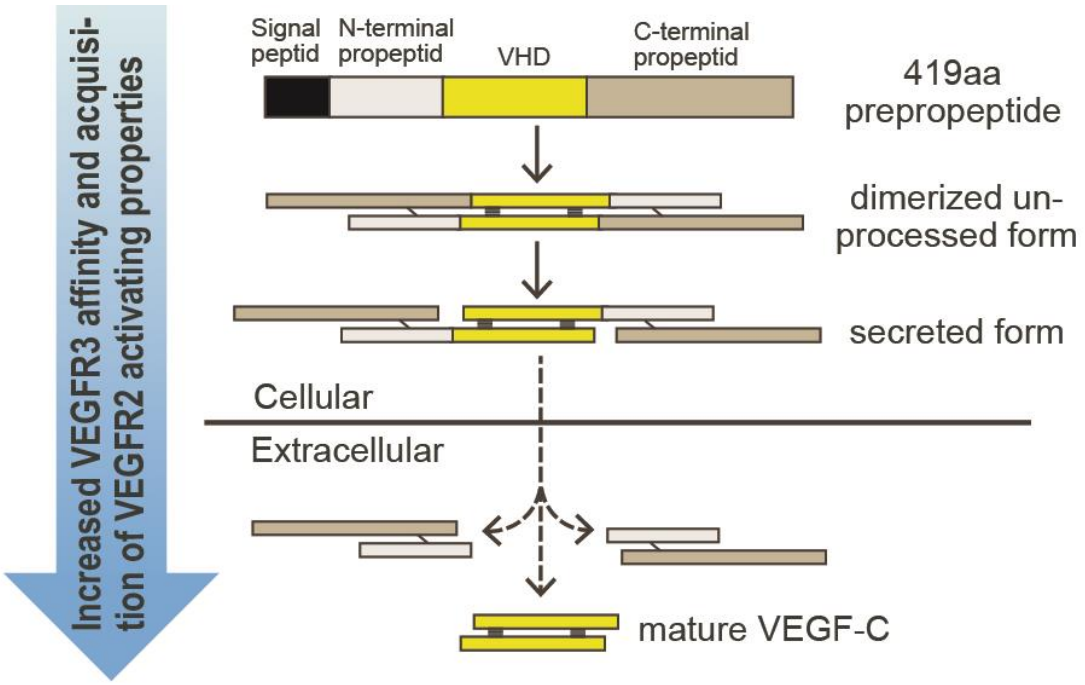

Figure 4. Processing of VEGF-C. VEGF-C is synthesized as a 419 aa prepropeptide, which dimerize after removal of a N-terminal signal peptide. Subsequently the C-terminal is cleaved off by enzymatic processing (by enzymes furin, PC5 and PC7), but remains attached by disulfide bridges. The protein is then secreted and undergoes further enzymatic processing extracellularly in a multi-step process driven by enzymes (ADAMTS3 in complex with CCB1 and/or plasmin) located either at the plasma membrane, at the extracellular matrix (ECM) or being soluble in the extracellular space. With each proteolytic cleavage affinity for VEGFR3 increases and the mature form acquire ability to activate VEGFR2 [98, 105-107].

Besides being expressed by endothelial cell, expression is found in non-endothelial cells such as various immune- and tumor cells [103]. The mechanisms behind VEGF-C upregulation are poorly understood, although VEGF-C overexpression has been linked to multiple transcription factors, growth factors and ECM components as well as with pro-inflammatory interleukin-mediated stimuli [108]. While there is a clear link between tumor hypoxia and stimulation of VEGF-A expression, this is not the case for VEGF-C. In contrast to VEGF-A, no putative HREs are found upstream of the VEGF-C gene. However, an internal ribosome entry site (IRES) with increased activity under hypoxia is located in the 5’ UTR of VEGF-C mRNA

[109]. Accordingly while hypoxia actually resulted in decreased VEGF-C transcription, VEGF-C protein translation was found to be increased during hypoxia in murine carcinoma models [110]. Whether this is also the case in glioblastoma is currently unknown. But our own examinations of glioblastoma cells (unpublished data) and published data from C6 rat glioma cells [111] only finding very little if any increase in VEGF-C mRNA following hypoxic growth, are not arguing against this.

Overexpression of VEGF-C has been described for a range of different cancers and is associated with adverse prognosis. There have been many reports directly linking increased VEGF-C tumor and serum levels with high lymphatic vessel density and through this promotion of metastasis to reginal lymph-nodes and distant organs [103]. Furthermore, VEGF-C has in preclinical studies of different cancer types, been shown to directly modulate tumor cell specific features important for cancer progression. This includes the stimulation of cell-proliferation, -migration and -invasion as well as maintenance of a cancer stem cell phenotype [108, 112]. Additionally, studies of VEGF-C knockdown in various cancer cells have associated decreased VEGF-C level with increased sensitivity to a number of different chemotherapeutic agents [113-115]. Results also points towards a role for VEGF-C in the interaction of tumor cells with infiltrative immune cells. Macrophages been shown to express VEGF-C, enabling these cells to stimulate tumor and endothelial cells and thereby cancer progression [108]. Moreover, VEGF-C has been associated with modulating an immune tolerating phenotype in cancer by direct immunosuppressive effects on various types of immune cells (including Natural killer (NK) cells, dendrite cells and T cells) [108]. A summary of the role for VEGF-C is shown in Figure 5.

1.6.3 VEGF-C in glioblastoma

In comparison to normal brain, where VEGF-C levels in general are low [96], upregulated VEGF-C expression is observed in glioblastoma patient tumors [116-119], with VEGF-C positivity in tumor cells, endothelial cells and infiltrating macrophages [117-119]. Examinations of a few conventional glioblastoma cell lines, have furthermore confirmed the expression of

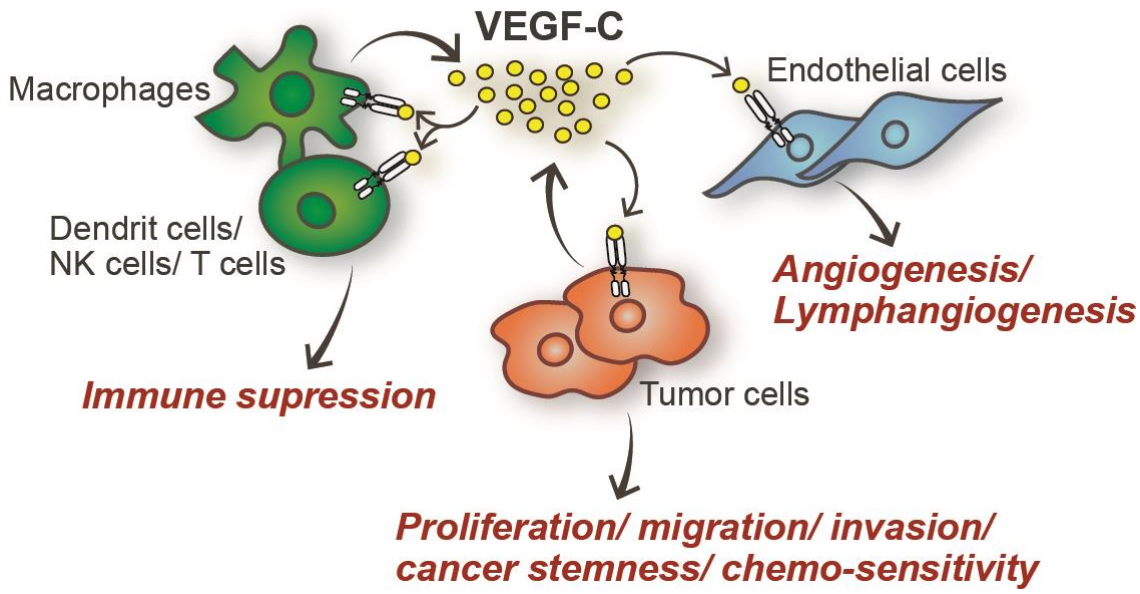

Figure 5. Expression and function of VEGF-C. While VEGF-C mainly is of importance for lymphangiogenesis in normal tissue, it exerts multiple functions in malignant tissue, by promoting lymphangiogenic/angiogenic mediated tumor spread; suppressing immune cancer directed reactivity as well as stimulating growth and treatment resistance directly in tumor cells. Illustration is based on information in Wang et al. [108].

VEGF-C in glioblastoma tumor cells [120, 121]. VEGF-C level has been found to be especially high in glioblastoma tumors and derived cultures with periventricular as compared to cortical brain location [122, 123]. Moreover, higher VEGF-C expression has been associated with a more angiogenic phenotype in glioblastoma tumors having high levels of a truncated variant of the glioma-associated oncogene homolog 1 (tGLI1) [116]. Same study also found higher VEGF-C mRNA expression to correlate with worse glioblastoma patient prognosis [116]. Another study comparing survival of VEGF-C-high and -low expressing glioblastoma patients, as evaluated by immunohistochemistry (IHC), did not show significance, although a trend towards shorter survival for VEGF-C high expressing patients was observed. However, this study found that concurrent high expression of both VEGF-C and NRP-2 led to significant poorer survival, also in multivariate testing together with selected clinical markers [121].

The functionality of VEGF-C in glioblastoma, including its putative effect on bevacizumab sensitivity, is only sparsely studied. Grau et al., showed increased VEGF-C mRNA expression in glioblastoma culture cells following bevacizumab therapy. This study also demonstrated exogenous VEGF-C to have minor stimulating effect on cell proliferation under bevacizumab treatment of both glioblastoma cells and human brain microvascular endothelial cells (HBMVECs) [120]. In C6 rat glioma cells, stimulation with VEGF-C was likewise shown to increase cell proliferation as well as activity in transwell-migration assay [124]. Beside this, *in vitro* angiogenesis assay investigations have confirmed stimulation of HBMVECs by glioblastoma tumor cell derived VEGF-C [116, 120].

1.6.4 Notch signaling, its role in glioblastoma and approaches for targeting

In mammals four Notch receptors exist (Notch-1, -2, -3 and -4), which are transmembrane molecules expressed at the cell surface as non-covalently linked heterodimers. The receptors are activated via binding to its ligands (Delta-like (Dll) -1, -3, -4 and Jagged 1-2), also transmembrane proteins but located on the neighboring cell. This binding leads to a conformational change in the receptor, exposing two proteolytic sites. These sites are in turn cleaved by a disintegrin and metalloprotease (ADAM), proteases ADAM10 and -17 and a γ-secretase complex, respectively, ultimately releasing the Notch intracellular domain (NICD) into the cytoplasm. NICD translocate to the nucleus where it forms a transcriptional activation complex with the DNA binding protein CSL (CBF1, Suppressor of Hairless, Lag-1) thereby stimulating gene transcription [125, 126]. Multiple targets are transcriptionally stimulated by Notch signaling, of which some of the best characterized belong to the Hairy/Enhancer of Split (Hes 1-7) and Hey (Hey 1-2, L) families of basic helix-loop-helix transcriptional repressors [126]. Figure 6 illustrates signaling via Notch.

Notch signaling play an important role in maintenance of neural progenitor cells in an undifferentiated state, but can also promote glial differentiation and accordingly correct Notch signaling is critical for brain development during embryogenesis [126-128]. In the adult brain, expression of Notch molecules is strongly reduced. However in adult gliomas, including glioblastomas, overexpression of Notch and its ligands is commonly observed [129-133]. High

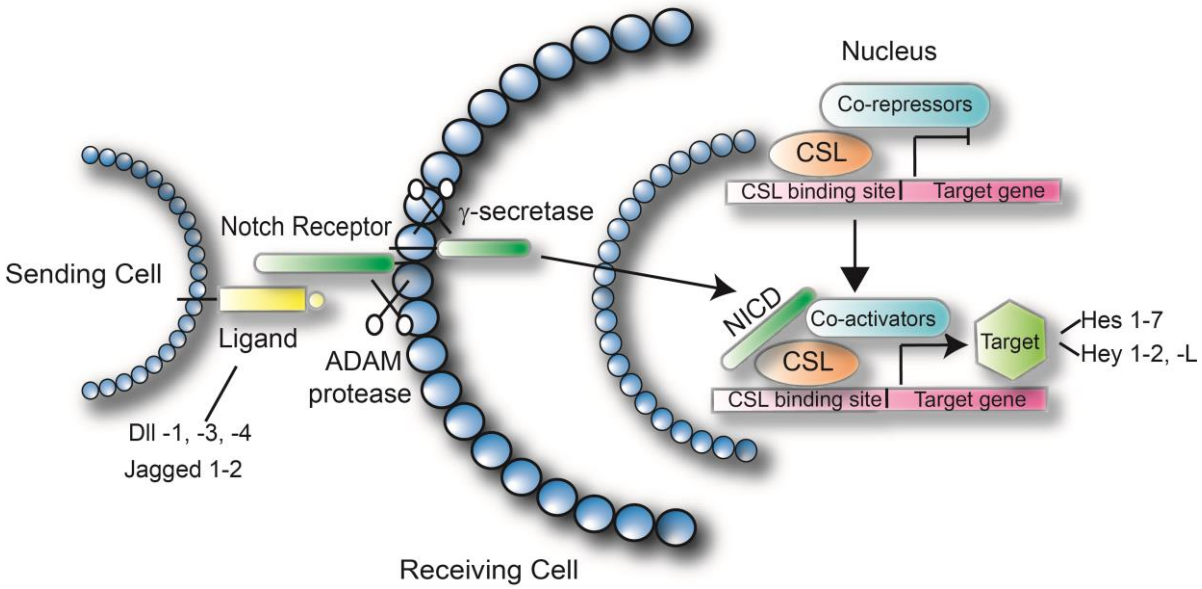

Figure 6. Activation of Notch signaling. In the absence of Notch signaling, CSL is bound to co-repressors at the promoter of target genes, thereby inhibiting gene transcription. Binding between Notch and its ligands allow for proteolytic processing of Notch releasing the NICD, which traverses to the nucleus. Here it interacts with CSL, resulting in exchange of the co-repressors with co-activators for interacting molecules for CSL, thereby initiating transcription of target genes. Modified from Stockhausen et al. [126].

expression of Notch downstream targets Hey-1, Hes-1 and Hes-4 as well as ligands Dll-4 and Jagged-1 have been associated with inferior survival of glioblastoma patients [133-136].

Functional studies in glioblastoma have found Notch signaling to be important for maintaining the tumor cells in an undifferentiated fast proliferating state. Concordantly, overexpression of NICD results in decreased expression of differentiation markers for astrocytes (glial fibrillary acidic protein, GFAP), oligodendrocytes (CNPase) and neurons (βIII-tubulin) [38], while inhibited Notch signaling has been shown to upregulate GFAP expression [131] and deplete expression of stem cell markers such as CD133, Nestin and Sox2 [137-139]. Further on, expression of Notch-1 and -3 were shown to be increased in GSCs subpopulation in glioblastoma tumors [139, 140]. In line with this, as compared to monolayer serum cultured cells, increased expression of Notch 1-4 was found in cells grown under stem cell conditions

and specifically upregulated in these cells under hypoxic growth [134], a condition known to increase expression of various stem cell markers in glioblastoma [141].

Besides being an important stimulator of viability, clonal capacity and cell cycle progression of glioblastoma cells [38, 130, 133, 137, 142] members of the Notch signaling pathway play pivotal functions in regulation of angiogenesis. This includes opposing roles of Dll-4 and Jagged-1 in vascular tip *versus* stalk fate decision of endothelial cells under initiation of angiogenesis sprouting [143]. Along with this, inhibition of the Notch pathway led to dysregulated VEGFR signaling and vessel formation in glioblastoma [144] and overexpression of either Dll-4 or Jagged-1 were associated with presence of specific microvascular patterns in glioblastoma tumors [135]. Further on, a tight link between Notch signaling and angiogenesis is indicated by studies finding a positive correlation between expression of several Notch signaling cascade members and HIF1α and VEGF-A, respectively, in glioblastoma tumors [134, 135].

For clinical targeting of Notch signaling, several strategies are under development. These include blocking antibodies directed against specific Notch- or Dll-variants as well as soluble ligand- or receptor decoys. However, the by far most studied approach is the abrogation of Notch downstream signaling by γ-secretase inhibitors (GSIs) [127]. While these GSIs have the advantages of targeting signaling from all Notch receptors, they are not specific for Notch inhibition, as γ-secretase also has a range of other targets [145]. Further on, systemic delivery of GSIs can lead to gastrointestinal toxicity, related to accumulation of goblet cells in the intestine as a result of increased differentiation of stem cells located in this tissue [146]. The potential of GSIs for glioblastoma targeting, has been shown by preclinical studies finding GSI therapy to decrease glioblastoma xenograft growth substantially and sensitize glioblastoma cells for radiation- and chemotherapy [138, 147-149]. Recently published early clinical testing of the GSI RO4929097 in glioblastoma patients in combination with radiation- plus temozolomide therapy or bevacizumab therapy, respectively, further showed that the treatment was well tolerated. However, the survival data, although inconclusive, indicated that effect of the treatment was minimal [150, 151].

1.6.5 Signaling and targeting of EGFR and mutation EGFRvIII in glioblastoma

The epidermal growth factor receptor (EGFR) is a RTK of the ErbB/HER receptor family. Ligands are several, including EGF and TGF-α, and ligand binding results in receptor homodimerization with another EGFR monomer or heterodimerization with other ErbB family members. This promotes autophosphorylation of the cytoplasmatic domain, initiating intracellular downstream signaling pathways, including PI3K-Akt, RAS-MAPK, PLCγ-PKC and JAK-STATs [152, 153]. EGFR is overexpressed in over 50% of glioblastomas [154, 155] compared to normal adult brain tissue, where EGFR expression is low and restricted to areas of neurogenesis in the subventricular zone [156]. Overexpression is most often a result of gene amplification with expanding number of genomic copies, but can also be caused by increased EGFR promoter activity or deregulation at the translational or post-translational level [153]. Alternatively mutations in the extracellular domain, given rise to constitutive activated truncated receptors are frequently seen in glioblastoma. Most common is the variant EGFRvIII, resulting from an *in-frame* deletion of exon 2-7 of the EGFR gene, leading to a receptor lacking most of the ligand binding area [153]. Despite being unable to bind ligands, EGFRvIII exhibits constitutive low activation, given rise to constitutive downstream signaling [157, 158]. EGFRvIII further escapes receptor degradation via a lowered internalization rate combined with recycling to the membrane rather than to lysosomes, thereby avoiding the control mechanism normally terminating receptor signaling [159]. Moreover, the EGFRvIII mutation modifies the downstream signaling pattern of the receptor [158], presumably related to the generation of a new amino acid at the fusion junction causing a tumor specific epitope [160]. While EGFR amplification is often seen alone, EGFRvIII almost exclusively is observed in tumors also harboring EGFR amplification with around 40 % of EGFR amplified gliomas harboring EGFRvIII [155]. Figure 7 shows signaling via EGFR.

Functionally, EGFR signaling adds to the aggressive growth in glioblastoma via stimulation of cell proliferation and survival pathways [161]. Additionally highlighting EGFR as an attractive target in glioblastoma is involvement of EGFR signaling in maintenance of the GSC subpopulation [162-164]. Moreover, EGFR signaling stimulates angiogenesis. Besides, that EGF and TGF-α directly can stimulate endothelial cells and thereby trigger angiogenesis [165], EGFR

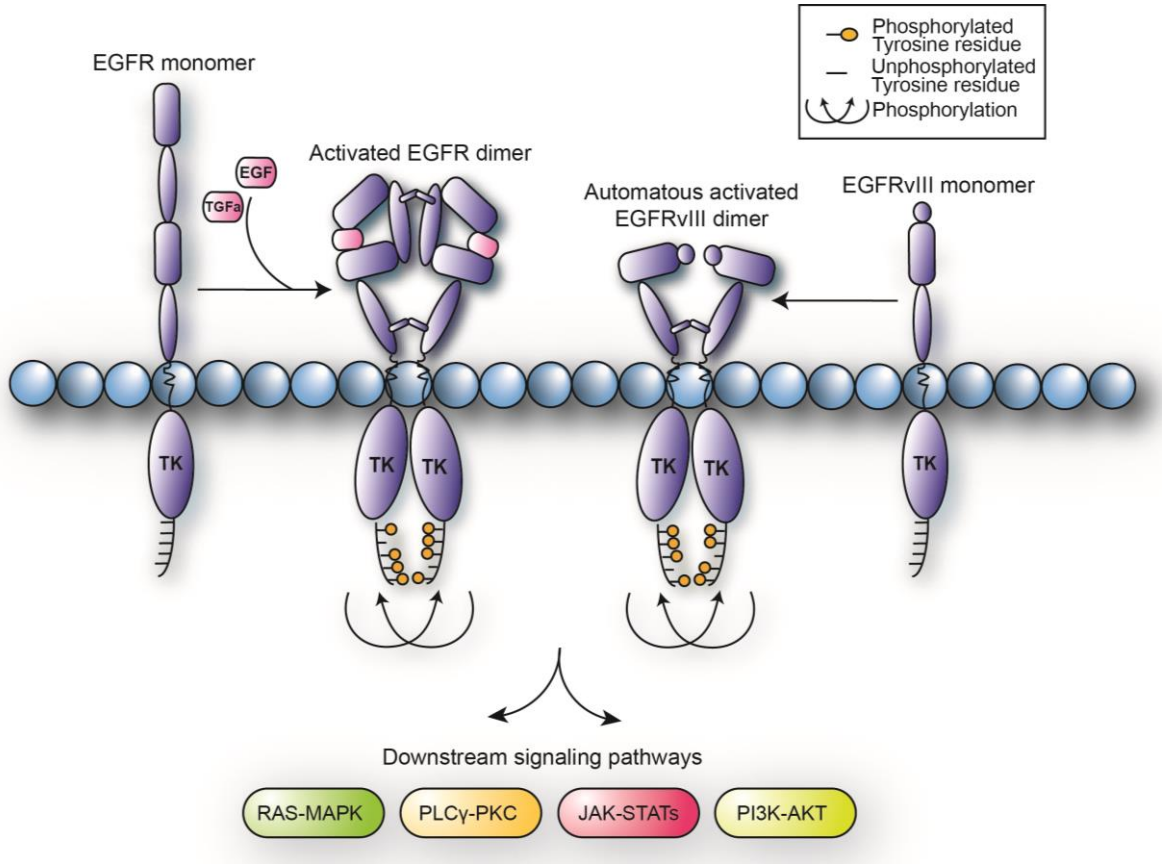

Figure 7. EGFR signaling. While the wildtype EGFR need ligand binding to dimerize and undergo autophosphorylation, the EGFRvIII mutated receptor missing large parts of the extracellular domain is constitutively activated. Receptor activation stimulates downstream signaling pathways promoting cancer cell proliferation, invasion and survival, besides playing a role in promotion of angiogenesis and maintenance of the GSC subpopulation. Amplification and mutation in EGFR is an important event in initiation and progression of glioblastoma [153, 166-168].

signaling in glioblastoma cells promotes VEGF-A expression, via both direct stimulation of its transcription and indirect via stimulation of HIF1α expression [169, 170]. Finally, EGFR signaling has, in studies of glioblastoma, been shown to induce upregulation of ECM modulating molecules such as matrix metalloproteases, important for both invasion and angiogenesis [168].

The most advanced and best studied targeting strategies for EGFR are TKIs, preventing auto-phosphorylation of the cytoplasmatic tyrosin kinase domain, of which Iressa (gefitinib) is an example [161]. Other strategies include monoclonal antibodies targeting the extracellular domain, including cetuximab, which competes for the ligand binding site, hindering EGFR dimerization and reducing receptor expression on cell surface [171, 172]. However, common for all EGFR targeting strategies is, that despite promising pre-clinical data, they have not been successful in clinical trials in glioblastoma patients [161, 173]. This lack of effect has been linked to inadequate drug delivery presumably related to problems with BBB penetration [161] and heterogeneity within the tumors presenting both positive (EGFR signaling dependent) and negative (EGFR signaling independent) cell clones [154]. Also, the EGFRvIII add to the resistant phenotype, as it was shown for Iressa, where EGFRvIII positive cells did not respond at doses efficiently inhibiting signaling of wildtype EGFR cells [174]. A recent study also showed ability of EGFRvIII positive tumor cells to protect EGFR wildtype cells from targeted therapy via a mechanism involving secretion of interleukin-6 from the EGFRvIII positive cells, promoting anti-apoptotic signaling in the wildtype cells [175]. Mechanisms behind decreased sensitivity towards EGFR inhibiting drugs moreover include activation of redundant signaling pathways of which multiple have been described [166]. Also, receptor relocation to intracellular compartments can give rise to resistance by protecting the receptors from drugs aimed for targeting at the membrane and by enabling new kinase independent functions, such as direct effects on transcriptional regulation [166].

1.6.6 Cross-talk of Notch and EGFR signaling – rationale for concurrent targeting

Several lines of evidence indicate synergy between the EGFR and Notch pathways in glioblastoma suggesting a rationale for increased therapeutic efficacy for dual targeting of both pathways (Summarized in Figure 8). At the level of expression, Purrow et al. demonstrated in glioblastoma cells, EGFR to be under transcriptional control of Notch-1 signaling via a p53 dependent mechanism [176]. On the contrary, the EGFR downstream signaling mediator Akt was found to sustain Notch-1 expression in a mouse glioma model [177]. Ability of the EGFR pathway to induce Notch levels was likewise supported by results

demonstrating increased Notch-1 level in Ras (also a EGFR downstream mediator) - transformed human astrocytes as compared to their untransformed counterparts [131]. This study further indicated direct interplay between the pathways, as inhibition of notch signaling reduced the aggressive phenotype of the transformed cells. In line with this, several studies in glioblastoma cells have demonstrated Notch-1 activation being capable of inducing Akt phosphorylation, and conversely Notch inhibition to decrease Akt activity [142, 178]. Further on, treatment of glioma cells with the TGF-α, an EGFR ligand whose expression is also stimulated by EGFR signaling, resulted in upregulation of the Notch pathway member Hes-1 [179]. Likewise EGFR was indirectly demonstrated to stimulate Hes-1 expression via inhibition of a Hes1 targeting micro RNA [180]. Underlining the potential of combined EGFR and Notch inhibition in glioblastoma, are results from other cancer types finding increased growth inhibitory effect of the combination compared to single pathway inhibition [181, 182].

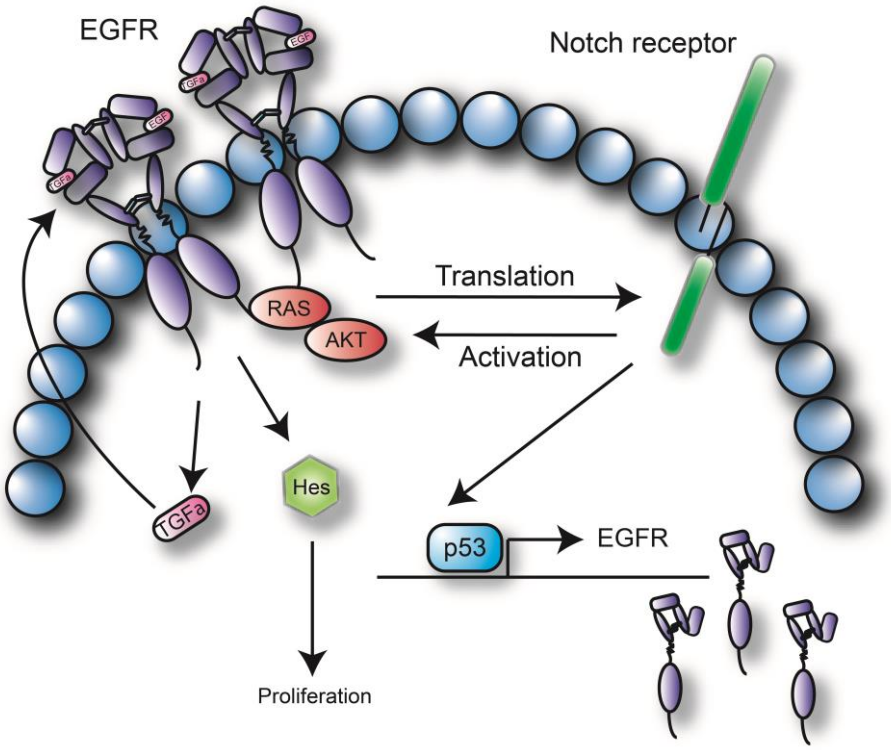

Figure 8. Cross-talk between EGFR and Notch signaling. EGFR and Notch receptors influence activity of each other by both stimulating increased protein levels as well as being able to activate down-stream mediators of the other pathway. Reprint from Stockhausen et al. [183].

2. Objectives and aims

Overall objective of this thesis is to examine biomarkers related to angiogenesis or efficacy of anti-angiogenic therapy for potential in therapeutic optimization for treatment of glioblastoma patients.

Aims of the three included studies were:

I) Evaluate VEGF-C as therapeutic target by examine its role for glioblastoma autocrine VEGFR2 signaling, bevacizumab efficacy and glioblastoma cell phenotype.

II) Test potential of combined Notch and EGFR targeting as therapeutic approach for inhibition of glioblastoma cell maintenance and angiogenesis stimulation.

III) Identifying biomarkers for identification of survival outliers of glioblastoma patients treated with radiation-, chemo- and bevacizumab therapy.

3.1 Results - Study I

VEGF-C sustains VEGFR-2 activation under bevacizumab therapy and promotes cellular maintenance in glioblastoma

By

Signe R. Michaelsen, Mikkel Staberg, Mette K. Nedergaard, Wiktor Majewski, Helle Broholm, Christopher Meulengracht, Thomas Urup, Mette Villingshøj, Slávka Lukacova, Andreas Kjær, Ulrik Lassen, Marie-Thérése Stockhausen, Hans S. Poulsen and Petra Hamerlik

Submitted, 2017

Summary study I:

This study examined the role of VEGF-C as an alternative activator of VEGFR2 as well as an oncogenic driver in glioblastoma. Examinations of VEGFR2/ VEGF-A/VEGF-C positive GSC cultures found a growth inhibiting effect of VEGFR2 targeting, while cells were nearly unaffected by bevacizumab therapy. Interaction between VEGF-C and VEGFR2 were demonstrated in GSCs via an antibody directed visualization technique (proximity ligation assay) and increased levels of activated VEGFR2 as well as secretion of VEGF-C were found under bevacizumab therapy of the cells. This implied ability of VEGF-C to maintain VEGFR2 signaling under bevacizumab therapy via involvement in autocrine activation of the receptor. Results were further supported by IHC and proximity ligation assay staining demonstrating VEGF-C expression and VEGF-C/VEGFR2 interaction in glioblastoma patient tumor samples from surgery before and after bevacizumab treatment. Although, these analyses demonstrated a heterogeneous expression pattern for VEGF-C with both positive and negative tumor cells, VEGF-C positivity were also found in endothelial and immune cells, indicating abundant VEGF-C levels in glioblastoma tumors. Treatment of cells with VEGF-C protein were found to promote activation of pro-survival signaling and contrary expression analysis conducted following siRNA mediated VEGF-C knockdown in glioblastoma cells downregulated genes important for cellular growth. In line with this, VEGF-C knockdown reduced cell viability, increased apoptotic signaling and abrogated cell cycle progression. Moreover, invasive capacity of glioblastoma cells was found to be reduced following VEGF-C knockdown. Finally, findings of central influence of VEGF-C for cell maintenance translated into reduced tumor growth and prolonged survival of VEGF-C knockdown *versus* control tumor cells upon orthotopic transplantation into brain of mice. Overall, this preclinical study highlight VEGF-C as a driver of VEGFR2 signaling as well as bevacizumab resistance and suggest VEGF-C directed therapy as a mean to target glioblastoma tumor cells. However, data also points to that VEGF-C targeting may only be relevant in selective cell clones of glioblastoma tumors, suggesting the possibility of VEGF-C targeting therapy to be most effect in combination with other treatments.

VEGF-C sustains VEGFR-2 activation under bevacizumab therapy and promotes cellular maintenance in glioblastoma

Signe R. Michaelsen[1,2], Mikkel Staberg[1,2], Mette K. Nedergaard[3], Wiktor Majewski[4], Helle Broholm[5], Christopher Meulengracht[2], Thomas Urup[1], Mette Villingshøj[1], Slávka Lukacova[6], Andreas Kjær[3], Ulrik Lassen[7], Marie-Thérése Stockhausen[1], Hans S. Poulsen[1,7,*] and Petra Hamerlik[1,2,*]

[1]*Department of Radiation Biology, The Finsen Center, Copenhagen University Hospital, Copenhagen, Denmark.*

[2]*Brain Tumor Biology, Danish Cancer Society Research Center, Copenhagen, Denmark*

[3]*Department of Clinical Physiology, Nuclear Medicine & PET and Cluster for Molecular Imaging, Copenhagen University Hospital & University of Copenhagen, Copenhagen, Denmark.*

[4]*Center for Genomic Medicine, Copenhagen University Hospital, Copenhagen, Denmark.*

[5]*Department of Neuropathology, Center of Diagnostic Investigation, Copenhagen University Hospital, Copenhagen, Denmark.*

[6]*Department of Oncology, Aarhus University Hospital, Aarhus, Denmark*

[7]*Department of Oncology, The Finsen Center, Copenhagen University Hospital, Copenhagen, Denmark.*

[*]**Correspondence:**

Petra Hamerlik, email: pkn@cancer.dk

Hans S. Poulsen, email: hans.skovgaard.poulsen@regionh.dk

RUNNING TITLE

VEGF-C promotes glioblastoma resistance to bevacizumab

KEYWORDS

Glioblastoma, VEGF-C, bevacizumab, survival, resistance

ABSTRACT

Glioblastoma (GBM) ranks among the most lethal cancers with current therapies offering only palliation. GBM tumors are highly angiogenic and additionally direct tumor promoting effects have been demonstrated for pro-angiogenic receptor for vascular endothelial growth factor (VEGF) –A. Yet, clinical trials with anti-angiogenic agent bevacizumab targeting VEGF-A have shown only modest efficacy, suggesting potential utility in targeting resistance mechanisms to these agents. Here, we demonstrate that VEGF ligand family member, VEGF-C, is expressed by patient-derived xenograft lines and GBM tumors prior and after VEGF-A sequestration by bevacizumab. VEGF-C activates VEGFR2 tyrosine kinase in GBM tumor cells in an autocrine manner, thereby stimulating cell survival pathways. Targeting VEGF-C expression reprograms cellular transcription to block survival, invasion, cell cycle progression and induce apoptosis. Most importantly, targeting VEGF-C impairs tumor growth *in vivo*. Collectively, our results support VEGF-C as a potential resistance mechanism to bevacizumab therapy, permitting sustained VEGFR2 activation, tumor growth and invasion, suggesting that targeting multiple VEGF ligands may improve tumor management in GBM patients.

INTRODUCTION

Glioblastoma (GBM, World Health Organization grade IV astrocytoma) ranks among the most lethal primary central nervous system (CNS) tumors in adults with median survival rates of less than 15 months, despite maximal therapy.[1, 2] Robust vascularization, often associated with the overexpression of vascular endothelial growth factor A (VEGF-A), is a hallmark of GBM.[3] The tyrosine kinase VEGF receptor 2 (VEGFR2) is a primary effector of VEGF-A signaling, expressed by both endothelial and tumor cells to stimulate paracrine and autocrine effects of VEGF signaling. VEGF-A/VEGFR2 signaling has been associated with a number of functions in GBM cells, including cell proliferation, invasion as well as self-renewal of GBM stem-like cells (GSCs),[4, 5, 6, 7, 8] leading to the development of targeted therapeutics against VEGF-A/ VEGFR2.[9, 10] Despite initial enthusiasm from preclinical and clinical studies, targeting VEGF-A using a humanized anti-VEGF antibody bevacizumab (Avastin) failed to show improvement in overall survival for GBM patients.[9] GBMs evade bevacizumab through multiple mechanisms, revealing the complexity of

molecules associated with pro-angiogenic signaling [11]. These evasive responses, together with the lack of any inhibitory effect of bevacizumab on VEGF-A/VEGFR2 expressing GBM cells,[4, 8, 12] suggest alternative ligand-mediated activation of VEGFR2 upon bevacizumab treatment.

The VEGF ligand family comprises other ligands, including VEGF-C and VEGF-D, for which overexpression have been associated with disease progression in various solid tumors;[13, 14, 15, 16] though their roles in GBM remain to be elucidated. VEGF-C, a main driver of lymphatic vessel formation, serves critical roles during embryogenesis,[17] tumorigenesis and metastasis.[18] It is produced as an immature protein undergoing extensive proteolytic processing to form mature VEGF-C.[19, 20, 21] Mature VEGF-C binds VEGFR3 and VEGFR2, which are primarily located on lymphatic and vascular endothelial cells, respectively.[19] Additionally VEGF-C and its receptors are expressed on tumor cells, including leukemic, skin and gastric cells; facilitating tumor progression in an autocrine manner. [22, 23, 24] In GBM, VEGF-C is expressed by endothelial cells, tumor cells, and infiltrating macrophages.[25, 26, 27, 28] In contrast to VEGF-D, VEGF-C is overexpressed in GBM compared to non-neoplastic brain tissue.[25, 26, 27, 29] Moreover, high VEGF-C levels have been documented to inform poor prognosis for GBM patients.[27, 28, 29] Most previous studies focused either on this prognostic significance of VEGF-C or its role in endothelial stimulation,[29, 30] why functional studies interrogating the role of VEGF-C signaling in GBM tumor cells are still missing.
In the present study, we investigated the role of autocrine VEGF-C/VEGFR2 signaling in GBM. Our results demonstrate that VEGF-C expressed by GBM cells mediates their survival, cell cycle progression and invasion, promotes tumorigenicity and contributing at least in part to bevacizumab resistance.

RESULTS

VEGFR2 activation is driven by VEGF-C in bevacizumab treated cells

We previously demonstrated that GBM tumor cells can express VEGFR2, which stimulates tumor growth[4]. To evaluate VEGFR2 expression in our collection of primary GBM models, we performed qRT-PCR and western blot (WB) analysis, using human microvascular endothelial cells (HMVECs)

as a positive control. *VEGFR2* expression pattern was heterogeneous, ranging from negative (CPH036; CPH047; CPH048) to moderate (IN326; IN1123) and high positivity (CPH017; 1966). *VEGFR2* levels in the high-expressing GBM cultures were comparable to that of HMVECs (**Figures 1a and b**). qRT-PCR analysis further confirmed *VEGF-A* positivity in all tested cultures as compared to HMVEC cells (**Figure 1b**). We selected representative VEGFR2-high (CPH017) and VEGFR2-moderate (IN1123) GBM cells to interrogate the functionality of autocrine VEGF-A/VEGFR2 signaling and exposed these to VEGFR2-specific receptor tyrosine kinase inhibitor SU1498 and/or exogenous ligand (40 ng/ml of human recombinant VEGF-A_{165}). While both CPH017 and IN1123 cells showed significant sensitivity to 10 µM SU1498 (**Figure 1c**), this concentration had no effect on VEGFR2-negative CPH036 cells (**Supplementary Figure S1**). Pre-treatment of CPH017 cells with SU1498 decreased VEGFR2 activated phosphorylation upon stimulation with recombinant VEGF-A (**Figures 1d and e**); further confirming specific effect of SU1498 and functionality of VEGFR2 in the GBM cells. Although bevacizumab (0.5 mg/ml) treatment of GBM cells sequestered secreted VEGF-A as assessed by ELISA, no significant impairment of GBM cell viability was observed (**Figures 1f and g**). WB analysis of cells indicated increased activated phosphorylation of VEGFR2 as well as total VEGFR2 levels after bevacizumab treatment (**Figure 1h**), an observation confirmed by confocal microscopy and quantification of mean phospho-VEGFR2 fluorescence intensity per cell (**Figures 1i and j**). Collectively, these data demonstrate that tumor cell VEGFR2 remains activated in the absence of VEGF-A, suggesting that other VEGF ligands may be stimulating VEGFR2 in the absence of VEGF-A to promote resistance to bevacizumab.

To determine the potential role of alternative VEGF ligands, we interrogated our patient-derived models for VEGF-C expression, given its increased expression in GBM. As shown in **Figure 2a**, five out of 7 GBM cultures tested expressed *VEGF-C* at levels comparable to control Human Dermal Lymphatic Endothelial Cells (HDLECs), previously demonstrated to express both *VEGF-C* and *VEGFR3.*[31] While *VEGF-C* positivity in most cultures correlated with *VEGFR2* positivity, *VEGFR3* expression was detected only in 2 cell cultures at very low levels (**Figure 2a**). When treated with bevacizumab (0.5 mg/mL), GBM cells presented significantly increased (CPH017) or had a trend

for increased (IN1123) VEGF-C secretion (**Figure 2b**), supporting the notion that VEGF-C drives VEGFR2 activation in the absence of VEGF-A.

VEGF-C interacts with VEGFR2 *in vitro* and *ex vivo*

To verify that VEGF-C binds VEGFR2, we performed proximity ligation assay (PLA). This assay confirmed VEGF-C – VEGFR2 protein interaction in GBM cells, as shown by quantification of PLA spots and confocal microscopy (**Figures 2c and d**). To rule out effects of culture, we interrogated VEGF-C expression and interaction with VEGFR2 in formalin fixed paraffin-embedded (FFPE) GBM specimens collected prior and post bevacizumab treatment. The cohort (patient and treatment characteristics are shown in **Supplementary Table S1**) consisted of 12 pairs of parallel tumor samples from surgery *before* treatment with combined bevacizumab and CPT-11 chemotherapy (Pre-Bev samples) and *after* treatment relapse (Post-Bev samples), with an average of 64.2 days after treatment termination until tissue collection (range: 23-236 days). Immunohistochemistry (IHC) staining showed a heterogeneous granular expression pattern for VEGF-C in tumor cells, endothelial cells of both neoplastic and non-neoplastic vessels, tumor infiltrating microglia and macrophages and in some areas also in cortical neurons (**Figure 2e and Supplementary Fig. S2**). Although heterogeneous, no systematic changes associated with bevacizumab treatment was found in VEGF-C expression pattern upon pair-wise comparisons of samples taken *before* and *after* bevacizumab therapy. Of the 12 patients, five presented slightly increased levels, five comparable levels and two slight decreased levels in Post-BEV *vs.* Pre-BEV samples. Importantly, PLA assay performed on FFPE specimens from 6 selected patients of our cohort confirmed interaction between VEGF-C and VEGFR2 both *before* and *after* bevacizumab therapy (**Figure 2f and Supplementary Fig. S3**). Staining for VEGF-C - VEGFR2 interaction supported these results. These data indicate that VEGF-CVEGFR2 signaling will persist, despite bevacizumab therapy.

VEGF-C signaling regulates genes critical for survival, cell cycle and immunomodulatory functions in glioblastoma

Our previous studies demonstrated that VEGF-A-mediated activation of VEGR2 leads to activation of Akt/Erk/PLC signaling in GBM cells.[32] Therefore, we measured activation of these signaling pathways in response to exogenous VEGF-C. As shown in **Figure 3a**, VEGF-C treatment

(0.2 µg/mL) induced activation of VEGFR2 and its downstream signaling kinases, PLC and ERK1/2, in GBM cells. In contrast, AKT activation was largely unaffected. To better delineate autocrine signaling and identify the biological role of VEGF-C in GBM cells, we performed gene expression profiling. First, we validated siRNA -mediated knockdown of VEGF-C using a non-targeting control siRNA (siCtrl) or two independent siRNAs against VEGF-C (siVEGF-C-1; siVEGF-C-2) in GBM cells by qRT-PCR and WB (**Figure 3b and c**). Of note, siVEGF-C did not decrease VEGF-A expression. Rather, VEGF-C knockdown resulted in increased VEGF-A secretion as assessed by qRT-PCR and ELISA (**Figure 3d and e**). The effect of VEGF-C knockdown on gene expression changes was analyzed by Affymetrix GeneChip® Human Gene 2.0 ST arrays. A total of 222 genes with absolute log2 fold change in expression above 2 (log2fc ≥ 2) were found to be significantly ($P \leq 0.05$) altered (98 genes were down-regulated and 124 genes up-regulated) (**Figure 4a; Supplementary Table S2 and S3**). A gene set enrichment analysis (GSEA, REACTOME pathway dataset) showed significant down-regulation of pathways regulating the cell cycle, DNA replication and mitosis (**Figure 4b and Supplementary Fig. S4**). This was concordant with cyclin-family member-, cell-division cycle (*CDC*)- and histones - coding genes scoring among the top down-regulated candidates (**Supplementary Table S2).** The interferon/cytokine signaling associated with immunomodulatory responses were among the top up-regulated GSEA pathways following VEGF-C knockdown (**Figure 4b and Supplementary Fig. S5**).

VEGF-C positively regulates survival, cell cycle progression and invasion of glioblastoma cells

To examine the biological impact of VEGF-C in GBM cells, we transfected GBM cells with either siCtrl or the two independent siRNAs targeting VEGF-C. Targeting VEGF-C expression reduced cell viability, as measured by MTT assay (**Figure 4c**) and induced apoptosis, as evaluated by WB analysis of cleaved caspase-3 (**Figure 4d**). In addition, we observed increased protein levels of *STAT1* and *IRF1*, mediators of interferon signaling with anti-proliferative effects in cancer, following VEGF-C knockdown (**Supplementary Fig. S6**).[33, 34] The adaptive responses of GBM cells to bevacizumab treatment (increased VEGF-C) and VEGF-C knockdown (increased VEGF-A) prompted us to evaluate the combinatory effect of VEGF-C knockdown and bevacizumab (0.5 mg/mL) treatment. Indeed, the combination of bevacizumab treatment with VEGF-C knockdown

reduced viability by another 10 % when compared to VEGF-C knockdown alone, indicating combinational anti-proliferative effect of simultaneous VEGF-C/VEGF-A inhibition (**Figure 4e**).

To examine the effects of VEGF-C knockdown on cell cycle progression, we performed a flow cytometry-based cell cycle analysis, including incorporation of EdU (DNA intercalating agent marking S phase cells) and staining for phosphorylated H3 Ser10 (marking mitotic cells). VEGF-C knockdown induced the apoptotic sub-G1 phase population (from 2.4% for siCtrl to 4.8 and 4.3% for siVEGF-C-1 and siVEGF-C-2, respectively) (**Figure 5a and b**). The proliferative index (= percentage of EdU-positive cells) decreased from 15% (siCtrl cells) to 1 (siVEGF-C-1) and 3% (siVEGF-C-2) cells, respectively. Furthermore, we observed a marked accumulation of cells at G2/M cell cycle phase following VEGF-C knockdown (**Figure 5b**). Mitotic index (= percentage of mitotic cells positive for phosphorylated H3 Ser10) was decreased from 1.45% (siCtrl) to 0.39 and 0.36% for siVEGF-C-1 and siVEGF-C-2, respectively (**Figure 5c**). As GSEA showed downregulation of genes involved in mitosis/chromosome segregation, we investigated whether cells transfected with siRNA-targeting VEGF-C entered mitosis. Cells were treated with nocodazole, an inhibitor of microtubule polymerization, which arrests cells at metaphase. **Figure 5c** shows that, unlike siCtrl cells, cells with VEGF-C knockdown did not enrich at G2/M after nocodazole treatment, demonstrating that these cells do not enter mitosis and cell death occurs either at the entry to S-phase or at G2-phase prior entering mitosis. Corresponding to cell cycle arrest, WB analysis confirmed reduced RB hyperphosphorylation and cyclin E2 levels, supporting impaired G1-S phase transition in siVEGF-C-1/siVEGF-C-2 cells compared to siCtrl cells. Similarly, cells lacking VEGF-C showed reduced cyclin B1 & A2, an indication of impeded G2-M transition (**Figure 5d**). As bevacizumab treatment has been associated with increased invasion,[7, 35] we hypothesized that VEGF-C could stimulate invasion. Indeed, targeting VEGF-C impaired invasion from 1.5-fold (siCtrl) to 1.1 or 1.3-fold (siVEGF-C-1 and -2, respectively) 24 hours after stimulation with exogenous EGF/bFGF (**Figure 5e and f**). VEGF-C knockdown led to upregulation of two factors known to negatively regulate cancer cell migration: ATF-3 and CXCL16 (**Supplementary Fig. S6**), [36, 37] thereby further supporting the role of VEGF-C in GBM cell invasion. Collectively, these results demonstrate an autocrine role of VEGF-C in cellular proliferation, survival, and invasion.

Targeting of VEGF-C reduces GBM tumor growth *in vivo*

To assess the contribution of VEGF-C signaling to tumorigenic capacity of GBM cells, we performed an *in vivo* survival study using orthotopic implantation of cells transfected with siCtrl (n = 9) or with siVEGF-C-1 (n = 10). Three days post intracranial implantation, *in vivo* bioluminescence imaging (BLI) analysis showed comparable BLI signal between the two groups, a confirmation that equal number of viable cells was present in both groups at start of the experiment (**Figure 6a**). BLI signal (a surrogate measure of tumor volume) increased over a month for both groups, but siRNA-mediated knockdown of VEGF-C slowed the increase in BLI signal (**Figure 6b and c**). Difference in tumor size between the two groups was further validated by volumetric measurement of magnetic resonance imaging (MRI) brain scans performed on day 28, which showed the presence of larger tumor lesions in siCtrl mice compared to siVEGF-C-1 mice and which correlated to BLI signal (**Figure 6b and d**). These differences (BLI signal, MRI) translated into significantly extended survival of animals injected with cells lacking VEGF-C (55 *vs*. 34 days for siCtrl vs. siVEGF-C-1, respectively) (**Figure 6e**).

Collectively, these results support an important role of VEGF-C for *in vivo* GBM tumor growth and identify a novel evasion mechanism, where GBM cells (possibly accompanied by infiltrating immuno- and endothelial cells) secrete VEGF-C in response to bevacizumab treatment, thereby facilitating sustained VEGFR2-mediated pro-survival signaling, invasion, cell proliferation and cell cycle progression under bevacizumab therapy (**Figure 6f**).

DISCUSSION

Since the establishment of tumor angiogenesis as therapeutic target, notable efforts were made to develop anti-angiogenic agents such as anti-VEGF-A targeting agent bevacizumab. Clinical data of current therapeutic setting clearly indicate transient efficacy with fast recurrence and limited survival benefit following bevacizumab treatment.[9] Although recent clinical and experimental studies suggested a number of escape mechanism for anti-VEGF-A therapy,[11, 38] the molecular and cellular underpinnings of the rebound effect after bevacizumab in GBM remain poorly understood.

Our results demonstrate for the first time that autocrine VEGF-C/VEGFR2 signaling regulates GBM cell viability, cell cycle progression and tumorigenic potential, thereby underscoring the global requirement for VEGF signaling in GBM maintenance. The experimental data presented here show that despite of efficient VEGF-A sequestration by bevacizumab, GBM cell-expressed VEGFR2 tyrosine kinase remains active (**Figures 1h-j**). This is presumably at least partly related to observed increase in VEGFR2 levels upon bevacizumab treatment, also recently reported in various other cancer cell types.[39] The sustained VEGFR2 activation may at least in part explain the limited effect of bevacizumab on GBM cells (**Figure 1f**) observed by us and others.[4, 12] In the light of our previous work, which underlined the importance of autocrine VEGF-A/VEGFR2 signaling in GBM maintenance, this observation prompted us to investigate alternative mechanisms for VEGFR2 activation in the absence of VEGF-A.

In addition to its well-defined role in lymphangiogenesis, VEGF-C represents a multifaceted factor participating in the regulation of angiogenesis, cancer progression as well as metastasis.[16] qRT-PCR analysis of tumor-derived primary cultures confirmed *VEGF-C* expression in GBM cells. Interestingly, the two model lines chosen for this study co-expressed *VEGFR2* and *VEGF-C* but lacked (CPH017) or expressed very low (IN1123) levels of *VEGFR3*, indicating that VEGF-C may operate via VEGFR2 (**Figures 1a, b and 2a**). Importantly, we confirmed VEGF-C – VEGFR2 interaction *in vitro* and observed concordance between the VEGF-C protein levels (evaluated by IHC) and VEGF-C - VEGFR2 interaction *ex vivo* (**Figures 2c-f**). Notably, VEGF-C expression and its interaction with VEGFR2 were sustained in GBM tumors after bevacizumab treatment (**Figures 2e and f, Supplementary Figure S2 & Supplementary Table S1**). In line with the heterogeneous pattern of *VEGF-C* expression observed in cell cultures, IHC staining revealed highly variable VEGF-C expression in our cohort of GBM specimens (**Figure 2e**). This heterogeneity may be driven by cellular environmental factors like hypoxia, which was found to induce VEGF-C expression in metastatic cancer cells.[40] IHC analysis confirmed previously reported VEGF-C expression by tumor infiltrating macrophages and other non-tumor cell types (**Supplementary Figure S2),**[26, 41, 42] suggesting that even VEGF-C-low expressing GBM tumor cells could be exposed to substantial amounts of VEGF-C ligand *in vivo*. Still, data indicate VEGF-C driven cell maintenance to be restricted to a subset of GBM tumor cells, as also previously found for

VEGFR2, [4, 7] and accordingly that VEGF-C as a treatment target would have highest clinical potential in an combination regimen.

The stimulation of GBM cells with exogenous VEGF-C was potent enough to trigger the canonical VEGFR2 downstream signaling pathways such as ERK and PLCγ with kinetics similar to that of VEGF-A (**Figure 3a**). By studying the effect of VEGF-C knockdown, we found that VEGF-C positively stimulates GBM cell viability, cell cycle progression and invasion (**Figure 4-5**, **Supplementary Figure S6**). Our findings are in line with previous studies, which reported autocrine VEGF-C signaling in other cancers.[16] In Barret cells, autocrine VEGF-A/VEGFR2 signaling induced cell proliferation via PLCγ /protein kinase-C/ERK signaling.[43] Rodriguez et al. (2010) reported that ERKs promote cell cycle entry by dislodging Rb from lamin A, thereby facilitating its rapid phosphorylation and cell cycle entry.[44] In our study, we observed both, changes in Rb phosphorylation and cyclin levels upon siRNA-mediated VEGF-C knockdown (**Figure 5d**), suggesting that an early (mediated by Rb phosphorylation changes) as well as a late (transcriptional reprograming of cyclin levels) cell cycle response take place in GBM. Signaling via VEGFR1/2 was previously positively associated with both activation of ERK and invasive capacity of GBM cancer cells.[8] This is concordant with our data, where VEGF-C stimulation induces ERK activation and VEGF-C loss impairs the invasive capacity of GBM cells (**Figure 5e and f**).

While bevacizumab did not affect GBM cell survival *in vitro* (**Figure 1f**), our data showed increase in VEGF-C secretion after bevacizumab treatment (**Figure 2b**). Moreover, VEGF-A secretion was increased after siRNA-mediated knockdown of VEGF-C (**Figure 3d and e**). These observations prompted us to evaluate the impact of combined VEGF-A (bevacizumab)/VEGF-C (siRNA) targeting in GBM cells. As shown in **Figure 4e**, combination of bevacizumab and siRNA-VEGF-C was superior at reducing cell viability in comparison to either treatment alone. The mechanism(s) by which VEGF-C stimulates the expression of VEGF-A is not clear. Interestingly, an increase in *VEGF-C* mRNA levels was previously demonstrated in GBM and endothelial cells following bevacizumab therapy.[30] Zhao et al. (2006) reported that VEGF-A have up-regulatory effect on VEGF-C expression in retinal pigment epithelial cells.[28] Since ERKs are ubiquitous enzymes involved in signal transduction and activation of numerous cellular functions, it is plausible that ERK activation, possibly in alliance with PLC-γ, may be responsible for VEGF-A/VEGF-C

compensatory expression in GBM cells. Importantly, the compensatory mechanism described in our study points to a global requirement for VEGF signaling route in GBM maintenance.

Previous studies showed that VEGF-C knockdown in GBM tumor cells decreases their ability to induce endothelial cell reactivity.[29] Moreover, Grau et al. (2011) have validated the potential of exogenous VEGF-C to stimulate reactivity of both endothelial cells derived from normal brain and GBM specimens under bevacizumab therapy.[30] As observed in other cancer types, including gastric and esophageal cancer,[31, 45] our data showed that VEGF-C knockdown delays tumor growth and prolongs survival of tumor-bearing mice (**Figure 6**). Taken together, findings presented herein and/or reported by others underline the crucial role of VEGF-C in both tumor growth and angiogenesis.

In conclusion, we provide direct evidence that VEGF-C/VEGFR2 signaling operates in an autocrine manner thereby promoting GBM cell viability, cell cycle progression and invasion. Since VEGF-C expression and VEGF-C/VEGFR2 interaction remained stable under bevacizumab treatment, we believe that autocrine VEGF-C signaling represents a novel escape mechanism developed by GBM tumors to counteract bevacizumab therapy.

MATERIALS AND METHODS

Cell culture

Patient-derived GBM cell cultures CPH017 (p4), CHP036 (p6), CPH047 (p3m1), CPH048 (p6) were described previously.[46] 1966 cells were provided by Dr. Rich (Cleveland Clinic, USA).[4] IN326[47] and IN1123[48] were kindly provided from Dr. Nakano (The University of Alabama at Birmingham, USA). The cells were maintained in Neurobasal®–A media supplemented with B-27® Supplement, GlutaMAX™, basic fibroblast growth factor (bFGF) (10 ng/ml), epidermal growth factor (EGF) (10 ng/ml), penicillin (50 U/mL), streptomycin (50 µg/mL) and N-2 Supplement (only CPH017, CPH036, CPH047 and CPH048) (all from ThermoFisher Scientific, Hvidovre, Denmark). Human dermal microvascular endothelial cells (HMVEC) were purchased from Lonza (Basel, Switzerland) and grown in EGM-2MV endothelial growth medium according to the manufacturer's instructions (Lonza). Human dermal lymphatic endothelial cells (HDLEC) adult cell pellet was

purchased from PromoCell (Heidelberg, Germany). All cells were maintained in an incubator with 5% CO2 at 37°C.

Inhibitors, growth factors & blocking antibodies

SU1498 (10 mM stock dissolved in DMSO, Merck Millipore), bevacizumab (Avastin®, 25 mg/mL, Roche, Basel, Switzerland), recombinant VEGF-A-165aa (50 µg/mL dissolved in buffered saline with 0.1% bovine BSA, Miltenyi Biotec, Lund, Sweden), recombinant human mature VEGF-C, Thr103-Arg227 ~ 21kDa (10 µg/mL dissolved in buffered saline with 0.1 % BSA, R&D Systems, Minneapolis, MN, USA).

siRNA transfection

Cells were transfected using 75 pmol of either VEGF-C-siRNA (siVEGF-C-1: esiRNA pool, EHU013781, Sigma-Aldrich; siVEGF-C-2: single siRNA, HSS111277, ThermoFisher Scientific) or scrambled control siRNA (siCtrl: Stealth™ RNAi Negative Control Duplex Med CG, ThermoFisher Scientific) and 5-7,5 µL of Lipofectamine RNAiMax in Opti-MEM reduced serum medium (ThermoFisher Scientific). For CPH017 cells standard transfection method was employed, while reverse transfections were used for IN1123 cells in which cells diluted in Opti-MEM media added 0.1 % Geltrex were plated on top of prior plated siRNA/lipid complexes in 24 wells.

Patient material

Paired Formalin Fixed Paraffin Embedded (FFPE) samples (n= 12 pathologically confirmed GBM; WHO grade IV) collected before and after bevacizumab treatment in combination with CPT-11 (Irinotecan) administered according to a published treatment protocol.[49] Post bevacizumab samples were obtained at re-surgery performed immediately after progression on bevacizumab treatment. The surgeries were performed at Copenhagen University Hospital, Denmark (Center 1, 9 patients), and at Aarhus University Hospital, Denmark (Center 2, 3 patients). Patient material was used according to Declaration of Helsinki and Danish legislation under permission from Danish Data Protection Agency (2006-41-6979) and the scientific ethical committee for Copenhagen and Frederiksberg (KF-01-327718, H-2-2012-069).

Western Blot (WB)

WB analysis was performed as described previously.[50] For signal development SuperSignal West Dura Extended Duration Substrate or SuperSignal West Femto Maximum Sensitivity Substrate was used (both ThermoFisher Scientific). Semi-quantification of band intensities was performed using the ImageJ software. Antibodies are listed in Supplementary Table S5.

RNA purification and Quantitative Real-Time PCR (qRT-PCR)

RNA was purified using the QIAshredder/RNeasy Mini kit (Qiagen, Ballerup, Denamrk). cDNA synthesis and qRT-PCR reactions were performed using SuperscriptTM III Platinum® qRT-PCR kit with SYBR® Green (ThermoFisher Scientific). Quantification of gene expression levels was done according to the comparative Ct method and normalized to expression of reference genes human TOP1, EIF4A2 and CYC1. Primer-sequences are listed in Supplementary Table S4.

MTT Cell Viability Assay

0.7-2x10^4 cells/well were plated in 96-well plates and incubated up to 7 days with either 100 µl growth medium or medium containing the indicated additives. In viability assays using siRNA, cells were plated immediately after transfection. Cell viability was measured using 3-(4,5-dimethylthiazol-2-yl)-2,5-diphenyl-tetrazolium bromide (MTT) assay as previously described[50].

ELISA

Cells were plated at a density of 1.25x10^6 cells/mL in growth media and conditioned media collected 48-72 hours later was submitted to Human VEGF Quantikine ELISA or the Human VEGF-C Quantikine ELISA (both R&D Systems) following manufacturer's instructions. Quantification was done by measuring absorbance at 450 nm with 570 nm as a reference using a Synergy2 microplate reader with Gen5 software (BioTek, Winooski, VT, USA).

Immunofluorescence

Cells treated with bevacizumab or IgG were attached to coverslips by cytospin, fixed for 10 min with 4% Paraformaldehyde (PFA), washed and then permeabilized with 0.25 % Triton-X-100 (Sigma-Aldrich, Munich, Germany) in PBS for 5 min. Coverslips were then washed, blocked for 30

min by 1 % BSA in PBS and incubated over night at 4˚C with primary antibody diluted in DMEM media + 10 % FCS (ThermoFisher Scientific). Next day, after washing coverslips were incubated with secondary antibody diluted in PBS for 1 hour at RT and thereafter counterstained with DAPI for nuclear detection and mounted using Fluoromount-G (Southern Biotech, Birmingham, AL, USA). Imaging was performed using a Zeiss LSM 700META/imager.Z1 microscope (Plan-Apochromat 63x/1.40 Oil DIC M27 objective, Carl Zeiss, Inc., Oberkochen, Germany) and processed with Zen 2008 and Zen Black software (Carl Zeiss, Inc.). Quantification of relative mean fluorescence intensity per cell of p-VEGFR2 staining was performed by examining 50 cells per condition from projection of Z-stack images encompassing the entire depth of the cells using the Cell Profiler 2.0 Software (http://cellprofiler.org/). Antibodies and dilutions can be found in Supplementary Table S5.

Proximity Ligation Assay (PLA)

Cells were grown on Geltrex™ LDEV-Free Reduced Growth Factor Basement Membrane Matrix (ThermoFisher Scientific)-coated coverslips, fixed with 4 % PFA for 10 min, washed and then permeabilized with 0.25 % Triton-X-100 (Sigma-Aldrich) in PBS for 5 min. For tissue, four µm sections of FFPE material were used. These were deparaffinized, hydrated, blocked for endogen peroxidases using methanol with H_2O_2 and pre-treated in a microwave oven with citrate buffer (pH 6.0). For both cells and tissue VEGF-C and VEGFR2 co-localization was detected using the Duolink® In Situ Red starter kit Mouse/Rabbit (Sigma-Aldrich) according to manufacturer's instructions with overnight incubation with primary antibody at 4˚C. Before mounting the cytoskeleton (F-actin) was stained by 30 min incubation with Alexa Fluor 488 Phalloidin. Antibodies and dilutions are shown in Supplementary Table S5.

Samples were imaged using a Zeiss LSM 700META/imager.Z1 microscope (EC Plan-Neofluar 40x/1.30 oil DIC M27 objective, Carl Zeiss, Inc.) and processed with Zen 2008 and Zen Black software (Carl Zeiss, Inc.). Quantification of mean PLA spots per cells was evaluated on merged projection of Z-stack images encompassing the entire depth of the cells using Blobfinder Software[51] (http://www.cb.uu.se/~amin/BlobFinder/), examining 10 different fields on each coverslip and in total a minimum of 40 cells per condition.

Immunohistochemistry (IHC)

Four µm sections of FFPE material were used for IHC. These were deparaffinized, hydrated, blocked for endogen peroxidase using H_2O_2 and pre-treated in a microwave oven with a Tris/ethylene glycol tetra-acetic acid buffer (pH 9.0) before immunostaining. Staining was conducted on a DAKO (Glostrup, Denmark) Cytomation autostainer using antibody for VEGF-C (described in Supplementary Table S5). Staining was evaluated using an Olympus BX51 microscope.

Gene expression analysis by microarray

RNA (250 ng input) was amplified, labeled using the WT Plus Expression Kit (Affymetrix, Santa Clara, CA, USA) according to manufactures instructions and hybridized to the HumanGene 2.0 ST GeneChip® array (Affymetrix). The arrays were washed and stained with phycoerytrin conjugated streptavidin (SAPE) using the Affymetrix Fluidics Station® 450, and the arrays were scanned in the Affymetrix GeneArray® 3000 scanner to generate fluorescent images, as described in the Affymetrix GeneChip® protocol. Cell intensity files (CEL files) were generated in the GeneChip® Command Console® Software (AGCC; Affymetrix).

Raw CEL files were pre-processed by quantile normalization, and gene summaries were extracted via robust multi-array average (RMA).[52] The probe level data (.CEL files) were transformed into expression measures using R version 3.2.2 (https://www.R-project.org/).[53] Differential expression analysis was conducted using R package limma[54] with p-value threshold of 0.05 and Bonferroni-Hochberg adjustment. A cutoff of 2 was applied to log2 fold change in order to filter the results. NetAffx Release 36 Transcript Cluster Annotation (Affymetrix) was used to translate probe set information into genes.

Gene Set Enrichment Analysis (GSEA) was performed using the GSEA Desktop Application (build#0045) from Broad Institute (Cambridge, MA, USA) by analyzing gene sets (with applied set size filters: min=15, max=500) from REACTOME pathway database available in MSigDB (v5.2, build=Sep22,2016).[55]

Invasion assay

Cell spheroids were obtained by plating 1000 cells in non-adherent round-bottomed 96-well plates in 50µL of media lacking EGF and bFGF. Next day, 50 µL of Geltrex was added to each well and allowed to solidify at 37˚C before addition of 100 µL (growth factor enriched)-media containing 2x the normal concentrations of EGF and FGF to reach normal growth factor levels in total volume (200 µL). An Olympus (Tokyo, Japan) IX71 microscope was used to capture images of each well at individual time points (0 and 24 hours following stimulation). The migratory capacity was evaluated by comparing the relative total pixel area covered by cells at time point 0 and 24 hours using ImageJ software.

Cell cycle analysis

Analysis of cell cycle profiles (cells in subG1, G1, S or G2/M phases) and mitotic index was done as previously described[48, 50] using the FACS Verse Cell Sorter (BD Biosciences, Kgs. Lyngby, Denmark) for sample acquisition and the FlowJo software for cell cycle analysis. For the cell cycle analysis, cells were pulse-labeled with EdU (5-ethyl-2'-deoxyuridine) for 60 min at end of incubation, fixed and stained using the Click-iT EdU Alexa Flour 647 Flow Cytometry Assay Kit (ThermoFisher Scientific) following manufacturer's instructions and counterstained using Hoechst 33342 dye (ThermoFisher Scientific). For determination of the mitotic index, cells were incubated with 0.04 µM/mL Nocadazole (Sigma-Aldrich) or DMSO 12 hours prior to fixation and staining using anti-$H3^{Ser10}$.

***In vivo* tumor formation and imaging**

Intracranial GBM xenografts were established by in brain injection of $0.1x10^6$ cells in 8-10 week old NMRI nude female mice (Taconic Europe, Lille Skensved, Denmark) as previously described.[56] A variant of the CPH017 cell culture (CHP017-LUC) having stable expression of luciferase[57] was used and cells were transfected with siRNA constructs 1 day prior to injection. In total, 10 mice received siVEGF-C-1 transfected cells and 9 mice received siCtrl transfected cells. Tumor growth and size was monitored by Bioluminescence (BLI) performed on all mice at day 3, 13, 23, 34 and 42 following cell injection and Magnetic resonance imaging (MRI) performed on selected mice at day 28 following injection. Both methods have been described previously[57]. In short,

measurement of the BLI intensity was done by i.p. injection of D-luciferin followed by scanning which was continued until the peak signal was captured for each mouse. A two-dimensional region of interest (ROI) at a fixed size was manually drawn covering the skull of the mouse and total photon flux was measured. For MRI a TurboRare T2w protocol was used for generation of 8 transverse and 12 coronal images (slices) with a thickness of 0.5 mm which were acquired using a repetition time of 2500 ms and an echo time of 33 ms. A field of view of 20×20 mm was chosen and sampled into a matrix size of 256×256 mm resulting in a spatial resolution of 0.078. ROIs covering the total tumor area were manually drawn on each slice and tumor volume was obtained by interpolating the ROIs from all transverse images and coronal images, respectively. The total tumor volume was calculated as the mean of the tumor volume in the transverse and coronal images. Mice were humanely euthanized when presenting tumor related symptoms such as neurological signs and/or 20% weight loss. Animal care and all experimental procedures were performed under the approval of the Danish Animal Welfare Council (2012-15-2934-00267).

Statistical analysis

Quantified *in vitro* data are expressed as Mean ± SD, ± SEM or ± 95% Confidence Interval as indicated. For all *in vitro* experiments, n indicates the number of independent performed experiments, while for the *in vivo* data it represents the number of animals used. Statistical analysis was performed using Graphpad Prism (v. 7.02, GraphPad Software). Choice of statistical method and definitions of significance levels are described in figure legends.

CONFLICT OF INTEREST

The authors declare no potential conflicts of interest.

ACKNOWLEDGEMENTS

We thank Pia Pedersen and the Erler group for technical assistance. Funding was provided from the University of Copenhagen, the Danish Cancer Society, NovoNordisk Foundation, Arvid Nilssons Foundation, Torben and Alice Frimodts Fond, King Christian IX's foundation, Dansk

Kraeftforsknings Foundation, Fabrikant Ejner Willumsens Memorial Fund and Sejer Perssons and Lis Klüwers Foundation. An unrestricted grant was also provided from Roche A/S.

AUTHOR CONTRIBUTIONS

SRM has contributed to overall study design, experimental designs, performing experiments, analysis and interpretation of data and manuscript writing; MS, MKN, CM, MV contributed by performing and analyzing experiments; WM performed the bioinformatic analysis; SL and TU have contributed by preparing patient material used for analyses; HB has contributed to staining and analysis of IHC data; AK contributed to experimental design of animal study; M-TS have contributed to overall study design and experimental design; HSP and UL contributed to overall study design and manuscript drafting; PH contributed to overall study design, experimental design, interpretation of data and manuscript writing. All authors red and approved the manuscript.

REFERENCES

1. Stupp R, Hegi ME, Mason WP, van den Bent MJ, Taphoorn MJ, Janzer RC*, et al.* Effects of radiotherapy with concomitant and adjuvant temozolomide versus radiotherapy alone on survival in glioblastoma in a randomised phase III study: 5-year analysis of the EORTC-NCIC trial. *Lancet Oncol* 2009, **10**(5)**:** 459-466.

2. Ohgaki H. Epidemiology of brain tumors. *Methods Mol Biol* 2009, **472:** 323-342.

3. Brem S, Cotran R, Folkman J. Tumor angiogenesis: a quantitative method for histologic grading. *J Natl Cancer Inst* 1972, **48**(2)**:** 347-356.

4. Hamerlik P, Lathia JD, Rasmussen R, Wu Q, Bartkova J, Lee M*, et al.* Autocrine VEGF-VEGFR2-Neuropilin-1 signaling promotes glioma stem-like cell viability and tumor growth. *J Exp Med* 2012, **209**(3)**:** 507-520.

5. Paul-Samojedny M, Pudelko A, Suchanek-Raif R, Kowalczyk M, Fila-Danilow A, Borkowska P*, et al.* Knockdown of the AKT3 (PKBgamma), PI3KCA, and VEGFR2 genes by RNA interference suppresses glioblastoma multiforme T98G cells invasiveness in vitro. *Tumour Biol* 2015, **36**(5)**:** 3263-3277.

6. Xu C, Wu X, Zhu J. VEGF promotes proliferation of human glioblastoma multiforme stem-like cells through VEGF receptor 2. *ScientificWorldJournal* 2013, **2013:** 417413.

7. Kessler T, Sahm F, Blaes J, Osswald M, Rubmann P, Milford D*, et al.* Glioma cell VEGFR-2 confers resistance to chemotherapeutic and antiangiogenic treatments in PTEN-deficient glioblastoma. *Oncotarget* 2015, **6**(31)**:** 31050-31068.

8. Szabo E, Schneider H, Seystahl K, Rushing EJ, Herting F, Weidner KM*, et al.* Autocrine VEGFR1 and VEGFR2 signaling promotes survival in human glioblastoma models in vitro and in vivo. *Neuro Oncol* 2016, **18**(9)**:** 1242-1252.

9. Wang N, Jain RK, Batchelor TT. New Directions in Anti-Angiogenic Therapy for Glioblastoma. *Neurotherapeutics* 2017.

10. Chi AS, Sorensen AG, Jain RK, Batchelor TT. Angiogenesis as a therapeutic target in malignant gliomas. *Oncologist* 2009, **14**(6)**:** 621-636.

11. Tamura R, Tanaka T, Miyake K, Yoshida K, Sasaki H. Bevacizumab for malignant gliomas: current indications, mechanisms of action and resistance, and markers of response. *Brain Tumor Pathol* 2017, **34**(2)**:** 62-77.

12. Francescone R, Scully S, Bentley B, Yan W, Taylor SL, Oh D*, et al.* Glioblastoma-derived tumor cells induce vasculogenic mimicry through Flk-1 protein activation. *J Biol Chem* 2012, **287**(29)**:** 24821-24831.

13. Lin W, Jiang L, Chen Y, She F, Han S, Zhu J*, et al.* Vascular endothelial growth factor-D promotes growth, lymphangiogenesis and lymphatic metastasis in gallbladder cancer. *Cancer Lett* 2012, **314**(2)**:** 127-136.

14. Yasuoka H, Kodama R, Hirokawa M, Takamura Y, Miyauchi A, Inagaki M*, et al.* Neuropilin-2 expression in papillary thyroid carcinoma: correlation with VEGF-D expression, lymph node metastasis, and VEGF-D-induced aggressive cancer cell phenotype. *J Clin Endocrinol Metab* 2011, **96**(11)**:** E1857-1861.

15. Tanaka M, Kitadai Y, Kodama M, Shinagawa K, Sumida T, Tanaka S*, et al.* Potential role for vascular endothelial growth factor-D as an autocrine factor for human gastric carcinoma cells. *Cancer Sci* 2010, **101**(10)**:** 2121-2127.

16. Wang CA, Tsai SJ. The non-canonical role of vascular endothelial growth factor-C axis in cancer progression. *Exp Biol Med (Maywood)* 2015, **240**(6)**:** 718-724.

17. Karkkainen MJ, Haiko P, Sainio K, Partanen J, Taipale J, Petrova TV*, et al.* Vascular endothelial growth factor C is required for sprouting of the first lymphatic vessels from embryonic veins. *Nat Immunol* 2004, **5**(1)**:** 74-80.

18. Chen JC, Chang YW, Hong CC, Yu YH, Su JL. The role of the VEGF-C/VEGFRs axis in tumor progression and therapy. *Int J Mol Sci* 2012, **14**(1)**:** 88-107.

19. Joukov V, Sorsa T, Kumar V, Jeltsch M, Claesson-Welsh L, Cao Y*, et al.* Proteolytic processing regulates receptor specificity and activity of VEGF-C. *EMBO J* 1997, **16**(13)**:** 3898-3911.

20. Jha SK, Rauniyar K, Karpanen T, Leppanen VM, Brouillard P, Vikkula M*, et al.* Efficient activation of the lymphangiogenic growth factor VEGF-C requires the C-terminal domain of VEGF-C and the N-terminal domain of CCBE1. *Sci Rep* 2017, **7**(1)**:** 4916.

21. Siegfried G, Basak A, Cromlish JA, Benjannet S, Marcinkiewicz J, Chretien M*, et al.* The secretory proprotein convertases furin, PC5, and PC7 activate VEGF-C to induce tumorigenesis. *J Clin Invest* 2003, **111**(11)**:** 1723-1732.

22. Cho HJ, Kim IK, Park SM, Baek KE, Nam IK, Park SH*, et al.* VEGF-C mediates RhoGDI2-induced gastric cancer cell metastasis and cisplatin resistance. *Int J Cancer* 2014, **135**(7)**:** 1553-1563.

23. Yeh YW, Cheng CC, Yang ST, Tseng CF, Chang TY, Tsai SY*, et al.* Targeting the VEGF-C/VEGFR3 axis suppresses Slug-mediated cancer metastasis and stemness via inhibition of KRAS/YAP1 signaling. *Oncotarget* 2017, **8**(3)**:** 5603-5618.

24. Dias S, Choy M, Alitalo K, Rafii S. Vascular endothelial growth factor (VEGF)-C signaling through FLT-4 (VEGFR-3) mediates leukemic cell proliferation, survival, and resistance to chemotherapy. *Blood* 2002, **99**(6)**:** 2179-2184.

25. Grau SJ, Trillsch F, Herms J, Thon N, Nelson PJ, Tonn JC*, et al.* Expression of VEGFR3 in glioma endothelium correlates with tumor grade. *J Neurooncol* 2007, **82**(2)**:** 141-150.

26. Jenny B, Harrison JA, Baetens D, Tille JC, Burkhardt K, Mottaz H*, et al.* Expression and localization of VEGF-C and VEGFR-3 in glioblastomas and haemangioblastomas. *J Pathol* 2006, **209**(1)**:** 34-43.

27. Xu Y, Zhong Z, Yuan J, Zhang Z, Wei Q, Song W*, et al.* Collaborative overexpression of matrix metalloproteinase-1 and vascular endothelial growth factor-C predicts adverse prognosis in patients with gliomas. *Cancer Epidemiol* 2013, **37**(5)**:** 697-702.

28. Zhao H, Hou C, Hou A, Zhu D. Concurrent Expression of VEGF-C and Neuropilin-2 Is Correlated with Poor Prognosis in Glioblastoma. *Tohoku J Exp Med* 2016, **238**(2)**:** 85-91.

29. Carpenter RL, Paw I, Zhu H, Sirkisoon S, Xing F, Watabe K*, et al.* The gain-of-function GLI1 transcription factor TGLI1 enhances expression of VEGF-C and TEM7 to promote glioblastoma angiogenesis. *Oncotarget* 2015, **6**(26)**:** 22653-22665.

30. Grau S, Thorsteinsdottir J, von BL, Winkler F, Tonn JC, Schichor C. Bevacizumab can induce reactivity to VEGF-C and -D in human brain and tumour derived endothelial cells. *J Neurooncol* 2011, **104**(1)**:** 103-112.

31. Liu P, Zhou J, Zhu H, Xie L, Wang F, Liu B*, et al.* VEGF-C promotes the development of esophageal cancer via regulating CNTN-1 expression. *Cytokine* 2011, **55**(1)**:** 8-17.

32. Knizetova P, Ehrmann J, Hlobilkova A, Vancova I, Kalita O, Kolar Z*, et al.* Autocrine regulation of glioblastoma cell cycle progression, viability and radioresistance through the VEGF-VEGFR2 (KDR) interplay. *Cell Cycle* 2008, **7**(16)**:** 2553-2561.

33. Wu TH, Pabin CN, Qin Z, Blankenstein T, Philip M, Dignam J*, et al.* Long-term suppression of tumor growth by TNF requires a Stat1- and IFN regulatory factor 1-dependent IFN-gamma pathway but not IL-12 or IL-18. *J Immunol* 2004, **172**(5)**:** 3243-3251.

34. Papageorgiou A, Dinney CP, McConkey DJ. Interferon-alpha induces TRAIL expression and cell death via an IRF-1-dependent mechanism in human bladder cancer cells. *Cancer Biol Ther* 2007, **6**(6)**:** 872-879.

35. Lu KV, Chang JP, Parachoniak CA, Pandika MM, Aghi MK, Meyronet D*, et al.* VEGF inhibits tumor cell invasion and mesenchymal transition through a MET/VEGFR2 complex. *Cancer Cell* 2012, **22**(1)**:** 21-35.

36. Fang Y, Henderson FC, Jr., Yi Q, Lei Q, Li Y, Chen N. Chemokine CXCL16 expression suppresses migration and invasiveness and induces apoptosis in breast cancer cells. *Mediators Inflamm* 2014, **2014:** 478641.

37. Guenzle J, Wolf LJ, Garrelfs NW, Goeldner JM, Osterberg N, Schindler CR*, et al.* ATF3 reduces migration capacity by regulation of matrix metalloproteinases via NFkappaB and STAT3 inhibition in glioblastoma. *Cell Death Discov* 2017, **3:** 17006.

38. Lu KV, Bergers G. Mechanisms of evasive resistance to anti-VEGF therapy in glioblastoma. *CNS Oncol* 2013, **2**(1)**:** 49-65.

39. Mahfouz N, Tahtouh R, Alaaeddine N, El Hajj J, Sarkis R, Hachem R*, et al.* Gastrointestinal cancer cells treatment with bevacizumab activates a VEGF autoregulatory mechanism involving telomerase catalytic subunit hTERT via PI3K-AKT, HIF-1alpha and VEGF receptors. *PLoS One* 2017, **12**(6)**:** e0179202.

40. Morfoisse F, Kuchnio A, Frainay C, Gomez-Brouchet A, Delisle MB, Marzi S*, et al.* Hypoxia induces VEGF-C expression in metastatic tumor cells via a HIF-1alpha-independent translation-mediated mechanism. *Cell Rep* 2014, **6**(1)**:** 155-167.

41. Ding M, Fu X, Tan H, Wang R, Chen Z, Ding S. The effect of vascular endothelial growth factor C expression in tumor-associated macrophages on lymphangiogenesis and lymphatic metastasis in breast cancer. *Mol Med Rep* 2012, **6**(5)**:** 1023-1029.

42. Spiric Z, Eri Z, Eric M. Significance of Vascular Endothelial Growth Factor (VEGF)-C and VEGF-D in the Progression of Cutaneous Melanoma. *Int J Surg Pathol* 2015, **23**(8)**:** 629-637.

43. Domigan CK, Ziyad S, Iruela-Arispe ML. Canonical and noncanonical vascular endothelial growth factor pathways: new developments in biology and signal transduction. *Arterioscler Thromb Vasc Biol* 2015, **35**(1)**:** 30-39.

44. Rodriguez J, Calvo F, Gonzalez JM, Casar B, Andres V, Crespo P. ERK1/2 MAP kinases promote cell cycle entry by rapid, kinase-independent disruption of retinoblastoma-lamin A complexes. *J Cell Biol* 2010, **191**(5)**:** 967-979.

45. Yao J, Da M, Guo T, Duan Y, Zhang Y. RNAi-mediated gene silencing of vascular endothelial growth factor-C inhibits tumor lymphangiogenesis and growth of gastric cancer in vivo in mice. *Tumour Biol* 2013, **34**(3)**:** 1493-1501.

46. Stockhausen MT, Broholm H, Villingshoj M, Kirchhoff M, Gerdes T, Kristoffersen K*, et al.* Maintenance of EGFR and EGFRvIII expressions in an in vivo and in vitro model of human glioblastoma multiforme. *Exp Cell Res* 2011, **317**(11)**:** 1513-1526.

47. Flavahan WA, Wu Q, Hitomi M, Rahim N, Kim Y, Sloan AE*, et al.* Brain tumor initiating cells adapt to restricted nutrition through preferential glucose uptake. *Nat Neurosci* 2013, **16**(10)**:** 1373-1382.

48. Rasmussen RD, Gajjar MK, Tuckova L, Jensen KE, Maya-Mendoza A, Holst CB*, et al.* BRCA1-regulated RRM2 expression protects glioblastoma cells from endogenous replication stress and promotes tumorigenicity. *Nat Commun* 2016, **7:** 13398.

49. Poulsen HS, Grunnet K, Sorensen M, Olsen P, Hasselbalch B, Nelausen K*, et al.* Bevacizumab plus irinotecan in the treatment patients with progressive recurrent malignant brain tumours. *Acta Oncol* 2009, **48**(1)**:** 52-58.

50. Staberg M, Michaelsen SR, Rasmussen RD, Villingshoj M, Poulsen HS, Hamerlik P. Inhibition of histone deacetylases sensitizes glioblastoma cells to lomustine. *Cell Oncol (Dordr)* 2017, **40**(1)**:** 21-32.

51. Allalou A, Wahlby C. BlobFinder, a tool for fluorescence microscopy image cytometry. *Comput Methods Programs Biomed* 2009, **94**(1)**:** 58-65.

52. Bolstad BM, Irizarry RA, Astrand M, Speed TP. A comparison of normalization methods for high density oligonucleotide array data based on variance and bias. *Bioinformatics* 2003, **19**(2)**:** 185-193.

53. Team RC. R: A Language and Environment for Statistical Computing. 2011, Vienna, Austria: R Foundation for Statistical Computing. ISBN 3-900051-07-0. Available from: http://www. R-project. org; 2011.

54. Phipson B, Lee S, Majewski IJ, Alexander WS, Smyth GK. Robust hyperparameter estimation protects against hypervariable genes and improves power to detect differential expression. *Ann Appl Stat* 2016**:** 946-963.

55. Subramanian A, Tamayo P, Mootha VK, Mukherjee S, Ebert BL, Gillette MA*, et al.* Gene set enrichment analysis: a knowledge-based approach for interpreting genome-wide expression profiles. *Proc Natl Acad Sci U S A* 2005, **102**(43)**:** 15545-15550.

56. Kristoffersen K, Nedergaard MK, Villingshoj M, Borup R, Broholm H, Kjaer A*, et al.* Inhibition of Notch signaling alters the phenotype of orthotopic tumors formed from glioblastoma multiforme neurosphere cells but does not hamper intracranial tumor growth regardless of endogene Notch pathway signature. *Cancer Biol Ther* 2014, **15**(7)**:** 862-877.

57. Nedergaard MK, Michaelsen SR, Urup T, Broholm H, El AH, Poulsen HS*, et al.* 18F-FET microPET and microMRI for anti-VEGF and anti-PlGF response assessment in an orthotopic murine model of human glioblastoma. *PLoS One* 2015, **10**(2)**:** e0115315.

FIGURES AND FIGURE LEGENDS

Figure 1. VEGFR2 tyrosine kinase expressed by GBM cells remains active under bevacizumab therapy. (A) Western Blot (WB) for VEGFR2 and Tubulin in a panel of patient derived GBM cultures. (B) qRT-PCR analysis of VEGF-A and VEGFR2 expression in GBM cell panel standardized to expression in HMVEC cells (Mean of duplicates ± SD, n=1, Y-scale is log10 transformed). (C) Viability of CHP017 and IN1123 cells treated with SU1498 (10 µM) or left unstimulated (Mean ± SEM, n=3). (D) Representative WB of VEGFR2, p-VEGFR2 or tubulin in CPH017 cells plated overnight in NB media without EGF and bFGF and thereafter treated with either SU1498 (30 µM for 3 h), VEGF-A (40 ng/mL for 15 min) or a combination (30 µM SU1498 for 3 h followed by 40 ng/mL VEGF-A for 15 min). (E) Quantification of relative p-VEGFR2/tubulin levels from WB analysis in D (Mean ± SEM, n=3). (F) Viability of CPH017 and IN1123 cells treated 7 days with bevacizumab (Bev) (0-1 mg/mL), (Mean ± SEM, n=3). (H) Representative WB of VEGFR2, p-VEGFR2 or tubulin in CPH017 cells treated for 72 h with Bev (0.5 mg/mL) or IgG. (G) ELISA quantification of VEGF-A protein in conditioned media from CPH017 cells treated for 48 h with bevacizumab (Bev, 0.5 mg/mL) or IgG control (Mean ± SD, n=1 in technical triplicates, n.d. denotes that signal could not be detected). (I) Representative confocal image of immunofluorescent staining for p-VEGFR2 (red) and DAPI (blue) of CPH017 cells treated for 72 h with Bev (0.5 mg/mL) or IgG. (J) Quantification of mean fluorescence intensity per cell for p-VEGFR2 staining shown in I (Mean ± SD, n=1 with 50 analyzed cells for each condition). Statistics are in C and F: 2-way ANOVA with Bonferroni post test, and in E: One-way ANOVA with Dunnett's post test for comparison of treatments with control and paired 2-sample t-test for comparison of VEGF-A and SU1498+VEGF-A treatments, and in J: Unpaired 2-sample t-test. Significance levels are: * $P \leq 0.05$, ** $P \leq 0.01$, **** $P \leq 0.0001$, NS: Non-significant.

Figure 2. VEGF-C expression and interaction with VEGFR2 is not affected by bevacizumab therapy. (A) qRT-PCR analysis of VEGF-C and VEGFR3 expression in a GBM cell panel standardized to expression in HDLEC cells (Mean of duplicates ± SD, n=1, Y-scale is log10 transformed, n.d. denotes that signal could not be detected). (B) ELISA quantification of VEGF-C protein in conditioned media from CPH017 and IN1123 cells treated 72 h with bevacizumab (Bev) (0.5 mg/mL) or IgG (Mean ± SEM, n=3). Statistic analysis is a paired 2-sample t-test with significance levels: * $P \leq 0.05$. (C) Quantification of PLA dots in CPH017 and IN1123 cells. (Mean ± SEM, n=3-4 each quantifying a minimum of 40 cells). (D) Representative confocal images showing PLA signal (red), F-Actin (grey) and DAPI (blue) of CPH017 and IN1123 cells. Staining with only VEGF-C antibody (AB) was used a negative control. (E) IHC evaluation of VEGF-C in parallel GBM samples before and after bevacizumab therapy. Representative images of 2 out of 12 analyzed patients show are shown. Scale bar: 50 µm. (F) Confocal images of PLA signal (red), F-Actin (green) and DAPI (blue) in FFPE GBM tissue before and after bevacizumab therapy. Representative images from tumor samples of 2 out of 6 analyzed patients are shown and are the same also shown in E for VEGF-C IHC.

Figure 3. VEGF-C regulates canonical VEGFR2 signaling pathway. (A) WB for p-VEGFR2, VEGFR2, p-PLCγ1, PLCγ1, p-Akt, Akt, p-ERK, Erk and Tubulin in CPH017 cells plated in media lacking EGF/bFGF for 24 hours and then stimulated with VEGF-A (40 ng/mL) or VEGF-C (0.2 µg/mL) in indicated intervals. The WB shown is a representative of one of 3 independently conducted experiments. (B) qRT-PCR analysis of VEGF-C expression in CPH017 and IN1123 cells 48 h following transfection with either siCtrl (scrambled control) or siVEGF-C (VEGF-C targeting siRNA), (Mean± SEM, n=3-4). (C) WB for VEGF-C and Tubulin in CPH017 cells 72 h following siCtrl or siVEGF-C transfection. (D) qRT-PCR analysis of VEGF-A expression in CPH017 and IN1123 cells 48 h following siCtrl or siVEGF-C transfection (Mean ± SEM, n=3-4). (E) ELISA quantification of VEGF-A in conditioned media from CPH017 cells transfected with either siCtrl or siVEGF-C (Mean± SD, n=1 in technical duplicates). In panels B and D: One-sample t-tests setting the hypothetical value to one, and in panel E: One-way ANOVA with Dunnett's post test. Significance levels are: * $P \leq 0.05$, *** $P \leq 0.001$, **** $P \leq 0.0001$.

Figure 4. VEGF-C loss leads to transcriptional changes and reduces the viability of GBM cells. (A) Heat map of significantly de-regulated genes (log2 fc ≥ 2 and adjusted $P \leq 0.05$) after VEGF-C knockdown compared to siCtrl. (B) Gene set enrichment analysis (GSEA) using a 479-gene set from the REACTOME pathway database. Top 10 most significant down-regulated and 10 most up-regulated gene sets are shown with Normalized Enrichment Score (NES). (C) Development in viability of CHP017 and IN1123 cells transfected with siCtrl or siVEGF-C (Mean ± SEM, n=3-5). (D) WB of Cleaved (Cl.) Caspase-3 and Tubulin in CPH017 cells 72 h following siCtrl or siVEGF-C transfection. (E) Viability of IN1123 cells transfected with either siCtrl or siVEGF-C-2 alone or combined with 0.5 mg/mL bevacizumab (Bev) (Mean ± SEM, n=3). Statistics are in C: 2-way ANOVA with Bonferroni post test and in E: One-way ANOVA with Dunnett's post test. Significance levels are defined as: * $P \leq 0.05$, ** $P \leq 0.01$, *** $P \leq 0.001$, **** $P \leq 0.0001$.

Figure 5. VEGF-C promotes cell cycle progression and invasion of GBM cells. (A) Representative FACS plot showing cell cycle profile CPH017 cells 72 h post transfection with siCtrl or siVEGF-C. (B) Quantification of SubG1, G1, S and G2/M cell cycle populations based on FACS analysis also shown in A. (Mean ± SEM, n=3-4, Y-scale is log10 transformed). (C) Mitotic index (%)of CPH017 cells 72 h post siCtrl and siVEGF-C knockdown. Cells were treated with nocadozole or DMSO control for 12 hrs prior analysis. (D) WB of phosphorylated Retinoblastoma protein (ppRB) and non-phosphorylated RB protein (pRB), Cyclin A2, Cyclin B1, Cyclin E2 and GAPDH of CPH017 cells 72 hrs post siCtrl and siVEGF-C transfection. (E) Representative images of invasion assay for siCtrl and siVEGF-C-2 treated cells. (F) Quantification of invasive capacity of siCtrl and siVEGF-C transfected IN1123 cells 24 h post stimulation compared to time zero (Mean ± SEM, n=2 each analyzing 6-7 individual cell aggregates per treatment). Statistics are in B and F: One-way ANOVA. Significance levels are: * $P \leq 0.05$, ** $P \leq 0.01$, **** $P \leq 0.0001$, NS: Non-significant.

Figure 6. VEGF-C loss impairs GBM growth *in vivo*. (A) Bioluminescence (BLI) signal in mice 3 days after orthotopically transplantation of CPH017 cells transfected with either siCtrl (9 mice) or siVEGF-C-1 (10 mice). (B) Representative images of BLI and MRI scans of siCtrl mice (M1, M2) and siVEGF-C1 mice (M3, M4). (C) Development in BLI signal over time as compared to the signal at day 3 following transplantation (Mean ± SEM). (D) Correlation between volume (mm^3) on MRI

scans on 28 post transplantation and BLI signal (photons/sec) at day 23. (E) Kaplan-Meier survival analysis of cumulative survival from tumor cell injection until sacrifice of VEGF-C-siRNA and Ctrl-siRNA mice. Statistics are in A: Non-paired t-test, C: 2-way ANOVA with Bonferroni's post test, D: Spearman correlation analysis and E: Log-rank test. Significance levels are: **** $P \leq 0.0001$, NS: Non-significant. (F) Schematic illustration of our hypothesis that VEGF-C stimulates VEGFR2 expressed by GBM cells (both autocrine and paracrine manner) to promote survival, proliferation and invasion. In contrast to VEGF-A signaling, that is abrogated upon bevacizumab treatment, remains VEGF-C secretion and signaling active under bevacizumab therapy and thus represents a novel evasion mechanism developed by GBM cells.

Figure 1

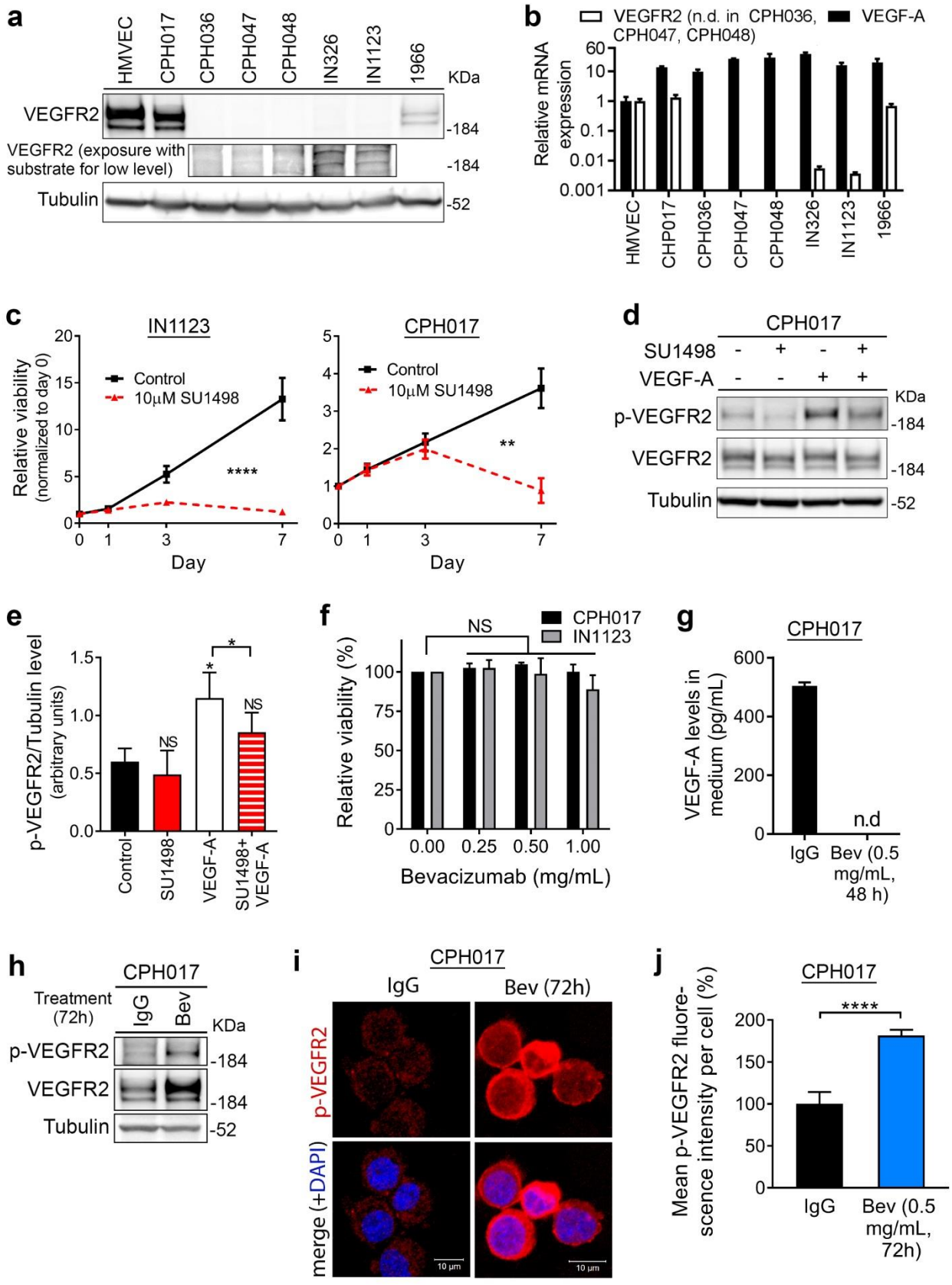
a
HMVEC
CPH017
CPH036
CPH047
CPH048
IN326
IN1123
1966
KDa
VEGFR2
-184
VEGFR2 (exposure with substrate for low level)
-184
Tubulin
-52
b
VEGFR2 (n.d. in CPH036, CPH047, CPH048)
VEGF-A
Relative mRNA expression
60
10
1
0.1
0.01
0.001
HMVEC
CHP017
CPH036
CPH047
CPH048
IN326
IN1123
1966
c
IN1123
Relative viability (normalized to day 0)
Control
10μM SU1498
****
Day
CPH017
Control
10μM SU1498
**
Day
d
CPH017
SU1498 - + - +
VEGF-A - - + +
KDa
p-VEGFR2
-184
VEGFR2
-184
Tubulin
-52
e
p-VEGFR2/Tubulin level (arbitrary units)
*
*
NS
NS
Control
SU1498
VEGF-A
SU1498+ VEGF-A
f
NS
CPH017
IN1123
Relative viability (%)
0.00
0.25
0.50
1.00
Bevacizumab (mg/mL)
g
CPH017
VEGF-A levels in medium (pg/mL)
n.d
IgG
Bev (0.5 mg/mL, 48 h)
h
CPH017
Treatment (72h)
IgG
Bev
KDa
p-VEGFR2
-184
VEGFR2
-184
Tubulin
-52
i
CPH017
IgG
Bev (72h)
p-VEGFR2
merge (+DAPI)
10 μm
10 μm
j
CPH017
****
Mean p-VEGFR2 fluorescence intensity per cell (%)
IgG
Bev (0.5 mg/mL, 72h)

Figure 2

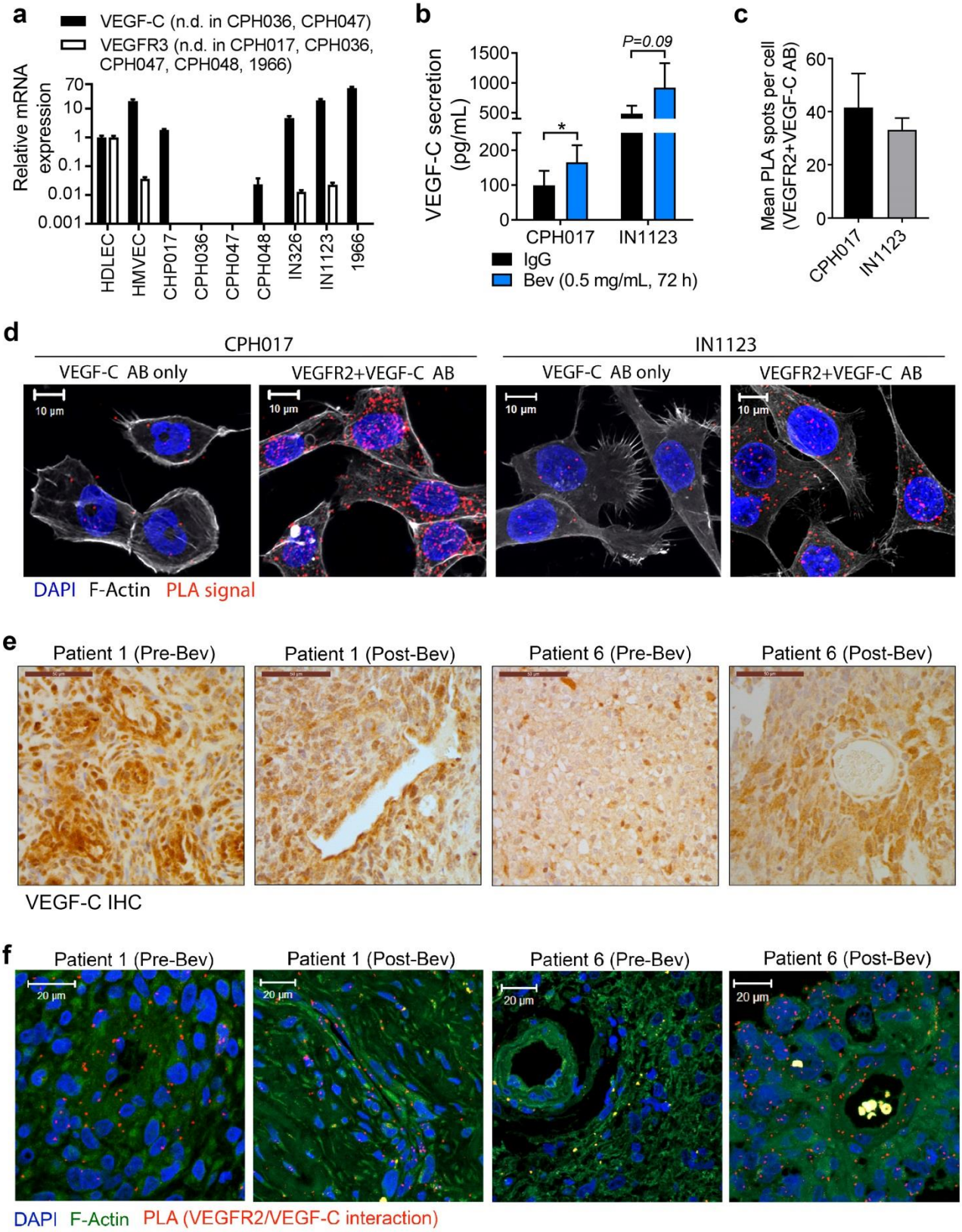
a
VEGF-C (n.d. in CPH036, CPH047)
VEGFR3 (n.d. in CPH017, CPH036, CPH047, CPH048, 1966)
Relative mRNA expression
70
10
1
0.1
0.01
0.001
HDLEC
HMVEC
CHP017
CPH036
CPH047
CPH048
IN326
IN1123
1966
b
VEGF-C secretion (pg/mL)
1500
1000
500
200
100
0
P=0.09
*
CPH017
IN1123
IgG
Bev (0.5 mg/mL, 72 h)
c
Mean PLA spots per cell (VEGFR2+VEGF-C AB)
60
40
20
0
CPH017
IN1123
d
CPH017
IN1123
VEGF-C AB only
VEGFR2+VEGF-C AB
VEGF-C AB only
VEGFR2+VEGF-C AB
10 µm
DAPI F-Actin PLA signal
e
Patient 1 (Pre-Bev)
Patient 1 (Post-Bev)
Patient 6 (Pre-Bev)
Patient 6 (Post-Bev)
VEGF-C IHC
f
Patient 1 (Pre-Bev)
Patient 1 (Post-Bev)
Patient 6 (Pre-Bev)
Patient 6 (Post-Bev)
20 µm
DAPI F-Actin PLA (VEGFR2/VEGF-C interaction)

Figure 3

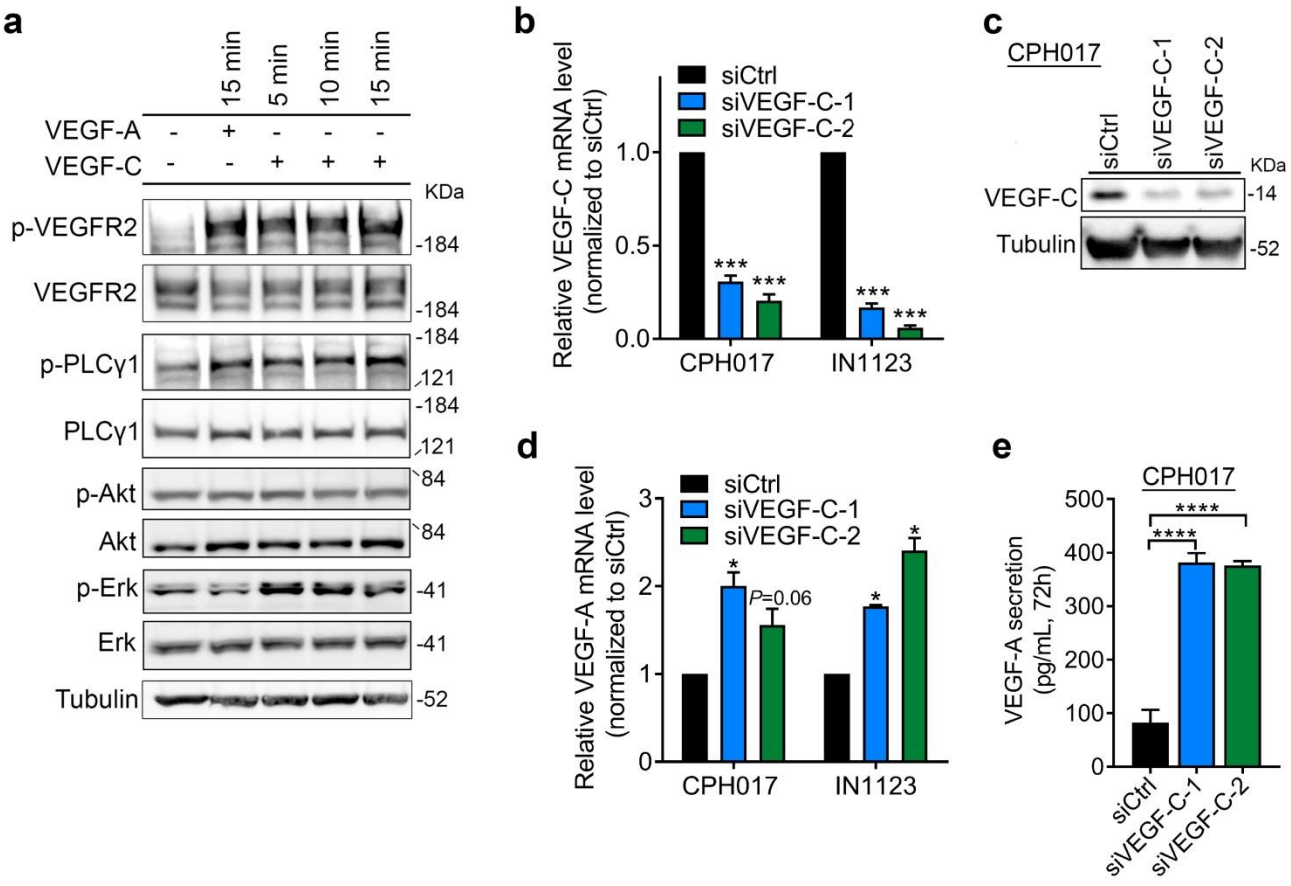
a
15 min
5 min
10 min
15 min
VEGF-A - + - - -
VEGF-C - - + + +
KDa
p-VEGFR2
-184
VEGFR2
-184
p-PLCγ1
-184
-121
PLCγ1
-184
-121
p-Akt
-84
Akt
-84
p-Erk
-41
Erk
-41
Tubulin
-52
b
Relative VEGF-C mRNA level (normalized to siCtrl)
siCtrl
siVEGF-C-1
siVEGF-C-2
1.0
0.5
0.0
***
***
***
***
CPH017
IN1123
c
CPH017
siCtrl
siVEGF-C-1
siVEGF-C-2
KDa
VEGF-C
-14
Tubulin
-52
d
Relative VEGF-A mRNA level (normalized to siCtrl)
siCtrl
siVEGF-C-1
siVEGF-C-2
3
2
1
0
*
*
P=0.06
*
*
CPH017
IN1123
e
CPH017
VEGF-A secretion (pg/mL, 72h)
500
400
300
200
100
0
****
****
siCtrl
siVEGF-C-1
siVEGF-C-2

Figure 4

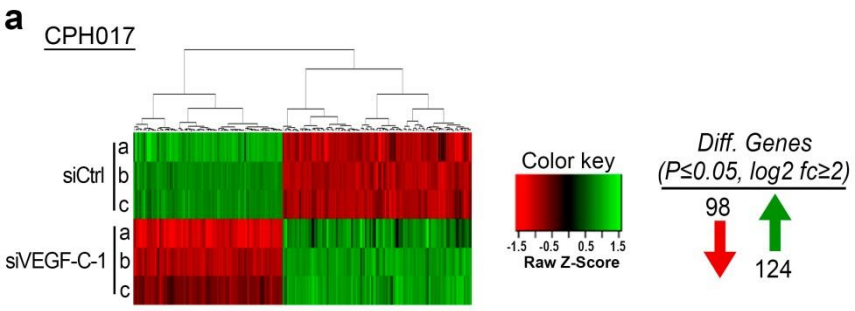

b

Top 10 down-regulated gene sets following VEGF-C knockdown	NES*
Cell Cycle	-2.95
DNA Replication	-2.92
Cell Cycle Mitotic	-2.92
Mitotic M-M/G1 phases	-2.76
Chromosome Maintenance	-2.74
Mitotic Prometaphase	-2.70
Deposition of new CENPA-containing nucleosomes at the centromere	-2.60
Meiosis	-2.59
Meiotic Recombination	-2.59
Telomere Maintenance	-2.57

Top 10 up-regulated gene sets following VEGF-C knockdown	NES*
Interferon signaling	3.06
Interferon alpha/beta signaling	3.00
Cytokine Signaling in Immune system	2.94
Interferon gamma signaling	2.83
Rig-I/MDA5 mediated induction of IFN-alpha/beta pathways	2.30
Antiviral mechanism by IFN stimulated genes	2.24
Regulation of IFNA signaling	2.22
TRAF6 mediated IRF7 activation	2.18
Chemokine receptors bind chemokines	2.18
Antigen procession-Cross presentation	2.08

*Normalized Enrichment Score

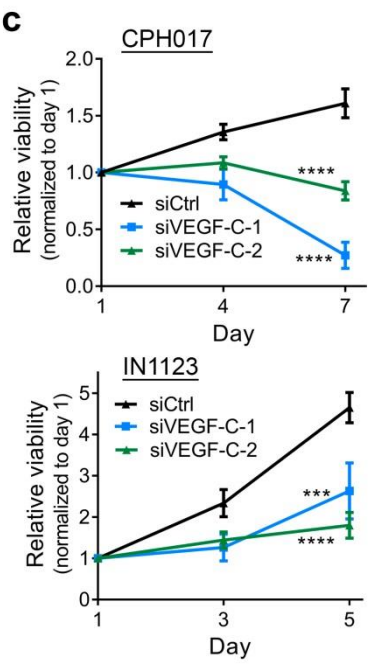

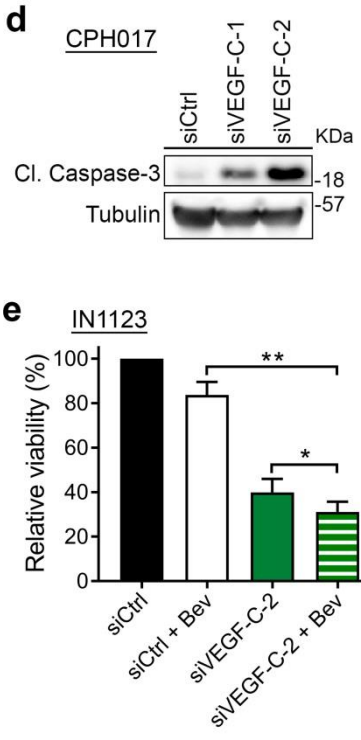

Figure 5

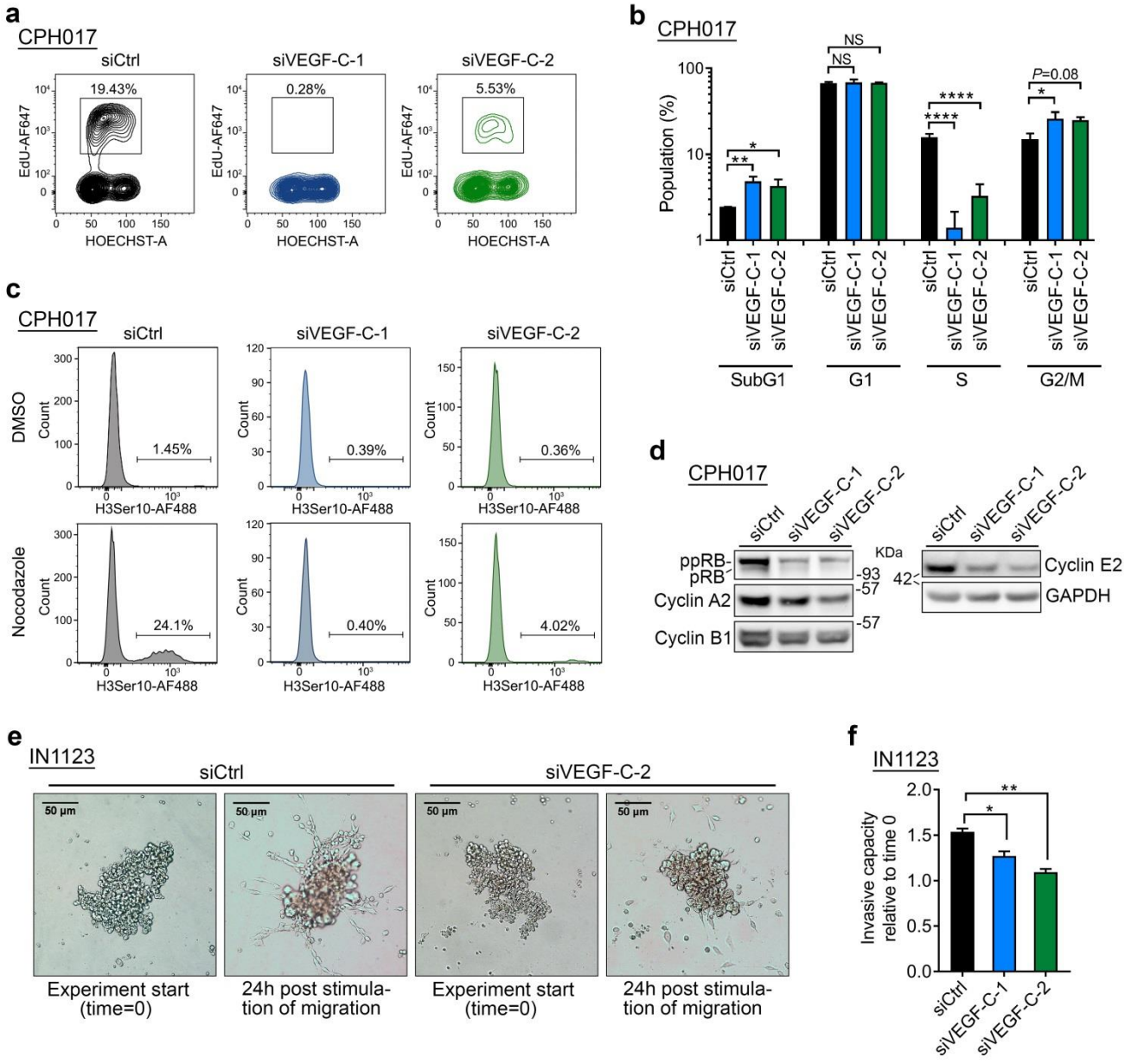
a
CPH017
siCtrl
siVEGF-C-1
siVEGF-C-2
19.43%
0.28%
5.53%
EdU-AF647
HOECHST-A
b
CPH017
Population (%)
NS
NS
P=0.08
SubG1
G1
S
G2/M
siCtrl
siVEGF-C-1
siVEGF-C-2
c
CPH017
DMSO
Nocodazole
Count
H3Ser10-AF488
1.45%
0.39%
0.36%
24.1%
0.40%
4.02%
d
CPH017
ppRB-
pRB
Cyclin A2
Cyclin B1
KDa
Cyclin E2
GAPDH
e
IN1123
siCtrl
siVEGF-C-2
50 µm
Experiment start (time=0)
24h post stimulation of migration
f
IN1123
Invasive capacity relative to time 0

Figure 6

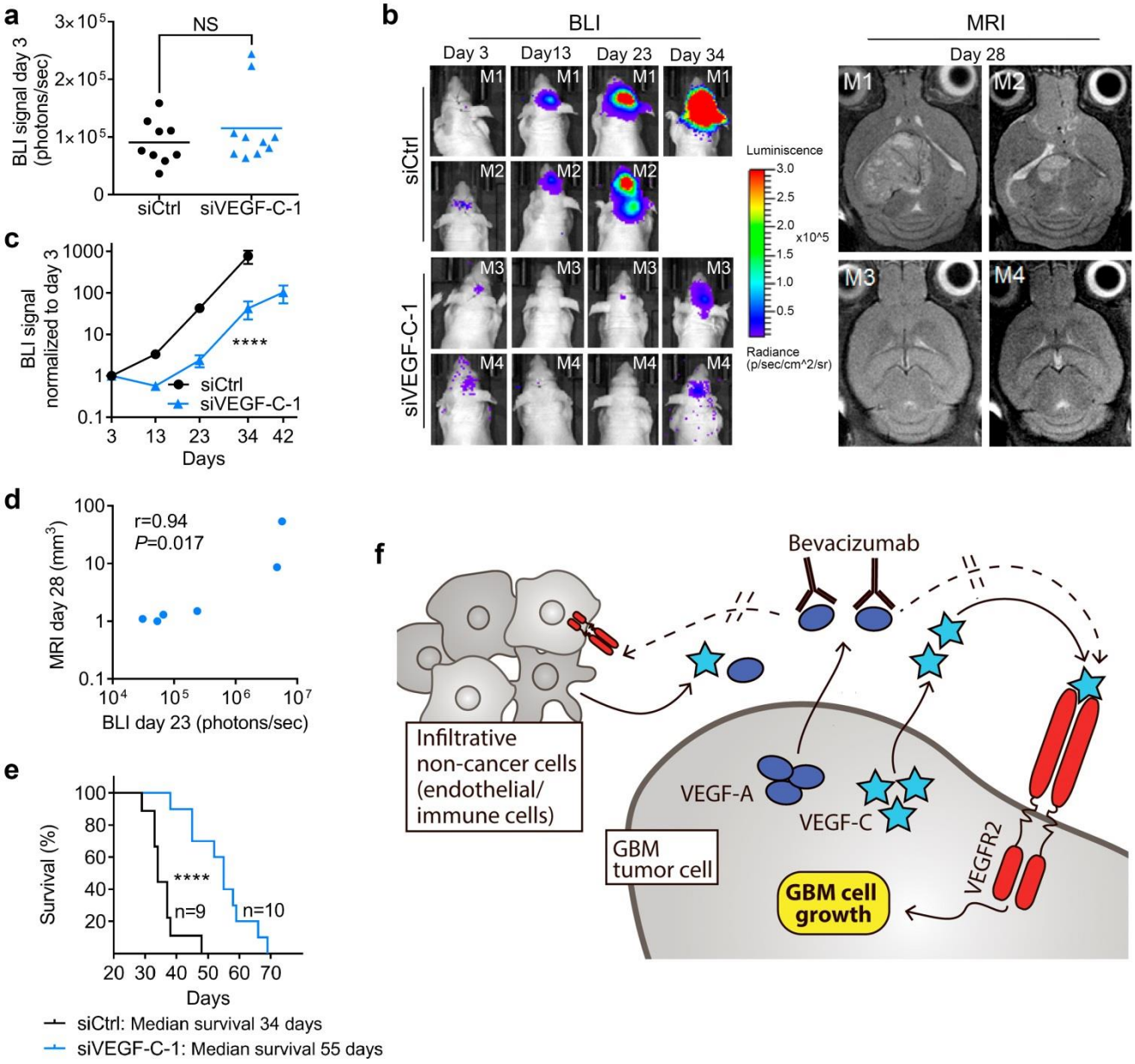
a
BLI signal day 3 (photons/sec)
NS
siCtrl
siVEGF-C-1
b
BLI
MRI
Day 3
Day13
Day 23
Day 34
Day 28
siCtrl
siVEGF-C-1
Luminiscence
Radiance (p/sec/cm^2/sr)
c
BLI signal normalized to day 3
****
siCtrl
siVEGF-C-1
Days
d
MRI day 28 (mm3)
r=0.94
P=0.017
BLI day 23 (photons/sec)
e
Survival (%)
****
n=9
n=10
Days
siCtrl: Median survival 34 days
siVEGF-C-1: Median survival 55 days
f
Bevacizumab
Infiltrative non-cancer cells (endothelial/ immune cells)
VEGF-A
VEGF-C
VEGFR2
GBM tumor cell
GBM cell growth

SUPPLEMENTARY MATERIAL

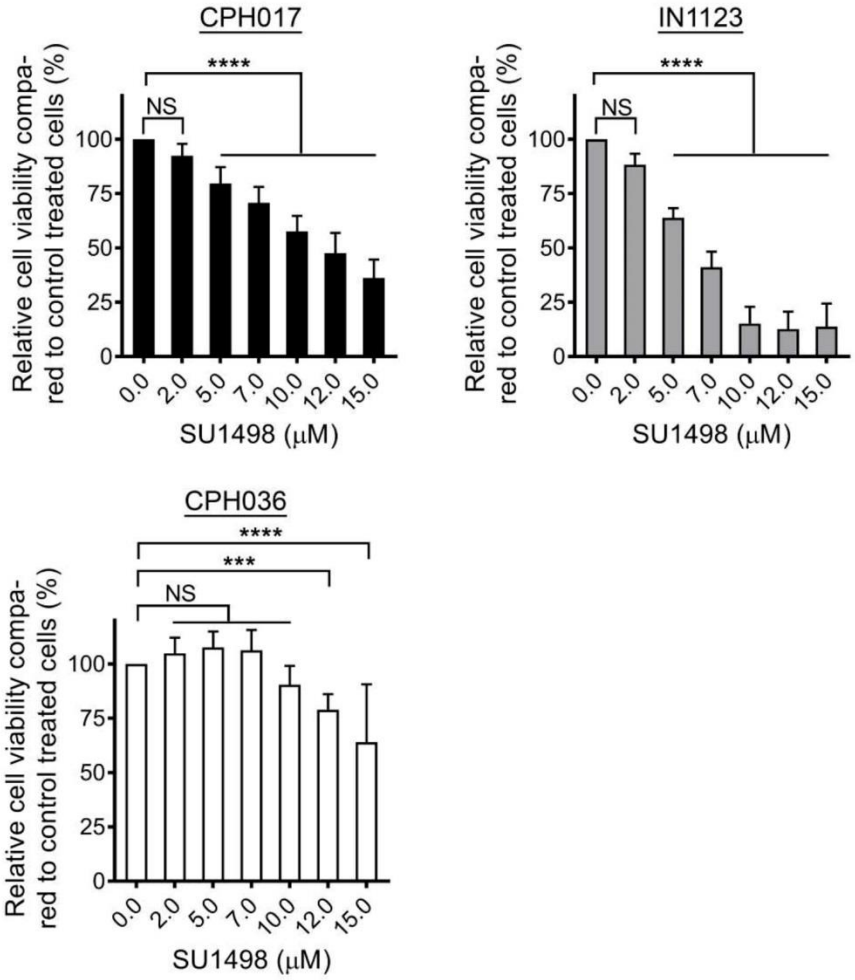

Supplementary Figure S1. Effect of VEGFR2 inhibitor SU1498 in GBM cultures. Relative viability of CPH017 (VEGFR2 high), IN1123 (VEGFR2 moderate) and CPH036 (VEGFR2 negative) cells exposed to 0-15μM SU1498 for 7 days (Mean ± 95% Confidence Interval, n=3). Statistical test is result of a 2-way ANOVA with Bonferroni post test.

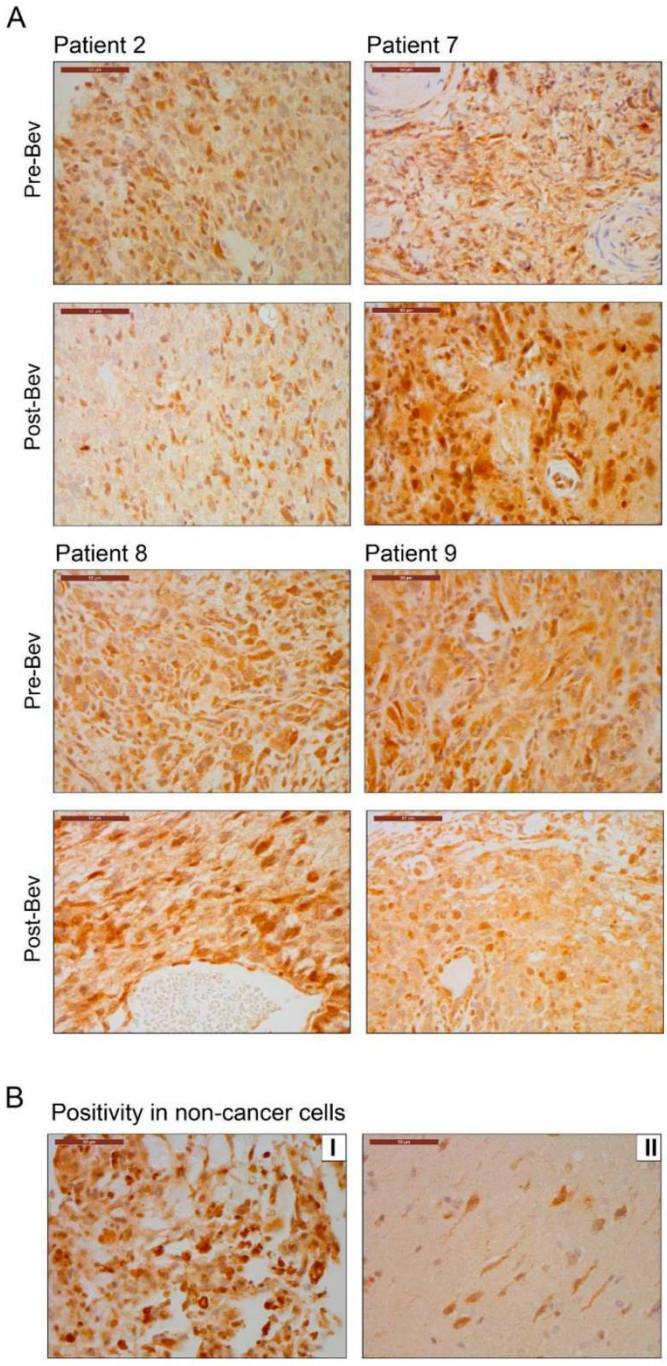

Supplementary Figure S2. VEGF-C IHC staining of GBM tumor tissue. (A) Representative images of IHC staining showing VEGF-C positivity of tumor cells in parallel tumor samples from routine surgery of 4 GBM patients before and after therapy with Bev. Heterogeneous positivity for VEGF-C was observed in astrocytic tumor cells. Positivity was also found in endothelial cells of non-neoplastic as well as neoplastic vessels. Patient characteristics can be found in Table S1. (B) Representative images of stained tumors showing VEGF-C IHC positivity in tumor-infiltrating macrophages (I) and normal neurons in tumor periphery (II) as identified based on morphology. Scale bar shows 50 µm.

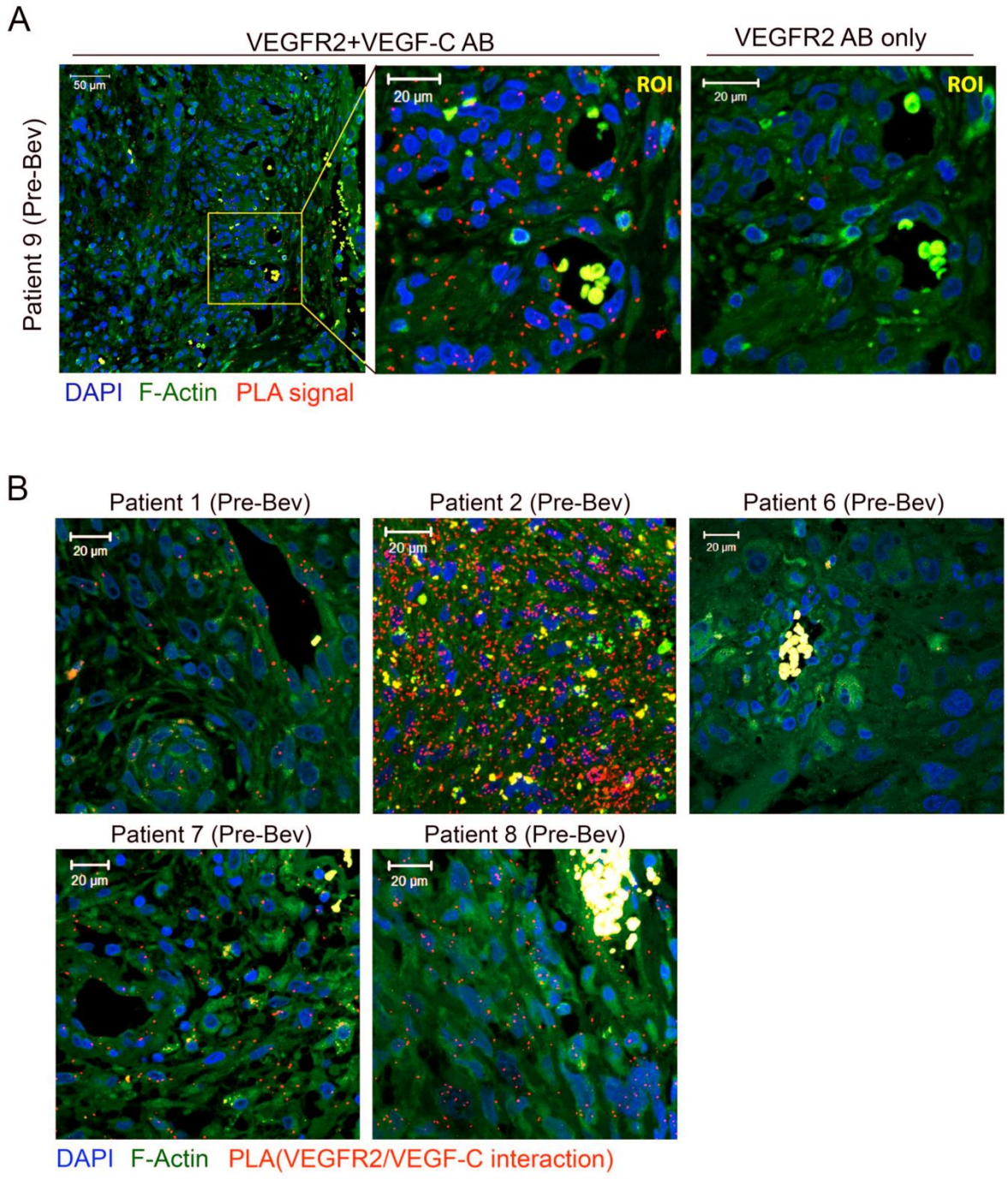

Supplementary Figure S3. Visualization of VEGFR2 and VEGF-C interaction in GBM tumor tissue using PLA Duolink technology. (A) Representative images of signal in parallel tissue sections from a bevacizumab (Bev) -naïve patient tumor sample incubated with either both VEGFR2 and VEGF-C antibody (AB) or VEGFR2 AB alone to show background staining. (B) Images of signal in 5 additional Bev-naïve patient samples, of which for some other regions are shown in main figure 3. Patient characteristics can be found in Table S1.

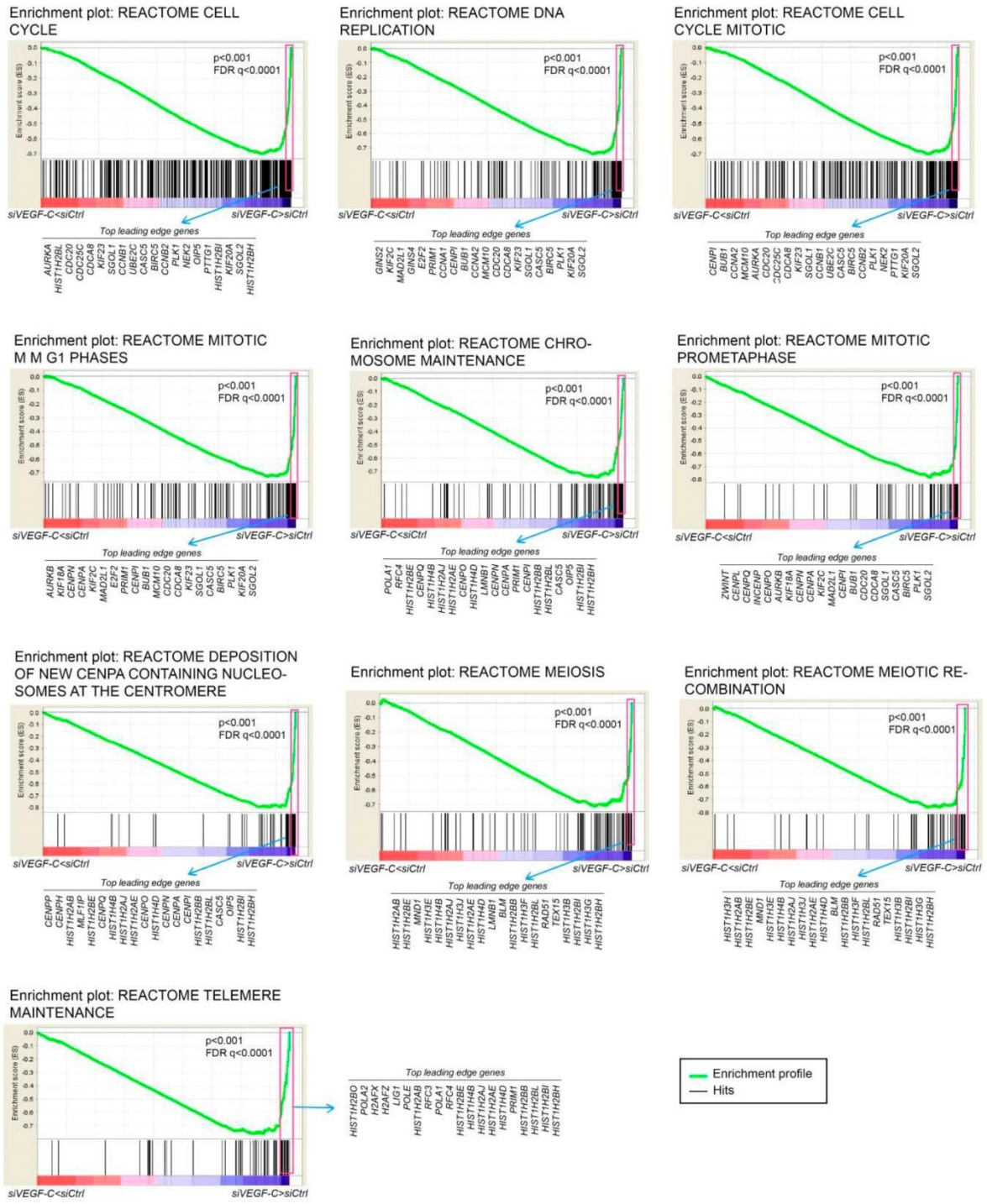

Supplementary Figure S4. Top 10 down-regulated gene sets following VEGF-C knockdown. GSEA plots and top leading edge genes for top 10 down-regulated REACTOME gene signature pathways.

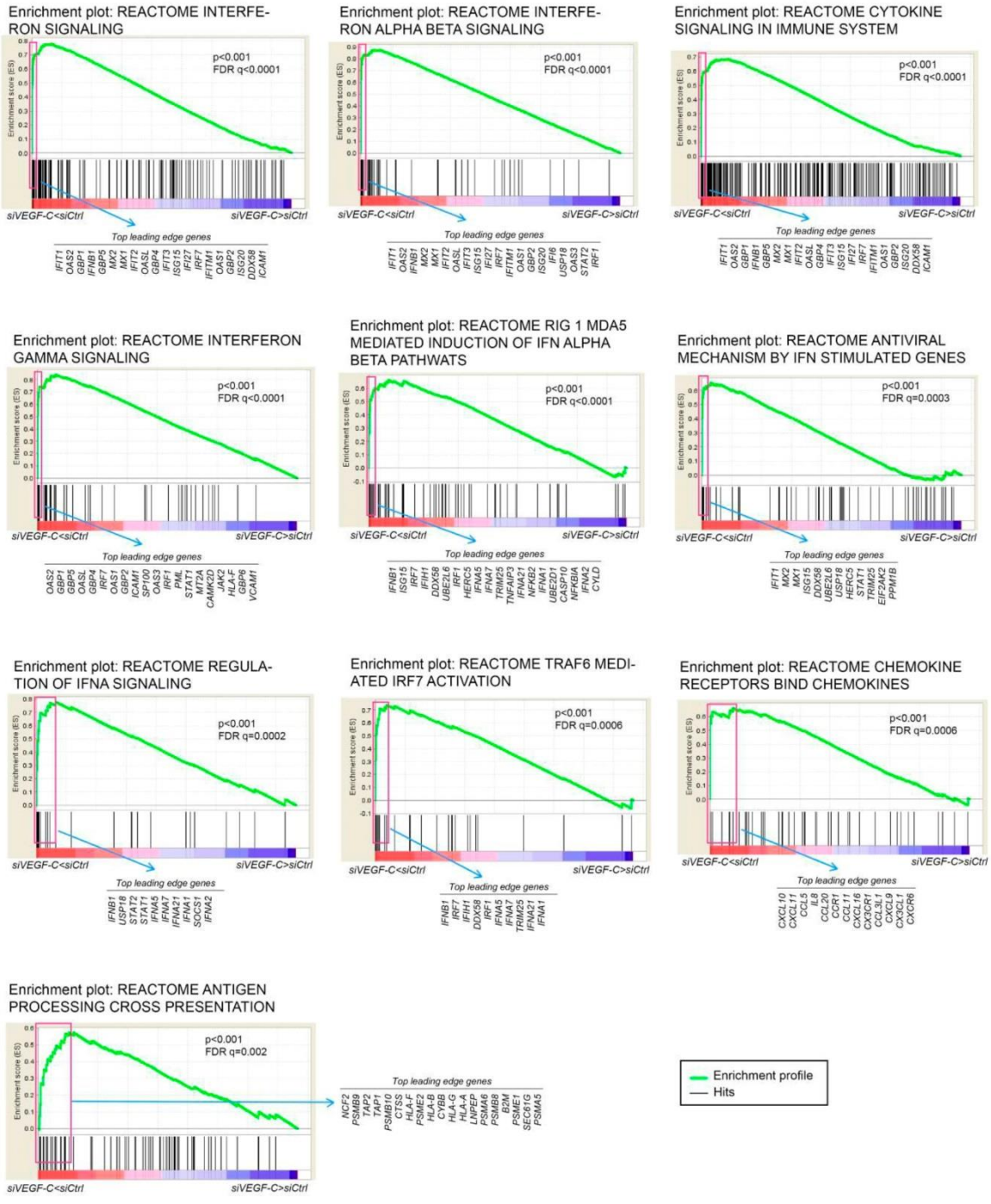

Supplementary Figure S5. Top 10 up-regulated gene sets following VEGF-C knockdown. GSEA plots and top leading edge genes for top 10 up-regulated REACTOME gene signature pathways.

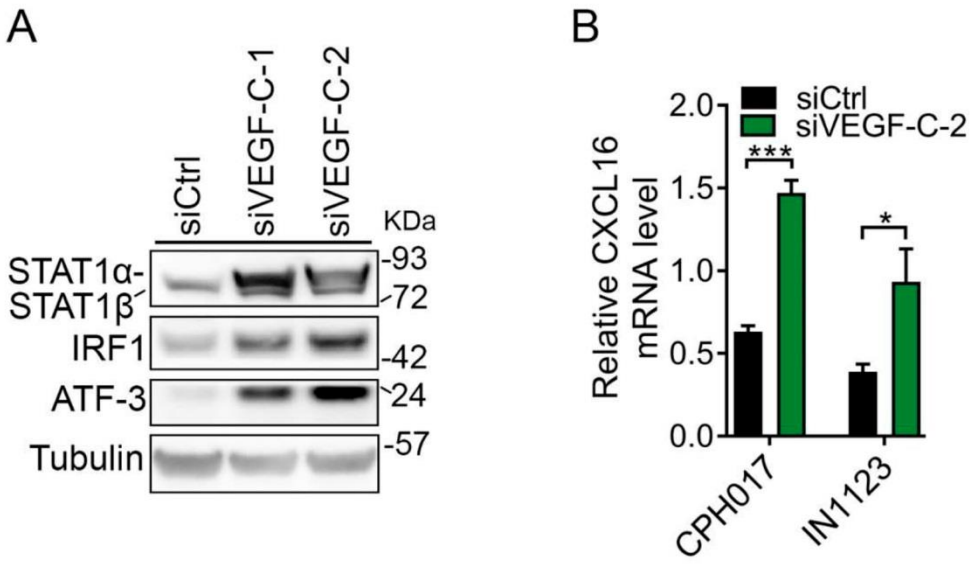

Supplementary Figure S6. Expression changes of selected markers following VEGF-C knockdown. (A) WB analysis for pro survival molecules STAT1α/β and IRF1, pro-migratory molecule ATF-3 and Tubulin in CPH017 cells 72 h following siCtrl or siVEGF-C treatment. (B) qRT-PCR measurements of relative mRNA expression of the migratory related molecule CXCL16 in siCtrl and siVEGF-C-2 CPH017 and IN1123 cells (Mean ± SEM, n=2-3). For STAT1α/β, IRF1, ATF-3 and CXCL16, WB and qRT-PCR changes correlates with changes seen in microarray analysis (Figure S5, Table S3).

Supplementary Table S1. Patient and treatment characteristics for samples examined by VEGF-C IHC and VEGFR2/VEGF-C PLA interaction assay

Patient case number	Age at start of Bev treatment (Years)	Gender	Duration of Bev treatment (Weeks)	Agent combined with Bev	Time from last dose of Bev until surgery (Days)	Survival from time of Bev resistance (Weeks)	Best Response on Bev treatment (RANO)
Patient 1 (C1)	65	F	6	CPT-11	27	23	R
Patient 2 (C1)	56	F	16	CPT-11	23	12	PD
Patient 3 (C1)	54	M	22	CPT-11	125	36	SD
Patient 4 (C1)	61	M	63	CPT-11	36	82	SD
Patient 5 (C1)	66	M	22	CPT-11	34	11	SD
Patient 6 (C1)	21	F	10	CPT-11	29	17	SD
Patient 7 (C1)	52	M	46	CPT-11	36	13	R
Patient 8 (C1)	51	M	22	CPT-11	49	18	R
Patient 9 (C1)	53	F	28	CPT-11	101	22	R
Patient 10 (C2)	45	M	14	CPT-11	236	41	R
Patient 11 (C2)	61	F	14	CPT-11	29	14	PD
Patient 12 (C2)	56	M	115	CPT-11	45	30	R
AVERAGE	**53.4**	**F:5, M:7**	**31.5**	**CPT-11**	**64.2**	**26.6**	**R:6, SD:4, PD:2**

Abbreviations: C1, Center 1; C2, Center 2; F, female; M, male; PD, progressive disease; R, either complete or partial response; SD, stable disease.

Supplementary Table S2. Genes with decreased expression in siVEGF-C samples compared to siCtrl samples (log2 fold change (fc) ≤ -2 and adj *P* ≤ 0.05)

Gene	Probeset_id	log2fc	adj. *P*-val	Gene	Probeset_id	log2fc	adj. *P*-val
KIF20A	16989636	-3.60	0.00510	SKA3	16777278	-2.38	0.00873
HIST1H3G	17016403	-3.59	0.00181	ESCO2	17067332	-2.37	0.02975
PLK1	16817017	-3.56	0.00116	DEPDC1	16688386	-2.36	0.00190
STMN2	17070249	-3.29	0.00032	ARHGAP11A	16798919	-2.36	0.00185
PI15	17070110	-3.23	0.00185	OIP5	16807605	-2.34	0.00871
DLGAP5	16793225	-3.21	0.00130	GPSM2	16668079	-2.32	0.00164
TUBB1	16915395	-3.14	0.00565	CEP55	16707551	-2.32	0.00229
CENPE	16978568	-3.03	0.00130	HIST1H1C	17016372	-2.31	0.00157
TOP2A	16844312	-3.03	0.00085	LINC00403	16776620	-2.28	0.01860
ASPM	16697544	-3.02	0.00134	SGOL2	16889251	-2.28	0.00878
HJURP	16909700	-2.95	0.00101	MAOB	17110289	-2.27	0.00708
PRR11	16836492	-2.94	0.00085	FAM72D	16691883	-2.26	0.00246
SHCBP1	16826160	-2.94	0.00395	AURKA	16920548	-2.26	0.00058
KIF23	16802519	-2.93	0.00761	SGOL1	16951485	-2.24	0.00695
KIF4A	17104484	-2.89	0.00101	CKAP2L	16901957	-2.23	0.00854
BIRC5	16838359	-2.89	0.00056	CDC25C	17000439	-2.20	0.01075
HMMR	16991859	-2.88	0.00076	SMC2	17087716	-2.20	0.00263
HIST1H3B	17016363	-2.88	0.00950	KIF4B	16991460	-2.19	0.00287
TPX2	16912379	-2.84	0.00085	HIST1H2BB	17016369	-2.19	0.00871
KIF14	16697695	-2.76	0.00050	AURKB	16840902	-2.18	0.00106
CCNB2	16801557	-2.75	0.00019	---	17121912	-2.18	0.01090
CCNB1	16985599	-2.72	0.00108	CCNF	16815090	-2.17	0.00241
CDC20	16663514	-2.72	0.00357	HIST1H2BH	17005600	-2.17	0.00324
SPC24	16868838	-2.66	0.01504	ANLN	17045198	-2.17	0.00156
KRT13	16844735	-2.66	0.04176	SPC25	16904780	-2.17	0.00234
HIST1H3F	17016400	-2.62	0.00139	HIST1H4D	17016383	-2.17	0.00051
HIST1H2AI	17005858	-2.61	0.00162	NEIL3	16972616	-2.16	0.01027
NDC80	16850517	-2.59	0.00206	DIAPH3	16779546	-2.16	0.00997
SLC6A14	17106398	-2.58	0.00203	ACO1	17084184	-2.15	0.00081
CDK1	16705159	-2.57	0.00071	CDCA3	16760621	-2.13	0.00030
PBK	17075776	-2.56	0.00134	POMK	17068636	-2.11	0.00085
CASC5	16799598	-2.55	0.00086	TICRR	16804631	-2.11	0.00181
CDCA8	16662648	-2.55	0.00059	GTSE1	16931384	-2.10	0.00112
SPAG5	16842673	-2.55	0.00017	GAS2L3	16755692	-2.10	0.00344
CENPF	16677425	-2.55	0.00037	PRC1	16813342	-2.10	0.00085
CCNA2	16979515	-2.54	0.00376	NCAPD2	16747287	-2.09	0.00070
UBE2C	16914315	-2.50	0.00102	RAD51	16799637	-2.08	0.00556
ST6GALNAC1	16849286	-2.50	0.00556	NUSAP1	16799793	-2.08	0.00287
TTK	17010552	-2.49	0.00159	LMNB1	16988703	-2.07	0.00037
CCL24	17058870	-2.48	0.00190	ERP27	16761830	-2.07	0.01010
FAM64A	16830173	-2.48	0.00184	NCAPH	16882975	-2.07	0.00355
CDCA2	17067102	-2.44	0.00253	KLHDC8A	16698476	-2.06	0.00253
NUF2	16673154	-2.44	0.00167	E2F8	16736638	-2.06	0.01326
MKI67	16719515	-2.42	0.00472	HTR1D	16683264	-2.05	0.01340
NCAPG	16965346	-2.42	0.00574	SLC26A9	16698590	-2.03	0.00544
NEK2	16698984	-2.41	0.00063	GPA33	16695974	-2.02	0.00017
CENPI	17105401	-2.41	0.00156	MCM10	16702571	-2.02	0.00548
DSCC1	17080595	-2.40	0.02231	KIF15	16939960	-2.01	0.00157
BUB1	16901755	-2.39	0.00287	FAM83D	16913681	-2.01	0.00415

Supplementary Table S3. Genes with increased expression in siVEGF-C samples compared to siCtrl samples (log2 fold change (fc) ≥ 2 and adj *P* ≤ 0.05)

Gene	Probeset_id	log2fc	adj. *P*-val	Gene	Probeset_id	log2fc	adj. *P*-val
CXCL10	16977052	7.64	0.000760	SLFN5	16833327	2.65	0.006861
BST2	16870200	6.75	0.000034	SAMD9	17059771	2.65	0.000647
CXCL11	16977058	6.74	0.000062	GBP2	16689354	2.65	0.009284
IFIT1	16707196	6.50	0.000034	GDF15	16859795	2.63	0.006950
XAF1	16830202	6.38	0.000499	ZNFX1	16920121	2.61	0.000089
OAS2	16757373	6.34	0.000933	GBP2	16689352	2.61	0.001885
IFI44	16666509	6.13	0.000048	OAS3	16757347	2.59	0.000166
RSAD2	16876764	6.12	0.000065	---	17123260	2.58	0.003065
MX1	16923031	5.19	0.000028	ANKRD1	16716478	2.58	0.006234
IFI44L	16666485	5.01	0.000055	---	17123268	2.56	0.041163
CMPK2	16894127	4.98	0.000048	---	17121624	2.55	0.000366
IFIT2	16707180	4.92	0.000034	---	16790260	2.54	0.008344
IFIT3	16707184	4.88	0.000041	ESM1	16996146	2.53	0.016163
CCL5	16843511	4.65	0.000499	UBE2L6	16738544	2.53	0.000892
ISG15	16657594	4.51	0.000034	C19orf66	16858080	2.51	0.000795
MX2	16922959	4.51	0.002477	---	17121622	2.51	0.000366
OASL	16771417	4.38	0.001837	RASGRP3	16878994	2.50	0.002142
IFITM1	16720085	4.33	0.000028	APOL1	16929631	2.49	0.002163
RTP4	16949442	3.99	0.001454	PARP14	16944695	2.48	0.000123
DHX58	16844999	3.93	0.003549	IFIT5	16707202	2.47	0.001158
TMEM140	17051943	3.87	0.003947	---	16947873	2.45	0.000499
CXCL8	16967771	3.80	0.000043	---	16766130	2.44	0.011052
GBP1	16689332	3.79	0.000193	---	17123270	2.43	0.037227
IFNB1	17092809	3.74	0.002392	LOC105370924	16803891	2.39	0.006456
IFIH1	16904365	3.67	0.000068	RPLP0P2	16725664	2.36	0.001158
CSAG3	17107896	3.67	0.000193	HERC5	16968765	2.36	0.000499
CSAG3	17115039	3.67	0.000193	STAT1	16906534	2.35	0.000118
EPSTI1	16778559	3.61	0.000499	LGALS9B	16842403	2.33	0.001449
OAS1	16757324	3.61	0.000277	CEACAM1	16872803	2.30	0.001482
SAMD9L	17059776	3.58	0.000092	KLHDC7B	16931766	2.30	0.004432
IFI27	16787814	3.51	0.011131	SP140L	16891890	2.29	0.013278
IFI6	16684080	3.42	0.000123	---	16770471	2.27	0.009033
DDX58	17093090	3.41	0.000034	---	16790259	2.25	0.004486
SSTR2	16837426	3.38	0.002247	TNFRSF9	16681288	2.23	0.009284
IRF7	16733995	3.37	0.000109	TRIM22	16721280	2.23	0.000504
GBP5	16689400	3.36	0.000062	UBA7	16954217	2.21	0.011233
HELZ2	16921289	3.35	0.000499	PLSCR1	16960186	2.21	0.000762
---	17123262	3.34	0.014172	TRIM14	17096436	2.20	0.000499
CD68	16830577	3.31	0.000193	RIN2	16911835	2.20	0.005884
HERC6	16968735	3.13	0.000118	ATF3	16677278	2.17	0.001102
DDX60L	16981266	3.12	0.000048	---	17119920	2.15	0.000647
AIM2	16695121	3.10	0.021243	IDO1	17068296	2.15	0.017506
---	17121224	3.07	0.023709	IRF9	16782687	2.12	0.000321
---	17123266	3.02	0.041514	---	16790258	2.10	0.006950
TRANK1	16952118	3.01	0.002090	GBP3	16689312	2.10	0.000853
USP18	16926942	3.00	0.000118	LOC100507460	16885802	2.09	0.007747
SP110	16909413	2.99	0.000286	TLR3	16972993	2.07	0.011052
---	17122070	2.96	0.028330	PARP9	16958124	2.07	0.000533
---	17119916	2.95	0.001974	IFNL2	16861953	2.06	0.029544
---	17123264	2.94	0.023709	ICAM1	16858137	2.05	0.020840
---	16917440	2.89	0.001393	IFITM4P	17016760	2.05	0.000500
SP100	16891922	2.88	0.000062	---	17036173	2.05	0.000500
MAB21L2	16971409	2.85	0.001567	TGM2	16919158	2.03	0.025617
IFNL1	16861961	2.74	0.005950	PARP12	17063480	2.03	0.000167
CD274	17083357	2.70	0.007376	---	17031434	2.02	0.000508
TNFSF10	16961616	2.70	0.000754	RUFY4	16890723	2.02	0.000795
ANO7P1	16682144	2.70	0.004408	---	17033890	2.02	0.000499
MMP13	16743764	2.70	0.005823	---	17038932	2.02	0.000499
DDX60	16981219	2.69	0.000118	PML	16802918	2.02	0.000769
---	16997835	2.69	0.037332	PLEKHA4	16874109	2.02	0.000947
GBP4	16689384	2.67	0.010364	LGMN	16796060	2.01	0.002477
STAT2	16766093	2.66	0.000118	FBXO6	16659036	2.00	0.000528

Supplementary Table S4. Sequences and cycling conditions for primers used for qRT-PCR detection

Gene	Primer sequences (5'-3')	Cycling conditions
VEGFR3	F: CATCCAGCTGTTGCCCAGG R: GAGCCACTCGACGCTGATGAA	95ºC for 45s, 65ºC for 45s and 72ºC for 45s for 50 cycles, with initial melting at 95ºC for 2 min.
VEGF-C	F: CACGAGCTACCTCAGCAAGA R: GCTGCCTGACACTGTGGTA	95ºC for 10s, 62ºC for 5s, 72ºC for 8s for 50 cycles, with initial melting at 95ºC for 2 min.
VEGF-A	F: CCTTGCTGCTCTACCTCCAC R: ATCTGCATGGTGATGTTGGA	95ºC for 15s and 60ºC for 60s for 50 cycles, with initial melting at 95ºC for 2 min.
VEGFR2	F: GTGACCAACATGGAGTCGTG R: TGCTTCACAGAAGACCATGC	
CXCL16	F: CCTATGTGCTGTGCAAGAGGAG R: CTGGGCAACATAGAGTCCGTCT	
TOP1. CYC1 and EIF4A2 (human specific)	From Primer Design geNorm housekeeping gene selection kit	

Manufacturer: TOP1, CYC1 and EIF4A2 primers were purchased from Primer Design (Chandler's Ford, United Kingdom) and the remaining from TAG Copenhagen (Frederiksberg. Denmark)

Supplementary Table S5. Application. dilution and manufacturer of utilized primary and secondary antibodies

Antibody	***Application with dilution***	***Manufacturer***
	Primary antibodies	
p-PLCγ1 (tyr783) (rabbit polyclonal)	WB: 1:1000	Cell Signaling Technology (#2821)
PLCγ1 (rabbit polyclonal)	WB: 1:1000	Cell Signaling Technology (#2822)
p-Akt (ser473) (rabbit polyclonal)	WB: 1:1000	Cell Signaling Technology (#9271)
Akt (rabbit polyclonal)	WB: 1:1000	Cell Signaling Technology (#9272)
p-Erk (thr202/tyr204) (mouse monoclonal)	WB: 1:2000	Cell Signaling Technology (#9106)
Erk (rabbit polyclonal)	WB: 1:1000	Cell Signaling Technology (#9102)
Cl. Capase-3 (rabbit monoclonal)	WB: 1:1000	Cell Signaling Technology (#9664)
ppRb/pRB (mouse monoclonal)	WB: 1:1000	BD Pharmingen (#554136)
Cyclin A2 (mouse monoclonal)	WB: 1:2000	Cell Signaling Technology (#4656)
Cyclin B1 (rabbit monoclonal)	WB: 1:1000	Cell Signaling Technology (#12231)
Cyclin E2 (rabbit polyclonal)	WB: 1:1000	Cell Signaling Technology (#4132)
STAT1 (mouse monoclonal)	WB: 1:1000	Cell Signaling Technology (#9176)
ATF-3 (rabbit polyclonal)	WB: 1:1000	Santa Cruz Biotechnology (#188)
IRF1 (rabbit polyclonal)	WB: 1:1000	Santa Cruz Biotechnology (#13041)
PTEN (mouse monoclonal)	WB: 1:200	Santa Cruz Biotechnology (#7974)
GAPDH (rabbit polyclonal)	WB: 1:10000	Santa Cruz Biotechnology (#25778)
α-Tubulin (rabbit monoclonal)	WB:1:1000, IF: 1:1000	Cell Signaling Technology (#2125S)
VEGFR2 (rabbit monoclonal)	WB: 1:1000	Cell Signaling Technology (#2479)
VEGFR2 (mouse monoclonal)	PLA: 1:500	Abcam (#Ab9530)
p-VEGFR2 (tyr1175) (rabbit monoclonal)	WB: 1:1000	Cell Signaling Technology (#2478)
p-VEGFR2 (tyr951) (mouse monoclonal)	IF: 1:1000	Cell Signaling Technology (#2476)
VEGF-C (rabbit polyclonal)	WB:1:1000, IHC: 1:250, PLA: 1:500	GeneTex (GTX113574)
F-actin: Alexa Fluor 488 Phalloidin	PLA: 1:500	ThermoFisher Scientific (#A12379)
	Secondary antibodies	
Rabbit anti mouse Igg	WB: 1:1000	DAKO # P0260
Swine anti rabbit Igg	WB: 1:1000	DAKO # P0217
Alexa Fluor 568 goat anti mouse	IF: 1:1000	ThermoFisher Scientific (#A11004)

Abbreviations: WB. Western blot; IF. Immunofluorescence; PLA. Proximity Ligation Assay; IHC. Immunohistochemistry.

3.2 Results - Study II

Combined EGFR- and notch inhibition display additive inhibitory effect on glioblastoma cell viability and glioblastoma-induced endothelial cell sprouting in vitro

By

Mikkel Staberg, Signe R. Michaelsen*, Louise S Olsen, Mette K. Nedergaard, Mette Villingshøj, Marie-Thérése Stockhausen, Petra Hamerlik and Hans S. Poulsen*

**authors contributed equally*

Published in *Cancer Cell International* 2016

Summary study II:

This preclinical study tested the effect of targeting of EGFR and Notch signaling in combination on cellular viability and angiogenesis in glioblastoma. Two GSC models were used and an initial characterization showed positivity of EGFR or EGFRvIII as well as various Notch pathway components. Additional the GSCs were shown to express VEGF-A and other proangiogenic factors and conditioned media from the cells were found to stimulate endothelial cell sprouting in an *in vitro* angiogenesis assay. Results thereby verified that the models were of relevance for evaluation of study endpoints. Exposure to single-line therapy with EGFR inhibitor Iressa and GSI DAPT showed direct inhibition of the respective pathways. These analyses also verified previously findings of crosstalk between the Notch and EGFR pathways, including effect of EGFR signaling for Hes1 expression and Notch signaling for Akt activity. Upon combinational therapy, we found in comparison to single-line therapy, increased inhibition of Hes-1 expression and decrease of activity of pro-survival mediators Akt and Erk. In line with this, combination of both drugs was also found to reduce cell viability more than upon treatment with either drug alone. Single-line therapy with both drugs was further found to abrogate glioblastoma induced endothelial cell sprouting, with reduction of both length and number of sprouts, and additive effect was demonstrated upon combined drug treatment. This effect could at least partly be attributed to drug induced reduction in VEGF-A expression and -secretion in the glioblastoma cells. Overall, study data confirm crosstalk between Notch and EGFR pathways and effect of both pathways in stimulation of angiogenesis in glioblastoma. Further, data imply therapeutic benefit of combinational targeting of the two pathways, both via direct effect on glioblastoma tumor cells and indirectly via inhibition of angiogenesis. However, more studies are needed, including thorough *in vivo* testing, to verify potential for clinical implementation.

Staberg *et al. Cancer Cell Int (2016) 16:34*
DOI 10.1186/s12935-016-0309-2

Cancer Cell International

PRIMARY RESEARCH Open Access

Combined EGFR- and notch inhibition display additive inhibitory effect on glioblastoma cell viability and glioblastoma-induced endothelial cell sprouting in vitro

Mikkel Staberg[1*†], Signe Regner Michaelsen[1†], Louise Stobbe Olsen[1], Mette Kjølhede Nedergaard[2], Mette Villingshøj[1], Marie-Thérése Stockhausen[1], Petra Hamerlik[1,3] and Hans Skovgaard Poulsen[1]

Abstract

Background: For Glioblastoma (GBM) patients, a number of anti-neoplastic strategies using specifically targeting drugs have been tested; however, the effects on survival have been limited. One explanation could be treatment resistance due to redundant signaling pathways, which substantiates the need for combination therapies. In GBM, both the epidermal growth factor receptor (EGFR) and the notch signaling pathways are often deregulated and linked to cellular growth, invasion and angiogenesis. Several studies have confirmed cross-talk and co-dependence of these pathways. Therefore, this study aimed at testing a combination treatment strategy using inhibitors targeting the notch and EGFR pathways.

Methods: For evaluation of cell viability a standard MTT assay was used. Western blotting (WB) and Q-RT-PCR were employed in order to assess the protein- and mRNA expression levels, respectively. In order to determine angiogenic processes, we used an endothelial spheroid sprouting assay. For assessment of secreted VEGF from GBM cells we performed a VEGF-quantikine ELISA.

Results: GBM cells were confirmed to express EGFR and Notch and to have the capacity to induce endothelial cell sprouting. Inhibition of EGFR and Notch signaling was achieved using either Iressa (gefitinib) or the gamma-secretase inhibitor DAPT. Our data showed that DAPT combined with Iressa treatment displayed increased inhibitory effect on cell viability and abrogated expression and activation of major pro-survival pathways. Similarly, the combinational treatment significantly increased abrogation of GBM-induced endothelial cell sprouting suggesting reduced GBM angiogenesis.

Conclusion: This study finds that simultaneous targeting of notch and EGFR signaling leads to enhanced inhibitory effects on GBM-induced angiogenesis and cell viability, thereby stressing the importance of further evaluation of this targeting approach in a clinical setting.

Keywords: Glioblastoma, Angiogenesis, Endothelial spheroid sprouting, Notch, EGFR, DAPT, Iressa, Gamma-secretase inhibitor, Tyrosine-kinase inhibitor

*Correspondence: mikkel.staberg@regionh.dk
†Mikkel Staberg and Signe Regner Michaelsen contributed equally to this work
[1] Department of Radiation Biology, The Finsen Center, Copenhagen University Hospital, Copenhagen, Denmark
Full list of author information is available at the end of the article

Background

Glioblastoma (GBM) is a devastating tumor of the brain and current therapies have only a palliative effect. GBM tumors are proliferative and infiltrative with a prominent angiogenic phenotype [1]. Thus, therapies targeting angiogenesis have become interesting in the treatment of GBM and the humanized antibody bevacizumab targeting vascular endothelial growth factor A (VEGF) are approved for patients with recurrent GBM [2]. However, as the effect of this and other anti-angiogenic therapies tested in GBM are very limited [3], new alternative strategies for targeting GBM in general and angiogenesis in particular are needed.

GBM is often associated with mutation and amplification of the epidermal growth factor receptor (EGFR) gene and consequently, the importance of EGFR signaling for tumor development and maintenance has gained much attention [4]. Overexpression of EGFR has been correlated to the malignant phenotype of GBM and the most common EGFR mutation in GBM EGFRvIII leads to constitutive active signaling [5–8]. Activation of EGFR downstream signaling pathways leads to increased proliferation and tumorigenesis, and stimulates angiogenesis via upregulation of pro-angiogenic molecules in the tumor cells [9, 10]. In line with this finding, anti-EGFR therapies have been shown to reduce the production of the pro-angiogenic factor VEGF and reduce vascular formation [11, 12]. Similarly to EGFR, the Notch pathway has also gained attention as a potential target in GBM. The notch gene family consists of four transmembrane receptors (notch1–4) and their ligands (jagged1–2 and Dll1, Dll2 and Dll4) [13]. Ligand binding to the receptor results in two successive proteolytic cleavages which activate downstream signaling resulting in transcription of downstream targets such as Hes1 and Hey1 [14]. The Notch pathway has been linked to a number of GBM specific processes including cellular responses to hypoxia, angiogenesis and tumor growth [15, 16]. Thus, the Notch pathway represents a highly interesting therapeutic target.

Increasing evidence points to a cross-talk between the Notch and EGFR pathway [17, 18]. In line with this, GBM tumors with EGFR amplification display overexpression of notch-regulated genes [19] and it has been shown that notch signaling can induce EGFR upregulation through a P53-dependent mechanism in GBM [20]. It is also believed that the interplay between notch and EGFR is involved in the genesis and maintenance of tumor cells in various cancers including GBM [18, 21]. Thus, this study aimed at investigating the functional interplay between EGFR and notch signaling and elucidating its role in GBM cell maintenance and GBM-induced endothelial cell (EC) sprouting as a surrogate marker for angiogenesis-like processes.

This was done by evaluating the effect of mono- or combined therapy using the tyrosine-kinase inhibitor iressa (TKI; targeting EGFR) and the gamma-secretase inhibitor DAPT (GSI; targeting notch signaling). In the present study, we have used two primary GBM cell cultures with confirmed notch and EGFR expression. Both iressa as well as DAPT single-agent treatment abrogated EGFR and notch signaling, respectively, leading to reduced cell viability, and decreased VEGF expression and GBM-induced EC sprouting. Upon combinational treatment with both iressa and DAPT, the inhibitory effect on cell viability and EC sprouting was even more pronounced. Our data indicate that the cross-talk between EGFR and Notch signaling pathways are crucial for GBM maintenance and vascular phenotype.

Methods

Cell cultures

GBM cell cultures used in this study were CPH036 (p6) and CPH047 (p3m1). These were established from patient tumor tissue derived from initial surgery before any other treatment and have previously been described in regard to EGFR status and expression of markers related to stemness and the neuronal lineages [22]. We further analyzed the IDH status of the cell cultures by dideoxy sequencing of *IDH1* codon 132 and *IDH2* codon 140 and 172. Both cell lines were found to be *IDH1/2* wild-type (unmutated). Cells were cultured as floating neurospheres in Neurobasal®-A media (NB media) supplemented with N2, B27, bFGF (10 ng/ml), EGF (10 ng/ml), L-glutamine, penicillin (50 U/ml), and streptomycin (50 µg/ml) (all from Invitrogen) and incubated in cell culture flasks (NUNC) in a humidified chamber with 5 % CO_2 at 37 °C. Spheres were dissociated at every experiment and at new passage to obtain single cells. Endothelial cells (EC) used in this study represents primary human dermal microvascular endothelial cells (HMVEC) from Lonza. EC were incubated in endothelial growth medium-2 (EGM-2) added EGM-2 microvascular (MV) supplements (VEGF, EGF, bFGF, long R3 insulin-like growth factor (R^3-IGF-1), ascorbic acid, hydrocortisone, GA-1000 and 5 % fetal calf serum (FCS); all from Lonza. Cells were incubated at 5 % CO_2 at 37 °C and passaged at sub-confluence.

Reagents

Drugs used in experiments were DAPT (*N*-[(3,5-difluorophenyl)acetyl]-L-alanyl-2-phenyl]glycine-1,1-dimethylethyl ester) obtained from Merck Millipore and iressa (Gefitinib) from tocris bioscience. All drugs were dissolved in DMSO which was also used for treatment controls. Recombinant human $VEGF_{165}$ from Miltenyi Biotec was used to induce a pro-angiogenic response.

Western blotting

Protein lysates for western blotting (WB) were prepared and obtained from cell pellets by sonication in ice-cold modified RIPA buffer [50 mM Tris–HCl (pH 7.4), 1 % NP40, 0.25 % Na-deoxycholate, 150 mM NaCl, 1 mM EDTA] supplemented with protease and phosphatase inhibitor mixture II and III (calbiochem). Determination of protein concentrations was done by the BCA protein assay (pierce). WB was performed by separation of protein lysates on NuPage 4–12 % Bis–Tris gels following electroblotting onto nitrocellulose membranes using the Novex NuPAGE SDS-PAGE gel system (invitrogen). Membranes were blocked in 5 % non-fat dry-milk in wash buffer for one hour at room temperature following incubation with primary antibodies overnight at 4 °C. Primary antibodies used are displayed in Additional file 1: Figure S4. The following day membranes were washed and incubated with HRP-conjugated secondary antibodies for 1 h at room temperature and developed using the SuperSignal West Dura Extended Duration Substrate (pierce biotechnology) and the biospectrum imaging system (UVP).

Quantitative real-time PCR (Q-RT-PCR)

Total RNA was purified from GBM cell pellets as previously described [23]. In short, RNA was obtained by using the RNeasy Mini kit and QIAshredder and submitted to a DNase treatment (all from Qiagen). For cDNA synthesis and Q-RT-PCR reactions the SuperscriptTM III platinum® two step qRT-PCR kit with SYBR® Green (Invitrogen) was used. Gene expression levels were quantified according to the comparative Ct method and normalized to expression of the three housekeeping genes TOP1, EIF4A2, and CYC1 (primerdesign). Primers used in Q-RT-PCR reactions for amplification of target genes are displayed in Additional file 1: Figure S5.

Cell viability assay

Cells were plated at concentrations of 2.5–3.5 × 10^4 cells per well in 96-well plates and incubated for 7 days with either 100 µl of growth medium or medium containing indicated treatments or control. Cell viability was measured using a 3-(4,5-dimethylthiazol- 2-yl)-2,5-diphenyltetrazolium bromide (MTT) assay (sigma) by the addition of 20 µl of MTT solution (5 mg/ml, dissolved in sterile water) to each well and incubation for 4 h before the addition of 100 µl of solubilization buffer (10 % sodium dodecyl sulfate, 0.01 M HCl). Absorbance at 570 nm was measured the next day using Synergy2 microplate reader with Gen5 software.

VEGF enzyme-linked immunosorbent assay (ELISA)

One million cells were grown for 14 days in 10 ml of culture media added vehicle or inhibitors for 14 days. Conditioned media was collected and VEGF (-A) levels were quantified using the Human VEGF Quantikine ELISA kit (R&D Systems) following manufacturer's instructions. Quantification was done by measuring the absorbance at 450 nm with 570 as a reference using the Synergy2 microplate reader.

Spheroid sprouting assay

A spheroid sprouting assay was employed in order to assess the angiogenic-like sprouting process in response to pro-angiogenic stimulus and principally performed as described previously [24]. Cell spheroid formation was obtained by seeding 2000 HMVEC (EC) in each well in non-adherent round-bottomed 96-well plates in growth medium (EGM-2MV) containing 0.3 % methylcellulose (Sigma-Aldrich) and incubated at 37 °C and 5 % CO_2 for 24 h. Next, the single spheroids from the wells were collected and embedded into collagen gels, consisting of a collagen solution (1 mg/ml rat tail collagen from BD Biosciences) with 0.2 M NaOH, 1 × Medium 199 (Sigma-Aldrich), 0.6 % methylcellulose, (Sigma-Aldrich) in HMVEC basal medium (EBM-2), in 4-well plates. For each well containing spheres, these were stimulated with 50 % FCS in EBM-2 medium added the experimental factor. In the cases where this was conditioned media from GBM cells, the media was collected from 1 × 10^6 cells grown for 14 days with or without the indicated treatments and subsequently up-concentrated around 10 times by centrifugation at max speed using Amicon Ultra Centrifugal Filter Units (Merck Millipore). Spheres were incubated for 16 h and spheroid sprouting was visualized by using an Eclipse TS100 phase-contrast microscope, Digital Sight imaging system and the NIS Elements F3.2 software (all from Nikon). Quantification of spheroid sprouting (number of sprouts and total sprout length per sphere) was determined using ImageJ software.

Statistics

Statistics were performed using a one-way Analysis of Variance test (ANOVA) to compare multiple data groups, followed by Tukeys post hoc test, for comparison of multiple samples or by an un-paired two-tailed student's t test when comparing two samples. The software used for the above statistics and creation of figures was Graphpad Prism 6.0. The effect of combination therapy was done in SAS version 9.4 (SAS Institute, Denmark) by general linear modeling and analysis of the response levels was done on the log scale. Tests for additivity were made by comparing the sum of the two treatment effects on the log scale with the combination treatment and the hypothesis of additive effect were rejected if the comparison demonstrated significant interaction i.e. evidence of synergistic

or sub-additive effect. A p value < 0.05 was considered statistically significant.

Results

Characterization of GBM cell cultures for EGFR- and notch signaling pathway component expression

Q-RT-PCR and western blotting (WB) were employed in order to determine the expression levels of EGFR and EGFRvIII and Notch family molecules in two primary GBM cell cultures (CPH036 and CPH047). Both mRNA and protein analysis found that the two cultures were positive for EGFR, whereas only CPH047 displayed expression of the mutated EGFR variant, EGFRvIII, (Fig. 1a, b). Further, mRNA analysis found that both cell cultures express notch receptors 1–3 and their notch receptor ligands jagged-1, jagged-2, Dll-1 and Dll-4 (Fig. 1c) and the expression was confirmed when examining a selection of these molecules at the protein level (Fig. 1d). Protein expression of the notch downstream effector protein, Hes-1, confirmed active Notch signaling in both cultures (Fig. 1d).

Iressa and DAPT abrogates downstream survival pathway signaling through the EGFR- and notch pathways and reduces cell viability in vitro

Following verification that the GBM cells expressed components of the EGFR- and notch signaling pathways, we wanted to investigate the effect of EGFR and Notch inhibition. We used the EGFR inhibitor iressa, and the notch inhibitor DAPT for investigating the effect of EGFR and notch signaling abrogation on the downstream survival kinases Akt and Erk. In CPH036 cells, mono-therapy with iressa (5 μM) inhibited EGFR phosphorylation (pY1086) but had no effect on phosphorylation of the downstream effector proteins Akt (p-Akt) and Erk (p-Erk) as seen in Fig. 2a. DAPT (5 μM) mono-therapy had minor effect on p-EGFR and displayed inhibition of p-Akt but without effect on p-Erk. Upon combined Iressa and DAPT treatment this resulted in both inhibition of p-Akt and p-Erk in CPH036 cells. In CPH047 cells mono-therapy with either Iressa or DAPT reduced p-Akt and p-Erk levels to some degree and upon combined treatment this effect was even more pronounced (Fig. 2a). Furthermore, as seen in Fig. 2b, mono-therapy, with Iressa or DAPT, decreased Hes-1 expression in CPH047 cells whereas only DAPT could inhibit Hes-1 expression in CPH036 cells. Upon combinational treatment with Iressa and DAPT an additive downregulation of Hes-1 expression was seen in CPH047 cells, whereas no direct additive effect could be seen in the CPH036 cells.

Following confirmation that the inhibitors abrogated downstream signaling through survival pathways Akt and Erk, we examined the effect of Iressa and DAPT on cell viability in vitro. As seen in Fig. 2c single-agent treatment of the CPH036 cells, with either DAPT or Iressa, was able to significantly decrease cell viability compared to control. Upon co-administration of both drugs, this effect was even further potentiated and confirmed to be additive, as a test for additivity was not rejected ($p = 0.56$ for 0.5 μM iressa + 5 μM DAPT and $p = 0.50$ for 2 μM Iressa + 20 μM DAPT). In CPH047 cells, higher concentrations (20 μM DAPT or 2 μM iressa) of each inhibitor were needed to significantly inhibit cell viability and upon combined treatment this inhibitory effect was further enhanced and again confirmed to be additive ($p = 0.98$) (Fig. 2d). In conclusion, combinational therapy with Iressa and DAPT display pronounced inhibitory effect as compared to mono-therapy in GBM cells on both downstream signaling of the EGFR- and notch pathway and cell viability.

Capacity of GBM cell cultures to secrete and express VEGF and to induce endothelial cell sprouting

VEGF is a well-known inducer of angiogenesis in GBM [25]. This prompted us to investigate the level of VEGF expression and secretion in CPH036 and CPH047 cells. We found that both cell cultures were positive for VEGF mRNA expression and protein secretion (Fig. 3a) together with other pro-angiogenic factors (Additional file 1: Figure S1). The expression of VEGF receptors (VEGFR-1 and -2) could not be detected in the GBM cells (Additional file 1: Figure S2), suggesting only paracrine effects of VEGF upon secretion from the tumor cells. Knowing that the GBM cells secrete VEGF into the culture media we assessed whether conditioned media from CPH036 and CPH047 was sufficient in inducing angiogenic-like processes in EC. We performed a cell sprouting assay which measures the cells ability to migrate, proliferate and form tube-like structures, all processes required in angiogenesis. Upon exposure of EC to conditioned media obtained from either CPH036 or CPH047 cells this clearly induced sprouting as displayed in Fig. 3b. The relative number of sprouts per sphere and relative total sprout length per sphere was quantified to be significantly increased compared to control (NB unconditioned media) as shown in Fig. 3c, d. These data implied that the examined GBM cells have the capacity of inducing angiogenesis-like processes of EC in vitro possibly through secretion of VEGF.

Iressa and DAPT abrogates GBM-induced endothelial cell sprouting and reduces VEGF expression and secretion by GBM cells

Following confirmation that the GBM cells displayed capacity to induce EC sprouting, we investigated how this ability was affected by EGFR and Notch inhibition.

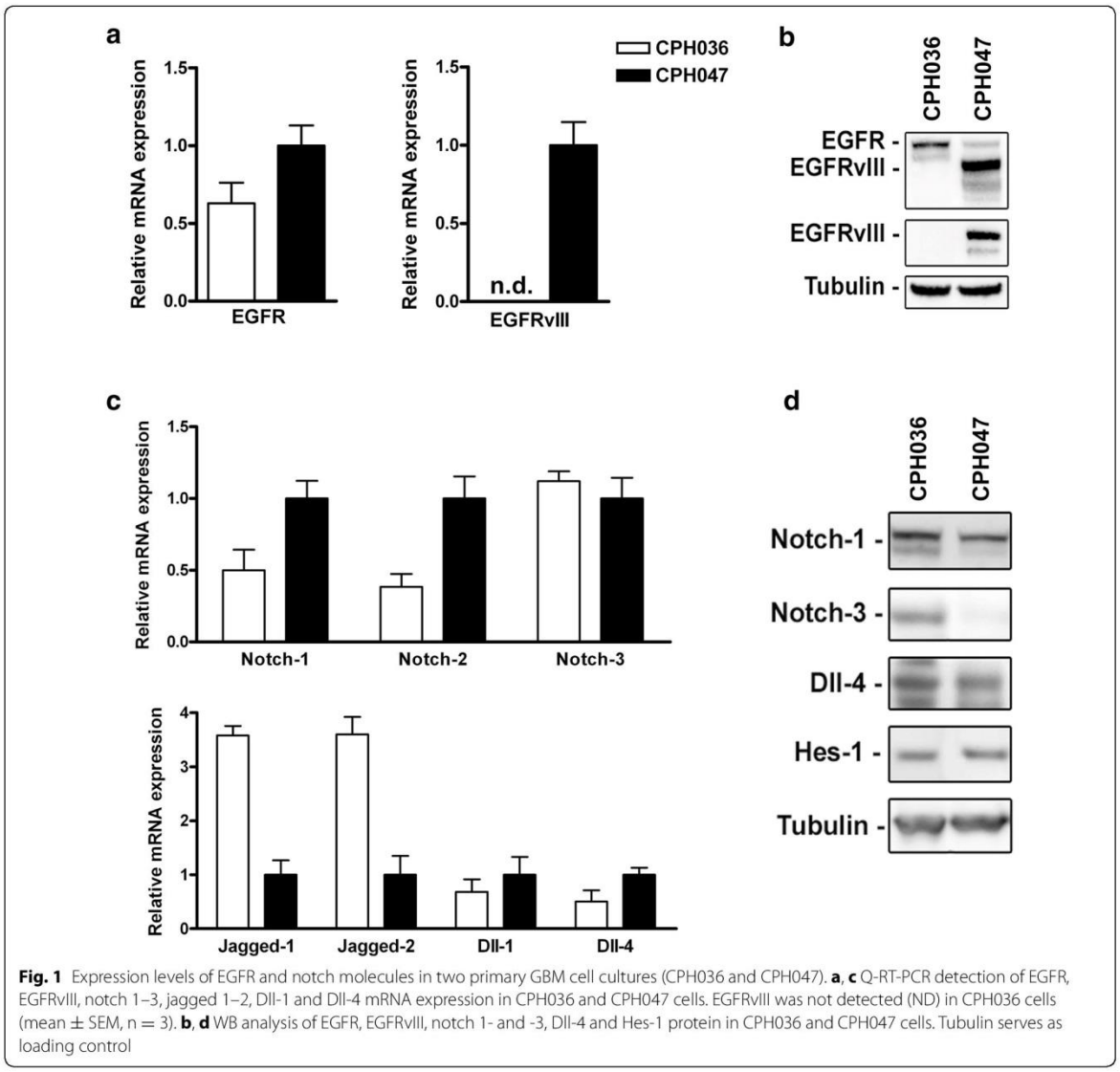

Fig. 1 Expression levels of EGFR and notch molecules in two primary GBM cell cultures (CPH036 and CPH047). **a**, **c** Q-RT-PCR detection of EGFR, EGFRvIII, notch 1–3, jagged 1–2, Dll-1 and Dll-4 mRNA expression in CPH036 and CPH047 cells. EGFRvIII was not detected (ND) in CPH036 cells (mean ± SEM, n = 3). **b**, **d** WB analysis of EGFR, EGFRvIII, notch 1- and -3, Dll-4 and Hes-1 protein in CPH036 and CPH047 cells. Tubulin serves as loading control

EC were subjected to conditioned media collected from GBM cells receiving either no treatment (DMSO) or treatment with 5 μM iressa and 5 μM DAPT alone or in combination (5 μM DAPT +5 μM iressa). We found that mono-therapy with Iressa or DAPT of CPH036 and CPH047 cells significantly reduced the capacity of GBM-induced EC spheroid sprouting (Fig. 4a–c, e). Upon treatment with combined DAPT and iressa an increased co-inhibitory effect of quantified EC sprouting could be seen compared to mono-therapy (Fig. 4c, e). In CPH036 cells, the co-inhibitory effect was confirmed to be additive for both the number ($p = 0.62$) and length ($p = 0.59$) of spouts. For the CPH047 cells the length of spouts was borderline non-significant ($p = 0.080$), demonstrating a trend towards additivity. Conversely, the co-inhibitory effect for the number of sprouts in CPH047 cells showed a significant interaction ($p = 0.046$), but with an effect that was less (76 % reduction) than would be expected if additive (83 % reduction), suggesting that the combination was sub-additive. Further, the inhibitory effect of DAPT and Iressa on EC sprouting could be confirmed not to be a result of non-metabolized inhibitor leftovers inducing EC death since conditioned media from GBM cells treated with DAPT, Iressa or a combination had no

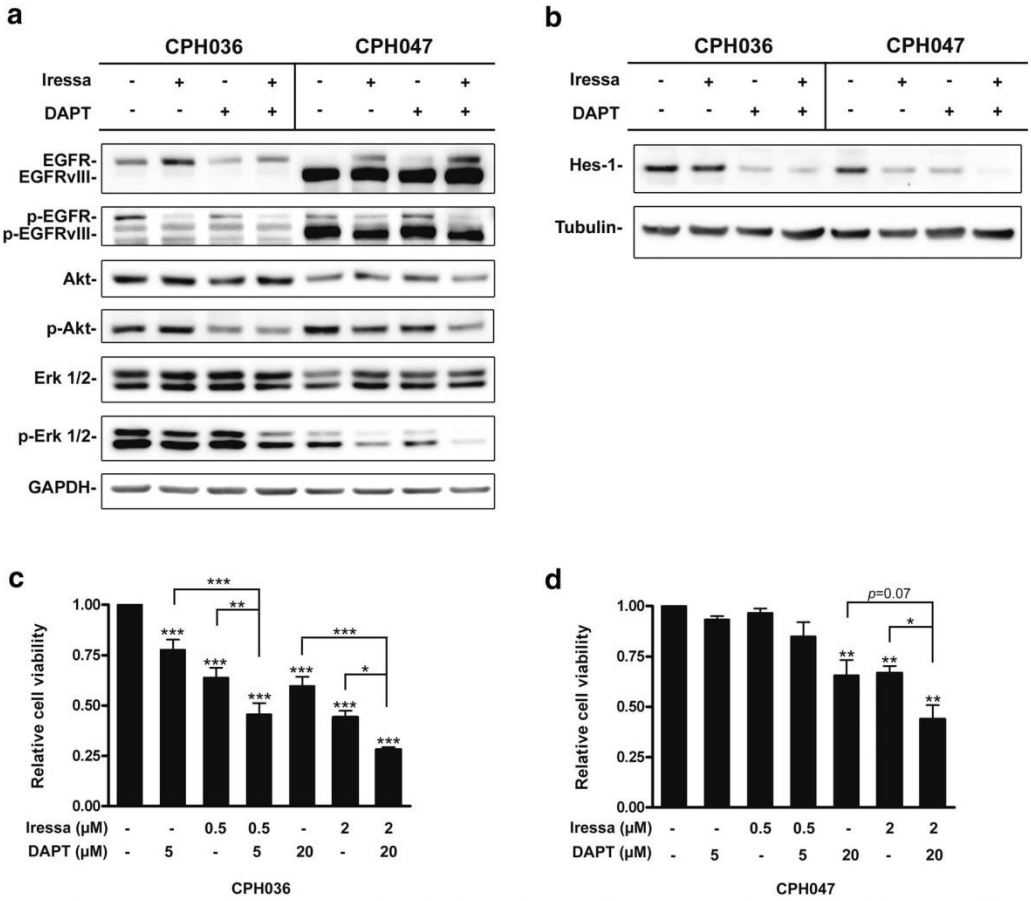

Fig. 2 Iressa and DAPT treatment inhibits the EGFR- and notch pathways abrogating downstream signaling and cell viability in vitro. **a**, **b** WB analysis of CPH36 and CPH047 cells treated with 5 μM iressa, 5 μM DAPT or a combination for 24 h. WB was investigated for expression of EGFR, EGFRvIII, Akt, p-Akt, Erk, p-Erk and Hes-1. GAPDH and tubulin serves as loading controls. **c**, **d** Cell viability of CPH036 or CPH047 cells following 7 days of treatment with iressa, DAPT or a combination in the indicated doses (mean ± SEM, n = 5). *$p < 0.05$, **$p < 0.01$, ***$p < 0.001$

effect on EC proliferation (Additional file 1: Figure S3). To examine whether the effect of inhibited GBM-induced EC sprouting could be due to the effect of Iressa and DAPT on VEGF expression and secretion by the GBM cells, we measured VEGF secretion following treatment. Iressa treatment resulted in almost complete inhibition of VEGF expression and secretion in CPH036 and CPH047 cells (Fig. 4d, f), while DAPT treatment was able to partially abrogate VEGF expression and secretion, however with less potency, compared to iressa. Upon combined treatment no additive effect could be observed as a result of almost complete inhibition of VEGF secretion and expression by Iressa treatment (Fig. 4d, f). Summed, both iressa and DAPT display capacity to inhibit GBM-induced cell sprouting in EC and upon combinational treatment this effect is even further enhanced. Further, the results indicate that this effect, at least partly, could be a result of inhibition of VEGF expression.

Discussion

EGFR and notch are both involved in regulation of GBM cancer cells by promoting their survival, therapeutic resistance and pro-angiogenic signaling [13, 26, 27]. Thus, there is a rationale for treatment with inhibitors targeting both the EGFR and Notch signaling axis in GBM. The main focus of this study was to investigate the effect of simultaneous EGFR and notch abrogation on GBM cell maintenance and EC sprouting.

Aberrant expression of components of the EGFR and notch pathway has in GBM been confirmed previously [27,

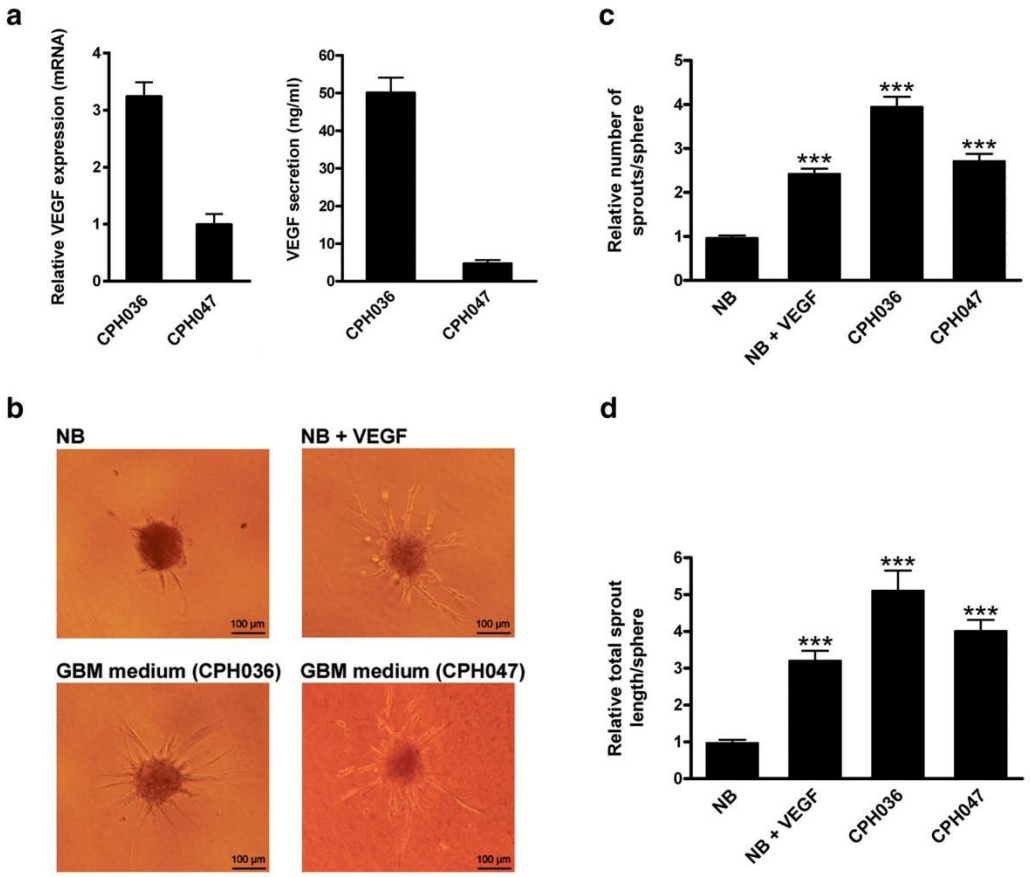

Fig. 3 EC cell sprouting stimulation by GBM-conditioned cell culture media. CPH036 and CPH047 cells were grown for 14 days and the conditioned media was collected and concentrated. EC were grown in presence of 20 ng/ml VEGF or conditioned media from CPH036 or CPH047 cells. **a** Relative VEGF expression analyzed by Q-RT-PCR, and VEGF secretion (ng/ml) analyzed by ELISA of CPH036 and CPH047 cells (mean ± SEM, n = 6 for Q-RT-PCR and n = 3 for ELISA). **b** Representative pictures showing sprouting of EC upon stimulation with VEGF or conditioned media from either CPH036 or CPH047 cells. **c**, **d** EC sprouting quantified as number of sprouts and total length of sprouts per sphere, respectively, and displayed relative to NB unconditioned media (mean ± SEM, n = 3 measuring an average of 10 spheres per condition in each experiment). *Scale bar* shows 100 µm. ***$p < 0.001$ vs. NB medium

28]. In accordance with this, we identified heterogeneous expression of EGFR/EGFRvIII, notch ligands and notch receptors in our GBM cell cultures. EGFR and Notch are important regulators of angiogenesis and abrogation of either of these pathways results in reduced angiogenesis in GBM [15, 29]. In the examined GBM cells, we confirmed endogenous expression and secretion of the key pro-angiogenic cytokine VEGF [25], for which increased expression has been correlated with increased glioma malignancy and poor prognosis [30, 31]. Furthermore, we confirmed that the examined GBM cells were able to induce EC sprouting (Fig. 3b–d) indicating that these cells had the capacity to induce neo-angiogenesis of surrounding EC by the secretion of pro-angiogenic factors.

Upon abrogation of Notch and EGFR signaling by DAPT or Iressa treatment, respectively, this inhibited the expression and secretion of VEGF in our GBM cells (Fig. 4d, f). This supports that VEGF-induced angiogenesis is dependent of active signaling through the notch and EGFR pathways as also shown by others [32–34]. Recently, Wang et al. [29] showed that combined treatment with the anti-EGFR antibody Cetuximab together with DAPT displayed downregulation of VEGF in Head Neck Squamous Cell Carcinoma [29], which is in line with our observations. VEGF is generally considered to be a positive upstream regulator of Notch with Notch acting as an upstream regulator of VEGFRs [35]. Moreover, our data demonstrate that Notch regulates VEGF

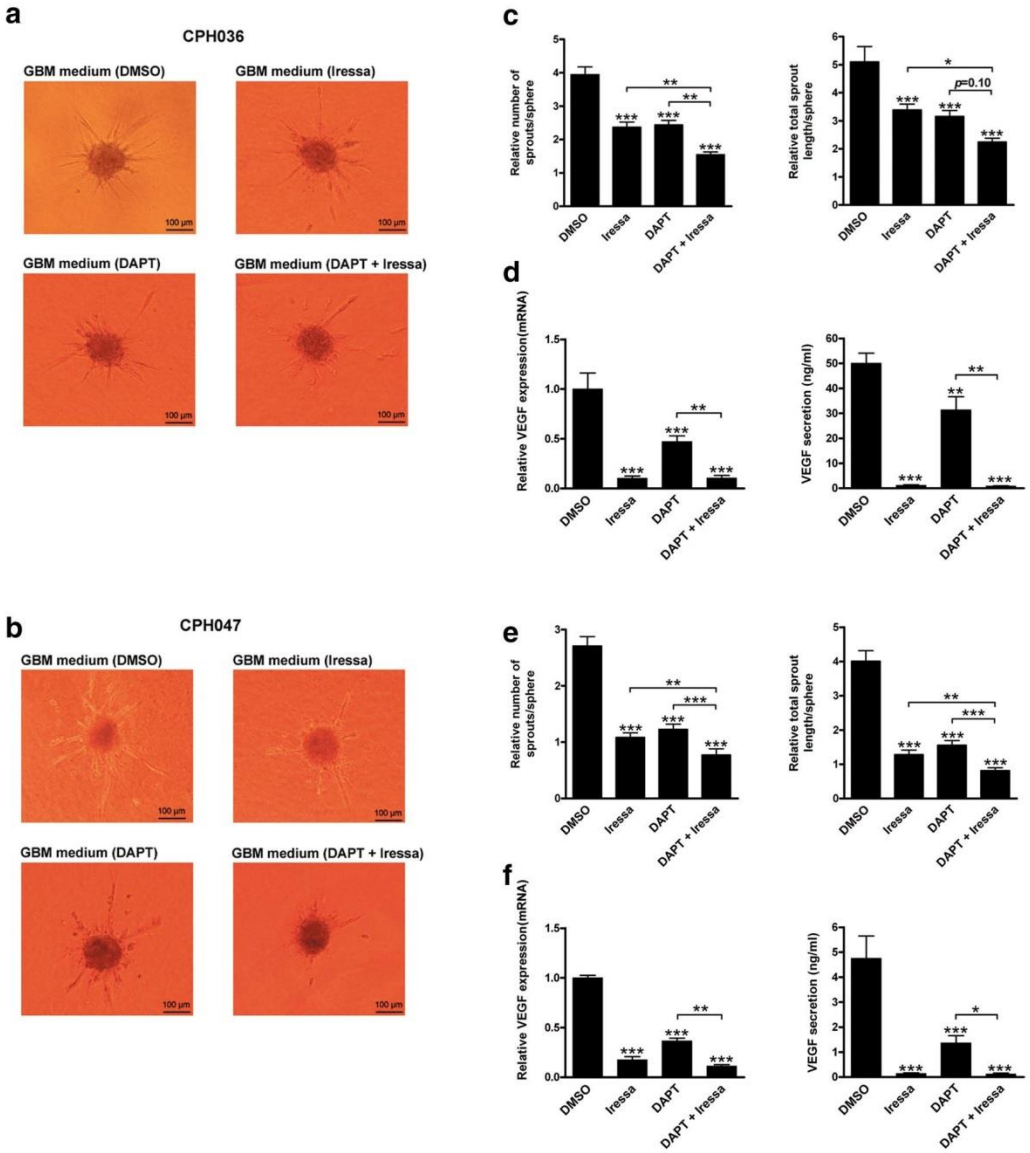

Fig. 4 Iressa and DAPT treatment abrogates GBM-induced EC sprouting, and inhibits VEGF expression and secretion in GBM cells. CPH036 and CPH047 cells were treated with 5 µM iressa, 5 µM DAPT or a combination for 14 days. The conditioned GBM media was concentrated and subjected to EC for sprouting analysis. **a**, **b** Representative pictures showing sprouting of EC upon administration of conditioned media obtained from CPH036 or CPH047 cells treated with indicated inhibitors. **c**, **e** Relative EC sprouting quantified as total number of sprouts and total length of sprouts per sphere upon stimulation with conditioned inhibitor-treated media from either CPH036 or CPH047 cells, respectively (mean ± SEM, n = 3 measuring an average of 10 spheres per condition in each experiment). **d**, **f** VEGF mRNA levels in inhibitor-treated CPH036 and CPH047 cells were analyzed by Q-RT-PCR and normalized to the mean gene expression of the control. VEGF secretion levels (ng/ml) analyzed by ELISA from inhibitor-treated CPH036 and CPH047 cells as measured by VEGF-ELISA (mean ± SEM, n = 3). *Scale bar* shows 100 µm. *$p < 0.05$, **$p < 0.01$, ***$p < 0.001$

expression, indicating the existence of a positive feed-back-loop regulatory mechanism.

Studies have shown that treatment with small molecule inhibitors targeting EGFR or Notch is able to inhibit GBM angiogenesis in vitro [36, 37]. We observed that treatment with DAPT plus iressa was not sufficient to fully block EC sprouting (Fig. 4c, e) despite almost complete inhibition of VEGF secretion upon combined treatment (Fig. 4d, f)

suggesting that other angiogenic stimulators are involved in GBM-induced EC sprouting. Factors including angiogenin, PDGF-AA, IGFBP-3 are known to be implicated in angiogenesis [38–40] and were confirmed to be present in the GBM-conditioned media at comparable levels to VEGF (Additional file 1: Figure S1) which could explain additional stimulation of EC sprouting.

Aberrant EGFR and notch signaling regulate cell viability and therapeutic resistance of GBM cells [17, 27, 41]. Both, EGFR and notch regulated signaling are in GBM linked to the RAS-RAF-MEK-ERK and the PI3K-Akt-mTOR signaling pathways [42, 43]. Interestingly, it has been shown that Notch signaling is dependent on mTOR in lung and kidney tumor cells [44], indicating the existence of a positive feedback loop between Notch and EGFR signaling. Our results show that the inhibition of EGFR signaling results in decreased Hes-1 levels supporting that EGFR signaling stimulate activity of the Notch pathway. Further, we found upon combined treatment targeting both Notch and EGFR an increased inhibition of GBM cell viability compared to mono-therapy alone. This was probably a result of more effective inhibition of the pro-survival pathways Akt and Erk which we observed upon combination therapy (Fig. 2a). Cenciarelli et al. [28] showed that co-treatment with GSI-X and AG1478 (targeting Notch and EGFR, respectively) displayed synergistic anti-proliferative effects in GBM in vitro [28]. Taken together, our data and those of others indicate redundant signaling between EGFR and Notch, which indicate a need for further preclinical and clinical evaluation of simultaneous inhibition of Notch and EGFR which are upstream of key pro-survival regulatory pathways as the RAS-RAF-MEK-ERK and PI3K-Akt-mTOR.

Over the last years, a number of pharmacological studies have been conducted testing either EGFR or Notch pathway inhibitors in patients with various cancer types including GBM (http://www.clinicaltrial.gov). For GBM patients a number of different EGFR targeting drugs have been tested in the clinic, but overall results have been disappointing with non or very limited clinical benefits [45]. So far, only one study has been reported for the use of a notch-specific inhibitor in glioma patients. In this study, the Merck-developed GSI termed MK-0752 was tested in various advanced solid tumors and the results indicated some clinical benefits especially in glioma patients [46]. Still, the anti-tumor activity was not impressive with most patients obtaining stable disease as best response [46]. Data from a currently ongoing phase II trial, treating patients with recurrent or progressive GBM with another GSI (RO4929097), are yet to be published, but will further shed light on the effect of single-agent treatment with Notch inhibitors. Overall, the results from recent and/or ongoing clinical trials evaluating EGFR- and notch-specific inhibitors as mono-therapies imply certain clinical limitations of this approach.

In this study, we find that a combined treatment strategy that targets both EGFR and notch signaling pathways results in enhanced inhibitory effect on cell viability and EC sprouting, compared to either of the mono-therapies, supporting the important role of notch/EGFR signaling cross-talk in GBM. Taken together, this fact and the above mentioned clinical studies support the rationale for combined treatment strategy employing both EGFR and notch inhibitors.

Additional file

Additional file 1: Figure S1. Evaluation of angiogenic factors secreted by GBM cells. **Figure S2.** Expression of VEGF receptors (VEGFR-1 and VEGFR-2) in GBM cell cultures CPH036 and CPH047 and in endothelial cells (HMVEC). **Figure S3.** Effect of conditioned cell media from GBM cell cultures treated with inhibitors on endothelial cell proliferation. **Figure S4.** Overview of primary antibodies used for western blotting. **Figure S5.** Overview of primer sets used for Q-RT-PCR.

Abbreviations

GBM: glioblastoma; EGFR: epidermal growth factor receptor; VEGF: vascular endothelial growth factor A; TKI: tyrosine-kinase inhibitor; GSI: gamma-secretase inhibitor; EC: endothelial cell.

Authors' contributions

MTS and HSP designed the study. MS, SRM, LSO and MV all participated in the experimental work. PH and MKN assisted in data interpretation and revision of the manuscript. MS and SRM drafted the manuscript. All authors read and approved the final manuscript.

Author details

[1] Department of Radiation Biology, The Finsen Center, Copenhagen University Hospital, Copenhagen, Denmark. [2] Department of Clinical Physiology, Nuclear Medicine & PET and Cluster for Molecular Imaging, Copenhagen University Hospital and University of Copenhagen, Copenhagen, Denmark. [3] Brain Tumor Biology Group, Danish Cancer Society Research Center, Copenhagen, Denmark.

Acknowledgements

We would like to thank Katerina Tritsaris for advice regarding the in vitro endothelial sprouting assay, Pia Pedersen for practical assistance with the experiments, Linea Melchior for helping with IDH status analysis of the cell cultures and Ib Jarle Christensen, Statistician, for help with the statistical evaluation of the combination therapy.

Competing interests

The authors declare that they have no competing interests.

Funding

Financial support was kindly provided by the Faculty of Health Sciences, University of Copenhagen and Dansk Kræftforsknings Fond.

Received: 15 January 2016 Accepted: 18 April 2016
Published online: 26 April 2016

References

1. Plate KH, Risau W. Angiogenesis in malignant gliomas. Glia. 1995;15(3):339–47.
2. Ghiaseddin A, Peters KB. Use of bevacizumab in recurrent glioblastoma. CNS Oncol. 2015;4(3):157–69.
3. Thomas AA, Omuro A. Current role of anti-angiogenic strategies for glioblastoma. Curr Treat Options Oncol. 2014;15(4):551–66.

4. Ekstrand AJ, James CD, Cavenee WK, Seliger B, Pettersson RF, Collins VP. Genes for epidermal growth-factor receptor, transforming growth factor-alpha, and epidermal growth-factor and their expression in human gliomas in vivo. Cancer Res. 1991;51(8):2164–72.
5. Wikstrand CJ, Reist CJ, Archer GE, Zalutsky MR, Bigner DD. The class III variant of the epidermal growth factor receptor (EGFRvIII): characterization and utilization as an immunotherapeutic target. J Neurovirol. 1998;4(2):148–58.
6. Sugawa N, Ekstrand AJ, James CD, Collins VP. Identical splicing of aberrant epidermal growth factor receptor transcripts from amplified rearranged genes in human glioblastomas. Proc Natl Acad Sci USA. 1990;87(21):8602–6.
7. Ekstrand AJ, Sugawa N, James CD, Collins VP. Amplified and rearranged epidermal growth factor receptor genes in human glioblastomas reveal deletions of sequences encoding portions of the N- and/or C-terminal tails. Proc Natl Acad Sci USA. 1992;89(10):4309–13.
8. Normanno N, De LA, Bianco C, Strizzi L, Mancino M, Maiello MR, Carotenuto A, De FG, Caponigro F, Salomon DS. Epidermal growth factor receptor (EGFR) signaling in cancer. Gene. 2006;366(1):2–16.
9. Bos JL. Ras oncogenes in human cancer: a review. Cancer Res. 1989;49(17):4682–9.
10. De LA, Carotenuto A, Rachiglio A, Gallo M, Maiello MR, Aldinucci D, Pinto A, Normanno N. The role of the EGFR signaling in tumor microenvironment. J Cell Physiol. 2008;214(3):559–67.
11. Petit AM, Rak J, Hung MC, Rockwell P, Goldstein N, Fendly B, Kerbel RS. Neutralizing antibodies against epidermal growth factor and ErbB-2/neu receptor tyrosine kinases down-regulate vascular endothelial growth factor production by tumor cells in vitro and in vivo: angiogenic implications for signal transduction therapy of solid tumors. Am J Pathol. 1997;151(6):1523–30.
12. Hirata A, Uehara H, Izumi K, Naito S, Kuwano M, Ono M. Direct inhibition of EGF receptor activation in vascular endothelial cells by gefitinib ('Iressa', ZD1839). Cancer Sci. 2004;95(7):614–8.
13. Teodorczyk M, Schmidt MH. Notching on cancer's door: notch signaling in brain tumors. Front Oncol. 2014;4:341.
14. Li JL, Harris AL. Crosstalk of VEGF and notch pathways in tumour angiogenesis: therapeutic implications. Front Biosci (Landmark Ed). 2009;14:3094–110.
15. Rehman AO, Wang CY. Notch signaling in the regulation of tumor angiogenesis. Trends Cell Biol. 2006;16(6):293–300.
16. Sahlgren C, Gustafsson MV, Jin S, Poellinger L, Lendahl U. Notch signaling mediates hypoxia-induced tumor cell migration and invasion. Proc Natl Acad Sci USA. 2008;105(17):6392–7.
17. Aguirre A, Rubio ME, Gallo V. Notch and EGFR pathway interaction regulates neural stem cell number and self-renewal. Nature. 2010;467(7313):323–7.
18. Fassl A, Tagscherer KE, Richter J, Berriel DM, Alcantara Llaguno SR, Campos B, Kopitz J, Herold-Mende C, Herzig S, Schmidt MH, et al. Notch1 signaling promotes survival of glioblastoma cells via EGFR-mediated induction of anti-apoptotic Mcl-1. Oncogene. 2012;31(44):4698–708.
19. Brennan C, Momota H, Hambardzumyan D, Ozawa T, Tandon A, Pedraza A, Holland E. Glioblastoma subclasses can be defined by activity among signal transduction pathways and associated genomic alterations. PLoS One. 2009;4(11):e7752.
20. Purow BW, Sundaresan TK, Burdick MJ, Kefas BA, Comeau LD, Hawkinson MP, Su Q, Kotliarov Y, Lee J, Zhang W, et al. Notch-1 regulates transcription of the epidermal growth factor receptor through p53. Carcinogenesis. 2008;29(5):918–25.
21. Fitzgerald K, Harrington A, Leder P. Ras pathway signals are required for notch-mediated oncogenesis. Oncogene. 2000;19(37):4191–8.
22. Stockhausen MT, Broholm H, Villingshoj M, Kirchhoff M, Gerdes T, Kristoffersen K, Kosteljanetz M, Spang-Thomsen M, Poulsen HS. Maintenance of EGFR and EGFRvIII expressions in an in vivo and in vitro model of human glioblastoma multiforme. Exp Cell Res. 2011;317(11):1513–26.
23. Stockhausen MT, Kristoffersen K, Stobbe L, Poulsen HS. Differentiation of glioblastoma multiforme stem-like cells leads to downregulation of EGFR and EGFRvIII and decreased tumorigenic and stem-like cell potential. Cancer Biol Ther. 2014;15(2):216–24.
24. Korff T, Augustin HG. Tensional forces in fibrillar extracellular matrices control directional capillary sprouting. J Cell Sci. 1999;112(Pt 19):3249–58.
25. Bao S, Wu Q, Sathornsumetee S, Hao Y, Li Z, Hjelmeland AB, Shi Q, McLendon RE, Bigner DD, Rich JN. Stem cell-like glioma cells promote tumor angiogenesis through vascular endothelial growth factor. Cancer Res. 2006;66(16):7843–8.
26. Andersson U, Guo D, Malmer B, Bergenheim AT, Brannstrom T, Hedman H, Henriksson R. Epidermal growth factor receptor family (EGFR, ErbB2-4) in gliomas and meningiomas. Acta Neuropathol. 2004;108(2):135–42.
27. Kanamori M, Kawaguchi T, Nigro JM, Feuerstein BG, Berger MS, Miele L, Pieper RO. Contribution of notch signaling activation to human glioblastoma multiforme. J Neurosurg. 2007;106(3):417–27.
28. Cenciarelli C, Marei HE, Zonfrillo M, Pierimarchi P, Paldino E, Casalbore P, Felsani A, Vescovi AL, Maira G, Mangiola A. PDGF receptor alpha inhibition induces apoptosis in glioblastoma cancer stem cells refractory to anti-notch and anti-EGFR treatment. Mol Cancer. 2014;13:247.
29. Wang WM, Zhao ZL, Ma SR, Yu GT, Liu B, Zhang L, Zhang WF, Kulkarni AB, Sun ZJ, Zhao YF. Epidermal growth factor receptor inhibition reduces angiogenesis via hypoxia-inducible factor-1alpha and notch1 in head neck squamous cell carcinoma. PLoS One. 2015;10(2):e0119723.
30. Takano S, Yoshii Y, Kondo S, Suzuki H, Maruno T, Shirai S, Nose T. Concentration of vascular endothelial growth factor in the serum and tumor tissue of brain tumor patients. Cancer Res. 1996;56(9):2185–90.
31. Nam DH, Park K, Suh YL, Kim JH. Expression of VEGF and brain specific angiogenesis inhibitor-1 in glioblastoma: prognostic significance. Oncol Rep. 2004;11(4):863–9.
32. Zhou L, Wang DS, Li QJ, Sun W, Zhang Y, Dou KF. Downregulation of the notch signaling pathway inhibits hepatocellular carcinoma cell invasion by inactivation of matrix metalloproteinase-2 and -9 and vascular endothelial growth factor. Oncol Rep. 2012;28(3):874–82.
33. Wang Z, Banerjee S, Li Y, Rahman KM, Zhang Y, Sarkar FH. Down-regulation of notch-1 inhibits invasion by inactivation of nuclear factor-kappaB, vascular endothelial growth factor, and matrix metalloproteinase-9 in pancreatic cancer cells. Cancer Res. 2006;66(5):2778–84.
34. Pore N, Jiang Z, Gupta A, Cerniglia G, Kao GD, Maity A. EGFR tyrosine kinase inhibitors decrease VEGF expression by both hypoxia-inducible factor (HIF)-1-independent and HIF-1-dependent mechanisms. Cancer Res. 2006;66(6):3197–204.
35. Thurston G, Kitajewski J. VEGF and delta-notch: interacting signalling pathways in tumour angiogenesis. Br J Cancer. 2008;99(8):1204–9.
36. Paris D, Quadros A, Patel N, DelleDonne A, Humphrey J, Mullan M. Inhibition of angiogenesis and tumor growth by beta and gamma-secretase inhibitors. Eur J Pharmacol. 2005;514(1):1–15.
37. Li JL, Sainson RC, Oon CE, Turley H, Leek R, Sheldon H, Bridges E, Shi W, Snell C, Bowden ET, et al. DLL4-notch signaling mediates tumor resistance to anti-VEGF therapy in vivo. Cancer Res. 2011;71(18):6073–83.
38. Raghu H, Lakka SS, Gondi CS, Mohanam S, Dinh DH, Gujrati M, Rao JS. Suppression of uPA and uPAR attenuates angiogenin mediated angiogenesis in endothelial and glioblastoma cell lines. PLoS One. 2010;5(8):e12458.
39. Nicosia RF, Nicosia SV, Smith M. Vascular endothelial growth factor, platelet-derived growth factor, and insulin-like growth factor-1 promote rat aortic angiogenesis in vitro. Am J Pathol. 1994;145(5):1023–9.
40. Granata R, Trovato L, Lupia E, Sala G, Settanni F, Camussi G, Ghidoni R, Ghigo E. Insulin-like growth factor binding protein-3 induces angiogenesis through IGF-I- and SphK1-dependent mechanisms. J Thromb Haemost. 2007;5(4):835–45.
41. Zadeh G, Bhat KP, Aldape K. EGFR and EGFRvIII in glioblastoma: partners in crime. Cancer Cell. 2013;24(4):403–4.
42. Azuaje F, Tiemann K, Niclou SP. Therapeutic control and resistance of the EGFR-driven signaling network in glioblastoma. Cell Commun Signal. 2015;13:23.
43. Stockhausen MT, Kristoffersen K, Poulsen HS. Notch signaling and brain tumors. Adv Exp Med Biol. 2012;727:289–304.
44. Ma J, Meng Y, Kwiatkowski DJ, Chen X, Peng H, Sun Q, Zha X, Wang F, Wang Y, Jing Y, et al. Mammalian target of rapamycin regulates murine and human cell differentiation through STAT3/p63/jagged/notch cascade. J Clin Invest. 2010;120(1):103–14.
45. Reardon DA, Wen PY, Mellinghoff IK. Targeted molecular therapies against epidermal growth factor receptor: past experiences and challenges. Neuro Oncol. 2014;16(Suppl 8):viii7–13.
46. Krop I, Demuth T, Guthrie T, Wen PY, Mason WP, Chinnaiyan P, Butowski N, Groves MD, Kesari S, Freedman SJ, et al. Phase I pharmacologic and pharmacodynamic study of the gamma secretase (notch) inhibitor MK-0752 in adult patients with advanced solid tumors. J Clin Oncol. 2012;30(19):2307–13.

SUPPLEMENTARY MATERIAL

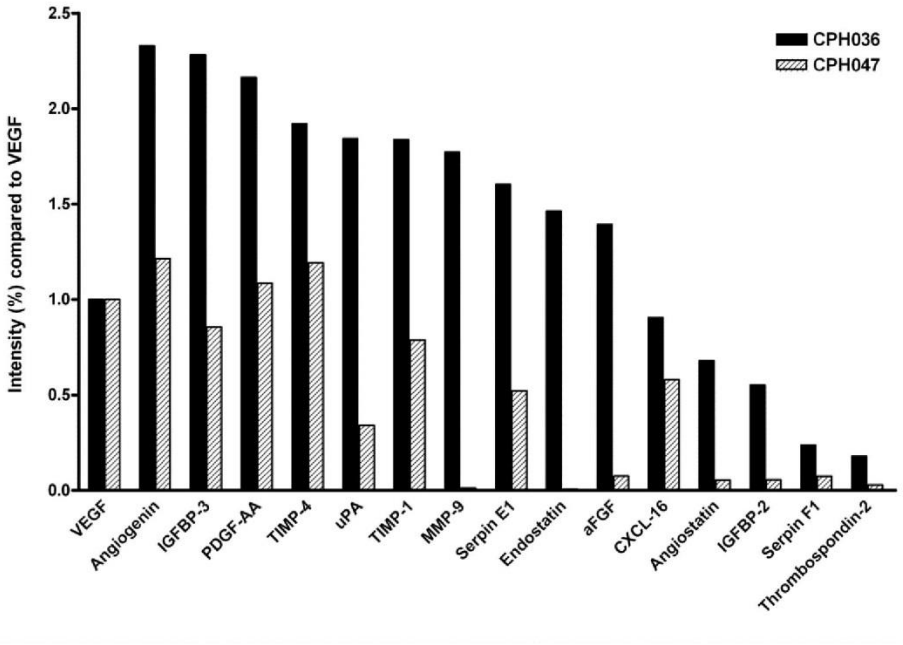

Supplementary Figure 1. Evaluation of angiogenic factors secreted by GBM cells. Relative secretion of angiogenic factors set relative to VEGF secretion. One million GBM cells (CPH036 and CPH047) were incubated for 14 days and the conditioned cell media was harvested, concentrated around 10 times and subjected to the Proteome Profiler human angiogenesis array kit (R&D systems) used in accordance with the manufacturer's instructions. Signal was detected utilizing the Super-Signal West Dura extended Duration Substrate (Pierce Biotechnology) in the UVP Biospectrum AC imaging system which also was used for quantification of relative protein expression. Mean of one experiment performed in duplicate is shown.

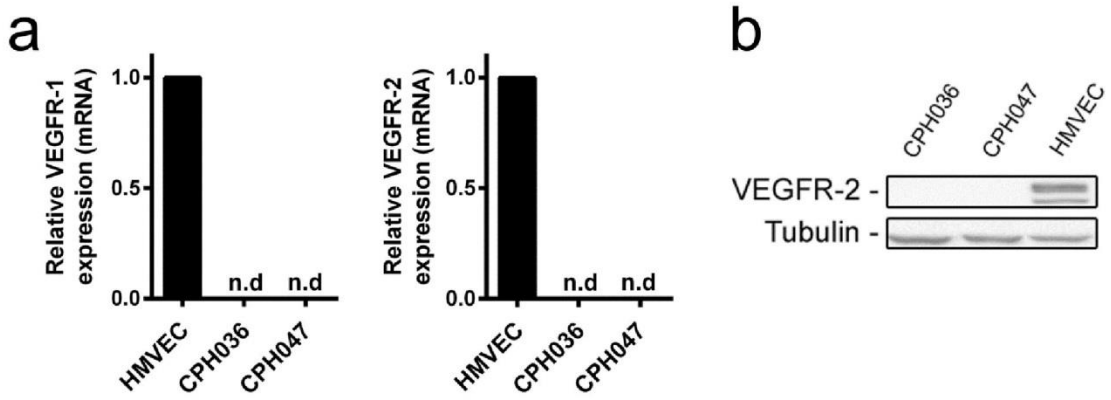

Supplementary Figure 2. Expression of VEGF receptors (VEGFR-1 and VEGFR-2) in GBM cell cultures CPH036 and CPH047 and in endothelial cells (HMVEC). (a) Expression levels of VEGFR-1 and VEGFR-2 evaluated by Q-RT-PCR. (b) Expression of VEGFR-2 identified by western blotting using primary antibody against VEGFR-2 and tubulin.

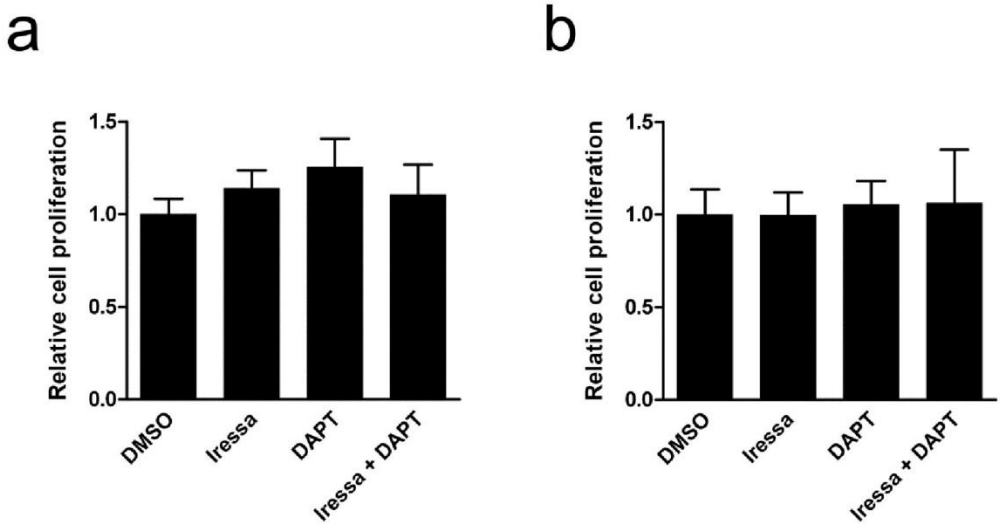

Supplementary Figure 3. Effect of conditioned cell media from GBM cell cultures treated with inhibitors on endothelial cell proliferation. Conditioned media was obtained from $1x10^6$ cells of either CPH036 (a) or CPH047 (b) cells treated for 14 days with DMSO, 5µM Iressa, 5µM DAPT or a combination. HMVEC (EC) cells were plated in 96-well plates (2,000 cells in 0.1 mL EC media) and the following day the media was changed to EC media added 10% of conditioned media from the GBM cells that had been concentrated around 10 times. Cells were incubated for 20 hrs and level of proliferation was examined by BrdU assay using the Cell Proliferation ELISA, BrdU kit (Roche A/S) using a 20 hrs BrdU incubation step and otherwise following the instructions by the manufacturer. Quantification was done by measuring the absorbance at 370nm with 492nm as a reference using Synergy2 microplate reader with Gen5. Data are shown as mean ± SEM obtained from three independent experiments. Significant difference was tested with a one-way ANOVA with a Tukey post-hoc test.

Dilution	Antibody	Manufacturer
1:1000	Rabbit anti-Akt	Cell Signaling, #9272
1:1000	Rabbit anti-pAkt	Cell Signaling, #9271
1:1000	Rabbit anti-Erk 1/2	Cell Signaling, #9102
1:1000	Mouse anti-pErk 1/2	Cell Signaling, #9106
1:20.000	Sheep anti-EGFR	Fitzgerald, #20-ES04
1:1000	Rabbit anti-pEGFR	Invitrogen, #44-790G
1:50	Mouse anti-EGFRvIII	Duke University, L8A4
1:100	Goat anti-Notch 1	Santa Cruz, #SC-23304
1:1000	Rabbit anti-Notch 3	Cell Signaling, #5276
1:1000	Rabbit anti-Dll 4	Abcam, #ab7280
1:2000	Rabbit anti-Hes 1	Toray Industries inc, Japan
1:1000	Rabbit anti-VEGFR-2	Cell signaling, #55b11
1:1000	Rabbit anti-Tubulin	Cell Signaling, #2125

Supplementary Figure 4. Overview of primary antibodies used for western blotting. Antibodies are listed with dilution, manufacturer (university) and catalog number.

Target gene	Forward primer (5' - 3')	Reverse primer (5' - 3')
EGFR	GGC ATA GGA ATT TTC GTA GTA CAT	TCC TTG GGA ATT TGG AAA TT
EGFRvIII	ATG CGA CCC TCC GGG ACG	ATC TGT CAC ATA ATT ACC T
Dll-1	GCC GAC AAG AAT GGC TTC	CCG GCC TTT TTC TTT CAG
Dll-4	GGT CAG ACC TGG TTA TTG G	CGA AAG ACA GAT AGG CTG
Hes-1	AGC GGG CGC AGA TGA C	CGT TCA TGC ACT CGC TGA A
Notch-1	CTT CCC CTA CGG CCG CGA	CAG GTA GAC GAT GGA GCC GCG GA
Notch-2	GCC TGT ATG TGC CCT GTG CAC C	AGC CTC CAT TGC GGT TGG CAC
Notch-3	CTG GCT GAC AGC TCG GTC ACG C	AGT GGC AGT GGC AGC TGC ATA G
Jagged-1	ATG GGG AGT GTG ATA CCA	GAG ACT GGA AGA CCG ACA
Jagged-2	CGG CCA CCT GGA CAA TAA	CAA CCG TCT CCA CCT TGA
VEGF	CCT TGC TGC TCT ACC TCC AC	ATC TGC ATG GTG ATG TTG GA
VEGFR-1	GGC TCT GTG GAA AGT TCA GC	GTG ACC AAC ATG GAG TCG TG
VEGFR-2	GTG ACC AAC ATG GAG TCG TG	TGC TTC ACA GAA GAC CAT GC

Supplementary Figure 5. Overview of primer sets used for Q-RT-PCR. All primers were obtained from DNA Technology A/S.

3.3 Results - Study III

Molecular profiling of short-term and long-term surviving patients identifies CD34 mRNA levels as prognostic for glioblastoma survival

By

Signe R. Michaelsen, Thomas Urup, Lars Rønn Olsen, Helle Broholm, Ulrik Lassen and Hans S. Poulsen

Submitted, 2017

Summary study III:

This study examined RNA expression level of 792 genes for prognostic value for OS of glioblastoma. A study cohort of 93 patients was selected from a population of patients previously examined for gene expression in the diagnostic tumor specimen using the NanoString platform. All included patients had primary glioblastomas and all had been treated with concomitant radiation- and chemotherapy therapy as well as bevacizumab in either the first-line or relapse setting. For identification of potential biomarkers an analysis strategy was applied with an initial screening in patients being extreme in regards to survival. Among the 93 patients, 14 short-term survivors (STS, OS ≤ 12 months) and 6 long-term survivors (LTS, OS ≥ 36 months) were identified, all confirmed being IDH wildtype. Comparison of these patients found no differences between the STS and LTS groups in regard to glioblastoma subtype, but 14 single genes were significantly differently expressed; a number reduced to 12 upon univariate analysis in whole patient cohort. In multivariate analysis in the patient cohort adjusting for known prognostic markers (age, corticosteroid use, performance status and MGMT status) increased IFNG, CXCL9, LGALS4, CD34 levels and decreased MGMT level remained significant associated with prolonged OS. Lastly, these genes were tested in an independent validation cohort consisting of 349 patients participating in the AVAglio study. These patients had been examined with a similar NanoString platform as in our study cohort. Upon multivariate analysis of the candidate genes in the validation cohort, CD34 and MGMT level remained significantly associated with OS, but only CD34 were significantly differently expressed between STS and LTS patients in the validation cohort. Besides confirming previously findings for association of MGMT expression with survival in glioblastoma, study support increased CD34 mRNA level as an identifier of LTS patients as well as an independent prognostic marker for increased OS in newly diagnosed glioblastoma. CD34 is a vessel marker and data therefore argue for further analysis of vessel architecture for treatment effect and survival in glioblastoma.

Molecular profiling of short-term and long-term surviving patients identifies CD34 mRNA levels as prognostic for glioblastoma survival

AUTHORS

Signe Regner Michaelsen[1*], Thomas Urup[1,2], Lars Rønn Olsen[3], Helle Broholm[4], Ulrik Lassen[2], Hans Skovgaard Poulsen[1,2]

AFFILIATIONS

[1]Department of Radiation Biology, Rigshospitalet, Copenhagen, Denmark.

[2]Department of Oncology, Rigshospitalet, Copenhagen, Denmark.

[3]Department of Bio and Health Informatics, Technical University of Denmark, Lyngby, Denmark.

[4]Department of Pathology, Rigshospitalet, Copenhagen, Denmark.

*Corresponding Author:

Signe Regner Michaelsen, Tel: (+45) 35 45 63 03, Fax (+45) 35 45 63 01,

Email: signe.regner.michaelsen@regionh.dk; signerm@gmail.com

RUNNING TITLE

CD34 is prognostic for glioblastoma survival

KEYWORDS

Prognostic markers, GBM, NanoString, CD34, MGMT, LTS

ABSTRACT

Despite extensive treatment, overall survival (OS) for glioblastoma (GBM) remains poor. A small proportion of patients present long survival over 3 years, but the underlying molecular background separating these long-term survivors (LTS) from short-term survivors (STS) are insufficiently understood. Accordingly, study aim was to identify independent prognostic biomarkers for survival.

Study cohort consisted of 93 primary GBM patients treated with radiation-, chemo- and bevacizumab therapy, among which 14 STS (OS ≤ 12 months) and 6 LTS (OS ≥ 36 months) were identified, all confirmed being IDH wild-type. RNA expression levels in diagnostic tumor specimen for 792 genes were analyzed by NanoString technology. While no differences were found with regard to GBM subtype between LTS *vs.* STS, comparative analysis of individual genes identified 14 significantly differently expressed candidate genes. Univariate analysis in the whole patient cohort found that 12 of these were significantly associated with OS, of which increased *IFNG*, *CXCL9*, *LGALS4*, *CD34* and decreased *MGMT* levels remained significant associated with prolonged OS in multivariate analysis correcting for known prognostic variables. Validation of study results in an independent dataset from the AVAglio study confirmed *CD34* as significant in comparative analysis between STS and LTS patients and in multivariate analysis together with clinicopathological factors. The external validation cohort thereby supports association of increased *CD34* mRNA level in the diagnostic specimen with prolonged survival in primary GBM patients receiving radiation-, chemo- and bevacizumab therapy. Accordingly, measuring *CD34* expression can be useful as biomarker of GBM patient survival and to identify potential STS and LTS.

BACKGROUND

Glioblastoma (GBM) is a devastating disease with median overall survival (OS) rate under 15 months [1]. However, despite a large proportion of the GBM patient population dying within the first 12 months from diagnosis, around 15 % live past 36 months [1, 2]. Access to a reliable method to predict which patients that will turn into short-term-survivors (STS) and long-term-survivors (LTS) could prove beneficial for both clinical trial design and development of individualized treatment programs for GBM.

Patient characteristics reported associated with GBM prognosis includes patient age, performance status (PS), extent of resection, multiple lesion sites and corticosteroids use [2-6]. On the molecular side promoter methylation of the O^6-methylguanine-DNA methyltransferase (MGMT) gene, inversely correlated to gene expression, has been established as a prognostic marker [7-9]. Also mutation of isocitrate dehydrogenase 1 (IDH1) gene warrants a better prognosis [10]. However, the IDH mutant patient group consists mainly of secondary GBMs developing from lower grade glioma [11] and deviates from IDH wild-type GBMs by having separate methylation and gene expression profile [12-15]. Both MGMT promoter methylation and IDH mutation has specifically been confirmed overrepresented in LTS [16-19], but otherwise information on the molecular background for what differentiate LTS from the general GBM population is sparse. The few conducted studies using genome wide approaches have had difficulties identifying a solid LTS signature profile [20-22] and also attempts to associate the LTS patient group with specific GBM molecular subtypes have failed [20, 21, 23]. Reports have though indicated increased genomic instability [22] and co-gain of chromosome 19/20 [21] in LTS patient tumors. Contrary, GBMs of STS have a tendency towards general DNA hypomethylation [20, 22] as well as overrepresentation of a pro-tumorigenic inflammation phenotype [21-23].

Study aim was to identify novel prognostic factors for OS of GBM patients. With specific focus on STS and LTS, we explored expression level of 792 genes in a cohort of newly diagnosed GBM patients undergoing treatment with radiation, chemotherapy and bevacizumab, a vascular endothelial growth factor (VEGF) -targeting antibody.

MATERIAL AND METHODS

Patient population

Patients for this study were identified among a cohort of 112 patients which all had pathologically confirmed GBM (WHO grade IV) and who had received bevacizumab as either first-line or relapse therapy at Rigshospitalet, Copenhagen, between May 2005 and December 2011. Furthermore, these patients were bevacizumab response evaluable and had available tumor tissue from which sufficient RNA could be purified for analysis of gene expression using the Nanostring method (selection criteria are described in detail in Urup et al. [24]). Additionally, inclusion criteria were patients with newly diagnosed primary GBM, excluding 16 patients having a prior diagnosis with lower grade glioma, and first-line treatment with radiation therapy with concomitant and adjuvant chemotherapy, excluding one patient. Bioinformatics analysis excluded additional two patients due to poor gene expression quality (see below), resulting in a final cohort of biomarker evaluable patients of 93. Among these long-term survivors (LTS, OS ≥ 36 months from GBM diagnosis) and short-term survivors (STS, OS ≤ 12 months from GBM diagnosis) were identified. Patient selection for this study is described in the REMARK diagram shown in Figure 1.

Treatment

Among the final cohort of 93 patients, 66 patients had received first-line therapy according to the Stupp regimen (ie, concomitant radiation- and temozolomide therapy, followed by up to 6 courses of adjuvant temozolomide therapy) as previously described [2]. As relapse therapy these patients had received bevacizumab given every two weeks either together with irinotecan according to a previously published treatment protocol (BI, 51 patients) [25] or together with both irinotecan and cetuximab in a phase 2 trial (CBI, 15 patients) [26]. After progression on primary therapy 31 of the 66 patients receiving Stupp regimen underwent reoperation and 9 received different types of experimental treatment either before or after bevacizumab relapse therapy.

The remaining 27 of the 93 patients had been enrolled in a phase 2 trial randomizing for concomitant radiation-, bevacizumab- and irinotecan-therapy (BI) or concomitant radiation-, bevacizumab- and temozolomide-therapy (BT) with neoadjuvant and adjuvant treatment with bevazicumab-irinitocan or bevacizumab-temozolomide, respectively [27]. Upon disease progression two of these BI-BT treated patients underwent reoperation and 14 patients received protocol crossover therapy.

Gene expression analysis of tumor samples

RNA purified from the diagnostic tumor sample of included patients had previously been examined by NanoString gene expression analysis as described in Urup et. al [24], in which data regarding a proportion of the patients in this study were also analyzed. In short, RNA was purified at HistogeneX, Belgium, from tissue sections of formalin-fixed paraffin embedded (FFPE) tumor material using microdissection to remove non-tumor material and using the High Pure RNA Paraffin Isolation kit (Roche, Ca. No. 03.270.289.001). NanoString gene expression measurement (NanoString Technologies, Seattle, WA) was conducted using a customized platform of 800 genes designed by Genentech, San Francisco, CA, to allow for classification according to the Phillips GBM subtypes [28] and evaluation of genes estimated central for various GBM features. Full gene list is shown in Supplementary Table 1.

Subtype classification was conducted by Genentech without knowledge of clinical outcome using a 31 gene classifier previously described [29]. All other bioinformatics analysis was conducted using R version 3.1 (R Development Core Team, Vienna, Austria, http://www.R-project.org). Raw counts for included samples were log2 transformed and expression of 792 genes was normalized to 8 reference genes *ACTB*, *AL-137727*, *GUSB*, *PPIA*, *RPLP0*, *TUBB*, *UBC*, and *VPS33B* as in our previous study [24]. Based on distribution from normalization analysis two outlier samples with poor gene expression data quality were identified and removed from further analysis.

Assessment of IDH mutation status

IDH analysis was conducted for selected patients using parallel sections from same FFPE tumor samples also analyzed for RNA expression. For most of these patients IDH was analyzed by immunohistochemistry on sections using the OptiView DAB IHC v4 Protocol (v1.00.0108) plus the BenchMark ULTRA IHC staining Module (Ventana Medical System, Tucson, AZ). Primary antibody was anti-IDH1 R132H (clone H09, Dianova) at 1:700 dilution. In a few cases IDH1-R132 status was examined on purified DNA by Multiplex Ligation-dependent Probe Amplification (MLPA) analysis, using the SALSA MLPA kit P088 (MRC Holland, Amsterdam, the Netherlands) and following the instructions of the manufacturer.

Validation in AVAglio trial cohort

For validation purposes data on 349 patients with biomarker-evaluable samples from the AVAglio clinical trial previously analyzed using the NanoString techniques in Sandmann et al. [29] were used. NanoString data covered 743 of the 800 genes analyzed in the current study including the 8 housekeeping genes and were together with clinical data downloaded via the NCBI's GEO database, accession GSE84010. Data were log2 transformed and normalized as described for the NanoString data of our study cohort.

Statistical analysis

Survival probabilities were estimated using the Kaplan-Meier method. Comparison of clinical characteristics for LTS and STS cohorts were done using the Fisher's exact test and the Mann-Whitney U test. The Welch's t-test was performed in the initial screen for differentially expressed genes between LTS and STS patients in our study cohort, while comparative analysis of single genes between STS and LTS as well as between MGMT promoter methylated and non-methylated patients in the validation cohort was done by Mann-Whitney U test. The Cox proportional hazards model was used for univariate and multivariate analyses of OS and results are presented as hazard ratios (HR) with 95% confidence interval (CI). For continues covariates, data were log transformed (log base 2) prior to these analysis. *P*-values < 0.05 were considered significant. Calculations were performed using SPSS (v22.0, IBM Corp., Armonk, NY) and R version 3.1.

RESULTS

Characteristics of patient cohort and LTS- and STS sub-populations

93 GBM patients were identified for study inclusion (REMARK diagram, Figure 1). These were all biomarker evaluable, had all no prior diagnosis with lower grade glioma and had all been treated with concomitant radiation- and chemotherapy, in form of temozolomide or irinotecan, as well as with bevacizumab therapy. Among this population, 14 STS and 6 LTS patients were identified, which by molecular analysis of diagnostic tumor sample were confirmed to be IDH1 wild-type.

Clinicopathological characteristics of the total patient cohort and STS plus LTS sub-populations are shown in Table 1. Median OS was for all patients 17.0 months, while for STS 9.9 months and for LTS 52.3 months. Two patients of the LTS group were still alive at study cut-off with follow-up times of 71 and 116 months. There were no significantly differences between LTS and STS patients

in regard to gender, WHO PS, presence of multifocal disease, extent of primary surgery, reception of tumor reoperation or GBM subtype. Significantly less LTS than STS received corticosteroid treatment at start of first-line therapy (33.3% *vs.* 92.9%; $P = 0.014$); while age at diagnosis had a non-significant trend for younger age in LTS (median: 54.4 years) *vs.* STS patients (median: 62.0 years), ($P = 0.098$). Patients had been enrolled in different therapeutic treatment protocols and type of treatment differed significantly between STS and LTS patients ($P = 0.014$). Among the LTS, all patients had received primary treatment with concomitant radiation- and temozolomide therapy followed by relapse bevacizumab therapy (RT/TMZ + BI or CBI therapy). In the STS sub-population only 5 had this type of treatment, while remaining patients had received first-line concomitant radiation-, chemo- and bevacizumab therapy (BI-BT therapy).

Identification of biomarkers associated with patient survival

RNA expression data for 800 genes obtained by NanoString analysis of the diagnostic tumor sample from included patients were analyzed in a 4 step process shown in Figure 2. After initial pre-processing (Step 1), we conducted specific analysis of LTS *vs.* STS sub-populations, based on the hypothesis that comparison of these survival-wise extreme groups could identify relevant prognostic variables (Step 2). A Welch's t-test was employed, thereby addressing potential problems of unequal variance and sample size, and out of 792 analyzed genes, 14 genes were significantly differently expressed ($P < 0.05$) between the LTS and STS sub-populations (Supplementary Table 2). Of these two genes (*MGMT* and *E2F5*) were downregulated in LTS compared to STS, while remaining 12 genes (*OX40*, *IFNG*, *CXCL9*, *LGALS4*, *RTN1*, *PTPRO*, *REN*, *NKX2-2*, *MDM2*, *POLK*, *NKG2D* and *CD34*) were upregulated in LTS compared to STS patients. The identified genes were screened for association with OS in an univariate analysis in the total population of 93 patients (Step 3), and 12 of the 14 analyzed genes were found to be significantly ($P < 0.05$) associated with OS (Supplementary Table 3). In step 4, these candidate genes were further individually tested in multivariate analysis together with clinicopathological factors that we previously have found being significantly associated with survival for patients receiving concomitant radiation- and chemotherapy at our institution [2, 8]. These included patient age at diagnosis (years), corticosteroid use (yes *vs.* no) and WHO PS (1 *vs.* 0); which all were confirmed by univariate analysis also being significantly associated with OS ($P < 0.05$) in the patient population of this study (Supplementary Table 3). Additionally MGMT status was included in these analyses. However, as we did not have access to MGMT promoter methylation status for our study cohort,

MGMT mRNA expression was included in multivariate analysis instead based on the anticipation of these factors being inversely correlated. This rationale was supported by finding of *MGMT* mRNA expression being significant in the univariate analysis (HR = 1.52; *P* = 0.001), (Supplementary Table 3), as well as in a reduced multivariate analysis together with age, WHO PS and corticosteroid use (HR = 1.52; *P* = 0.003), (Table 2). Of the remaining 11 candidate genes, four turned out significant upon individual testing in multivariate analysis adjusted for the four clinicopathological variables (Table 2). These were *IFNG* (HR = 0.61; *P* = 0.008), *CXCL9* (HR = 0.83; *P* = 0.037), *LGALS4* (HR = 0.61; *P* = 0.002) and *CD34* (HR = 0.64; *P* = 0.014).

Testing of identified survival associated biomarkers in AVAglio cohort

To further investigate if the identified biomarkers (*IFNG*, *CXLC9*, *LGALS4*, *CD34* and *MGMT*) can be used for identification of survival outliers and represent independent prognostic variables, we examined online available data generated for 349 of the patients in the AVAglio study; a clinical trial comparing radiation-temozolomide-bevacizumab *vs.* radiation-temozolomide-placebo treatment in the first-line setting for GBM [29]. As this study did not show survival differences dependent on treatment, analysis was done on patients from both treatment arms. Tumors had been examined with a NanoString platform very similar to the one used in this study, including both the five biomarkers of interest as well as the same housekeeping genes. Pre-processing of data was done in the same manner as described above and comparative analysis of IDH wild-type STS (n = 115) *vs.* LTS (n = 7) patients in the AVAglio cohort showed significantly increased *CD34* expression levels in LTS patients (log2 fold change = 0.58, *P* = 0.01, Mann-Whitney U test). In contrast, none of the other four variables were significantly differently expressed at mRNA level in STS and LTS patients in the AVAglio cohort (*P* = 0.19 – 0.74) and data thereby only support high *CD34* expression as an identifier of the LTS patient group.

Following, *IFNG*, *CXLC9*, *LGALS4*, and *CD34* were individually tested in multivariate analysis together with the clinicopathological factors, patient age (years), corticosteroid use (yes *vs.* no), WHO PS (1-2 *vs.* 0) and MGMT promoter methylation (yes *vs.* no). Results validated increased *CD34* (HR = 0.68; *P* = 0.010) as being independently associated with prolonged OS, while they were nonsignificant for *CXCL9, IFNG* and *LGALS4* (*P* > 0.05) (Table 3). Similar to our study cohort, *MGMT* mRNA level also remained significantly associated with OS in a reduced multivariate analysis not including MGMT promoter status (HR = 1.57; *P* < 0.001) (Table 3). Further, comparative analysis of *MGMT* mRNA level in MGMT promoter methylated *vs*. non-methylated patients in the AVAglio

cohort showed significantly decreased mRNA expression in methylated patients (log2 fold change = -0.75, $P < 0.001$, Mann-Whitney U test). These results thereby confirmed our anticipation of an inverted relationship between MGMT promoter methylation status and mRNA expression level evaluated by the NanoString method.

DISCUSSION

This study find increased *CD34* mRNA expression to be independently associated with prolonged survival of GBM patients as well as significantly overexpressed in LTS *vs*. STS in two separate datasets. CD34 is a transmembrane cell surface protein expressed by vascular endothelial cells, and consequently often used to estimate microvascular density (MVD) in tumor tissue [30]. A previous study also identified *CD34* as part of a 43 gene-based expression profile separating LTS and STS [31]. This study which had several similarities to our study as it examined the diagnostic sample of primary GBMs treated with combined radiation- and chemotherapy, verified significantly increased *CD34* expression in LTS *vs.* STS using both microarray and PCR methods. Contrary, we and others have not been able to show significantly association of MVD as estimated by CD34 immunohistochemistry with OS in GBMs undergoing combinations of radiation-, chemo- and bevacizumab therapy [32-34], although the study by Wang et al. observed a non-significant trend towards increased OS in patients with higher MVD [33]. This lack of prognostic value of MVD, could result from that MVD does not reflect CD34 protein expression precisely, as it does only estimate vessel number and neither take vessel size nor variant vessel architecture into account. Still, it could be speculated that prognostic value of CD34 in GBM is a product of better tumor vascularization resulting in improved drug delivery and/or higher effect of radiation therapy due to increased tumor oxygenation. Future investigations will need to verify this hypothesis.

By excluding secondary GBMs from our study population and securing that our LTS and STS cohorts did not contain tumors harboring IDH1 mutation, we eliminated analysis bias from this distinct GBM subgroup. Importance of such procedures is emphasized by almost exclusively clustering of IDH1 GBM tumors into the proneural GBM subtype [15, 35]. This has been shown to confer the survival advances previously reported for this subtype [28], with analysis only examining IDH1 negative proneural GBMs not finding this trend in comparison to the other subtypes [29, 36]. Accordingly we here report as by previous studies, the LTS to distribute into all GBM subtypes with no significant differences as compared to STS [21, 23].

In contrast to MGMT promoter methylation, relevance of *MGMT* expression as prognostic variable is questionable with both positive and negative studies [37]. Here we show *MGMT* RNA level to be independently associated with GBM survival in both our study- and validation cohorts and further confirm *MGMT* RNA level to be inversely correlated with MGMT promoter methylation status. *MGMT* RNA level were also significantly differently expressed in STS and LTS patients in our study cohort, being in line with findings for reduced frequency of *MGMT* promoter methylated patients among LTS [16-19]. Study results thereby acknowledge prognostic relevance of *MGMT* status estimated based on RNA expression.

Among clinical factors evaluated in LTS *vs.* STS sub-populations, we find significant increase of STS receiving corticosteroids. Lack of significance of other known prognostic factors, e.i. age and PS [2, 5], is presumable a result of the low patient number in the STS and LTS cohorts; a shortcoming of many studies of survival outliers in GBM, often including 10 or less LTS [17, 21-23]. Contrary, we find that type of treatment differed significantly between STS and LTS. The major difference between the treatments of our study cohort was whether bevacizumab was given in first-line or as relapse therapy. Therefore, when considering the lack of efficacy on OS of adding bevacizumab to first-line or relapse treatment in recent years randomized clinically phase 3 trials [38-40], we estimate that treatment differences have not influenced findings in this study.

CONCLUSION

This study finds *CD34* gene expression level to be significantly higher in LTS *vs.* STS GBM patients as well as being independently associated with improved OS in two GBM patient cohorts. This warrants that measurement of *CD34* level could improve prognostic models for OS in GBM and inform for further research of the influence of vascular heterogeneity on GBM tumor growth and treatment response.

NOTES

Acknowledgements

The authors would like to thank Kirsten Grunnet for contribution to assembly of clinical information and Genentech for generation of gene expression analysis and providing sample subtyping. Financial support was kindly received from The University of Copenhagen and the Sejer

Perssons and Lis Klüwers Foundation. Genentech funded RNA and DNA purification as well as the gene expression analysis, but was not involved in interpretation of results or manuscript drafting.

Compliance with ethical Standards

Conflict of interest

The authors declare no conflict of interest.

Ethical approval

Study was approved by the Danish Data Protection Agency (2006-41-6979) and the ethical committee for the Capital Region of Denmark (H-2-2012-069). Exemption from obtaining informed consent to participate was granted by the ethical committee as patients were either deceased or fatally ill.

REFERENCES

1. Stupp R, Hegi ME, Mason WP, van den Bent MJ, Taphoorn MJ, Janzer RC, Ludwin SK, Allgeier A, Fisher B, Belanger K, Hau P, Brandes AA, Gijtenbeek J, Marosi C, Vecht CJ, Mokhtari K, Wesseling P, Villa S, Eisenhauer E, Gorlia T, Weller M, Lacombe D, Cairncross JG, Mirimanoff RO (2009) Effects of radiotherapy with concomitant and adjuvant temozolomide versus radiotherapy alone on survival in glioblastoma in a randomised phase III study: 5-year analysis of the EORTC-NCIC trial. Lancet Oncol 10: 459-466

2. Michaelsen SR, Christensen IJ, Grunnet K, Stockhausen MT, Broholm H, Kosteljanetz M, Poulsen HS (2013) Clinical variables serve as prognostic factors in a model for survival from glioblastoma multiforme: an observational study of a cohort of consecutive non-selected patients from a single institution. BMC Cancer 13: 402 doi:1471-2407-13-402 [pii];10.1186/1471-2407-13-402 [doi]

3. Gittleman H, Lim D, Kattan MW, Chakravarti A, Gilbert MR, Lassman AB, Lo SS, Machtay M, Sloan AE, Sulman EP, Tian D, Vogelbaum MA, Wang TJC, Penas-Prado M, Youssef E, Blumenthal DT, Zhang P, Mehta MP, Barnholtz-Sloan JS (2017) An independently validated nomogram for individualized estimation of survival among patients with newly diagnosed glioblastoma: NRG Oncology RTOG 0525 and 0825. Neuro Oncol 19: 669-677 doi:10.1093/neuonc/now208

4. Field KM, Rosenthal MA, Yilmaz M, Tacey M, Drummond K (2014) Comparison between poor and long-term survivors with glioblastoma: review of an Australian dataset. Asia Pac J Clin Oncol 10: 153-161 doi:10.1111/ajco.12076

5. Gorlia T, van den Bent MJ, Hegi ME, Mirimanoff RO, Weller M, Cairncross JG, Eisenhauer E, Belanger K, Brandes AA, Allgeier A, Lacombe D, Stupp R (2008) Nomograms for predicting survival of patients with newly diagnosed glioblastoma: prognostic factor analysis of EORTC and NCIC trial 26981-22981/CE.3. Lancet Oncol 9: 29-38

6. Fekete B, Werlenius K, Orndal C, Rydenhag B (2016) Prognostic factors for glioblastoma patients--a clinical population-based study. Acta Neurol Scand 133: 434-441 doi:10.1111/ane.12481

7. Hegi ME, Diserens AC, Gorlia T, Hamou MF, de TN, Weller M, Kros JM, Hainfellner JA, Mason W, Mariani L, Bromberg JE, Hau P, Mirimanoff RO, Cairncross JG, Janzer RC, Stupp R (2005) MGMT gene silencing and benefit from temozolomide in glioblastoma. N Engl J Med 352: 997-1003

8. Kristensen LS, Michaelsen SR, Dyrbye H, Aslan D, Grunnet K, Christensen IJ, Poulsen HS, Gronbaek K, Broholm H (2016) Assessment of Quantitative and Allelic MGMT Methylation Patterns as a Prognostic Marker in Glioblastoma. J Neuropathol Exp Neurol 75: 246-255 doi:nlv024 [pii];10.1093/jnen/nlv024 [doi]

9. Lalezari S, Chou AP, Tran A, Solis OE, Khanlou N, Chen W, Li S, Carrillo JA, Chowdhury R, Selfridge J, Sanchez DE, Wilson RW, Zurayk M, Lalezari J, Lou JJ, Ormiston L, Ancheta K, Hanna R, Miller P, Piccioni D, Ellingson BM, Buchanan C, Mischel PS, Nghiemphu PL, Green R, Wang HJ, Pope WB, Liau LM, Elashoff RM, Cloughesy TF, Yong WH, Lai A (2013) Combined analysis of O6-methylguanine-DNA methyltransferase protein expression and promoter methylation provides optimized prognostication of glioblastoma outcome. Neuro Oncol 15: 370-381 doi:10.1093/neuonc/nos308

10. Cheng HB, Yue W, Xie C, Zhang RY, Hu SS, Wang Z (2013) IDH1 mutation is associated with improved overall survival in patients with glioblastoma: a meta-analysis. Tumour Biol 34: 3555-3559 doi:10.1007/s13277-013-0934-5

11. Dunn GP, Andronesi OC, Cahill DP (2013) From genomics to the clinic: biological and translational insights of mutant IDH1/2 in glioma. Neurosurg Focus 34: E2 doi:10.3171/2012.12.FOCUS12355

12. Turcan S, Rohle D, Goenka A, Walsh LA, Fang F, Yilmaz E, Campos C, Fabius AW, Lu C, Ward PS, Thompson CB, Kaufman A, Guryanova O, Levine R, Heguy A, Viale A, Morris LG, Huse JT, Mellinghoff IK, Chan TA (2012) IDH1 mutation is sufficient to establish the glioma hypermethylator phenotype. Nature 483: 479-483 doi:10.1038/nature10866

13. Hata N, Hatae R, Yoshimoto K, Murata H, Kuga D, Akagi Y, Sangatsuda Y, Suzuki SO, Iwaki T, Mizoguchi M, Iihara K (2017) Insular primary glioblastomas with IDH mutations: Clinical and biological specificities. Neuropathology 37: 200-206 doi:10.1111/neup.12362

14. Sturm D, Witt H, Hovestadt V, Khuong-Quang DA, Jones DT, Konermann C, Pfaff E, Tonjes M, Sill M, Bender S, Kool M, Zapatka M, Becker N, Zucknick M, Hielscher T, Liu XY, Fontebasso AM, Ryzhova M, Albrecht S, Jacob K, Wolter M, Ebinger M, Schuhmann MU, van Meter T, Fruhwald MC, Hauch H, Pekrun A, Radlwimmer B, Niehues T, von Komorowski G, Durken M, Kulozik AE, Madden J, Donson A, Foreman NK, Drissi R, Fouladi M, Scheurlen W, von Deimling A, Monoranu C, Roggendorf W, Herold-Mende C, Unterberg A, Kramm CM, Felsberg J, Hartmann C, Wiestler B, Wick W, Milde T, Witt O, Lindroth AM, Schwartzentruber J, Faury D, Fleming A, Zakrzewska M, Liberski PP, Zakrzewski K, Hauser P, Garami M, Klekner A, Bognar L, Morrissy S, Cavalli F, Taylor MD, van Sluis P, Koster J, Versteeg R, Volckmann R, Mikkelsen T, Aldape K,

Reifenberger G, Collins VP, Majewski J, Korshunov A, Lichter P, Plass C, Jabado N, Pfister SM (2012) Hotspot mutations in H3F3A and IDH1 define distinct epigenetic and biological subgroups of glioblastoma. Cancer Cell 22: 425-437 doi:10.1016/j.ccr.2012.08.024

15. Verhaak RG, Hoadley KA, Purdom E, Wang V, Qi Y, Wilkerson MD, Miller CR, Ding L, Golub T, Mesirov JP, Alexe G, Lawrence M, O'Kelly M, Tamayo P, Weir BA, Gabriel S, Winckler W, Gupta S, Jakkula L, Feiler HS, Hodgson JG, James CD, Sarkaria JN, Brennan C, Kahn A, Spellman PT, Wilson RK, Speed TP, Gray JW, Meyerson M, Getz G, Perou CM, Hayes DN, Cancer Genome Atlas Research N (2010) Integrated genomic analysis identifies clinically relevant subtypes of glioblastoma characterized by abnormalities in PDGFRA, IDH1, EGFR, and NF1. Cancer Cell 17: 98-110 doi:10.1016/j.ccr.2009.12.020

16. Zhang GB, Cui XL, Sui DL, Ren XH, Zhang Z, Wang ZC, Lin S (2013) Differential molecular genetic analysis in glioblastoma multiforme of long- and short-term survivors: a clinical study in Chinese patients. J Neurooncol 113: 251-258 doi:10.1007/s11060-013-1102-x

17. Millward CP, Brodbelt AR, Haylock B, Zakaria R, Baborie A, Crooks D, Husband D, Shenoy A, Wong H, Jenkinson MD (2016) The impact of MGMT methylation and IDH-1 mutation on long-term outcome for glioblastoma treated with chemoradiotherapy. Acta Neurochir (Wien) 158: 1943-1953 doi:10.1007/s00701-016-2928-8

18. Smrdel U, Popovic M, Zwitter M, Bostjancic E, Zupan A, Kovac V, Glavac D, Bokal D, Jerebic J (2016) Long-term survival in glioblastoma: methyl guanine methyl transferase (MGMT) promoter methylation as independent favourable prognostic factor. Radiol Oncol 50: 394-401 doi:10.1515/raon-2015-0041

19. Hartmann C, Hentschel B, Simon M, Westphal M, Schackert G, Tonn JC, Loeffler M, Reifenberger G, Pietsch T, von Deimling A, Weller M, German Glioma N (2013) Long-term survival in primary glioblastoma with versus without isocitrate dehydrogenase mutations. Clin Cancer Res 19: 5146-5157 doi:10.1158/1078-0432.CCR-13-0017

20. Lu J, Cowperthwaite MC, Burnett MG, Shpak M (2016) Molecular Predictors of Long-Term Survival in Glioblastoma Multiforme Patients. PLoS One 11: e0154313 doi:10.1371/journal.pone.0154313

21. Geisenberger C, Mock A, Warta R, Rapp C, Schwager C, Korshunov A, Nied AK, Capper D, Brors B, Jungk C, Jones D, Collins VP, Ichimura K, Backlund LM, Schnabel E, Mittelbron M, Lahrmann B, Zheng S, Verhaak RG, Grabe N, Pfister SM, Hartmann C, von Deimling A, Debus J, Unterberg A, Abdollahi A, Herold-Mende C (2015) Molecular profiling of long-term survivors identifies a subgroup of glioblastoma characterized by chromosome 19/20 co-gain. Acta Neuropathol 130: 419-434 doi:10.1007/s00401-015-1427-y

22. Peng S, Dhruv H, Armstrong B, Salhia B, Legendre C, Kiefer J, Parks J, Virk S, Sloan AE, Ostrom QT, Barnholtz-Sloan JS, Tran NL, Berens ME (2017) Integrated genomic analysis of survival outliers in glioblastoma. Neuro Oncol 19: 833-844 doi:10.1093/neuonc/now269

23. Gerber NK, Goenka A, Turcan S, Reyngold M, Makarov V, Kannan K, Beal K, Omuro A, Yamada Y, Gutin P, Brennan CW, Huse JT, Chan TA (2014) Transcriptional diversity of long-term glioblastoma survivors. Neuro Oncol 16: 1186-1195 doi:10.1093/neuonc/nou043

24. Urup T, Michaelsen SR, Olsen LR, Toft A, Christensen IJ, Grunnet K, Winther O, Broholm H, Kosteljanetz M, Issazadeh-Navikas S, Poulsen HS, Lassen U (2016) Angiotensinogen and HLA class II predict bevacizumab response in recurrent glioblastoma patients. Mol Oncol 10: 1160-1168 doi:10.1016/j.molonc.2016.05.005

25. Poulsen HS, Grunnet K, Sorensen M, Olsen P, Hasselbalch B, Nelausen K, Kosteljanetz M, Lassen U (2009) Bevacizumab plus irinotecan in the treatment patients with progressive recurrent malignant brain tumours. Acta Oncol 48: 52-58

26. Hasselbalch B, Lassen U, Hansen S, Holmberg M, Sorensen M, Kosteljanetz M, Broholm H, Stockhausen MT, Poulsen HS (2010) Cetuximab, bevacizumab, and irinotecan for patients with primary glioblastoma and progression after radiation therapy and temozolomide: a phase II trial. Neuro Oncol 12: 508-516

27. Hofland KF, Hansen S, Sorensen M, Engelholm S, Schultz HP, Muhic A, Grunnet K, Ask A, Costa JC, Kristiansen C, Thomsen C, Poulsen HS, Lassen U (2014) Neoadjuvant bevacizumab and irinotecan versus bevacizumab and temozolomide followed by concomitant chemoradiotherapy in newly diagnosed glioblastoma multiforme: A randomized phase II study. Acta Oncol 53: 939-944 doi:10.3109/0284186X.2013.879607

28. Phillips HS, Kharbanda S, Chen R, Forrest WF, Soriano RH, Wu TD, Misra A, Nigro JM, Colman H, Soroceanu L, Williams PM, Modrusan Z, Feuerstein BG, Aldape K (2006) Molecular subclasses of high-grade glioma predict prognosis, delineate a pattern of disease progression, and resemble stages in neurogenesis. Cancer Cell 9: 157-173

29. Sandmann T, Bourgon R, Garcia J, Li C, Cloughesy T, Chinot OL, Wick W, Nishikawa R, Mason W, Henriksson R, Saran F, Lai A, Moore N, Kharbanda S, Peale F, Hegde P, Abrey LE, Phillips HS, Bais C (2015) Patients With Proneural Glioblastoma May Derive Overall Survival Benefit From the Addition of Bevacizumab to First-Line Radiotherapy and Temozolomide: Retrospective Analysis of the AVAglio Trial. J Clin Oncol 33: 2735-2744 doi:10.1200/JCO.2015.61.5005

30. Nielsen JS, McNagny KM (2008) Novel functions of the CD34 family. J Cell Sci 121: 3683-3692 doi:10.1242/jcs.037507

31. Marko NF, Toms SA, Barnett GH, Weil R (2008) Genomic expression patterns distinguish long-term from short-term glioblastoma survivors: a preliminary feasibility study. Genomics 91: 395-406 doi:10.1016/j.ygeno.2008.01.002

32. Wood MD, Reis GF, Reuss DE, Phillips JJ (2016) Protein Analysis of Glioblastoma Primary and Posttreatment Pairs Suggests a Mesenchymal Shift at Recurrence. J Neuropathol Exp Neurol 75: 925-935 doi:10.1093/jnen/nlw068

33. Wang SY, Ke YQ, Lu GH, Song ZH, Yu L, Xiao S, Sun XL, Jiang XD, Yang ZL, Hu CC (2013) Vasculogenic mimicry is a prognostic factor for postoperative survival in patients with glioblastoma. J Neurooncol 112: 339-345 doi:10.1007/s11060-013-1077-7

34. Hasselbalch B, Eriksen JG, Broholm H, Christensen IJ, Grunnet K, Horsman MR, Poulsen HS, Stockhausen MT, Lassen U (2010) Prospective evaluation of angiogenic, hypoxic and EGFR-related biomarkers in recurrent glioblastoma multiforme treated with cetuximab, bevacizumab and irinotecan. APMIS 118: 585-594 doi:10.1111/j.1600-0463.2010.02631.x

35. Noushmehr H, Weisenberger DJ, Diefes K, Phillips HS, Pujara K, Berman BP, Pan F, Pelloski CE, Sulman EP, Bhat KP, Verhaak RG, Hoadley KA, Hayes DN, Perou CM, Schmidt HK, Ding L, Wilson RK, Van Den Berg D, Shen H, Bengtsson H, Neuvial P, Cope LM, Buckley J, Herman JG, Baylin SB, Laird PW, Aldape K, Cancer Genome Atlas Research N (2010) Identification of a CpG island methylator phenotype that defines a distinct subgroup of glioma. Cancer Cell 17: 510-522 doi:10.1016/j.ccr.2010.03.017

36. Brennan CW, Verhaak RG, McKenna A, Campos B, Noushmehr H, Salama SR, Zheng S, Chakravarty D, Sanborn JZ, Berman SH, Beroukhim R, Bernard B, Wu CJ, Genovese G, Shmulevich I, Barnholtz-Sloan J, Zou L, Vegesna R, Shukla SA, Ciriello G, Yung WK, Zhang W, Sougnez C, Mikkelsen T, Aldape K, Bigner DD, Van Meir EG, Prados M, Sloan A, Black KL, Eschbacher J, Finocchiaro G, Friedman W, Andrews DW, Guha A, Iacocca M, O'Neill BP, Foltz G, Myers J, Weisenberger DJ, Penny R, Kucherlapati R, Perou CM, Hayes DN, Gibbs R, Marra M, Mills GB, Lander E, Spellman P, Wilson R, Sander C, Weinstein J, Meyerson M, Gabriel S, Laird PW, Haussler D, Getz G, Chin L, Network TR (2013) The somatic genomic landscape of glioblastoma. Cell 155: 462-477 doi:10.1016/j.cell.2013.09.034

37. Mason S, McDonald K (2012) MGMT testing for glioma in clinical laboratories: discordance with methylation analyses prevents the implementation of routine immunohistochemistry. J Cancer Res Clin Oncol 138: 1789-1797 doi:10.1007/s00432-012-1312-1

38. Gilbert MR, Dignam JJ, Armstrong TS, Wefel JS, Blumenthal DT, Vogelbaum MA, Colman H, Chakravarti A, Pugh S, Won M, Jeraj R, Brown PD, Jaeckle KA, Schiff D, Stieber VW, Brachman DG, Werner-Wasik M, Tremont-Lukats IW, Sulman EP, Aldape KD, Curran WJ, Jr., Mehta MP (2014) A randomized trial of bevacizumab for newly diagnosed glioblastoma. N Engl J Med 370: 699-708 doi:10.1056/NEJMoa1308573

39. Chinot OL, Wick W, Mason W, Henriksson R, Saran F, Nishikawa R, Carpentier AF, Hoang-Xuan K, Kavan P, Cernea D, Brandes AA, Hilton M, Abrey L, Cloughesy T (2014) Bevacizumab plus radiotherapy-temozolomide for newly diagnosed glioblastoma. N Engl J Med 370: 709-722 doi:10.1056/NEJMoa1308345

40. van den Bent M, Gorlia T, Bendszus M, Sahm F, Domont J, Idbaih A, Platten M, Weller M, Golfoinopoulos V, Wick W EH1.3EORTC 26101 phase III trial exploring the combination of bevacizumab and lomustine versus lomustine in patients with first progression of a glioblastoma EANO meeting 2016. Neuro Oncol pp iv1-iv2

FIGURE LEGENDS

Fig. 1 REMARK diagram for biomarker examined patients.

Fig. 2 Flowchart for identification of differentially expressed genes associated with OS. Boxes to the right shows the number of genes identified according to each steps in our study cohort.

Figure 1

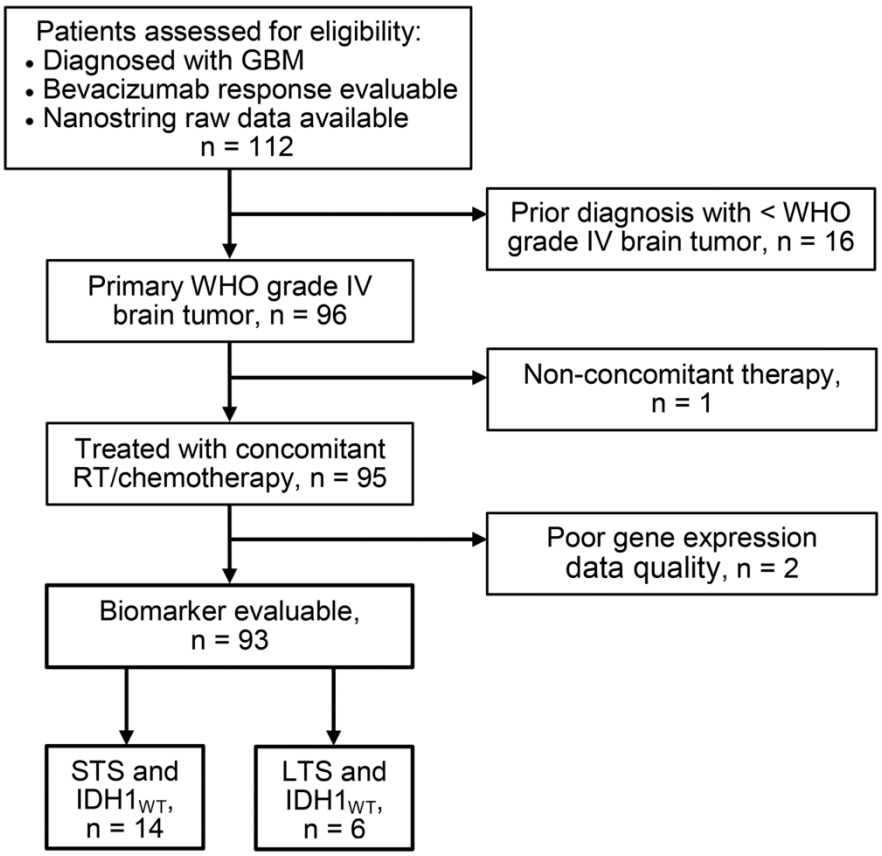
Patients assessed for eligibility:
• Diagnosed with GBM
• Bevacizumab response evaluable
• Nanostring raw data available
n = 112
Prior diagnosis with < WHO grade IV brain tumor, n = 16
Primary WHO grade IV brain tumor, n = 96
Non-concomitant therapy, n = 1
Treated with concomitant RT/chemotherapy, n = 95
Poor gene expression data quality, n = 2
Biomarker evaluable, n = 93
STS and IDH1WT, n = 14
LTS and IDH1WT, n = 6

Figure 2

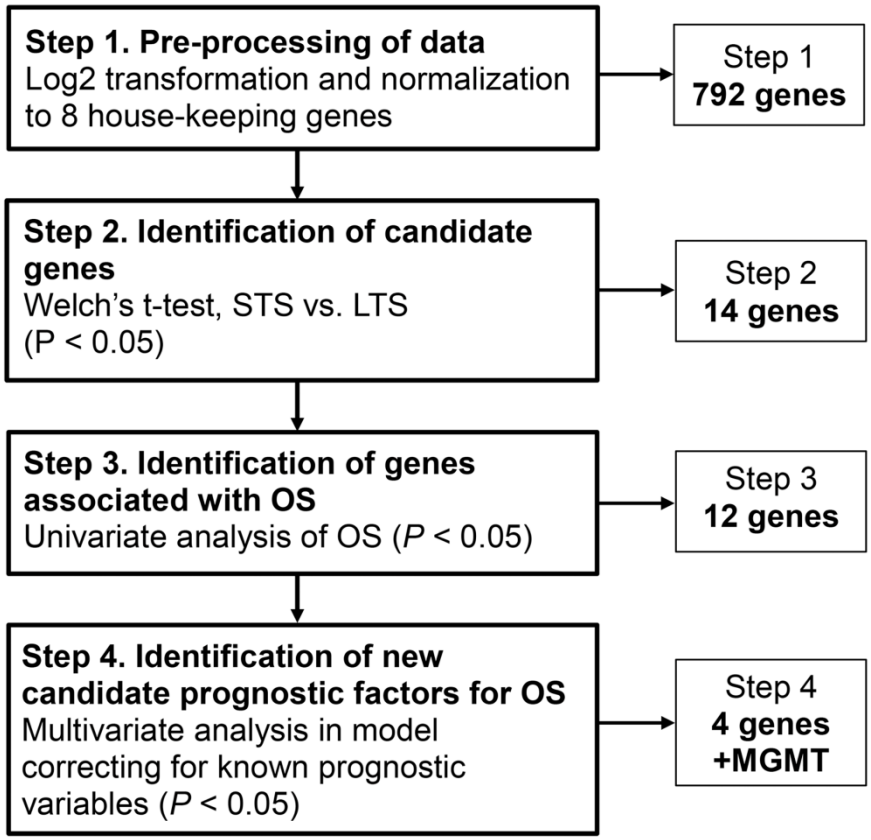
Step 1. Pre-processing of data
Log2 transformation and normalization to 8 house-keeping genes
Step 1
792 genes
Step 2. Identification of candidate genes
Welch's t-test, STS vs. LTS
(P < 0.05)
Step 2
14 genes
Step 3. Identification of genes associated with OS
Univariate analysis of OS (P < 0.05)
Step 3
12 genes
Step 4. Identification of new candidate prognostic factors for OS
Multivariate analysis in model correcting for known prognostic variables (P < 0.05)
Step 4
4 genes
+MGMT

Table 1 Patient characteristics

Variable	All patients *n* = 93	STS (OS < 12 mo) *n* = 14	LTS (OS > 36 mo) *n* = 6	*P*-value (LTS *vs.* STS)
OS (mo), median (range)	17.0 (6.7-116.1)	9.9 (6.7-11.9)	52.3 (40.8-116.1)	<0.0001
Gender, *n* (%)				
Male	60 (64.5)	10 (71.4)	3 (50.0)	0.613
Female	33 (35.5)	4 (28.6)	3 (50.0)	
Age at diagnosis (years), median (range)	58.0 (23-73)	62.0 (41-73)	54.4 (29-61)	0.098
WHO performance status, *n* (%)				
0	58 (62.4)	9 (64.3)	5 (83.3)	0.613
1	29 (31.2)	5 (35.7)	1 (16.7)	
Missing	6 (6.5)	0	0	
Corticosteroid use, *n* (%)				
No	29 (31.2)	1 (7.1)	4 (66.7)	0.014
Yes	58 (62.4)	13 (92.9)	2 (33.3)	
Missing	6 (6.4)	0	0	
Multifocal disease, *n* (%)				
No	83 (89.2)	12 (85.7)	5 (83.3)	1.000
Yes	10 (10.8)	2 (14.3)	1 (16.7)	
Extent of primary surgery, *n* (%)				
Biopsy	7 (7.5)	0 (0.0)	1 (16.7)	1.000
Partial or gross total resection	86 (92.5)	14 (100.0)	5 (83.3)	
Reoperation, *n* (%)				
No	60 (64.5)	13 (92.9)	4 (66.7)	0.202
Yes	33 (35.5)	1 (7.1)	2 (33.3)	
Treatment, *n* (%)				
RT/TMZ + BI or CBI	66 (71.0)	5 (35.7)	6 (100.0)	0.014
BI-BT	27 (29.0)	9 (64.3)	0 (0.0)	
GBM subtype, *n* (%)				
PN (proneural)	27 (29.0)	3 (21.4)	1 (16.7)	1.000
M (mesenchymal)	40 (43.0)	6 (42.9)	3 (50.0)	
PL (proliferative)	19 (20.5)	4 (28.6)	2 (33.3)	
UN (unknown)	7 (7.5)	1 (7.1)	0 (0.0)	
IDH status, *n* (%)				
No	20 (21.5)	14 (100.0)	6 (100.0)	
Yes	0	0	0	
Missing	73 (78.5)	0	0	

Statistical tests: Log-rank test (OS from patient diagnosis); Mann-Whitney U test (Age); Fisher's exact test (Gender, WHO performance status, Corticosteroid use (Prednisolone > 10mg), Multifocal disease, Extent of primary surgery, reoperation, Treatment, GBM Subtype).
Abbreviations: STS short-term survivor; *LTS* long-term survivor; *OS* overall survival; *RT/TMZ + BI or CBI* therapy with radiation/temozolomide in first-line and bevacizumab/irinotecan or cetuximab/bevacizumab/irinotecan in second-line; *BI-BT* therapy with radiation/bevacizumab/irinotecan or radiation/bevacizumab/temozolomide in first-line.

Table 2 Testing of individual genes in multivariate analysis modelling the probability of OS (Step 4)

2-fold change	**HR (95 % CI)**	***P*-value**
*OX40**	0.76 (0.57-1.01)	0.057
*IFNG**	0.61 (0.43-0.88)	0.008
*CXCL9**	0.83 (0.70-0.99)	0.037
*LGALS4**	0.61 (0.45-0.84)	0.002
*RTN1**	0.83 (0.68-1.01)	0.062
*PTPRO**	0.86 (0.65-1.15)	0.32
*NKX2-2**	0.78 (0.59-1.02)	0.064
*MDM2**	0.85 (0.69-1.05)	0.14
*NKG2D**	0.81 (0.62-1.05)	0.11
*E2F5**	1.41 (0.99-2.01)	0.055
*CD34**	0.64 (0.45-0.92)	0.014
*MGMT***	1.52 (1.16-2.00)	0.003

*Stratified for a prognostic index consisting of: Age at diagnosis (10 years increase), Corticosteroid use (yes *vs.* no), WHO performance status (1 *vs*. 0) and MGMT mRNA expression.
** Stratified for same prognostic index excluding MGMT status.
Abbreviations: OS overall survival; *HR* Hazard ratio; *CI* confidence interval.

Table 3 Testing of individual genes in multivariate analysis modelling the probability of OS in AVAglio cohort

2-fold change	HR (95 % CI)	*P*-value
*IFNG**	0.91 (0.65-1.27)	0.572
*CXCL9**	0.85 (0.71-1.02)	0.088
*LGALS4**	1.16 (0.74-1.82)	0.527
*CD34**	0.68 (0.50-0.91)	0.010
*MGMT***	1.57 (1.31-1.88)	<0.001

*Stratified for a prognostic index consisting of: Age (10 years increase), Corticosteroid use (yes *vs.* no), WHO performance status (1-2 *vs.* 0) and MGMT promotor methylation (yes *vs.* no).
** Stratified for same prognostic index excluding MGMT promotor methylation.
Abbreviations: OS overall survival; *HR* Hazard ratio; *CI* confidence interval.

SUPPLEMENTARY MATERIAL *Page 1 of 6*

Supplementary Table 1 Names and accession number for the 800 genes analyzed by NanoString technology

Gene name	Accession number	Gene name	Accession number	Gene name	Accession number	Gene name	Accession number
A2BP1	NM_145891.2	*CXCL13*	NM_006419.2	*INPP4B*	NM_001101669.1	*PSMD12*	NM_174871.2
AB13BP	NM_015429.3	*CXCL9*	NM_002416.1	*INSM1*	NM_002196.2	*PTCRA*	NM_138296.2
ABCC9	NM_020298.2	*CXCR3*	NM_001504.1	*IPO8*	NM_006390.2	*PTEN*	NM_000314.3
ABHD4	NM_022060.2	*CXCR4*	NM_003467.2	*IRS1*	NM_005544.2	*PTGDS*	NM_000954.5
ABHD6	NM_020676.5	*CXCR5*	NM_001716.3	*IRS2*	NM_003749.2	*PTGER4*	NM_000958.2
ABL1	NM_005157.3	*CYB5R2*	NM_016229.3	*ITM2B*	NM_021999.2	*PTPRB*	NM_002837.3
ACTB	NM_001101.2	*CYP27B1*	NM_000785.3	*JAG1*	NM_000214.2	*PTPRD*	NM_001040712.2
ACTN1	NM_001102.3	*Cd11c*	NM_000887.3	*JAK2*	NM_004972.2	*PTPRO*	NM_030671.2
ACVR2A	NM_001616.3	*Cox2*	NM_000963.1	*JAK3*	NM_000215.2	*PTRH2*	NM_016077.3
ADAMDEC1	NM_014479.2	*DAB2*	NM_001343.2	*JUN*	NM_002228.3	*PTX3*	NM_002852.3
ADAMTS3	NM_014243.2	*DARC*	NM_002036.2	*KANK3*	NM_198471.2	*PYCARD*	NM_013258.3
AGR2	NM_006408.2	*DBF4*	NM_006716.3	*KCNA1*	NM_000217.2	*PYCRL*	NM_023078.2
AGT	NM_000029.3	*DCX*	NM_000788.2	*KCND2*	NM_012281.2	*Pcp4l1*	NM_001102566.1
AIP	NM_003977.2	*DDX1*	NM_004939.1	*KCNE3*	NM_005472.4	*Perforin1*	NM_005041.3
AKR1C3	NM_003739.4	*DDX25*	NM_013264.3	*KEL*	NM_000420.2	*PlGF*	NM_002632.5
AKT1	NM_005163.2	*DEF6*	NM_022047.3	*KHDRBS2*	NM_152688.2	*RAB7B*	NM_177403.3
AKT1S1	NM_032375.3	*DENND2A*	NM_015689.3	*KIAA0101*	NM_014736.4	*RAC1B*	NM_198829.1
AKT2	NM_001626.2	*DEPTOR*	NM_022783.2	*KIAA0746*	NM_015187.3	*RAD51C*	NM_002876.2
AKT3	NM_181690.1	*DGKG*	NM_001346.2	*KIAA1102*	NM_014988.2	*RAD54B*	NM_012415.2
AL-137727	AL137727.1	*DHFR*	NM_000791.3	*KIAA1370*	NM_019600.2	*RASIP1*	NM_017805.2
ALDH1L1	NM_012190.2	*DHX40*	NM_001166301.1	*KIAA1462*	NM_020848.2	*RASL10A*	NM_001007279.1
ANGPT1	NM_001146.3	*DIDO1*	NM_001193369.1	*KIAABRAF16-9*	MSK_GMB2_003.1	*RB1*	NM_000321.1
ANGPT2	NM_001147.2	*DIRAS3*	NM_004675.2	*KIF13B*	NM_015254.3	*RBM24*	NM_153020.2
ANGPTL4	NM_139314.1	*DKK2*	NM_014421.2	*KLF4*	NM_004235.4	*RBP1*	NM_002899.3
ANKRD22	NM_144590.2	*DLL1*	NM_005618.3	*KLRC3*	NM_007333.2	*RBP7*	NM_052960.2
AP2B1	NM_001282.2	*DLL3*	NM_203486.2	*KPNA3*	NM_002267.3	*RDH14*	NM_020905.3
APC	NM_000038.3	*DLX2*	NM_004405.3	*KRIT1*	NM_004912.3	*RELB*	NM_006509.2
APLN	NM_017413.4	*DNAJC12*	NM_021800.2	*KRT19*	NM_002276.4	*REN*	NM_000537.3
APLNR	NR_027991.1	*DNM3*	NM_015569.3	*LAG3*	NM_002286.5	*RERE*	NM_012102.3
APPBP2	NM_006380.2	*DNMT1*	NM_001379.2	*LAMA4*	NM_001105209.1	*RFPL1S*	NR_002727.2
AQP1	NM_198098.1	*DPP10*	NM_020868.3	*LAMB1*	NM_002291.2	*RGN*	NM_152869.2
AR	NM_001011645.1	*DPYD*	NM_000110.3	*LAMP3*	NM_014398.3	*RGS12*	NM_198229.1
ARAP2	NM_015230.2	*DR5*	NM_003842.3	*LAPTM4A*	NM_014713.4	*RGS5*	NM_003617.2
ARAP3	NM_022481.5	*DTL*	NM_016448.2	*LCP2*	NM_005565.3	*RHEB*	NM_005614.3
ARC	NM_015193.3	*DUSP1*	NM_004417.2	*LDHA*	NM_001165414.1	*RHOB*	NM_004040.2
AREG	NM_001657.2	*DUSP12*	NM_007240.1	*LDHB*	NM_001174097.1	*RHOJ*	NM_020663.3
ARG1	NM_000045.2	*DUSP18*	NM_152511.3	*LGALS1*	NM_002305.3	*RNASE2*	NM_002934.2
ARHGDIB	NM_001175.4	*DYNLL1*	NM_003746.2	*LGALS13*	NM_013268.2	*RNF10*	NM_014868.3
ARID3A	NM_005224.2	*DYRK3*	NM_003582.2	*LGALS2*	NM_006498.2	*RNF13*	NM_007282.4
ASCL1	NM_004316.3	*DYRK4*	NM_003845.1	*LGALS3_all*	NM_002306.3	*ROBO4*	NM_019055.5
ASNS	NM_183356.2	*Dll4*	NM_019074.2	*LGALS4*	NM_006149.3	*RORC*	NM_001001523.1
ASPA	NM_000049.2	*E2F4*	NM_001950.3	*LGALS5*	NM_015973.3	*RPL13*	NM_000977.2
ATAR	NM_003820.2	*E2F5*	NM_001951.3	*LGALS7*	NM_002307.3	*RPL13A*	NM_012423.2
ATM	NM_138292.3	*E2F7*	NM_203394.2	*LGALS8_all*	NM_006499.3	*RPLP0*	NM_001002.3
ATOH1	NM_005172.1	*ECT2*	NM_018098.4	*LGALS9_all*	NM_002308.3	*RPS19*	NM_001022.3
ATOH8	NM_032827.6	*EDNRB*	NM_003991.2	*LIF*	NM_002309.3	*RPS6*	NM_001010.2
ATP1A2	NM_000702.3	*EFNA1*	NM_004428.2	*LIMK2*	NM_001031801.1	*RTN1*	NM_021136.2
ATP6V1G2	NM_130463.2	*EFNB2*	NM_004093.2	*LMO3*	NM_001001395.2	*RYR3*	NM_001036.3
AVIL	NM_006576.2	*EGFL11*	NM_198283.1	*LOC254531*	NM_153613.2	*RasGRP3*	NM_015376.2
AXIN2	NM_004655.3	*EGFL7*	NM_016215.3	*LOC390940*	XM_001129773.1	*S100A11*	NM_005620.1

AXL	NM_021913.2	*EGFR*	NM_201282.1	*LOC400796*	XM_001132413.2	*S100A4*	NM_002961.2
B2M	NM_004048.2	*EGFREX30*	MSK_GMB2_006.1	*LRP4*	NM_002334.2	*S100A9*	NM_002965.2
B4GALT1	NM_001497.3	*EGFRVII*	MSK_GMB2_005.1	*LRP8*	NM_033300.2	*SAA2*	NM_030754.3
B7H4	NM_024626.2	*EGFRVIII*	MSK_GMB2_008.1	*LTF*	NM_002343.2	*SALL3*	NM_171999.2
BAG2	NM_004282.3	*EGLN3*	NM_022073.3	*LUM*	NM_002345.3	*SAMD9*	NM_017654.2
BAX	NM_138761.3	*EHF*	NM_012153.3	*LY6G6D*	NM_021246.2	*SAMD9L*	NM_152703.2
BCAN	NM_198427.1	*ELTD1*	NM_022159.3	*MAOB*	NM_000898.4	*SASH1*	NM_015278.3
BCAS1	NM_003657.2	*EMCN*	NM_016242.3	*MAP2*	NM_031845.2	*SCD*	NM_005063.4
BCL11A	NM_022893.3	*EMP3*	NM_001425.2	*MAP3K8*	NM_005204.2	*SCG3*	NM_013243.2
BCL2L1	NM_138578.1	*EMX2*	NM_004098.3	*MAP4K1*	NM_007181.3	*SDCCAG8*	NM_006642.2
BCL2L2	NM_004050.2	*END1*	NM_021729.4	*MBP*	NM_002385.2	*SDHA*	NM_004168.1
BCL3	NM_005178.2	*ENG*	NM_001114753.1	*MCAM*	NM_006500.2	*SEC61G*	NM_001012456.1
BCL6	NM_138931.1	*ENO1*	NM_001428.2	*MDM2*	NM_006878.2	*SELE*	NM_000450.2
BDCA1	NM_001765.2	*ENPP4*	NM_014936.4	*MDM4*	NM_002393.3	*SELL*	NR_029467.1
BEST1	NM_004183.3	*ENTPD3*	NM_001248.2	*MDS032*	NM_018467.2	*SERPINA1*	NM_000295.4
BEST3	NM_032735.2	*EOMES*	NM_005442.2	*MEF2C*	NM_002397.3	*SERPINB13*	NM_012397.3
BEX1	NM_018476.3	*EPB41L3*	NM_012307.2	*MELK*	NM_014791.2	*SERPINE1*	NM_000602.2
BGN	NM_001711.3	*EPHA4*	NM_004438.3	*MEOX2*	NM_005924.4	*SERPINE2*	NM_006216.2
BIRC5	NM_001168.2	*EPPK1*	NM_031308.1	*MEST*	NM_177525.1	*SERPINH1*	NM_001235.2
BMF	NM_001003940.1	*ERBB2*	NM_004448.2	*MET*	NM_000245.2	*SETDB2*	NM_031915.1
BMP2	NM_001200.2	*ERBB3*	NM_001005915.1	*MFAP5*	NM_003480.2	*SFRP1*	NM_003012.3
BOP1	NM_015201.3	*ERBB4*	NM_001042599.1	*MGMT*	NM_002412.3	*SGCG*	NM_000231.2
BRAF	NM_004333.3	*ERCC2*	NM_000400.2	*MIA*	NM_006533.1	*SGK1*	NM_005627.2
BRIP1	NM_032043.1	*ERCC5*	NM_000123.2	*MICA*	NM_000247.1	*SHCBP1*	NM_024745.2
BTG3	NM_006806.3	*EREG*	NM_001432.2	*MICB*	NM_005931.3	*SHH*	NM_000193.2
BTK	NM_000061.1	*ERG*	NM_182918.3	*MLH1*	NM_000249.2	*SIDT2*	NM_001040455.1
C13orf15	NM_014059.2	*ESM1*	NM_007036.4	*MMP10*	NM_002425.1	*SKAP2*	NM_003930.3
C1ORF2	NM_006589.2	*ETS1*	NM_005238.3	*MMP2*	NM_004530.2	*SLC12A5*	NM_001134771.1
C2GnT3	NM_001097635.1	*ETV5*	NM_004454.2	*MMP3*	NM_002422.3	*SLC1A2*	NM_004171.3
C2GnT4	NM_001097636.1	*EVI2B*	NM_006495.3	*MMP7*	NM_002423.3	*SLC25A32*	NM_030780.2
C2GnT5	NM_001490.4	*EXOSC9*	NM_001034194.1	*MMRN2*	NM_024756.2	*SLC4A4*	NM_001098484.2
C2ORF80	NM_001099334.2	*EYA1*	NM_000503.4	*MOXD1*	NM_001031699.1	*SLIT1*	NM_003061.2
C8orf4	NM_020130.2	*EZH2*	NM_004456.3	*MS4A6A*	NM_152851.2	*SMAD4*	NM_005359.3
CA12	NM_001218.3	*EphB4*	NM_004444.4	*MSH2*	NM_000251.1	*SMARCB1*	NM_003073.3
CA9	NM_001216.2	*F13A1*	NM_000129.3	*MSH6*	NM_000179.1	*SMC4*	NM_001002800.1
CAB39L	NM_001031724.1	*FABP5*	NM_001444.1	*MTHFD1*	NM_005956.2	*SMG8*	NM_018149.6
CAD11	NM_001797.2	*FABP7*	NM_001446.3	*MTHFD1L*	NM_001242767.1	*SMO*	NM_005631.3
CAIV	NM_000717.2	*FAF1*	NM_007051.2	*MTHFD2*	NM_006636.3	*SNAP91*	NM_001242794.1
CAPN2	NM_001748.4	*FAK*	NM_005607.3	*MTOR*	NM_004958.2	*SNCA*	NM_000345.2
CAPZA2	NM_006136.2	*FAM119*	NM_206914.1	*MUC1*	NM_002456.5	*SNCB*	NM_001001502.1
CASP1	NM_001223.3	*FAM20C*	NM_020223.2	*MUC2*	NM_002457.2	*SNRNP200*	NM_014014.4
CASP2	NM_032982.2	*FAN176C*	NM_058187.3	*MXD4*	NM_006454.2	*SNRNP70*	NM_003089.4
CASP3	NM_032991.2	*FANCI*	NM_001113378.1	*MYB*	NM_005375.2	*SOCS2*	NM_003877.3
CASP4	NM_001225.3	*FAP*	NM_004460.2	*MYBL1*	XM_034274.14	*SORL1*	NM_003105.4
CCL2	NM_002982.3	*FAS*	NM_152876.1	*MYBL2*	NM_002466.2	*SOX11*	NM_003108.3
CCL22	NM_002990.3	*FBLIM1*	NM_001024215.1	*MYC*	NM_002467.3	*SOX13*	NM_005686.2
CCL28	NM_148672.2	*FBXO3*	NM_012175.3	*MYCN*	NM_005378.4	*SOX18*	NM_018419.2
CCL5	NM_002985.2	*FCGR2B*	NM_001002273.1	*MYCT1*	NM_025107.2	*SOX2*	NM_003106.2
CCNB1	NM_031966.2	*FCRL5*	NM_031281.2	*MYL9*	NM_181526.1	*SOX4*	NM_003107.2
CCND2	NM_001759.2	*FERMT*	NM_017671.4	*Map4k4*	NM_004834.3	*SOX8*	NM_014587.2
CCNE2	NM_057735.1	*FGF1*	NM_033137.1	*Mgat5*	NM_002410.4	*SOX9*	NM_000346.2

CCNG2	NM_004354.1	*FGF2*	NM_002006.4	*NAG*	NM_015909.2	*SPARC*	NM_003118.2
CCR5	NM_000579.1	*FGFR3*	NM_022965.2	*NARG1*	NM_057175.3	*SPOCD1*	NM_144569.4
CCR7	NM_001838.2	*FGR*	NM_005248.1	*NCAM1*	NM_000615.5	*SPQR1214*	NM_020340.2
CD11b	NM_000632.3	*FN1*	NM_212482.1	*NCOA3*	NM_181659.1	*SPRY2*	NM_005842.2
CD127	NM_002185.2	*FOS*	NM_005252.2	*NDRG2*	NM_016250.2	*SPRY4*	NM_030964.3
CD137	NM_001561.4	*FOSL2*	NM_005253.3	*NDRG4*	NM_001242835.1	*SPSB1*	NM_025106.3
CD137L	NM_003811.3	*FOXO1*	NM_002015.3	*NES*	NM_006617.1	*SQLE*	NM_003129.3
CD163	NM_004244.4	*FOXO4*	NM_005938.2	*NEUN*	NM_001082575.1	*SRD5A1*	NM_001047.2
CD20	NM_019010.1	*FOXP3*	NM_014009.3	*NF1*	NM_000267.2	*SRGN*	NR_036430.1
CD244	NM_016382.2	*FREM3*	NM_001168235.1	*NID1*	NM_002508.2	*SRPX*	NM_006307.2
CD247	NM_198053.1	*FSCN2*	NM_001077182.2	*NID2*	NM_007361.3	*SRRM2*	NM_016333.3
CD25	NM_000417.1	*FXYD5*	NM_001164605.1	*NIP7*	NM_016101.3	*ST3GAL2*	NM_006927.3
CD27	NM_001242.4	*Fmod*	NM_002023.3	*NKG2D*	NM_007360.1	*ST6GAL1_all*	NM_003032.2
CD274	NM_014143.3	*G0S2*	NM_015714.3	*NKX1-2*	XM_372331.4	*STAT1*	NM_007315.2
CD276	NM_001024736.1	*GABBR1*	NM_021903.1	*NKX2-1*	NM_003317.3	*STAT2*	NM_005419.2
CD28	NM_001243078.1	*GABRB2*	NM_000813.2	*NKX2-2*	NM_002509.2	*STAT3*	NM_139276.2
CD34	NM_001025109.1	*GAD2*	NM_000818.2	*NKX2-8*	NM_014360.2	*STEAP1*	NM_012449.2
CD36	NM_000072.3	*GALNT10*	NM_198321.2	*NKX3-1*	NR_046072.1	*STEAP3*	NM_001008410.1
CD3E	NM_000733.2	*GALNT13*	NM_052917.2	*NMU*	NM_006681.2	*STK11*	NM_000455.4
CD4	NM_000616.4	*GALNT14*	NM_024572.2	*NNMT*	NM_006169.2	*SUSD5*	NM_015551.1
CD40	NM_001250.4	*GALNT2*	NM_004481.3	*NOTCH2*	NM_024408.3	*SV2B*	NM_001167580.1
CD40L	NM_000074.2	*GAPDH*	NM_002046.3	*NPAS2*	NM_002518.3	*SYT1*	NM_005639.2
CD44	NM_001001392.1	*GATA3*	NM_001002295.1	*NPM1*	NM_002520.5	*SYT4*	NM_020783.3
CD45	NM_080921.2	*GATM*	NM_001482.2	*NPR3*	NM_000908.3	*TAF1a*	NM_005681.2
CD45RO	NM_080921.3	*GCNT1_all*	NM_001097633.1	*NPTX2*	NM_002523.1	*TAGLN*	NM_003186.3
CD48	NM_001778.2	*GEN1*	NM_182625.3	*NR2E1*	NM_003269.3	*TBET*	NM_013351.1
CD68	NM_001251.2	*GFAP*	NM_002055.4	*NRAS*	NM_002524.3	*TBP*	NM_001172085.1
CD69	NM_001781.1	*GGH*	NM_003878.2	*NRP1*	NM_003873.5	*TCF12*	NM_207037.1
CD70	NM_001252.2	*GGTA1P*	NR_045211.1	*NRP2*	NM_003872.2	*TCF4*	NM_001083962.1
CD80	NM_005191.3	*GINS1*	NM_021067.3	*NXPH1*	NM_152745.2	*TCL1A*	NR_049726.1
CD86	NM_175862.3	*GINS2*	NM_016095.2	*Notch1*	NM_017617.3	*TERT*	NM_198253.1
CD8A_1	NM_001768.5	*GLUT1*	NM_006516.2	*OAS1*	NM_016816.2	*TFRC*	NM_003234.1
CD8A_2	NM_001768.6	*GMNN*	NM_015895.3	*OLIG2*	NM_005806.2	*TGFb1*	NM_000660.3
CD8B	NM_172099.2	*GOLM1*	NM_016548.3	*OMG*	NM_002544.3	*THBS1*	NM_003246.2
CD93	NM_012072.3	*GPC4*	NM_001448.2	*OX40*	NM_003327.2	*TIM3*	NM_032782.3
CDC25A	NM_001789.2	*GPNMB*	NM_001005340.1	*OX40L*	NM_003326.2	*TIMP1*	NM_003254.2
CDC45	NM_003504.3	*GPR143*	NM_000273.1	*P2RY12*	NM_022788.3	*TIMP3*	NM_000362.4
CDC6	NM_001254.3	*GPR17*	NM_005291.1	*PAK3*	NM_002578.2	*TLR2*	NM_003264.3
CDCA5	NM_080668.3	*GPX3*	NM_002084.3	*PARK2*	NM_004562.2	*TLR4*	NR_024168.1
CDCA7	NM_031942.4	*GRB14*	NM_004490.2	*PCDH12*	NM_016580.2	*TLX*	NM_172350.1
CDCA7L	NM_001127371.2	*GRIA2*	NM_001083620.1	*PCDH17*	NM_001040429.2	*TMEFF2*	NM_016192.2
CDCP1	NM_022842.3	*GRIK1*	NM_000830.3	*PCNA*	NM_002592.2	*TMEM100*	NM_018286.2
CDH1	NM_004360.2	*GUSb*	NM_000181.1	*PD1*	NM_005018.1	*TMEM191A*	NR_026815.1
CDH19	NM_021153.2	*GZMA*	NM_006144.2	*PDCD1LG2*	NM_025239.3	*TMEM88*	NM_203411.1
CDH3	NM_001793.4	*GZMB*	NM_004131.3	*PDE4D*	NM_006203.4	*TMSB15A*	NM_021992.2
CDH4	NM_001794.2	*H6PD*	NM_004285.3	*PDE8B*	NM_003719.2	*TNC*	NM_002160.1
CDH5	NM_001795.3	*HBEGF*	NM_001945.1	*PDGFA*	NM_002607.5	*TNF1a*	NM_000594.2
CDHR1	NM_001171971.1	*HES1*	NM_005524.2	*PDGFRA*	NM_006206.3	*TNFRSF21*	NM_014452.3
CDK4	NM_000075.2	*HEY1*	NM_012258.3	*PDGFRAD89*	MSK_GMB2_001.1	*TNFSF10*	NM_003810.2
CDK6	NM_001259.6	*HGF*	NM_000601.4	*PDGFRADCt*	MSK_GMB2_004.1	*TNFSF13B*	NM_006573.4
CDKN2A	NM_000077.3	*HHIP*	NM_022475.1	*PDGFRb*	NM_002609.3	*TNIK*	NM_001161560.1
CDKN2B	NM_004936.3	*HIF1A*	NM_001530.2	*PDK1*	NM_002610.3	*TOP1*	NM_003286.2

CDKN2C	NM_001262.2	*HIPK3*	NM_005734.2	*PDLIM3*	NM_014476.4	*TOP2A*	NM_001067.2
CENPK	NM_022145.4	*HKR2*	NM_181846.1	*PDLIM4*	NM_001131027.1	*TP53*	NM_000546.2
CENPM	NM_001002876.1	*HLA-A*	NM_002116.5	*PDPN*	NM_006474.4	*TP53INP1*	NM_033285.3
CEP170	NM_001042404.1	*HLA-B*	NM_005514.6	*PDZK1IP1*	NM_005764.3	*TRADD*	NM_003789.2
CES2	NM_003869.5	*HLA-C*	NM_002117.4	*PECAM1*	NM_000442.3	*TRAF5*	NM_004619.3
CFB	NM_001710.5	*HLA-DQA1*	NM_002122.3	*PEDF*	NM_020376.3	*TRMT6*	NM_015939.3
CFI	NM_000204.3	*HLA-E*	NM_005516.4	*PERP*	NM_022121.3	*TSC1*	NM_000368.3
CHEK1	NM_001114121.1	*HMGCS2*	NM_005518.3	*PFDN4*	NM_002623.3	*TSC2*	NM_000548.3
CHGB	NM_001819.1	*HMMR*	NM_012484.2	*PFN2*	NM_002628.4	*TTC28*	XM_929318.3
CHI3L1	NM_001276.2	*HMOX1*	NM_002133.1	*PHF11*	NM_001040443.1	*TTK*	NM_003318.3
CHIC2	NM_012110.2	*HOXA5*	NM_019102.2	*PHF19*	NM_001009936.1	*TTL*	NM_153712.4
CLEC14	NM_175060.1	*HOXC6*	NM_153693.3	*PHLDA3*	NM_012396.3	*TUBB*	NM_178014.2
CLEC2B	NM_005127.2	*HP*	NM_005143.3	*PHLPP1*	NM_194449.1	*TUBB4A*	NM_006087.2
CLEC5a	NM_013252.2	*HPCAL1*	NM_002149.2	*PHLPP2*	NM_015020.2	*TUSC3*	NM_006765.2
CLTC	NM_004859.2	*HS1BP3*	NM_022460.3	*PHYHIP*	NM_014759.3	*TXNDC5*	NM_030810.2
CNGA3	NM_001079878.1	*HSPA4L*	NM_014278.2	*PI3*	NM_002638.3	*TYMS*	NM_001071.1
CNTN3	NM_020872.1	*Hey2*	NM_012259.2	*PIDD*	NM_145886.2	*UBC*	NM_021009.3
COL15A1	NM_001855.2	*HeyL*	NM_014571.3	*PIK3CA*	NM_006218.2	*UBE2T*	NM_014176.3
COL18A1	NM_030582.3	*Hhex*	NM_002729.4	*PIK3IP1*	NM_001135911.1	*USHBP1*	NM_031941.3
COL1A2	NM_000089.3	*ICAM1*	NM_000201.2	*PIK3R1*	NM_181504.2	*VAV3*	NM_001079874.1
COL4A1	NM_001845.4	*ICAM2*	NM_000873.3	*PKNOX2*	NM_022062.2	*VCAM1*	NM_001078.3
COL4A2	NM_001846.2	*ID1*	NM_002165.2	*PLA2G2A*	NM_000300.2	*VEGFA_new*	NM_001025366.2
COL6A3	NM_057164.4	*IDH1*	NM_005896.2	*PLA2G5*	NM_000929.2	*VEGFA_old*	NM_001025366.1
CRAT	NM_000755.2	*IDO1*	NM_002164.3	*PLAGL2*	NM_002657.2	*VEGFB*	NM_003377.3
CRIP2	NR_073084.1	*IFI27*	NM_005532.3	*PLAT*	NM_000931.2	*VEGFC*	NM_005429.2
CRKL	NM_005207.3	*IFIT3*	NM_001031683.2	*PLEK2*	NM_016445.1	*VEGFD*	NM_004469.2
CRYAB	NM_001885.1	*IFNg*	NM_000619.2	*PLVAP*	NM_031310.1	*VEGFR1*	NM_002019.4
CSDA	NM_003651.3	*IGF1R*	NM_000875.2	*PMAIP1*	NM_021127.2	*VEGFR2*	NM_002253.2
CSDC2	NM_014460.3	*IGF2*	NM_001127598.1	*PMM2*	NM_000303.2	*VEGFR3*	NM_002020.1
CSF1R	NM_005211.2	*IGF2BP3*	NM_006547.2	*PMS2*	NM_000535.5	*VIM*	NM_003380.2
CSF2	NM_000758.2	*IGFBP2*	NM_000597.2	*PODXL*	NM_005397.3	*VPS33B*	NM_018668.3
CSMD3	NM_198124.1	*IGFBP3*	NM_000598.4	*POFUT1*	NM_015352.1	*WIF1*	NM_007191.2
CSPG4	NM_001897.4	*IGFBP6*	NM_002178.2	*POLK*	NM_016218.2	*WT1*	NM_000378.3
CSPGS	NM_006574.3	*IGHA1*	AF067420.1	*POLR2A*	NM_000937.2	*YPEL2*	NM_001005404.3
CTDSP2	NM_005730.3	*IL10*	NM_000572.2	*POSTN*	NM_001135935.1	*ZAP70*	NM_001079.3
CTGF	NM_001901.2	*IL12A*	NM_000882.2	*PPAP2B*	NM_003713.3	*ZBTB10*	NM_023929.3
CTHRC1	NM_138455.2	*IL13*	NM_002188.2	*PPARA*	NM_001001928.2	*ZBTB16*	NM_006006.4
CTLA4	NM_005214.3	*IL17A*	NM_002190.2	*PPIA*	NM_021130.2	*ZFPM2*	NM_012082.3
CTNND2	NM_001332.2	*IL17F*	NM_052872.3	*PPM1D*	NM_003620.2	*ZNF217*	NM_006526.2
CTPS2	NM_175859.1	*IL1B*	NM_000576.2	*PRKCZ*	NM_002744.4	*ZNF238*	NM_205768.2
CTSF	NM_003793.3	*IL2*	NM_000586.2	*PROM1*	NM_006017.1	*ZNF367*	NM_153695.2
CX3CL1	NM_002996.3	*IL4*	NM_000589.2	*PRPF3*	NM_004698.2	*ZNF423*	NM_015069.2
CX3CR1	NM_001337.3	*IL6*	NM_000600.1	*PRPF31*	NM_015629.3	*ZNF711*	NM_021998.4
CXCL1	NM_001511.1	*IL7*	NM_000880.2	*PRPF6*	NM_012469.3	*egfr-sept14e7*	Fusion_0098.1
CXCL10	NM_001565.1	*IL8*	NM_000584.2	*PRPF8*	NM_006445.3	*iASPP*	NM_001142502.1
CXCL11	NM_005409.3	*ILR4*	NM_000418.2	*PSD3*	NM_015310.2	*p63*	NM_001114978.1
CXCL12	NM_000609.5	*IMPG2*	NM_016247.2	*PSIP1*	NM_021144.3	*p73*	NM_005427.2

Supplementary Table 2 Welch's t-test, comparing LTS (OS > 36 mo) *vs*. STS (OS < 12 mo) (Step 2)*

Gene name	Log2 fold change	*P*-value
OX40	1.38	0.003
IFNG	1.04	0.010
CXCL9	1.88	0.012
LGALS4	1.12	0.013
RTN1	1.82	0.013
PTPRO	1.25	0.015
REN	0.72	0.017
MGMT	-1.47	0.019
NKX2-2	1.05	0.020
MDM2	1.94	0.024
POLK	0.23	0.040
NKG2D	1.70	0.041
E2F5	-0.66	0.044
CD34	0.54	0.049

*Significant genes differentially expressed with $P < 0.05$. Minus indicates down-regulated genes in the LTS compared to STS group. *Abbreviations: STS* short-term survivor; *LTS* long-term survivor; *OS* overall survival.

Supplementary Table 3 Univariate analysis modelling the probability of OS (Step 3)

Covariate	HR (95 % CI)	*P*-value
Genes (2-fold change)		
OX40	0.61 (0.46-0.80)	0.000
IFNG	0.58 (0.41-0.82)	0.002
CXCL9	0.80 (0.68-0.94)	0.008
LGALS4	0.65 (0.48-0.88)	0.006
RTN1	0.80 (0.69-0.94)	0.006
PTPRO	0.77 (0.59-0.94)	0.012
REN	0.82 (0.64-1.05)	0.11
MGMT	1.52 (1.19-1.94)	0.001
NKX2-2	0.75 (0.59-0.96)	0.023
MDM2	0.78 (0.64-0.94)	0.011
POLK	0.46 (0.18-1.19)	0.11
NKG2D	0.74 (0.60-0.92)	0.006
E2F5	1.48 (1.04-2.11)	0.031
CD34	0.73 (0.54-0.98)	0.039
Clinical variables		
Age at diagnosis (per 10 years)	1.43 (1.14-1.78)	0.002
Corticosteroid use (yes *vs.* no)	1.80 (1.14-2.86)	0.012
WHO performance status (1 *vs.* 0)	1.66 (1.05-2.63)	0.032

Abbreviations: OS overall survival; *HR* Hazard ratio; *CI* confidence interval.

4. Supplement discussion

4.1 Choice of model for *in vitro* and *in vivo* examinations of glioblastoma

Thoughtful choice of study material is essential for obtaining clinical relevant research results. For many years dominating cellular model systems in preclinical glioblastoma research were the same few conventional cell lines established and managed in serum-containing media and used without considering of passage number or comparability to the original tumor. An example of this is the U87MG cell line, for which a recent study found that the commercial available version do not match the genetic profile of the original tumor and that these cells only was likely to be of glioblastoma origin [184]. Others are the U118MG and U138MG cell lines as well as the U251 and U373 cell lines, shown to be pair-wise identical [185], indicating cross-contamination. Besides being questionable in regard to their origin, these traditional cell models have been found to be poor representatives of glioblastoma tumors [42]. Consequently many research groups today have developed new advanced cell models. Similarly, cells used in ***Study I*** and ***-II*** were derived from subcutaneous xenografts on immune-deficient mice established from glioblastoma patient tumor material [186, 187]. Serum lacking neural-stem cell media were utilized for culturing based on the theory that this will maintain characteristics of the original tumor including the GSC phenotype [42, 43], and cells were only used in limited number of passages to avoid phenotypic and genotypic drifting. This method has been shown, in previous studies from our laboratory, to conserve molecular features of the original tumor in the model cultures, such as expression of EGFR, EGFRvIII and Notch-1 [38, 186].

Although the examined cell cultures used in ***Study I*** and ***-II*** displayed relevant molecular features, only two cultures were used in most experiments due to lack of time to include more models. While a very limited number of tested models are often the reality in preclinical cell based studies, it is also a major limitation as variation between glioblastoma patients cannot be properly recapitulated.

In vitro cell models do not capture the complexity of human tumors including interaction of tumor cells with environmental features such as infiltrative blood-vessels, and *in vivo* studies are therefore often necessary to complement *in vitro* findings. In ***Study I*** the effect of VEGF-C knockdown was investigated in a xenograft mouse model. Advantages of this type of model is that tumors develop relatively fast, it is highly reproducible and it allows for studying material of human origin, and thereby the full range of molecular alteration found in such tumors [188]. Tumor cells were transplanted orthotopically into the mouse brain, a method which in comparison to the subcutaneous xenograft model is more laborious both in regard to tumor establishment and measurement of tumor size [188]. However, this model allow for study of interaction of tumor cells with surrounding brain parenchyma and has been shown to reproduce the specific pathological features of human glioblastomas, although this is dependent of type of cell transplanted [189]. A disadvantage of the xenograft models is that they use immune-deprived animals, and therefore interaction between tumors and the immune system cannot be examined. Given previous demonstrated influence of VEGF-C on immune cells [108] as well as ***Study I*** findings of VEGF-C expression in infiltrative immune cells and upregulation of an immune regulatory expression profile upon VEGF-C knockdown, this presents a limitation for the conducted *in vivo* study. As such, this issue could have been overcome by use of chemically induced models or genetically modified models, in which tumors are developed in host cells. But these models have other limitations, such as low comparability with human glioblastoma or being more laborious [188, 189]. We found the orthotropic xenograft model as optimal for *in vivo* examination in ***Study I***, as it allowed us to investigate how human glioblastoma cells being highly positive for VEGFR2 and VEGF-C behave in the brain. Furthermore, the CPH017 cell model had in a previous *in vivo* study using same setup [190] been found to recapitulate bevacizumab sensitivity observed in the patient from which the cells were originally derived (unpublished data), indicating clinical relevance of this model.

4.2 Considerations regarding studies of clinical material

Retrospectively analysis of clinical patient data and tissue are strong methods for examining variations in molecular and clinical markers, and test hypothesis of correlation between these and survival endpoints. However, while being valuable for studying patient heterogeneity, such analyses are restricted by several factors. Among these, incorrect selection of study cohort can largely limit what conclusion that can be drawn. Moreover, improperly registered clinical information or highly limited amount of tissue, will result in an incomplete dataset with missing data reducing the statistical power. ***Study III*** examined primary glioblastoma patients all treated with radiation- , chemo- and bevacizumab therapy. Only a few missing values were found for the clinically characteristics of these patients, which distributed closely to those of a previous analyzed cohort of 225 consecutive non-selected glioblastoma patients treated according to Stupp's regimen at Rigshospitalet, Copenhagen [191]. Accordingly, we believe the ***Study III*** patients to be suitable for modelling the general population of newly diagnosed glioblastoma patients. Contrary, selection of patients for tissue examination in ***Study I*** depended on availability of paired tissue samples before and after bevacizumab therapy. As these patients are rare, only few were examined and additional analysis by other methods, as also presented in the manuscript, is necessary to draw conclusions.

Moreover, quality of tumor material can be varying depending on how it was handled as well as the way and time of storage. In both ***Study I*** and ***-III***, material was formalin-fixed paraffin embedded (FFPE) tumor blocks from routine operations and consequently tissue storage time was varying. While this have been shown not to affect protein analysis by IHC as conducted in ***Study I***, quality of RNA as analyzed in **Study III**, decline with prolonged storage time [192]. In general RNA analysis based on FFPE material is challenging, as this type of tissue preservation can result in RNA degradation, fragmentation and covalent modifications, compromising the quality and quantity of the RNA as well as inhibit its conversion to cDNA [193]. The NanoString method used in ***Study III*** is a barcode based technology, partly meeting these challenges by not requiring cDNA conversion and only using small amount of input material, thereby avoiding gene amplification bias from fragmented RNA [193]. Still, conclusions based on this technique should be drawn with care as varying comparability have

been found between NanoString data from FFPE material and RNA analysis made on fresh frozen material from same tumor tissue [194, 195]. Besides quality of tissue, also varying amount of normal tissue in the tissue blocks can influence results based on RNA quantification and accordingly material for ***Study III*** underwent laser microdissection removing non-malignant cells prior to the purification of RNA.

4.3 Effective treatment strategy for glioblastoma – a difficult task

Successful treatment for glioblastoma is subject to tremendous challenges. Given their location in the brain, these tumors are hardly accessible for surgery as well as drug treatment due to the only semi-permeable BBB. Further, these tumors are surrounded by delicate normal tissue prone for off-target effect. Also, an issue is heterogeneity among glioblastoma tumors with presentation of a pleomorphic range of inter-tumor gene expression differences, as shown by the identification of glioblastoma subtypes [14-16]. This makes discovery of one ubiquitous treatment for all glioblastoma patients extremely difficult, if not impossible. An approach to overcome this challenge could be development of programs for individualized treatment regimens (personalized therapy) for glioblastoma based on tumor specific molecular profile [196]. However, large heterogeneity is also present within the single glioblastoma tumor having both cells of varying subtype [19] and differentiation level [39, 197]. This supports that a polytherapeutic approach may be most effective; further underlined in the case of targeted drugs by high level of redundancy between different molecular pathways [196], e.g. as described in **Section 1.6.6** for the Notch and EGFR pathways. Also, as glioblastomas are extremely aggressively growing, there is very little time for decision on choice of treatment and the number of different treatments that can be tried is very restricted. Consequently, having easy measurable, reliable markers for patient selection in regard to personalized therapy will improve chance for successful results.

With basis in angiogenesis, this thesis examined molecular markers that could prove useful for such nuancing in glioblastoma treatment.

4.4 Potential of examined molecular targets in a clinical context

4.4.1 VEGF-C – a multifaceted treatment factor

Study I findings regarding the role of VEGF-C for promotion of glioblastoma tumor cell growth, survival signaling and invasion fits generally well with description from other tumor types indicating VEGF-C as an oncogenic driver in cancer cells [108]. The study thereby enlightens an area which until date has been very sparsely covered, with only few studies indicating function of VEGF-C for glioblastoma cell proliferation and motility via limited *in vitro* experiments examining effect of treatment with VEGF-C protein [116, 120, 124]. Also, our study support more global effects of VEGF-C in glioblastoma tumors. Although being far from conclusive, our data indicate involvement of VEGF-C for interaction between cancer- and immune cells in glioblastomas. Data is thereby consistent with previous reported expression of VEGF-C in tumor infiltrating macrophages in glioblastomas [118] and studies from models of other cancers demonstrating involvement of VEGF-C as a modulator of interplay between immune- and tumor cells [198, 199]. Further ***Study I*** verifies previously findings of VEGF-C expression in vascular endothelial cells in glioblastoma tumors [119, 120]. Together with demonstrated role of VEGF-C for stimulation of HBMVECs in *in vitro* angiogenesis assay [116, 120], this indicates an important role of VEGF-C for blood-vessel formation in glioblastoma. Collectively, this highlight a potential of VEGF-C directed treatment strategies in glioblastoma beyond tumor cell targeting.

A specific drug for clinical targeting of VEGF-C has been developed known as VGX-100, which is a humanized antibody. Early (phase I) clinical evaluation of this therapy in cancer patients reported that the drug was well tolerated and found some anti-tumor effect [200], but currently no testing has been conducted in glioblastoma patients. However, the treatment potential of VGX-100 for use in glioblastoma has been shown in a subcutaneous xenograft mouse model, where large reduction in tumor growth was found upon combinational treatment with VGX-100 and bevacizumab in comparison to control treatment [201, 202]. Notably, this examination did not find any effect of VGX-100 single treatment, being in contrast to our results from ***Study I***, where VEGF-C knockdown had large anti-tumor effect on itself. A reason for this contradiction could be that VGX-100 was tested in U87MG, that in

despite of being positive for both VEGF-C [120, 203] and VEGFR2 [66, 86] is problematic for glioblastoma modelling as described in **Section 4.1**. Further on, pharmacological targeting in animals is limited by *in vivo* drug stability, drug clearance and side effects restricting drug dose; elements avoided when testing cells treated before transplantation. Another possibility that partly could explain less effect of VGX-100 as compared to effect of knockdown is that VEGF-C, besides having autocrine and paracrine effects involving its secretion out of the cells, also has direct intracrine effects. Function of VEGF-C in glioblastoma would thereby be in line with findings regarding VEGF-A in colorectal cancer, where intracrine signaling was shown to promote pro-survival signaling, migration and invasion [95, 204]. Although no conclusions regarding this can be drawn from ***Study I***, IHC positivity for VEGF-C both in cytoplasm as well as in nucleus of glioblastoma cells could point in this direction (see Figure 9 for zoom in on Study I figure 2e). Also in support of intracrine VEGF-C signaling, is the prediction of nuclear localization signals (NLSs) in the VEGF-C sequence (Figure 10). Should intracrine signaling be of major importance for tumor promoting function of VEGF-C, an antibody based targeting strategy could be problematic as these bulk molecules cannot enter the cell, and alternative strategies should be investigated.

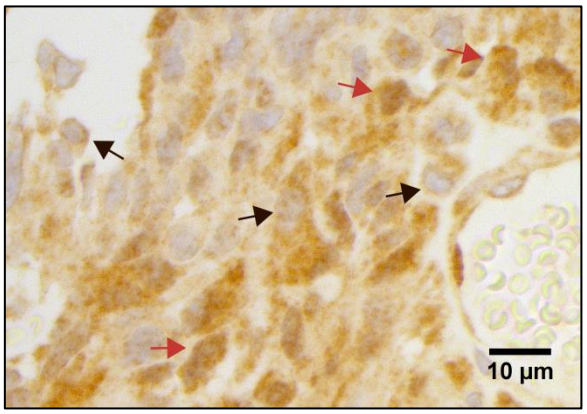

Figure 9. VEGF-C localization in glioblastoma tumor cells. Zoom in on ***Study I*** figure 2e (Patient 6 Post-Bev) showing VEGF-C IHC staining of glioblastoma tumor tissue. While staining was mainly cytoplasmic (black arrows), reaction was in selected cells also located over the nucleus (red arrows).

Intra-tumor heterogeneity in glioblastoma demonstrated for VEGF-C in ***Study I*** and in a previous study for its target VEGFR2 [65], further indicate that targeting VEGF-C will only have direct effect on a subset of glioblastoma cells. This argues for combination of anti-VEGF-C with other treatments. Our findings in ***Study I*** together with the study of VGX-100 [201, 202], support the use of combined anti-VEGF-C treatment with bevacizumab. Although bevacizumab

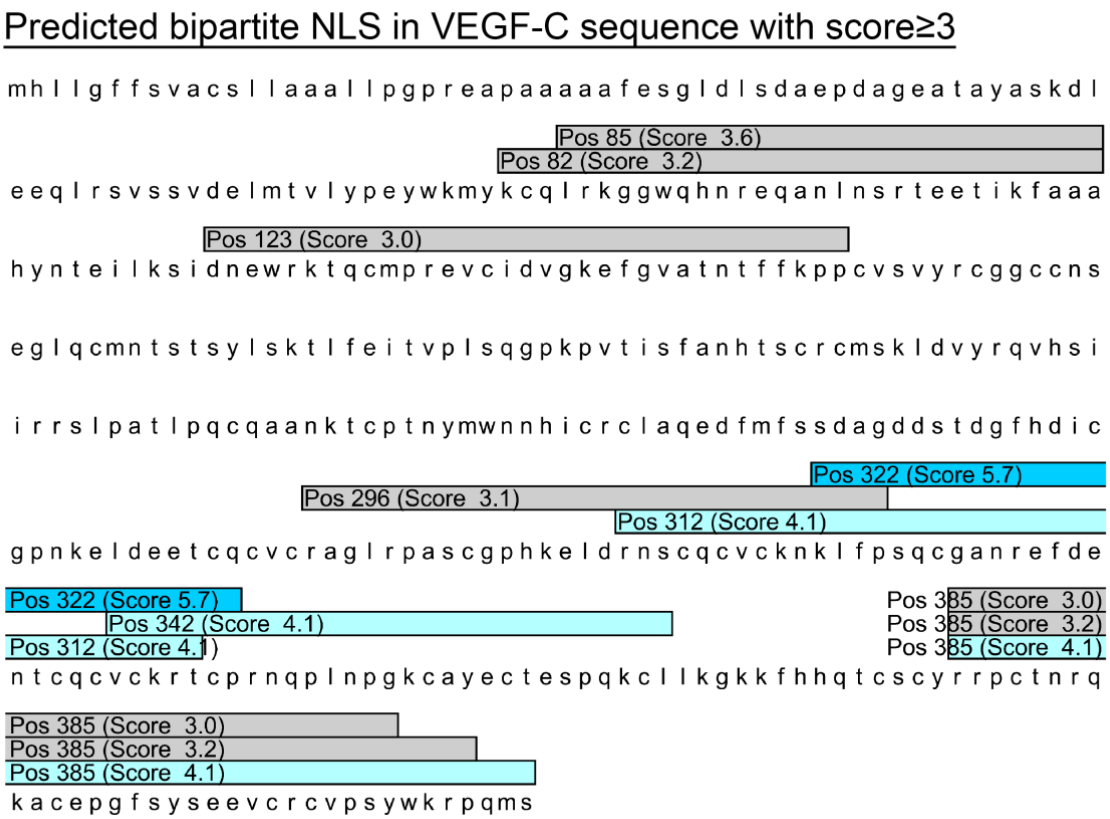

Figure 10. NLSs in VEGF-C. Prediction of NLSs in the full VEGF-C 419 aa sequence using the cNLS mapper software (http://nls-mapper.iab.keio.ac.jp/cgi-bin/NLS_Mapper_form.cgi). Higher scores indicate stronger NLS activity. A score of 5-6 (shown in turquoise) are mainly nuclear, but also localize to the cytoplasm, a score of 4 (shown in light blue) localize equally to the nucleus and cytoplasm, while a score of 3 (shown in grey) localize mainly in the cytoplasm, but are also partly nuclear.

is known not to cross react with VEGF-C [69], the treatment has been shown to change tumor gene expression profile and phenotype [65, 91, 92, 205]. Accordingly, VEGF-C level could in theory be decreased under long-term bevacizumab exposure making this combination less attractive. However, ***Study I*** data demonstrated that this was not the case indicated by presence of VEGF-C protein in patient tumors exposed to bevacizumab treatment. This was although bevacizumab drug, and thereby VEGF-A sequestration, presumable still was present in a proportion of samples as documented half-life of bevacizumab in patients is around 20 days [206] and mean time from treatment stop until surgery for ***Study I*** samples was 23 days.

Therefore, we find further preclinical testing of the combination of VEGF-C targeting and bevacizumab in more models attractive.

Finally, extended preliminary RNA analysis conducted in ten glioblastoma tumor samples showed large inter-tumor heterogeneity for VEGF-C expression (Figure 11 A). Similarly analysis of the TCGA dataset found varying expression for VEGF-C with significantly higher expression in tumors of mesenchymal subtype (Figure 11 B). This could indicate that potential effect of anti-VEGF-C therapy would vary considerably among patients, and patient selection based on either VEGF-C expression or subtype could increase treatment efficacy upon clinical testing of VEGF-C targeting.

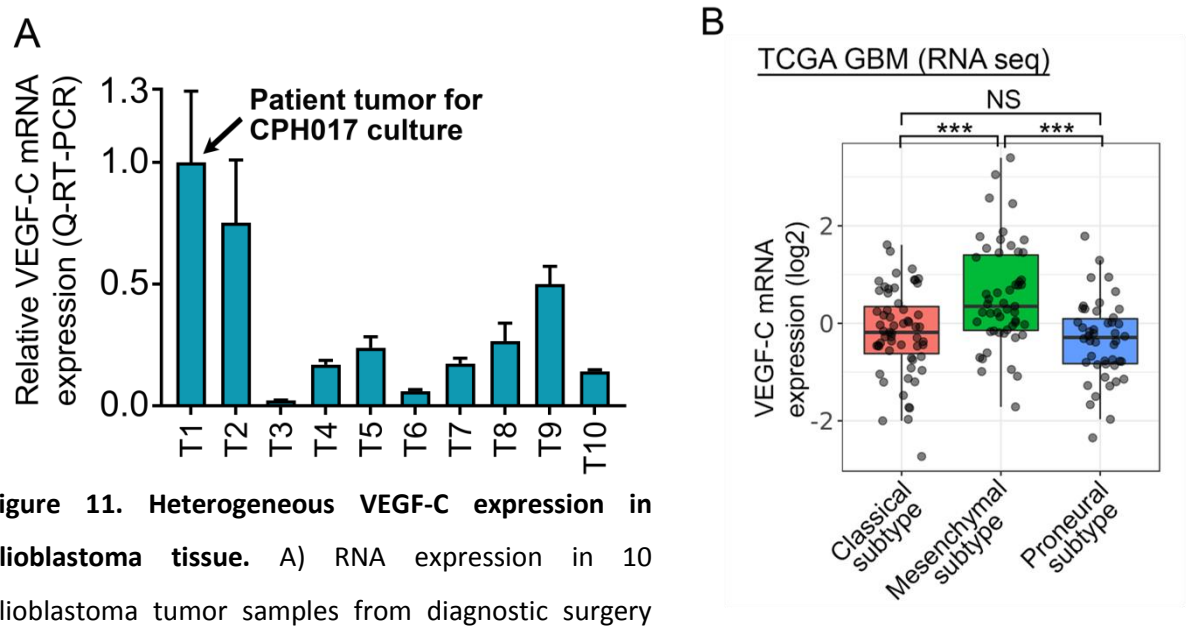

Figure 11. Heterogeneous VEGF-C expression in glioblastoma tissue. A) RNA expression in 10 glioblastoma tumor samples from diagnostic surgery measured by Q-RT-PCR. Sample T1 is patient sample from which the CPH017 cell culture used in Study I was derived. Mean ± SD is shown. B) Boxplot of VEGF-C mRNA levels in the glioblastoma patient tumors of the classical (n=59), mesenchymal (n=51) or proneural (n=46) subtype. Results are based on RNA sequencing data from TCGA glioblastoma dataset and obtained from the GlioVis website (http://gliovis.bioinfo.cnio.es/). Statistics are a result of a Tukey's Honestly Significant Difference Test. *** P≤0.001, NS: non-significant.

4.4.2 Notch and EGFR – improvement of therapeutic effect by a combinatory targeting strategy

Given fundamental roles of EGFR and Notch in glioblastoma maintenance, signaling via these molecules presents attractive treatment targets. However, the described redundancy between these pathways argues that a combinational approach may be necessary to obtain clinical effect. Accordingly, ***Study II*** found that combined inhibition of Notch and EGFR signaling to be superior in limiting viability and angiogenic potential *in vitro* of glioblastoma cells. ***Study II*** findings also confirmed direct interaction between the Notch and EGFR pathways in glioblastoma. This included verification of decreased Akt activation upon inhibition of Notch signaling [142, 178] and finding of lowered Hes-1 levels under EGFR inhibition, correlating with shown EGFR stimulatory effect on Hes-1 expression [180]. Moreover, we found in line with previous studies [142, 176], decreased EGFR expression when targeting the Notch signaling. Contrary, the EGFRvIII level was unaffected, proposing that the mutated receptor is not regulated via this mechanism. Correspondingly, the EGFRvIII positive cells were less sensitive in regard to cell viability when the two pathways were inhibited, consistent with previous results showing the EGFRvIII mutation to reduce the sensitivity towards Iressa treatment [174]. Still, we found efficient inhibition of VEGF-A level as well as angiogenic capacity of DAPT and Iressa in the EGFRvIII positive cells, suggesting that dual targeting of EGFR and Notch pathways should not be excluded as a potential treatment strategy for EGFRvIII positive tumors.

Following publication of ***Study II***, we conducted an *in vivo* study testing the combination of Iressa and DAPT. As seen in Figure 12, we did not observe a corresponding combinatory effect for tumor development as seen in our *in vitro* experiments. This could be a consequence of the combination being without effect in glioblastoma tumors due to compensatory effect by yet other mechanisms than Notch and EGFR. Alternatively, it could be a result of choice of study setup (e.g. inadequate dosing and drug delivery method) and therefore more *in vivo* studies testing other setups are needed to draw conclusions.

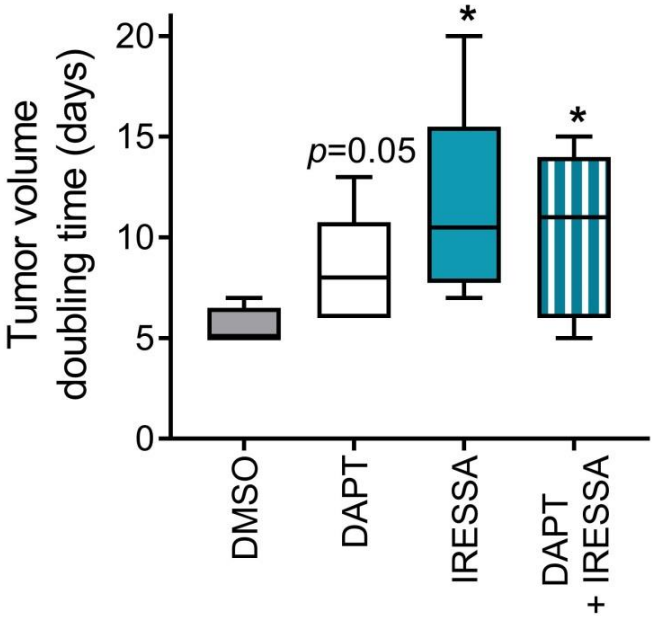

Figure 12. *In vivo* testing of DAPT and Iressa combinatory therapy. NMRI nude mice with subcutaneous xenografts established from the CPH036 glioblastoma cell culture, were divided in groups of 6 mice each. Mice were treated by oral gavage with control treatment (DMSO), DAPT (20 mg/kg), Iressa (40 mg/kg) or DAPT plus Iressa treatment diluted in corn oil. Treatment was given 4 days a week from tumor take until sacrifice and tumor size were measured by caliper every day. Doubling time was calculated as time for tumor to growth from 500 mm^3 to 1000 mm^3.

Of interest a recent preclinical study from non- small cell lung cancer found that a dual-targeting antibody, CT16, simultaneously inhibiting EGFR and Notch, to be superior over single targeting drugs for the two genes, both when used alone or in combination [207]. Testing of an identical strategy in glioblastoma is therefore intriguing. Moreover, this study found that effect of both single and dual targeting therapy was higher, when simultaneous combined with radiation therapy [207]. Due to the specific association of EGFR and Notch to the GSC population [139, 140, 162, 163, 167], Notch and EGFR targeting therapies could in theory be especially efficient in eliminating the GSC population, while other treatments such as radiation- or chemotherapy might be needed for eradicating more differentiated cells. However, in despite of preclinical studies suggesting increased *in vitro* and *in vivo* growth limiting effect for combining GSI treatment with radiation- and temozolomide therapy [138, 149], early clinical testing of GSI RO4929097 together with radiation- and temozolomide in glioblastoma patients indicated only modest survival efficacy [151]. Likewise, clinical phase I/II study in glioblastoma patients did not find improved survival of adding Iressa to radiation therapy [208]. Still, this does not exclude that simultaneous EGFR and Notch inhibition could display combinatory effect when applied in combination with radiation- or chemotherapy in

glioblastoma. Both Iressa and RO4929097 have been shown to enter human brain tumors and in these to modulate their respective targets [151, 209]. This suggests that the absence of effect, upon single targeted therapy of either Notch or EGFR, could be due to alternative mechanism sustaining down-stream signaling rather than inefficient drug function. In this light, more testing of the combination is relevant.

4.4.3 Clinical value of association of CD34 with glioblastoma patient survival

Reliable prognostic models can be an important tool for obtaining optimal patient balancing under randomization into treatment arms in clinical trials and therefore for correct evaluation of new therapeutic modalities. Likewise such models can be useful in daily decision making, selecting patients for available therapies or palliative care, thereby avoiding unnecessary treatment morbidity in patients where imminent death is expected. Among variables suggested for inclusion in such models for glioblastoma survival from retrospectively analysis conducted by us and others are: Patient age, performance status, corticosteroid use and MGMT promoter methylation status [26, 27, 191]. ***Study III*** propose higher gene expression level of CD34 as independently associated with prolonged glioblastoma survival and accordingly that estimation of CD34 level could improve prognostic modelling for OS in glioblastoma. Reason for this association can only be speculated, but given CD34 is a vessel marker [210], it could be a result of higher vascularization in glioblastomas allowing for better therapeutic efficacy. Alternatively, following the concept of glioblastomas expressing varying degree of angiogenesis dependent phenotype or invasive (angiogenesis independent) phenotype [211], the effect could simply be related to slower tumor growth rate and intracranial spread of more angiogenic tumors than of the more invasive tumors.

Correct assessment of CD34 expression level will be critical for its utilization as prognostic variable. As glioblastomas have been demonstrated being highly plastic over time, with changing expression pattern [14, 16], examination of tissue from surgery just prior to treatment start will be of importance for correct CD34 evaluation. Moreover, a recent study by Morrissey et al. showed that estimation of gene expression based on a single biopsy, which is most often what is used in today's clinical routine for glioblastoma diagnosis, is unreliable for

detection of gene expression [212]. By analyzing multi-region biopsies from glioblastoma tumors, the study found that 20% of regional biopsies presented a different subtype from the most common observed for each patient, and consequently that more biopsies are needed for correct marker assessment [212].

An alternative to direct measurement of CD34 level, could be estimation of tumor vascularity, but here again analysis of material not properly capturing regional heterogeneous vascularization of glioblastomas would be problematic. This could have caused failure in previous studies attempting to associate number of vessels, micro vascular density (MVD), to glioblastoma patient outcome [213-215]. Other reason could be that estimation of MVD is difficult, shown by low agreement and consequently inconsistent association of hot-spot assessed MVD with survival, in study having glioblastoma tumors independently evaluated by different observers [216]. Among alternative methods suggested for refinement of estimation in glioblastoma vascularization is tumor microvessel area (MVA), but although MVA has been significantly associated with survival in high grade glioma [217], this method is not easily assessable as it require analysis by optimized computer software. Also, vascular mimicry identified as CD34 negative, periodic acid-Schiff (PAS) positive vessel structures, has been correlated with inferior survival of glioblastoma patients [214]. Later studies have expanded this concept by subdividing glioblastoma tumors into two types based on five distinct microvascular patterns identified by dual CD34/PAS staining, which have been associated with different patient survival [135, 218]. Comparative studies of CD34 mRNA level and this range of suggested methods for vascular assessment are needed to shed light on how relevant the various vascular detection methods are as prognostic measures in glioblastoma.

4.5 Angiogenesis as a target – does it have a future in glioblastoma management?

The high level of vascularity in glioblastomas [44] denotes targeting of angiogenesis as an interesting treatment strategy. However, with later years failure of clinical trials testing bevacizumab in the upfront or recurrent setting [72-75], prospects of pursuing this strategy further is questionable.

With increasing insights into the complexity of blood-vessel formation in glioblastoma including description of multiple angiogenic drivers besides VEGF-A [219], a strategy of only targeting this marker may have been naïve and caused the lack of effect. In this regard ***Study I*** and ***-II***, via studying alternative angiogenesis related molecules, display the tumor heterogeneity and redundant signaling which can affect efficacy of molecular targeting and consequently support a strategy of combinational targeted treatment. Moreover, it is important to have in mind that many angiogenesis related molecules are multi-functional as described in this thesis for VEGF-C, VEGFR2, EGFR and Notch. Consequently effect on both tumor cells, tumor vessels and infiltrative immune cells should be considered.

Also, further optimization of bevacizumab administration should be considered in order to improve an anti-angiogenic treatment approach. Based on preclinical investigations it has been suggested that higher bevacizumab dosing induces an aggressive phenotype in glioblastoma. This is avoided by use of a lower dose, thereby prolonging the therapeutic window suggested to arise as response to anti-angiogenic therapy [220]. In support of this hypothesis, retrospective analysis have found longer survival in glioblastoma patients exposed to reduced bevacizumab dosing compared to patients treated more intensively with bevacizumab [221, 222]. However, a recent phase II clinical trial comparing low dose bevacizumab plus CCNU with high dose bevacizumab monotherapy for recurrent glioblastoma found no significant differences of PFS and OS between these groups [223]. Although this argues against improved effect upon lowering the bevacizumab dose, more studies testing other dose setups are necessary to fully enlighten this hypothesis.

Indications of some survival benefit from bevacizumab in subpopulations of glioblastoma patients experiencing a durable response [76-78], encourage that improvement in bevacizumab success can be obtained via biomarker driven patient selection. However, attempts to correlate bevacizumab efficacy to specific subtypes have been inconsistent. Retrospective studies have pointed at different subtypes for having best effect from bevacizumab therapy [20, 21], while a study from our laboratory did not find any significant association between subtype and bevacizumab response [224]. Consequently, based on current knowledge, patient selection for bevacizumab based on the molecular glioblastoma

subtypes is at present not a reliable method. Single tumor tissue biomarkers proposed of being associated with increased bevacizumab response include increased VEGF-A level [225] and decreased level of angiotensinogen, an effector of the renin-angiotensin system [224]. As such, also the association of CD34 with survival of glioblastoma patients found in ***Study III*** could be related to increased efficacy of bevacizumab therapy in CD34/vascular high patients; an association previously shown in breast cancer patients [226]. Alternatively early detection of blood biomarkers, such as VEGF-A, soluble VEGFR's and PlGF, or information from MRI and positron emission tomography (PET) scans, have been suggested usable for identifying which patients will benefit from anti-angiogenic therapy [68]. This information will be usable for deciphering, in which patient bevacizumab treatment should be continued or terminated. In general though, validation studies preferably via prospective trials are needed to evaluate if these markers are relevant for clinical implementation.

Per se, the era of ubiquitous distribution of bevacizumab for glioblastoma patients might be coming to its end. Yet, results presented and discussed in this thesis of angiogenesis related molecules and approaches for optimization of anti-angiogenic treatment, highlight that continued research within the field of angiogenesis in glioblastoma is meaningful and can bring important knowledge for improvement of glioblastoma management. But as also emphasized, to be effective such strategies will presumable have to take tumor composition, tumor expression pattern and clinical presentation of the individual patient into account.

5. Conclusions

Data presented in this thesis overall support that improvement in glioblastoma management can be obtained by employing molecules related to tumor blood-vessel formation. Specifically the thesis concludes:

VEGF-C is implicated in autocrine activation of VEGFR2 in glioblastoma tumor cells and of importance for sustaining VEGFR2 activation in glioblastoma under bevacizumab therapy. VEGF-C is a driver for cellular survival signaling, cell cycle progression, invasion and proliferation in glioblastoma tumor cells. Consequently, VEGF-C represents a therapeutic target for future investigation. In this regard a combinational treatment strategy will presumable be most effective given that VEGF-C is heterogeneously expressed in glioblastoma.

Crosstalk between the Notch and EGFR signaling pathways is present in glioblastoma tumor cells. This crosstalk signaling sustains cellular proliferation as well as angiogenesis-stimulating signaling of glioblastoma tumor cells upon single targeting of either pathway. Combined targeting of Notch and EGFR signaling results in additive inhibitory effects in glioblastoma tumor cells and is an appealing treatment strategy for further investigation in glioblastoma.

CD34 RNA expression is specifically upregulated in LTS compared to STS among newly diagnosed primary glioblastoma patients treated with radiation-, chemo- and bevacizumab therapy. CD34 is a prognostic marker associated with patient survival independently of patient age, corticosteroid use, performance status and MGMT status. Study of glioblastoma CD34 expression and tumor vessel composition represents a potential area of development for utilization in prognostic modelling of glioblastoma.

6. Future Perspectives

Results in this thesis suggest interesting perspectives for future investigations.

For VEGF-C appealing questions is, if VEGF-C besides having autocrine and paracrine function also has exclusively intracrine functions, and if so, whether this also involves VEGFR2. Besides given mechanistic insights into the effect of VEGF-C downregulation, this will shed light on the clinical potential of available antibody based method for VEGF-C targeting. Also, if and how VEGF-C influence interaction between glioblastoma tumor cells and immune cells is highly relevant to obtain a full picture of the potential for targeting VEGF-C. Moreover, it would be relevant to perform *in vivo* studies examining influence of VEGF-C for the growth- and vessel pattern of glioblastoma tumors. Lastly, testing of VEGF-C targeting *in vivo* together with bevacizumab and chemotherapy, will show if a combinatory approach should be examined as a potential future clinical therapy.

For the combinatory inhibition of Notch and EGFR signaling, additional *in vivo* testing is needed to examine if this strategy hold a future for treatment in glioblastoma patients. For such studies clinically relevant intracranial xenograft models should be employed. These should be established from glioblastoma cell models with varying expression of the molecular targets, including models with and without EGFRvIII, to test if possible efficacy is restricted to specific EGFR and Notch expression patterns. Different targeting drugs and optimized dosing schedules should be tested and efficacy at the expression level in the tumors should be confirmed. Finally, besides testing the combination of EGFR and Notch targeting alone, testing of combination with radiation- or chemotherapy would be relevant to investigate.

For the finding of CD34 association with glioblastoma survival, further studies of CD34 protein expression and vessel structures of glioblastoma tumors are needed to understand the underlying cause for this correlation. In this regard, tumor material from the LTS and STS patients of the Study III cohort, being extreme in regard to CD34 expression and survival, would be ideal for an initial study. Focus of such analysis should also be to identify a simple quantification method providing objective and robust results, as this will be necessary for utilization in the daily clinical routine.

7. References

1. Louis, D.N., et al., *WHO Classification of Tumors of the Central Nervous System*. Revised 4th edition ed. 2016: IACR: Lyon.
2. Walsh, K.M., H. Ohgaki, and M.R. Wrensch, *Epidemiology.* Handb Clin Neurol, 2016. **134**: p. 3-18.
3. Holland, E.C., *Glioblastoma multiforme: the terminator.* Proc Natl Acad Sci U S A, 2000. **97**(12): p. 6242-4.
4. Dunn, G.P., O.C. Andronesi, and D.P. Cahill, *From genomics to the clinic: biological and translational insights of mutant IDH1/2 in glioma.* Neurosurg Focus, 2013. **34**(2): p. E2.
5. Ohgaki, H. and P. Kleihues, *The definition of primary and secondary glioblastoma.* Clin Cancer Res, 2013. **19**(4): p. 764-72.
6. Paldor, I., et al., *Frontal glioblastoma multiforme may be biologically distinct from non-frontal and multilobar tumors.* J Clin Neurosci, 2016. **34**: p. 128-132.
7. Jiang, H., et al., *Impact of epidemiological characteristics of supratentorial gliomas in adults brought about by the 2016 world health organization classification of tumors of the central nervous system.* Oncotarget, 2017. **8**(12): p. 20354-20361.
8. Cheng, H.B., et al., *IDH1 mutation is associated with improved overall survival in patients with glioblastoma: a meta-analysis.* Tumour Biol, 2013. **34**(6): p. 3555-9.
9. Nonoguchi, N., et al., *TERT promoter mutations in primary and secondary glioblastomas.* Acta Neuropathol, 2013. **126**(6): p. 931-7.
10. Liu, X.Y., et al., *Frequent ATRX mutations and loss of expression in adult diffuse astrocytic tumors carrying IDH1/IDH2 and TP53 mutations.* Acta Neuropathol, 2012. **124**(5): p. 615-25.
11. Nobusawa, S., et al., *IDH1 mutations as molecular signature and predictive factor of secondary glioblastomas.* Clin Cancer Res, 2009. **15**(19): p. 6002-7.
12. Waitkus, M.S., B.H. Diplas, and H. Yan, *Isocitrate dehydrogenase mutations in gliomas.* Neuro Oncol, 2016. **18**(1): p. 16-26.
13. Crespo, I., et al., *Molecular and Genomic Alterations in Glioblastoma Multiforme.* Am J Pathol, 2015. **185**(7): p. 1820-33.
14. Phillips, H.S., et al., *Molecular subclasses of high-grade glioma predict prognosis, delineate a pattern of disease progression, and resemble stages in neurogenesis.* Cancer Cell, 2006. **9**(3): p. 157-73.
15. Verhaak, R.G., et al., *Integrated genomic analysis identifies clinically relevant subtypes of glioblastoma characterized by abnormalities in PDGFRA, IDH1, EGFR, and NF1.* Cancer Cell, 2010. **17**(1): p. 98-110.

16. Wang, Q., et al., *Tumor Evolution of Glioma-Intrinsic Gene Expression Subtypes Associates with Immunological Changes in the Microenvironment.* Cancer Cell, 2017. **32**(1): p. 42-56 e6.

17. Aldape, K., et al., *Glioblastoma: pathology, molecular mechanisms and markers.* Acta Neuropathol, 2015. **129**(6): p. 829-48.

18. Bhat, K.P.L., et al., *Mesenchymal differentiation mediated by NF-kappaB promotes radiation resistance in glioblastoma.* Cancer Cell, 2013. **24**(3): p. 331-46.

19. Patel, A.P., et al., *Single-cell RNA-seq highlights intratumoral heterogeneity in primary glioblastoma.* Science, 2014. **344**(6190): p. 1396-401.

20. Sandmann, T., et al., *Patients With Proneural Glioblastoma May Derive Overall Survival Benefit From the Addition of Bevacizumab to First-Line Radiotherapy and Temozolomide: Retrospective Analysis of the AVAglio Trial.* J Clin Oncol, 2015. **33**(25): p. 2735-44.

21. Erdem-Eraslan, L., et al., *Identification of Patients with Recurrent Glioblastoma Who May Benefit from Combined Bevacizumab and CCNU Therapy: A Report from the BELOB Trial.* Cancer Res, 2016. **76**(3): p. 525-34.

22. Stupp, R., et al., *Radiotherapy plus concomitant and adjuvant temozolomide for glioblastoma.* N Engl J Med, 2005. **352**(10): p. 987-96.

23. Perry, J.R., et al., *Short-Course Radiation plus Temozolomide in Elderly Patients with Glioblastoma.* N Engl J Med, 2017. **376**(11): p. 1027-1037.

24. Seystahl, K., W. Wick, and M. Weller, *Therapeutic options in recurrent glioblastoma--An update.* Crit Rev Oncol Hematol, 2016. **99**: p. 389-408.

25. *Retningslinjer for behandling af intrakranielle gliomer hos voksne*. 2016; Available from: www.dnog.dk.

26. Gorlia, T., et al., *Nomograms for predicting survival of patients with newly diagnosed glioblastoma: prognostic factor analysis of EORTC and NCIC trial 26981-22981/CE.3.* Lancet Oncol, 2008. **9**(1): p. 29-38.

27. Gittleman, H., et al., *An independently validated nomogram for individualized estimation of survival among patients with newly diagnosed glioblastoma: NRG Oncology RTOG 0525 and 0825.* Neuro Oncol, 2017. **19**(5): p. 669-677.

28. Fekete, B., et al., *Prognostic factors for glioblastoma patients--a clinical population-based study.* Acta Neurol Scand, 2016. **133**(6): p. 434-41.

29. Malmstrom, A., et al., *Temozolomide versus standard 6-week radiotherapy versus hypofractionated radiotherapy in patients older than 60 years with glioblastoma: the Nordic randomised, phase 3 trial.* Lancet Oncol, 2012. **13**(9): p. 916-26.

30. Kristensen, L.S., et al., *Assessment of Quantitative and Allelic MGMT Methylation Patterns as a Prognostic Marker in Glioblastoma.* J Neuropathol Exp Neurol, 2016. **75**(3): p. 246-55.

31. Hegi, M.E., et al., *MGMT gene silencing and benefit from temozolomide in glioblastoma.* N Engl J Med, 2005. **352**(10): p. 997-1003.

32. Lalezari, S., et al., *Combined analysis of O6-methylguanine-DNA methyltransferase protein expression and promoter methylation provides optimized prognostication of glioblastoma outcome.* Neuro Oncol, 2013. **15**(3): p. 370-81.

33. Verbeek, B., et al., *O6-Methylguanine-DNA methyltransferase inactivation and chemotherapy.* Br Med Bull, 2008. **85**: p. 17-33.

34. Jiang, Y., et al., *Glioblastoma Cell Malignancy and Drug Sensitivity Are Affected by the Cell of Origin.* Cell Rep, 2017. **18**(4): p. 977-990.

35. Parker, N.R., et al., *Molecular heterogeneity in glioblastoma: potential clinical implications.* Front Oncol, 2015. **5**: p. 55.

36. Bonavia, R., et al., *Heterogeneity maintenance in glioblastoma: a social network.* Cancer Res, 2011. **71**(12): p. 4055-60.

37. Bao, S., et al., *Glioma stem cells promote radioresistance by preferential activation of the DNA damage response.* Nature, 2006. **444**(7120): p. 756-60.

38. Kristoffersen, K., et al., *Level of Notch activation determines the effect on growth and stem cell-like features in glioblastoma multiforme neurosphere cultures.* Cancer Biol Ther, 2013. **14**(7): p. 625-37.

39. Guo, Y., et al., *Expression profile of embryonic stem cell-associated genes Oct4, Sox2 and Nanog in human gliomas.* Histopathology, 2011. **59**(4): p. 763-75.

40. Liu, G., et al., *Analysis of gene expression and chemoresistance of CD133+ cancer stem cells in glioblastoma.* Mol Cancer, 2006. **5**: p. 67.

41. Kenig, S., et al., *Topoisomerase IIbeta mediates the resistance of glioblastoma stem cells to replication stress-inducing drugs.* Cancer Cell Int, 2016. **16**: p. 58.

42. Lee, J., et al., *Tumor stem cells derived from glioblastomas cultured in bFGF and EGF more closely mirror the phenotype and genotype of primary tumors than do serum-cultured cell lines.* Cancer Cell, 2006. **9**(5): p. 391-403.

43. Vik-Mo, E.O., et al., *Brain tumor stem cells maintain overall phenotype and tumorigenicity after in vitro culturing in serum-free conditions.* Neuro Oncol, 2010. **12**(12): p. 1220-30.

44. Brem, S., R. Cotran, and J. Folkman, *Tumor angiogenesis: a quantitative method for histologic grading.* J. Natl. Cancer Inst, 1972. **48**(2): p. 347-356.

45. Scatliff, J.H., et al., *Vascular structure of glioblastomas.* Am. J. Roentgenol. Radium. Ther. Nucl. Med, 1969. **105**(4): p. 795-805.

46. Chi, A.S., et al., *Angiogenesis as a therapeutic target in malignant gliomas.* Oncologist, 2009. **14**(6): p. 621-36.

47. McKeown, S.R., *Defining normoxia, physoxia and hypoxia in tumours-implications for treatment response.* Br J Radiol, 2014. **87**(1035): p. 20130676.

48. Wigerup, C., S. Pahlman, and D. Bexell, *Therapeutic targeting of hypoxia and hypoxia-inducible factors in cancer.* Pharmacol Ther, 2016. **164**: p. 152-69.

49. Hjelmeland, A.B., et al., *Acidic stress promotes a glioma stem cell phenotype.* Cell Death Differ, 2011. **18**(5): p. 829-40.

50. Fukumura, D., et al., *Hypoxia and acidosis independently up-regulate vascular endothelial growth factor transcription in brain tumors in vivo.* Cancer Res, 2001. **61**(16): p. 6020-4.

51. Mammoto, T., et al., *Role of collagen matrix in tumor angiogenesis and glioblastoma multiforme progression.* Am J Pathol, 2013. **183**(4): p. 1293-305.

52. Yousfi, N., et al., *The impact of tumor nitric oxide production on VEGFA expression and tumor growth in a zebrafish rat glioma xenograft model.* PLoS One, 2015. **10**(3): p. e0120435.

53. Seystahl, K., et al., *Differential regulation of TGF-beta-induced, ALK-5-mediated VEGF release by SMAD2/3 versus SMAD1/5/8 signaling in glioblastoma.* Neuro Oncol, 2015. **17**(2): p. 254-65.

54. Koch, S. and L. Claesson-Welsh, *Signal transduction by vascular endothelial growth factor receptors.* Cold Spring Harb Perspect Med, 2012. **2**(7): p. a006502.

55. Krebs, R.J., M., *The lymphangiogenic growth factors VEGF-C and VEGF-D Part 1: Fundamentals and embryonic development.* LymphForsch, 2013. **17**(1): p. 30-37.

56. Dixelius, J., et al., *Ligand-induced vascular endothelial growth factor receptor-3 (VEGFR-3) heterodimerization with VEGFR-2 in primary lymphatic endothelial cells regulates tyrosine phosphorylation sites.* J Biol Chem, 2003. **278**(42): p. 40973-9.

57. Nilsson, I., et al., *VEGF receptor 2/-3 heterodimers detected in situ by proximity ligation on angiogenic sprouts.* EMBO J, 2010. **29**(8): p. 1377-88.

58. Claesson-Welsh, L., *VEGF receptor signal transduction - A brief update.* Vascul Pharmacol, 2016. **86**: p. 14-17.

59. Bae, O.N., et al., *Keratinocytic vascular endothelial growth factor as a novel biomarker for pathological skin condition.* Biomol Ther (Seoul), 2015. **23**(1): p. 12-8.

60. Folkman, J., *Tumor angiogenesis: therapeutic implications.* N Engl J Med, 1971. **285**(21): p. 1182-6.

61. Jain, R.K., *Antiangiogenesis strategies revisited: from starving tumors to alleviating hypoxia.* Cancer Cell, 2014. **26**(5): p. 605-22.

62. Hygino da Cruz, L.C., Jr., et al., *Pseudoprogression and pseudoresponse: imaging challenges in the assessment of posttreatment glioma.* AJNR Am J Neuroradiol, 2011. **32**(11): p. 1978-85.

63. Wang, N., R.K. Jain, and T.T. Batchelor, *New Directions in Anti-Angiogenic Therapy for Glioblastoma.* Neurotherapeutics, 2017.

64. Hamerlik, P., et al., *Autocrine VEGF-VEGFR2-Neuropilin-1 signaling promotes glioma stem-like cell viability and tumor growth.* J Exp Med, 2012. **209**(3): p. 507-20.

65. Kessler, T., et al., *Glioma cell VEGFR-2 confers resistance to chemotherapeutic and antiangiogenic treatments in PTEN-deficient glioblastoma.* Oncotarget, 2015. **6**(31): p. 31050-68.

66. Szabo, E., et al., *Autocrine VEGFR1 and VEGFR2 signaling promotes survival in human glioblastoma models in vitro and in vivo.* Neuro Oncol, 2016. **18**(9): p. 1242-52.

67. Xu, C., X. Wu, and J. Zhu, *VEGF promotes proliferation of human glioblastoma multiforme stem-like cells through VEGF receptor 2.* ScientificWorldJournal, 2013. **2013**: p. 417413.

68. Lu-Emerson, C., et al., *Lessons from anti-vascular endothelial growth factor and anti-vascular endothelial growth factor receptor trials in patients with glioblastoma.* J Clin Oncol, 2015. **33**(10): p. 1197-213.

69. Ferrara, N., et al., *Discovery and development of bevacizumab, an anti-VEGF antibody for treating cancer.* Nat Rev Drug Discov, 2004. **3**(5): p. 391-400.

70. Friedman, H.S., et al., *Bevacizumab alone and in combination with irinotecan in recurrent glioblastoma.* J Clin Oncol, 2009. **27**(28): p. 4733-40.

71. Kreisl, T.N., et al., *Phase II trial of single-agent bevacizumab followed by bevacizumab plus irinotecan at tumor progression in recurrent glioblastoma.* J Clin Oncol, 2009. **27**(5): p. 740-5.

72. Chinot, O.L., et al., *Bevacizumab plus radiotherapy-temozolomide for newly diagnosed glioblastoma.* N Engl J Med, 2014. **370**(8): p. 709-22.

73. Gilbert, M.R., et al., *A randomized trial of bevacizumab for newly diagnosed glioblastoma.* N Engl J Med, 2014. **370**(8): p. 699-708.

74. Herrlinger, U., et al., *Bevacizumab Plus Irinotecan Versus Temozolomide in Newly Diagnosed O6-Methylguanine-DNA Methyltransferase Nonmethylated Glioblastoma: The Randomized GLARIUS Trial.* J Clin Oncol, 2016. **34**(14): p. 1611-9.

75. van den Bent, M.G., T.; Bendszus, M.; Sahm, F.; Domont, J.; Idbaih, A.; Platten, M.; Weller, M; Golfoinopoulos, V.; Wick, W *EH1.3EORTC 26101 phase III trial exploring the combination of bevacizumab and lomustine versus lomustine in patients with first progression of a glioblastoma* in *EANO meeting 2016*. 2016. Neuro Oncol

76. Prados, M., et al., *Response as a predictor of survival in patients with recurrent glioblastoma treated with bevacizumab.* Neuro Oncol, 2011. **13**(1): p. 143-51.

77. Huang, R.Y., et al., *The Impact of T2/FLAIR Evaluation per RANO Criteria on Response Assessment of Recurrent Glioblastoma Patients Treated with Bevacizumab.* Clin Cancer Res, 2016. **22**(3): p. 575-81.

78. Urup, T., et al., *Development and validation of a prognostic model for recurrent glioblastoma patients treated with bevacizumab and irinotecan.* Acta Oncol, 2016. **55**(4): p. 418-22.

79. Balaña, C.E., A.; Pineda, E.; Sepúlveda, J.; Mesía, C.; del Barco, S.; Gil-Gil, M.; Hardy, M.; Indacoechea, A.; Cardona, A. F.;, *Prolonged survival after bevacizumab rechallenge in glioblastoma patients with previous response to bevacizumab.* Neurooncol Pract 2017. **4**(1): p. 15-23.

80. Reardon, D.A., et al., *Bevacizumab continuation beyond initial bevacizumab progression among recurrent glioblastoma patients.* Br J Cancer, 2012. **107**(9): p. 1481-7.

81. Baker, G.J., et al., *Mechanisms of glioma formation: iterative perivascular glioma growth and invasion leads to tumor progression, VEGF-independent vascularization, and resistance to antiangiogenic therapy.* Neoplasia, 2014. **16**(7): p. 543-61.

82. Holash, J., et al., *Vessel cooption, regression, and growth in tumors mediated by angiopoietins and VEGF.* Science, 1999. **284**(5422): p. 1994-8.

83. Zagzag, D., et al., *Vascular apoptosis and involution in gliomas precede neovascularization: a novel concept for glioma growth and angiogenesis.* Lab Invest, 2000. **80**(6): p. 837-49.

84. Soda, Y., et al., *Transdifferentiation of glioblastoma cells into vascular endothelial cells.* Proc. Natl. Acad. Sci. U. S. A, 2011. **108**(11): p. 4274-4280.

85. Wang, R., et al., *Glioblastoma stem-like cells give rise to tumour endothelium.* Nature, 2010. **468**(7325): p. 829-833.

86. Francescone, R., et al., *Glioblastoma-derived tumor cells induce vasculogenic mimicry through Flk-1 protein activation.* J. Biol. Chem, 2012. **287**(29): p. 24821-24831.

87. Scully, S., et al., *Transdifferentiation of glioblastoma stem-like cells into mural cells drives vasculogenic mimicry in glioblastomas.* J. Neurosci, 2012. **32**(37): p. 12950-12960.

88. Boer, J.C., A.M. Walenkamp, and W.F. den Dunnen, *Recruitment of bone marrow derived cells during anti-angiogenic therapy in GBM: the potential of combination strategies.* Crit Rev Oncol Hematol, 2014. **92**(1): p. 38-48.

89. Burrell, K., et al., *VEGF regulates region-specific localization of perivascular bone marrow-derived cells in glioblastoma.* Cancer Res, 2014. **74**(14): p. 3727-39.

90. Flanigan, P.M. and M.K. Aghi, *Adaptation to antiangiogenic therapy in neurological tumors.* Cell Mol Life Sci, 2015. **72**(16): p. 3069-82.

91. Lu, K.V., et al., *VEGF inhibits tumor cell invasion and mesenchymal transition through a MET/VEGFR2 complex.* Cancer Cell, 2012. **22**(1): p. 21-35.

92. Piao, Y., et al., *Acquired resistance to anti-VEGF therapy in glioblastoma is associated with a mesenchymal transition.* Clin Cancer Res, 2013. **19**(16): p. 4392-403.

93. Tamura, R., et al., *Bevacizumab for malignant gliomas: current indications, mechanisms of action and resistance, and markers of response.* Brain Tumor Pathol, 2017. **34**(2): p. 62-77.

94. Chen, T.T., et al., *MET Suppresses Epithelial VEGFR2 via Intracrine VEGF-induced Endoplasmic Reticulum-associated Degradation.* EBioMedicine, 2015. **2**(5): p. 406-20.

95. Bhattacharya, R., et al., *Intracrine VEGF Signaling Mediates the Activity of Prosurvival Pathways in Human Colorectal Cancer Cells.* Cancer Res, 2016. **76**(10): p. 3014-24.

96. Joukov, V., et al., *A novel vascular endothelial growth factor, VEGF-C, is a ligand for the Flt4 (VEGFR-3) and KDR (VEGFR-2) receptor tyrosine kinases.* EMBO J, 1996. **15**(7): p. 1751.

97. Achen, M.G., et al., *Vascular endothelial growth factor D (VEGF-D) is a ligand for the tyrosine kinases VEGF receptor 2 (Flk1) and VEGF receptor 3 (Flt4).* Proc Natl Acad Sci U S A, 1998. **95**(2): p. 548-53.

98. Joukov, V., et al., *Proteolytic processing regulates receptor specificity and activity of VEGF-C.* EMBO J, 1997. **16**(13): p. 3898-911.

99. Karpanen, T., et al., *Functional interaction of VEGF-C and VEGF-D with neuropilin receptors.* FASEB J, 2006. **20**(9): p. 1462-72.

100. Favier, B., et al., *Neuropilin-2 interacts with VEGFR-2 and VEGFR-3 and promotes human endothelial cell survival and migration.* Blood, 2006. **108**(4): p. 1243-50.

101. Davydova, N., et al., *Differential Receptor Binding and Regulatory Mechanisms for the Lymphangiogenic Growth Factors Vascular Endothelial Growth Factor (VEGF)-C and -D.* J Biol Chem, 2016. **291**(53): p. 27265-27278.

102. Karkkainen, M.J., et al., *Vascular endothelial growth factor C is required for sprouting of the first lymphatic vessels from embryonic veins.* Nat Immunol, 2004. **5**(1): p. 74-80.

103. Chen, J.C., et al., *The role of the VEGF-C/VEGFRs axis in tumor progression and therapy.* Int J Mol Sci, 2012. **14**(1): p. 88-107.

104. Krebs, R.J., M., *The lymphangiogenic growth factors VEGF-C and VEGF-D Part 2: The role of VEGF-C and VEGF.D in disease involving the lymphatic system.* LymphForsch, 2013. **17**(2): p. 96-103.

105. Siegfried, G., et al., *The secretory proprotein convertases furin, PC5, and PC7 activate VEGF-C to induce tumorigenesis.* J Clin Invest, 2003. **111**(11): p. 1723-32.

106. McColl, B.K., et al., *Plasmin activates the lymphangiogenic growth factors VEGF-C and VEGF-D.* J Exp Med, 2003. **198**(6): p. 863-8.

107. Jha, S.K., et al., *Efficient activation of the lymphangiogenic growth factor VEGF-C requires the C-terminal domain of VEGF-C and the N-terminal domain of CCBE1.* Sci Rep, 2017. **7**(1): p. 4916.

108. Wang, C.A. and S.J. Tsai, *The non-canonical role of vascular endothelial growth factor-C axis in cancer progression.* Exp Biol Med (Maywood), 2015. **240**(6): p. 718-24.

109. Morfoisse, F., et al., *Role of hypoxia and vascular endothelial growth factors in lymphangiogenesis.* Mol Cell Oncol, 2014. **1**(1): p. e29907.

110. Morfoisse, F., et al., *Hypoxia induces VEGF-C expression in metastatic tumor cells via a HIF-1alpha-independent translation-mediated mechanism.* Cell Rep, 2014. **6**(1): p. 155-67.

111. Enholm, B., et al., *Comparison of VEGF, VEGF-B, VEGF-C and Ang-1 mRNA regulation by serum, growth factors, oncoproteins and hypoxia.* Oncogene, 1997. **14**(20): p. 2475-83.

112. Yeh, Y.W., et al., *Targeting the VEGF-C/VEGFR3 axis suppresses Slug-mediated cancer metastasis and stemness via inhibition of KRAS/YAP1 signaling.* Oncotarget, 2017. **8**(3): p. 5603-5618.

113. Sun, P., et al., *RNA interference (RNAi)-mediated vascular endothelial growth factor-C (VEGF-C) reduction interferes with lymphangiogenesis and enhances epirubicin sensitivity of breast cancer cells.* Mol Cell Biochem, 2008. **308**(1-2): p. 161-8.

114. Cho, H.J., et al., *VEGF-C mediates RhoGDI2-induced gastric cancer cell metastasis and cisplatin resistance.* Int J Cancer, 2014. **135**(7): p. 1553-63.

115. Zhu, H., et al., *VEGF-C inhibition reverses resistance of bladder cancer cells to cisplatin via upregulating maspin.* Mol Med Rep, 2015. **12**(2): p. 3163-9.

116. Carpenter, R.L., et al., *The gain-of-function GLI1 transcription factor TGLI1 enhances expression of VEGF-C and TEM7 to promote glioblastoma angiogenesis.* Oncotarget, 2015. **6**(26): p. 22653-65.

117. Xu, Y., et al., *Collaborative overexpression of matrix metalloproteinase-1 and vascular endothelial growth factor-C predicts adverse prognosis in patients with gliomas.* Cancer Epidemiol, 2013. **37**(5): p. 697-702.

118. Jenny, B., et al., *Expression and localization of VEGF-C and VEGFR-3 in glioblastomas and haemangioblastomas.* J. Pathol, 2006. **209**(1): p. 34-43.

119. Grau, S.J., et al., *Expression of VEGFR3 in glioma endothelium correlates with tumor grade.* J Neurooncol, 2007. **82**(2): p. 141-50.

120. Grau, S., et al., *Bevacizumab can induce reactivity to VEGF-C and -D in human brain and tumour derived endothelial cells.* J Neurooncol, 2011. **104**(1): p. 103-12.

121. Zhao, H., et al., *Concurrent Expression of VEGF-C and Neuropilin-2 Is Correlated with Poor Prognosis in Glioblastoma.* Tohoku J Exp Med, 2016. **238**(2): p. 85-91.

122. Denicolai, E., et al., *Molecular heterogeneity of glioblastomas: does location matter?* Oncotarget, 2016. **7**(1): p. 902-13.

123. Tchoghandjian, A., et al., *Cortical and subventricular zone glioblastoma-derived stem-like cells display different molecular profiles and differential in vitro and in vivo properties.* Ann Surg Oncol, 2012. **19 Suppl 3**: p. S608-19.

124. Wang, Y., et al., *Temozolomide inhibits cellular growth and motility via targeting ERK signaling in glioma C6 cells.* Mol Med Rep, 2016. **14**(6): p. 5732-5738.

125. Zhang, R., A. Engler, and V. Taylor, *Notch: an interactive player in neurogenesis and disease.* Cell Tissue Res, 2017.

126. Stockhausen, M.T., K. Kristoffersen, and H.S. Poulsen, *The functional role of Notch signaling in human gliomas.* Neuro Oncol, 2010. **12**(2): p. 199-211.

127. Teodorczyk, M. and M.H. Schmidt, *Notching on Cancer's Door: Notch Signaling in Brain Tumors.* Front Oncol, 2014. **4**: p. 341.

128. Saito, T., *NEPRO: a novel Notch effector for maintenance of neural progenitor cells in the neocortex.* Adv Exp Med Biol, 2012. **727**: p. 61-70.

129. Xu, P., et al., *Differential expression of Notch family members in astrocytomas and medulloblastomas.* Pathol Oncol Res, 2009. **15**(4): p. 703-10.

130. Purow, B.W., et al., *Expression of Notch-1 and its ligands, Delta-like-1 and Jagged-1, is critical for glioma cell survival and proliferation.* Cancer Res, 2005. **65**(6): p. 2353-63.

131. Kanamori, M., et al., *Contribution of Notch signaling activation to human glioblastoma multiforme.* J Neurosurg, 2007. **106**(3): p. 417-27.

132. Dell'albani, P., et al., *Differential patterns of NOTCH1-4 receptor expression are markers of glioma cell differentiation.* Neuro Oncol, 2014. **16**(2): p. 204-16.

133. Hulleman, E., et al., *A role for the transcription factor HEY1 in glioblastoma.* J Cell Mol Med, 2009. **13**(1): p. 136-46.

134. Irshad, K., et al., *A combined gene signature of hypoxia and notch pathway in human glioblastoma and its prognostic relevance.* PLoS One, 2015. **10**(3): p. e0118201.

135. Qiu, X.X., et al., *The Vascular Notch Ligands Delta-Like Ligand 4 (DLL4) and Jagged1 (JAG1) Have Opposing Correlations with Microvascularization but a Uniform Prognostic Effect in Primary Glioblastoma: A Preliminary Study.* World Neurosurg, 2016. **88**: p. 447-58.

136. Jungk, C., et al., *Spatial transcriptome analysis reveals Notch pathway-associated prognostic markers in IDH1 wild-type glioblastoma involving the subventricular zone.* BMC Med, 2016. **14**(1): p. 170.

137. Fan, X., et al., *NOTCH pathway blockade depletes CD133-positive glioblastoma cells and inhibits growth of tumor neurospheres and xenografts.* Stem Cells, 2010. **28**(1): p. 5-16.

138. Yahyanejad, S., et al., *NOTCH blockade combined with radiation therapy and temozolomide prolongs survival of orthotopic glioblastoma.* Oncotarget, 2016. **7**(27): p. 41251-41264.

139. Yu, J.B., H. Jiang, and R.Y. Zhan, *Aberrant Notch signaling in glioblastoma stem cells contributes to tumor recurrence and invasion.* Mol Med Rep, 2016. **14**(2): p. 1263-8.

140. Ulasov, I.V., et al., *Inhibition of Sonic hedgehog and Notch pathways enhances sensitivity of CD133(+) glioma stem cells to temozolomide therapy.* Mol Med, 2011. **17**(1-2): p. 103-12.

141. Bar, E.E., *Glioblastoma, cancer stem cells and hypoxia.* Brain Pathol, 2011. **21**(2): p. 119-29.

142. Xu, P., et al., *The oncogenic roles of Notch1 in astrocytic gliomas in vitro and in vivo.* J Neurooncol, 2010. **97**(1): p. 41-51.

143. Benedito, R., et al., *The notch ligands Dll4 and Jagged1 have opposing effects on angiogenesis.* Cell, 2009. **137**(6): p. 1124-35.

144. Zou, Y., et al., *Gamma-secretase inhibitor DAPT suppresses glioblastoma growth via uncoupling of tumor vessel density from vessel function.* Clin Exp Med, 2013. **13**(4): p. 271-8.

145. Beel, A.J. and C.R. Sanders, *Substrate specificity of gamma-secretase and other intramembrane proteases.* Cell Mol Life Sci, 2008. **65**(9): p. 1311-34.

146. Milano, J., et al., *Modulation of notch processing by gamma-secretase inhibitors causes intestinal goblet cell metaplasia and induction of genes known to specify gut secretory lineage differentiation.* Toxicol Sci, 2004. **82**(1): p. 341-58.

147. Gilbert, C.A., et al., *Gamma-secretase inhibitors enhance temozolomide treatment of human gliomas by inhibiting neurosphere repopulation and xenograft recurrence.* Cancer Res, 2010. **70**(17): p. 6870-9.

148. Fan, X., et al., *Notch pathway inhibition depletes stem-like cells and blocks engraftment in embryonal brain tumors.* Cancer Res, 2006. **66**(15): p. 7445-52.

149. Wang, J., et al., *Notch promotes radioresistance of glioma stem cells.* Stem Cells, 2010. **28**(1): p. 17-28.

150. Pan, E., et al., *Phase I study of RO4929097 with bevacizumab in patients with recurrent malignant glioma.* J Neurooncol, 2016. **130**(3): p. 571-579.

151. Xu, R., et al., *Molecular and Clinical Effects of Notch Inhibition in Glioma Patients: A Phase 0/I Trial.* Clin Cancer Res, 2016. **22**(19): p. 4786-4796.

152. Nedergaard, M.K., C.J. Hedegaard, and H.S. Poulsen, *Targeting the epidermal growth factor receptor in solid tumor malignancies.* BioDrugs, 2012. **26**(2): p. 83-99.

153. Zandi, R., et al., *Mechanisms for oncogenic activation of the epidermal growth factor receptor.* Cell Signal, 2007. **19**(10): p. 2013-23.

154. Strommer, K., et al., *Cellular and tumoural heterogeneity of EGFR gene amplification in human malignant gliomas.* Acta Neurochir (Wien), 1990. **107**(3-4): p. 82-7.

155. Aldape, K.D., et al., *Immunohistochemical detection of EGFRvIII in high malignancy grade astrocytomas and evaluation of prognostic significance.* J Neuropathol Exp Neurol, 2004. **63**(7): p. 700-7.

156. Estrada, C.V., A., *Epidermal Growth Factor Receptor in the Adult Brain*, in *The Cell Cycle in the Central Nervous System* D. Janigro, Editor. 2006, Humana Press.

157. Huang, H.S., et al., *The enhanced tumorigenic activity of a mutant epidermal growth factor receptor common in human cancers is mediated by threshold levels of constitutive tyrosine phosphorylation and unattenuated signaling.* J Biol Chem, 1997. **272**(5): p. 2927-35.

158. Pedersen, M.W., et al., *Analysis of the epidermal growth factor receptor specific transcriptome: effect of receptor expression level and an activating mutation.* J Cell Biochem, 2005. **96**(2): p. 412-27.

159. Grandal, M.V., et al., *EGFRvIII escapes down-regulation due to impaired internalization and sorting to lysosomes.* Carcinogenesis, 2007. **28**(7): p. 1408-17.

160. Sugawa, N., et al., *Identical splicing of aberrant epidermal growth factor receptor transcripts from amplified rearranged genes in human glioblastomas.* Proc Natl Acad Sci U S A, 1990. **87**(21): p. 8602-6.

161. Padfield, E., H.P. Ellis, and K.M. Kurian, *Current Therapeutic Advances Targeting EGFR and EGFRvIII in Glioblastoma.* Front Oncol, 2015. **5**: p. 5.

162. Soeda, A., et al., *Epidermal growth factor plays a crucial role in mitogenic regulation of human brain tumor stem cells.* J Biol Chem, 2008. **283**(16): p. 10958-66.

163. Stockhausen, M.T., et al., *Differentiation of glioblastoma multiforme stem-like cells leads to downregulation of EGFR and EGFRvIII and decreased tumorigenic and stem-like cell potential.* Cancer Biol Ther, 2014. **15**(2): p. 216-24.

164. Mazzoleni, S., et al., *Epidermal growth factor receptor expression identifies functionally and molecularly distinct tumor-initiating cells in human glioblastoma multiforme and is required for gliomagenesis.* Cancer Res, 2010. **70**(19): p. 7500-13.

165. Schreiber, A.B., M.E. Winkler, and R. Derynck, *Transforming growth factor-alpha: a more potent angiogenic mediator than epidermal growth factor.* Science, 1986. **232**(4755): p. 1250-3.

166. Azuaje, F., K. Tiemann, and S.P. Niclou, *Therapeutic control and resistance of the EGFR-driven signaling network in glioblastoma.* Cell Commun Signal, 2015. **13**: p. 23.

167. Mazzoleni, S., et al., *Epidermal growth factor receptor expression identifies functionally and molecularly distinct tumor-initiating cells in human glioblastoma multiforme and is required for gliomagenesis.* Cancer Res, 2010. **70**(19): p. 7500-7513.

168. Keller, S. and M.H.H. Schmidt, *EGFR and EGFRvIII Promote Angiogenesis and Cell Invasion in Glioblastoma: Combination Therapies for an Effective Treatment.* Int J Mol Sci, 2017. **18**(6).

169. Pore, N., et al., *EGFR tyrosine kinase inhibitors decrease VEGF expression by both hypoxia-inducible factor (HIF)-1-independent and HIF-1-dependent mechanisms.* Cancer Res, 2006. **66**(6): p. 3197-204.

170. Maity, A., et al., *Epidermal growth factor receptor transcriptionally up-regulates vascular endothelial growth factor expression in human glioblastoma cells via a pathway involving phosphatidylinositol 3'-kinase and distinct from that induced by hypoxia.* Cancer Res, 2000. **60**(20): p. 5879-86.

171. Li, S., et al., *Structural basis for inhibition of the epidermal growth factor receptor by cetuximab.* Cancer Cell, 2005. **7**(4): p. 301-11.

172. Okada, Y., et al., *EGFR Down-regulation After anti-EGFR Therapy Predicts the Anti-tumor Effect in Colorectal Cancer.* Mol Cancer Res, 2017.

173. Reardon, D.A., P.Y. Wen, and I.K. Mellinghoff, *Targeted molecular therapies against epidermal growth factor receptor: past experiences and challenges.* Neuro Oncol, 2014. **16 Suppl 8**: p. viii7-13.

174. Pedersen, M.W., et al., *Differential response to gefitinib of cells expressing normal EGFR and the mutant EGFRvIII.* Br J Cancer, 2005. **93**(8): p. 915-23.

175. Zanca, C., et al., *Glioblastoma cellular cross-talk converges on NF-kappaB to attenuate EGFR inhibitor sensitivity.* Genes Dev, 2017.

176. Purow, B.W., et al., *Notch-1 regulates transcription of the epidermal growth factor receptor through p53.* Carcinogenesis, 2008. **29**(5): p. 918-25.

177. Rajasekhar, V.K., et al., *Oncogenic Ras and Akt signaling contribute to glioblastoma formation by differential recruitment of existing mRNAs to polysomes.* Mol Cell, 2003. **12**(4): p. 889-901.

178. Zhao, N., et al., *Akt-mTOR signaling is involved in Notch-1-mediated glioma cell survival and proliferation.* Oncol Rep, 2010. **23**(5): p. 1443-7.

179. Zheng, Y., L. Lin, and Z. Zheng, *TGF-alpha induces upregulation and nuclear translocation of Hes1 in glioma cell.* Cell Biochem Funct, 2008. **26**(6): p. 692-700.

180. Zhao, K., et al., *EGFR/c-myc axis regulates TGFbeta/Hippo/Notch pathway via epigenetic silencing miR-524 in gliomas.* Cancer Lett, 2017. **406**: p. 12-21.

181. Xie, M., et al., *Notch-1 contributes to epidermal growth factor receptor tyrosine kinase inhibitor acquired resistance in non-small cell lung cancer in vitro and in vivo.* Eur J Cancer, 2013. **49**(16): p. 3559-72.

182. Dong, Y., et al., *Synthetic lethality through combined Notch-epidermal growth factor receptor pathway inhibition in basal-like breast cancer.* Cancer Res, 2010. **70**(13): p. 5465-74.

183. Stockhausen, M.-T., K. Kristoffersen, and H.S. Poulsen, *Notch Signaling and Brain Tumors*, in *Notch Signaling in Embryology and Cancer*, J. Reichrath and S. Reichrath, Editors. 2012, Springer US: New York, NY. p. 289-304.

184. Allen, M., et al., *Origin of the U87MG glioma cell line: Good news and bad news.* Sci Transl Med, 2016. **8**(354): p. 354re3.

185. Bady, P., et al., *DNA fingerprinting of glioma cell lines and considerations on similarity measurements.* Neuro Oncol, 2012. **14**(6): p. 701-11.

186. Stockhausen, M.T., et al., *Maintenance of EGFR and EGFRvIII expressions in an in vivo and in vitro model of human glioblastoma multiforme.* Exp Cell Res, 2011. **317**(11): p. 1513-26.

187. Rasmussen, R.D., et al., *BRCA1-regulated RRM2 expression protects glioblastoma cells from endogenous replication stress and promotes tumorigenicity.* Nat. Commun, 2016. **7**: p. 13398.

188. Stylli, S.S., et al., *Mouse models of glioma.* J Clin Neurosci, 2015. **22**(4): p. 619-26.

189. Huszthy, P.C., et al., *In vivo models of primary brain tumors: pitfalls and perspectives.* Neuro Oncol, 2012. **14**(8): p. 979-93.

190. Nedergaard, M.K., et al., *18F-FET microPET and microMRI for anti-VEGF and anti-PlGF response assessment in an orthotopic murine model of human glioblastoma.* PLoS One, 2015. **10**(2): p. e0115315.

191. Michaelsen, S.R., et al., *Clinical variables serve as prognostic factors in a model for survival from glioblastoma multiforme: an observational study of a cohort of consecutive non-selected patients from a single institution.* BMC Cancer, 2013. **13**: p. 402.

192. Bass, B.P., et al., *A review of preanalytical factors affecting molecular, protein, and morphological analysis of formalin-fixed, paraffin-embedded (FFPE) tissue: how well do you know your FFPE specimen?* Arch Pathol Lab Med, 2014. **138**(11): p. 1520-30.

193. Zhang, P., et al., *The Utilization of Formalin Fixed-Paraffin-Embedded Specimens in High Throughput Genomic Studies.* Int J Genomics, 2017. **2017**: p. 1926304.

194. Reis, P.P., et al., *mRNA transcript quantification in archival samples using multiplexed, color-coded probes.* BMC Biotechnol, 2011. **11**: p. 46.

195. Chen, X., et al., *Comparison of Nanostring nCounter(R) Data on FFPE Colon Cancer Samples and Affymetrix Microarray Data on Matched Frozen Tissues.* PLoS One, 2016. **11**(5): p. e0153784.

196. Weathers, S.S. and M.R. Gilbert, *Toward Personalized Targeted Therapeutics: An Overview.* Neurotherapeutics, 2017. **14**(2): p. 256-264.

197. Ignatova, T.N., et al., *Human cortical glial tumors contain neural stem-like cells expressing astroglial and neuronal markers in vitro.* Glia, 2002. **39**(3): p. 193-206.

198. Chen, Z., et al., *Down-regulation of vascular endothelial cell growth factor-C expression using small interfering RNA vectors in mammary tumors inhibits tumor lymphangiogenesis and spontaneous metastasis and enhances survival.* Cancer Res, 2005. **65**(19): p. 9004-11.

199. Peppicelli, S., F. Bianchini, and L. Calorini, *Inflammatory cytokines induce vascular endothelial growth factor-C expression in melanoma-associated macrophages and stimulate melanoma lymph node metastasis.* Oncol Lett, 2014. **8**(3): p. 1133-1138.

200. Falchook, G.S., et al., *A first-in-human phase I study of VGX-100, a selective anti-VEGF-C antibody, alone and in combination with bevacizumab in patients with advanced solid tumors*. 2014, Journal of Clinical Oncology. p. 2524-2524.

201. Falchook, G.S., et al., *Phase I study of VGX-100, an anti-VEGF-C monoclonal antibody, with or without bevacizumab, in patients (pts) with advanced solid tumors.* Journal of Clinical Oncology, 2013. **31**(15_suppl): p. TPS2619-TPS2619.

202. Baldwin, M.E., *Combination treatment with vegf-c antagonists*. 2012, Google Patents.

203. Laakkonen, P., et al., *Vascular endothelial growth factor receptor 3 is involved in tumor angiogenesis and growth.* Cancer Res, 2007. **67**(2): p. 593-9.

204. Bhattacharya, R., et al., *Intracrine VEGF signalling mediates colorectal cancer cell migration and invasion.* Br J Cancer, 2017. **117**(6): p. 848-855.

205. Urup, T., et al., *Transcriptional changes induced by bevacizumab combination therapy in responding and non-responding recurrent glioblastoma patients.* BMC Cancer, 2017. **17**(1): p. 278.

206. Lu, J.F., et al., *Clinical pharmacokinetics of bevacizumab in patients with solid tumors.* Cancer Chemother Pharmacol, 2008. **62**(5): p. 779-86.

207. Hu, S., et al., *Antagonism of EGFR and Notch limits resistance to EGFR inhibitors and radiation by decreasing tumor-initiating cell frequency.* Sci Transl Med, 2017. **9**(380).

208. Chakravarti, A., et al., *RTOG 0211: a phase 1/2 study of radiation therapy with concurrent gefitinib for newly diagnosed glioblastoma patients.* Int J Radiat Oncol Biol Phys, 2013. **85**(5): p. 1206-11.

209. Hegi, M.E., et al., *Pathway analysis of glioblastoma tissue after preoperative treatment with the EGFR tyrosine kinase inhibitor gefitinib--a phase II trial.* Mol Cancer Ther, 2011. **10**(6): p. 1102-12.

210. Nielsen, J.S. and K.M. McNagny, *Novel functions of the CD34 family.* J Cell Sci, 2008. **121**(Pt 22): p. 3683-92.

211. Onishi, M., et al., *Angiogenesis and invasion in glioma.* Brain Tumor Pathol, 2011. **28**(1): p. 13-24.

212. Morrissy, A.S., et al., *Spatial heterogeneity in medulloblastoma.* Nat Genet, 2017. **49**(5): p. 780-788.

213. Wood, M.D., et al., *Protein Analysis of Glioblastoma Primary and Posttreatment Pairs Suggests a Mesenchymal Shift at Recurrence.* J Neuropathol Exp Neurol, 2016. **75**(10): p. 925-935.

214. Wang, S.Y., et al., *Vasculogenic mimicry is a prognostic factor for postoperative survival in patients with glioblastoma.* J Neurooncol, 2013. **112**(3): p. 339-45.

215. Hasselbalch, B., et al., *Prospective evaluation of angiogenic, hypoxic and EGFR-related biomarkers in recurrent glioblastoma multiforme treated with cetuximab, bevacizumab and irinotecan.* APMIS, 2010. **118**(8): p. 585-94.

216. Preusser, M., et al., *Histopathologic assessment of hot-spot microvessel density and vascular patterns in glioblastoma: Poor observer agreement limits clinical utility as prognostic factors: a translational research project of the European Organization for Research and Treatment of Cancer Brain Tumor Group.* Cancer, 2006. **107**(1): p. 162-70.

217. Hu, L.S., et al., *Correlations between perfusion MR imaging cerebral blood volume, microvessel quantification, and clinical outcome using stereotactic analysis in recurrent high-grade glioma.* AJNR Am J Neuroradiol, 2012. **33**(1): p. 69-76.

218. Chen, L., et al., *Classification of microvascular patterns via cluster analysis reveals their prognostic significance in glioblastoma.* Hum Pathol, 2015. **46**(1): p. 120-8.

219. Zhang, M., et al., *Recent advance in molecular angiogenesis in glioblastoma: the challenge and hope for anti-angiogenic therapy.* Brain Tumor Pathol, 2015. **32**(4): p. 229-36.

220. de Groot, J.F., *High-dose antiangiogenic therapy for glioblastoma: less may be more?* Clin Cancer Res, 2011. **17**(19): p. 6109-11.

221. Lorgis, V., et al., *Relation between bevacizumab dose intensity and high-grade glioma survival: a retrospective study in two large cohorts.* J Neurooncol, 2012. **107**(2): p. 351-8.

222. Levin, V.A., et al., *Impact of bevacizumab administered dose on overall survival of patients with progressive glioblastoma.* J Neurooncol, 2015. **122**(1): p. 145-50.

223. Weathers, S.P., et al., *A randomized phase II trial of standard dose bevacizumab versus low dose bevacizumab plus lomustine (CCNU) in adults with recurrent glioblastoma.* J Neurooncol, 2016. **129**(3): p. 487-494.

224. Urup, T., et al., *Angiotensinogen and HLA class II predict bevacizumab response in recurrent glioblastoma patients.* Mol Oncol, 2016. **10**(8): p. 1160-8.

225. Sathornsumetee, S., et al., *Tumor angiogenic and hypoxic profiles predict radiographic response and survival in malignant astrocytoma patients treated with bevacizumab and irinotecan.* J Clin Oncol, 2008. **26**(2): p. 271-8.

226. Tolaney, S.M., et al., *Role of vascular density and normalization in response to neoadjuvant bevacizumab and chemotherapy in breast cancer patients.* Proc Natl Acad Sci U S A, 2015. **112**(46): p. 14325-30.

8. Co-author declarations

GRADUATE SCHOOL OF HEALTH AND MEDICAL SCIENCES
UNIVERSITY OF COPENHAGEN

DECLARATION OF CO-AUTHORSHIP

Information on PhD student:	
Name of PhD student	Signe Regner Michaelsen
E-mail	signerm@gmail.com
Date of birth	07-08-1985
Work place	Department of Radiation Biology, Rigshospitalet, Denmark
Principal supervisor	Hans Skovgaard Poulsen

Title of PhD thesis:
Analysis of molecules related to angiogenesis for advancement of glioblastoma treatment

This declaration concerns the following article:
VEGF-C sustains VEGFR-2 activation under bevacizumab therapy and promotes cellular maintenance in glioblastoma

The PhD student's contribution to the article: *(please use the scale (A,B,C) below as benchmark*)*	(A,B,C)
1. Formulation/identification of the scientific problem that from theoretical questions need to be clarified. This includes a condensation of the problem to specific scientific questions that is judged to be answerable by experiments	C
2. Planning of the experiments and methodology design, including selection of methods and method development	C
3. Involvement in the experimental work	C
4. Presentation, interpretation and discussion in a journal article format of obtained data	C

**Benchmark scale of the PhD student's contribution to the article*		
A. refers to:	*Has contributed to the co-operation*	*0-33 %*
B. refers to:	*Has contributed considerably to the co-operation*	*34-66 %*
C. refers to:	*Has predominantly executed the work independently*	*67-100 %*

Signature of the co-authors:			
Date:	Name:	Title:	Signature:
12/10/2017	Petra Hamerlik	PhD	
19/10/17	Hans Skovgaard Poulsen	MD, DMSC	

Signature of the PhD student and the principal supervisor:	
Date: 26/10-17 PhD student: Signe Ulen	Date: Principal supervisor:

GRADUATE SCHOOL OF HEALTH AND MEDICAL SCIENCES
UNIVERSITY OF COPENHAGEN

DECLARATION OF CO-AUTHORSHIP

Information on PhD student:	
Name of PhD student	Signe Regner Michaelsen
E-mail	signerm@gmail.com
Date of birth	07-08-1985
Work place	Department of Radiation Biology, Rigshospitalet, Denmark
Principal supervisor	Hans Skovgaard Poulsen

Title of PhD thesis:
Analysis of molecules related to angiogenesis for advancement of glioblastoma treatment

This declaration concerns the following article:
Combined EGFR- and Notch inhibition display additive inhibitory effect on glioblastoma cell viability and glioblastoma-induced endothelial cell sprouting in vitro

The PhD student's contribution to the article: *(please use the scale (A,B,C) below as benchmark*)*	(A,B,C)
1. Formulation/identification of the scientific problem that from theoretical questions need to be clarified. This includes a condensation of the problem to specific scientific questions that is judged to be answerable by experiments	A
2. Planning of the experiments and methodology design, including selection of methods and method development	B
3. Involvement in the experimental work	B
4. Presentation, interpretation and discussion in a journal article format of obtained data	B

**Benchmark scale of the PhD student's contribution to the article*		
A. refers to:	*Has contributed to the co-operation*	*0-33 %*
B. refers to:	*Has contributed considerably to the co-operation*	*34-66 %*
C. refers to:	*Has predominantly executed the work independently*	*67-100 %*

Signature of the co-authors:			
Date:	Name:	Title:	Signature:
12/10/2017	Petra Hamerlik	PhD	
12/10-2017	Mikkel Staberg	PhD	
13/10-2017	Mette Villingshøj	Technician, MPH	
19/10/17	Hans Skovgaard Poulsen	MD, DMSC	

Signature of the PhD student and the principal supervisor:	
Date: 26/10-17	Date:
PhD student:	Principal supervisor:

GRADUATE SCHOOL OF HEALTH AND MEDICAL SCIENCES
UNIVERSITY OF COPENHAGEN

DECLARATION OF CO-AUTHORSHIP

Information on PhD student:	
Name of PhD student	Signe Regner Michaelsen
E-mail	signerm@gmail.com
Date of birth	07-08-1985
Work place	Department of Radiation Biology, Rigshospitalet, Denmark
Principal supervisor	Hans Skovgaard Poulsen

Title of PhD thesis:

Analysis of molecules related to angiogenesis for advancement of glioblastoma treatment

This declaration concerns the following article:

Molecular profiling of short-term and long-term surviving patients identifies CD34 mRNA levels as prognostic for glioblastoma survival

The PhD student's contribution to the article: *(please use the scale (A,B,C) below as benchmark*)*	(A,B,C)
1. Formulation/identification of the scientific problem that from theoretical questions need to be clarified. This includes a condensation of the problem to specific scientific questions that is judged to be answerable by experiments	C
2. Planning of the experiments and methodology design, including selection of methods and method development	C
3. Involvement in the experimental work	C
4. Presentation, interpretation and discussion in a journal article format of obtained data	C

**Benchmark scale of the PhD student's contribution to the article*		
A. refers to:	*Has contributed to the co-operation*	*0-33 %*
B. refers to:	*Has contributed considerably to the co-operation*	*34-66 %*
C. refers to:	*Has predominantly executed the work independently*	*67-100 %*

Signature of the co-authors:

Date:	Name:	Title:	Signature:
20/10-17	Thomas Urup	PhD	
19/10/17	Hans Skovgaard Poulsen	MD, DMSC	
26/10/17	Helle Broholm	MD	
24/10-17	Ulrik Lassen	MD, PhD	

Signature of the PhD student and the principal supervisor:	
Date: 26/10-17	Date:
PhD student: Signe Ulle	Principal supervisor: